Identification and Characterisation of Lipid Droplet-Localised Proteins

Dissertation

for the award of the degree

"*Doctor rerum naturalium*"

of the University of Göttingen

within the doctoral program

"Microbiology and Biochemistry"

of the Göttingen Graduate Center for Neurosciences, Biophysics, and Molecular Biosciences (GGNB)

Submitted by

Hannah Elisa Krawczyk

November 2020

Department of Plant Biochemistry

Albrecht-von-Haller-Institute for Plant Sciences

University of Göttingen

Thesis Advisory Committee

PD Dr. Till Ischebeck
Department of Plant Biochemistry, Albrecht-von-Haller-Institute for Plant Sciences, University of Göttingen

Prof. Dr. Jörg Stülke
Department of General Microbiology, Institute for Microbiology and Genetics, University of Göttingen

PD Dr. Marcel Wiermer
Molecular Biology of Plant-Microbe Interactions, Albrecht-von-Haller-Institute for Plant Sciences, University of Göttingen

Members of the Examination Board

Referee:
PD Dr. Till Ischebeck
Department of Plant Biochemistry, Albrecht-von-Haller-Institute for Plant Sciences, University of Göttingen

2nd referee:
Prof. Dr. Jörg Stülke
Department of General Microbiology, Institute for Microbiology and Genetics, University of Göttingen

Further members of the Examination Board:

PD Dr. Marcel Wiermer
Molecular Biology of Plant-Microbe Interactions, Albrecht-von-Haller-Institute for Plant Sciences, University of Göttingen
Prof. Dr. Christiane Gatz
Department Plant Molecular Biology and Physiology, Albrecht-von-Haller-Institute for Plant Sciences, University of Göttingen
Prof. Dr. Stefanie Pöggeler
Department Genetics of Eukaryotic Microorganisms, Institute of Microbiology and Genetics, University of Göttingen
Jun.-Prof. Dr. Jan de Vries
Department of Applied Bioinformatics, Institute for Microbiology and Genetics, University of Göttingen

Date of oral examination: 14.01.2021

“Science is not only a disciple of reason, but, also, one of romance and passion.”

Stephen Hawking (1942-2018)

Affidavit

I hereby confirm that the dissertation “Identification and characterisation of lipid droplet-localised proteins” is solely my own work and that I have used no sources or aids other than the ones stated. All passages in my thesis for which other sources, including electronic media, have been used, be it direct quotes or content references, have been acknowledged as such and the sources cited.

I agree to have my thesis checked in order to rule out potential similarities with other works and to have my thesis stored in a database for this purpose.

_____

Göttingen, November 2020
Hannah Elisa Krawczyk

Table of contents

List of important abbreviations

BR	brassinosteroid
CLO	CALEOSIN
CoA	Coenzym A
CPM	counts per million
DAG	diacylglycerol
DGAT	DIACYLGLYCEROL ACYLTRANSFERASE
DGDG	digalactosyldiacylglycerol
DOX	DIOXYGENASE
ERAD	ER-associated degradation
ESCRT	endosomal sorting complexes required for transport
FA	fatty acid
FAD	FATTY ACID DESATURASE
FID	flame ionisation detection
GABA	γ-aminobutyric acid
G3P	glycerol-3-phosphate
GC	gas chromatography
GPAT	GLYCEROL-3-PHOSPHATE ACYLTRANSFERASE
HS	heat stress
HSD	HYDROXYSTEROID DEHYDROGENASE
HSR	heat stress relief
LC	liquid chromatography
LD	lipid droplet
LDAP	LIPID DROPLET ASSOCIATED PROTEIN
LIPA	LIPID DROPLET PLASMA MEMBRANE ADAPTOR
LTP	lipid transfer protein
MAG	monoacylglycerol
MCS	membrane contact site
MGDG	monogalactosyldiacylglycerol
MS	mass spectrometry
OLE	OLEOSIN
PA	phophatidic acid
PC	phosphatidylcholine
PD	plasmodesmata
PDAT	PHOSPHOLIPID:DIACYLGLYCEROL ACYLTRANSFERASE
PE	phosphatidylethanolamine
PG	phosphatidylglycerol

PI	phosphatidylinositol
PLIN	PERILIPIN
PM	plasma membrane
PS	phosphatidylserine
PXA1	PEROXISOMAL ABC TRANSPORTER 1
RT	room temperature
SDP1	SUGAR DEPENDENT 1
SE	sterol ester
SLDP	SEED LIPID DROPLET PROTEIN
Snz	Snazarus
SYT	SYNAPTOTAGMIN
TAG	triacylglycerol
TE	total extract
VAP	VESICLE ASSOCIATED PROTEIN

Abstract

Lipid droplets (LD) are unique organelles, whose physiological relevance has been underestimated for a long time. Well-known in seed tissues for storing triacylglycerol (TAG) to fuel post-germinative seedling establishment, LDs in plants are nowadays known to be involved in many more processes. They also present a highly dynamic hub for cellular lipids through the short-term turnover of lipids. They are involved in lipid homeostasis and remodelling of various cellular membranes, e.g. through regulating the balance of lipid storage versus membrane expansion or by storing and buffering excess, unneeded or toxic lipids. This sink – rather than source – function of LDs is especially important during various stresses, such as e.g. heat stress. Here, membranes quickly have to adapt their membrane properties to maintain membrane integrity and prevent hyperfluidity, i.e. unsaturated fatty acids (FAs) with low melting points have to be replaced by saturated FAs with higher melting points. Indeed, LDs are observed to accumulate in response to different abiotic stresses, including heat stress, and with their lipid buffering functions they are often involved in amelioration of the stress. To fulfil their roles in maintaining lipid homeostasis of various organellar membranes, especially during stress conditions, contacts of LDs with these organelles are important. These membrane contact sites (MCS) of LDs are well-described in yeast and mammals and likewise often increase in response to stress. In mammals and yeast, they have been observed between LDs and nearly all other organelles. Data on plant LD contact sites, however, is scarce and limited to LD-ER and LD-peroxisome contacts.

In the present study, I shed light on the involvement of LD-stored TAG in the process of *Nicotiana tabacum* pollen tube heat adaptation. Pollen tubes are reproductive tissues highly sensitive to abiotic stresses and rich in LDs. Proper growth of the pollen tube is crucial for fertilisation and pollen competition and the ability to quickly react to changing environments is of upmost importance. We here show that heat-stress causes quick membrane lipid remodelling in *ex vivo* grown pollen tubes, leading to a pronounced decrease of unsaturated fatty acids (FAs) in nearly all phospholipid classes. Concomitantly, an unspecific increase in TAG and a significant increase in transcripts of several Tobacco *DIACYLGLYCEROL ACYLTRANSFERASE* (*DGAT)* isoforms is observed. We propose a model, where heat stress causes unspecific bulk membrane lipid degradation in growing pollen tubes, and released FAs are channelled into TAGs in a *DGAT1*-dependant way to be replaced in the membranes by newly synthesised saturated FAs, thereby ensuring correct membrane fluidity.

Furthermore, I identify a putative MCS between LDs and the plasma membrane (PM) in *Arabidopsis thaliana* seeds and seedlings. Two formerly undescribed proteins, SEED LIPID DROPLET PROTEIN (SLDP) 1 and 2, were shown to be LD-localised proteins. Mutations of these proteins cause aberrant clustering of LDs that normally evenly distribute along the PM during germination in *Arabidopsis thaliana*. Mutation of a putative interaction partner, PM-

localised LIPID DROPLET PM ANCHOR (LIPA), was found to cause the same phenotype. In addition, a mutual recruitment of ectopically expressed LIPA and SLDP to the PM and LDs, respectively, was observed in pollen tubes. By expressing both proteins in this non-native tissue, a seedling-like distribution of LDs could be reconstituted: LDs, that usually float dynamically through the cytoplasm in pollen tubes are immobilised along the PM when both proteins are co-expressed. Taken together, we suggest a model, where proper cellular LD distribution along the PM in germinating *A. thaliana* is achieved through a MCS between LD-localised SLDP and PM-localised LIPA.

1 Introduction

1.1 The lipid droplet (LD) – a long underestimated organelle

Lipid droplets (LDs) were first reported in the 1880s (Farmer, 1901), yet it took another 100 years for research on this phylogenetically highly conserved organelle to really pick up pace. Only when the link between obesity and several common illnesses, such as hypertension or diabetes, occurred to researchers in the 1980s, interest in the fat-storing organelles was sparked (reviewed in Murphy, 2012; Coleman, 2020). Still, they long remained considered as inert fat storage depots. Today, due to an increase in LD research over the last decade, it is widely appreciated that LDs are ubiquitous and versatile organelles present in many different cell and tissue types. It was found that LDs actively participate in many cellular processes such as lipid homeostasis, lipid signalling, and stress responses (reviewed in Welte and Gould, 2017; Thiam and Beller, 2017; Ischebeck *et al.*, 2020; de Vries and Ischebeck, 2020).

1.1.1 LD Biogenesis

To understand fundamental processes of LD biology and to grasp their versatile roles within the cell, it is important to regard their unique architecture. In contrast to most other organelles, LDs do not give rise to an aqueous compartment surrounded by a phospholipid bilayer, but instead have a lipophilic core surrounded by a phospholipid monolayer. A highly diverse protein coat decorates this monolayer, thereby contributing to the various functions of LDs.

LDs bud off the outer ER membrane leaflet

The unique architecture of LDs arises from their conserved mode of biogenesis, which occurs at the cytosolic leaflet of the ER membrane in a not entirely understood process: According to a widely accepted model, LD formation starts with the synthesis of neutral lipids such as triacylglycerol (TAG) or sterol esters (SEs). Enzymes involved in the final synthesis of these lipids reside in the ER membrane (Buhman *et al.*, 2001) and sequester the neutral lipids between the two leaflets of the ER membrane. There, they can freely diffuse laterally, but at one point, most likely when concentrations reach a critical threshold, a lipid lens forms that finally buds off towards the cytosol in an asymmetric manner (Figure 1: LD biogenesis). It is unclear how this lens formation and budding is facilitated, however lens structures may have phospholipid packing defects and a characteristic membrane curvature, which can be sensed by proteins that facilitate the asymmetric budding. The LD-surrounding phospholipid monolayer thus originates from the outer ER membrane leaflet. (Jacquier *et al.*, 2011; Kassan *et al.*, 2013; Choudhary *et al.*, 2015; Walther *et al.*, 2017; Nettebrock and Bohnert, 2020).

In recent years, evidence accumulated that LD biogenesis occurs at specialised ER subdomains, but generally, the temporal and spatial organisation of LD biogenesis still leaves many open questions. (Joshi *et al.*, 2018; Choudhary *et al.*, 2020; Choudhary and Schneiter, 2020; Nettebrock and Bohnert, 2020).

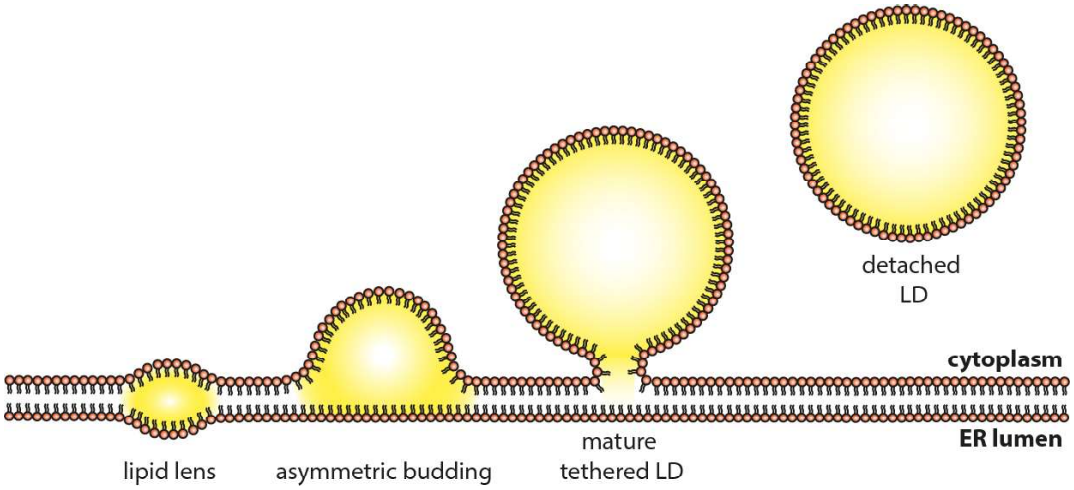

Figure 1: Simplified depiction of LD budding. Neutral lipids (yellow) accumulate between the two leaflets of the ER membrane until they reach a critical threshold. A lipid lens forms, that grows until it buds towards the cytosol. It continues to grow to a mature LD that stays connected to the ER via a lipidic bridge or completely detaches and forms a cytosolic LD.

Neutral lipid production initiates LD formation

LD biogenesis is initiated by the synthesis of neutral lipids in the ER membrane (reviewed in Chapman *et al.*, 2019). The main stored neutral lipid is triacylglycerol (TAG), which composes of a glycerol backbone esterified to three fatty acids (FAs). For the synthesis of the direct TAG precursor diacylglycerol (DAG) and subsequently TAG, different routes exist in plants: DAG can be completely synthesised *de novo* (via the Kennedy pathway), it can be synthesised *de novo* combined with phosphatidylcholine (PC)-FA modification and acyl-editing or it can completely be PC-derived. Depending on the pathway, DAG and TAG species with varying acyl chains arise. Differences in the substrate specificities of the involved enzymes and the respective activities and contributions of the different trafficking routes lead to differences in chain lengths or desaturation of the acyl-chains (reviewed in Bates and Browse, 2012; Bates *et al.*, 2013; Bates, 2016). *Arabidopsis thaliana* seeds use up to 48 % of PC-modified FAs for their TAG synthesis (reviewed in Bates and Browse, 2012). An exemplary overview of the different TAG synthesis routes in *Arabidopsis thaliana* seeds is shown in Figure 2.

The easiest way to produce DAG for TAG synthesis is via the Kennedy-pathway, where acyl-CoAs, *de novo* synthesised and exported from the chloroplast or from the existing cytosolic acyl-CoA pool, are directly used for *de novo* assembly of DAG. For this, fatty acyl-CoAs are subsequently esterified to the sn-1 and sn-2 positions of glycerol-3-phosphate (G3P) by glycerol-3-phosphate acyltransferase (GPAT) and lysophosphatidic acid acyltransferase (LPAAT) to yield first lysophosphatidic acid (LPA) and then phosphatidic acid (PA). Then, phosphatidic acid phosphatase (PAP) replaces the phosphate group of PA with a hydroxyl group to yield DAG. This way, if the acyl-CoA is derived from *de novo* synthesized fatty acids, mostly 16:0-, 18:0- and 18:1-FAs are incorporated into DAG/TAG. Many oilseeds however also

produce DAG from PC-derived FAs, which allows for modifications of the acyl-chains while they are in the PC-pool and leads to TAGs containing more diverse FA compositions. First of all, PC can provide free fatty acids or acyl-CoAs for the Kennedy pathway by the action of phospholipases A1 and A2, or lysophosphatidylcholine acyltransferases (LPCAT), respectively. Alternatively, PC from the membrane lipid pool can be converted to 1,2-DAG directly by action of phospholipase C (PLC) or diacylglycerol cholinephosphotransferase (PDCT), or it is first converted to phosphatidic acid as intermediate step by subsequent action of phospholipase D (PLD) and then to 1,2-DAG by PAP. Vice versa, 1,2-DAG that is not used for TAG production can be converted to PC by choline phosphotransferase (CPT) or PDCT. TAG is finally produced by acylation of 1,2-DAG. Diacylglycerol acyltransferase 1 (DGAT1) or phospholipid:diacylglycerol acyltransferase (PDAT) acylate 1,2-DAG to yield TAG, using acyl-CoA or PC as acyl-donor, respectively. (reviewed in Bates, 2016; Ischebeck *et al.*, 2020).

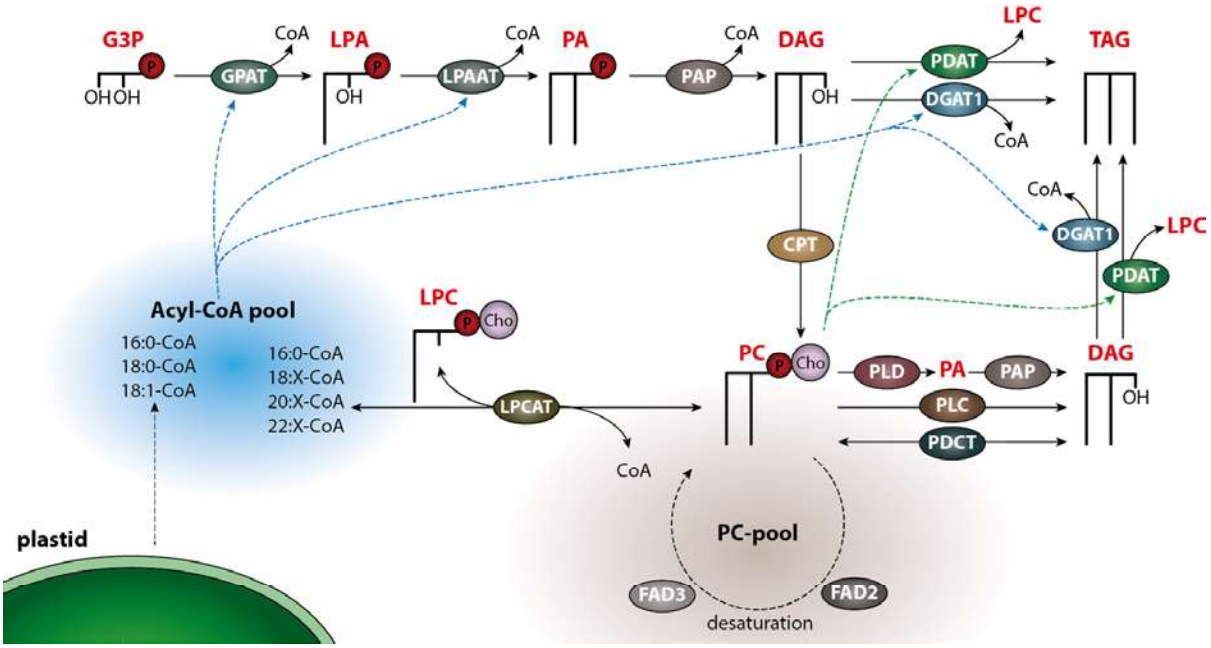

Figure 2: TAG synthesis routes in Arabidopsis. Fatty acids are either *de novo* synthesised in the plastid and exported as acyl-CoAs or fed into the cytosolic acyl-CoA pool by the action of LYSOPHOSPHATIDYLCHOLINE ACYLTRANSFERASE (LPCAT) on the phosphatidylcholine (PC)-pool. These acyl-CoAs can be converted to diacylglycerol (DAG) by the stepwise action of GLYCEROL-3-PHOSPHATE ACYLTRANSFERASE (GPAT), LYSOPHOSPHATIDIC ACID ACYLTRANSFERASE (LPAAT) and PHOSPHATIDIC ACID PHOSPHATASE (PAP), which subsequently add an acyl-chain to glycerol-3-phosphate (G3P) and lysophosphatidic acid (LPA) and replace the phosphate group of produced phosphatidic acid (PA) with a hydroxy group, respectively, to yield DAG. DAG is converted to TAG by addition of another acyl-group by DIACYLGLYCEROL ACYLTRANSFERASE 1 (DGAT1) and PHOSPHOLIPID:DIACYLGLYCEROL ACYLTRANSFERASE (PDAT), where DGAT1 uses acyl-CoA as acyl-donor and PDAT uses PC. Alternatively, DAG is converted to PC by a CHOLINE PHOSPHOTRANSFERASE (CPT) and feeds into the PC-pool, for further desaturation. PHOSPHOLIPASE D and C use the PC-pool to produce PA or DAG, resp., which again can be acylated to TAG by DGAT1 and PDAT. Thus, TAG is either synthesised using *de novo* produced acyl chains or derives from the membrane lipid pool. Figure from Ischebeck *et al.*, 2020.

Proper LD formation requires several proteins

Proper LD biogenesis relies not only on enzymes for neutral lipid synthesis, but on a wide array of other proteins. The ER bilayer has to be split into monolayers for lipid lens formation, asymmetric budding of the nascent LD (towards the cytosol but not towards the ER lumen) has to be controlled and also LD filling and growth, bridging of the ER and the LD as well as detaching of mature LDs suggests requirement of further proteins (reviewed in Nettebrock and Bohnert, 2020).

One protein family involved in proper LD biogenesis is the highly conserved Seipin family (Fld1p (few LDs 1) in yeast). Seipin has been found at LD-ER contact sites in different organisms, including humans, *Drosophila melanogaster*, *Caenorhabditis elegans* and *Saccharomyces cerevisiae* (in the following referred to as yeast) (reviewed in Hugenroth and Bohnert, 2020). Yeast Seipin homologue Fld1p has e.g. been shown to be involved in the directional budding of LDs into the cytosol (Cartwright *et al.*, 2015), in LD size regulation (Fei *et al.*, 2008) and in stabilising LD-ER contact sites via interaction with Ldb16p (Grippa *et al.*, 2015). In plants, unlike other organisms, several Seipin isoforms exist. These plant Seipin proteins, too, have been shown to be important for LD biogenesis: When expressed in leaves, they promote LD formation (Cai *et al.*, 2015), while their knockout leads to abnormal LD formation in seeds and pollen, causing negative effects on seed dormancy and pollen transmission (Taurino *et al.*, 2018). Recently, plant Seipins were found to interact with VESICLE ASSOCIATED PROTEIN (VAP) 27-1, a known ER-PM tether (Greer *et al.*, 2020).

A putative role in LD biogenesis is also attributed to members of the family of “LD associated proteins” (LDAPs). An LD-surface localised LDAP was initially identified in LD proteomes of avocado mesocarp tissue (Horn *et al.*, 2013), but later also found in e.g. Arabidopsis seedlings, senescent leaves and Tobacco pollen tubes (Brocard *et al.*, 2017; Kretzschmar *et al.*, 2018; Kretzschmar *et al.*, 2020). LDAPs are abundant on LDs in non-seed organs and are involved in LD maintenance and regulation, especially during abiotic stress and post-germinative growth. The Arabidopsis genome harbours three *LDAP* genes, but mammals and yeast lack homologues of LDAP (Gidda *et al.*, 2016). LDAPs directly interact with LDAP-interacting protein (LDIP), which is also plant-specific and LD-localised (Pyc *et al.*, 2017). Overexpression of LDAP resulted in an increased LD number, while suppression resulted in a decrease (Gidda *et al.*, 2016), knockout of LDIP likewise resulted in a decrease of LD abundance, but increase in neutral lipid content (Pyc *et al.*, 2017). The exact roles of LDAP and LDIP in plant LD biogenesis remain to be elucidated.

Other proteins potentially implicated in LD biogenesis are oleosins (OLEs). Oleosins are described as plant-specific structural proteins with some functional analogy to mammalian perilipins (PLINs) and are one of the major LD proteins in plants, especially in reproductive

tissues such as seeds or pollen. Oleosins, too, have been shown to promote LD biogenesis (Beaudoin *et al.*, 2000; Jacquier *et al.*, 2013; Ischebeck *et al.*, 2020). Expression of oleosins or PLINs in yeast (which completely lack oleosin or PLIN homologues) promotes LD formation (Jacquier *et al.*, 2013) and it was shown that proper targeting of oleosin to LD-ER contact sites is necessary for the directional budding of LDs towards the cytosol (Huang and Huang, 2017). Also, in soybean, RNAi-mediated suppression of oleosin leads to the formation of aberrant LD-ER complexes, a structure of interconnected ER and LDs, including micro- and giant LDs (Schmidt and Herman, 2008). Knockout of different oleosins in Arabidopsis seeds causes an enlargement of LDs (Siloto *et al.*, 2006; Shimada *et al.*, 2008). However, oleosins are not present in most vegetative tissues, such as leaves or stems. Instead, they are mostly found in organs that undergo desiccation processes, such as seeds and pollen. It is therefore assumed that oleosins, rather than functioning in LD biogenesis, play a role in preventing dehydration/rehydration-induced fusion of LDs and thereby influence LD size (Chapman *et al.*, 2019).

A current model of plant LD biogenesis at the ER membrane including oleosin, LDAP/LDIP, Seipin, DGAT1 and PDAT is depicted in Figure 3.

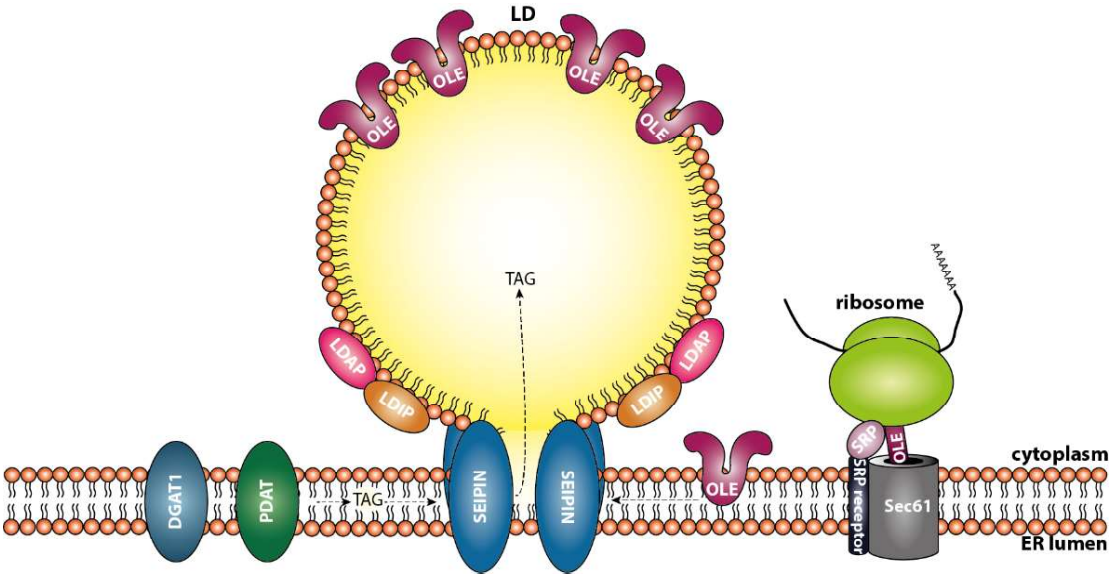

Figure 3: Current model of LD biogenesis and involved proteins. Triacylglycerol (TAG) is synthesized at the ER by DIACYLGLYCEROL ACYLTRANSFERASES 1 (DGAT1) and/or PHOSPHOLIPID:DIACYLGLYCEROL ACYLTRANSFEASE (PDAT), sequestered between the leaflets and channelled into a growing LD that is connected to the ER via a lipidic bridge. At this ER-LD junction, Seipin proteins are involved in regulating LD formation. Several proteins on the LD surface might play a role in proper LD formation, such as oleosin (OLE), LD-associated proteins (LDAPs), and LDIP (LDAP-interacting protein). Oleosins are co-translationally inserted into the ER membrane via SRP/Sec61 and reach the LD surface from the ER. Figure from Ischebeck et al., 2020.

1.1.2 LD Proteome

As already touched upon in section 1.1.1, an interplay of several proteins is needed for LD biogenesis, some of which are localised to the LD surface. Indeed LDs are not only comprised of their neutral lipid core and the surrounding phospholipid monolayer, but their surface is also heavily decorated with proteins involved in e.g. stress responses, metabolism or protein degradation. Some proteins, such as SEED LD PROTEIN (SLDP) and LIPID DROPLET PM ANCHOR (LIPA) identified and analysed in the present study, are of unknown function. The LD's protein coat is highly diverse and varies with the analysed organism, tissue type and developmental state. Focus here will be put on plant LD proteins. An overview of the diversity in LD-associated proteins and their respective functions in plants is shown in Figure 4.

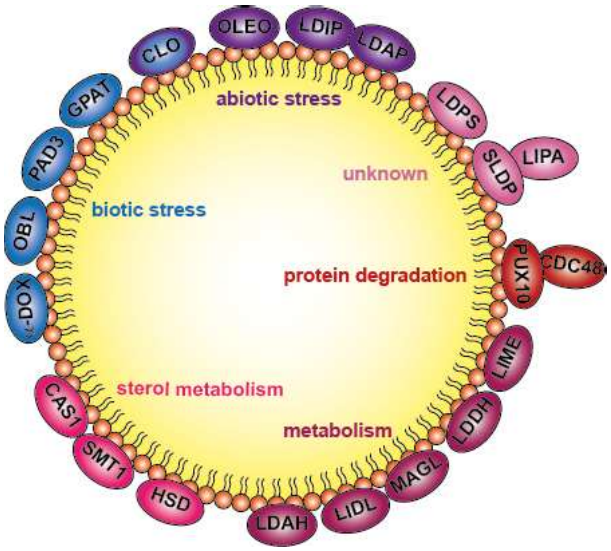

Figure 4: Selection of known plant LD proteins and their functions. A selection of published and confirmed LD-associated proteins and the respective cellular processes they are involved in. Many LD-associated proteins are involved in biotic or abiotic stress reactions. Also, many proteins are enzymes with metabolic functions, e.g. in sterol metabolism. Other functions are protein degradation or remain so far unknown. This study focuses on the two functionally undescribed protein families SEED LD PROTEIN (SLDP) and LIPID DROPLET MEMBRANE ADAPTOR (LIPA).

Several plant LD proteomes have been published

The first plant LD-localised proteins described were the major protein family of oleosins (Qu *et al.*, 1986), followed by lipoxygenases in 1992 (Feußner and Kindl, 1992). Two other major LD proteins followed, caleosins and steroleosins (also called hydroxysteroid dehydrogenases, HSDs), that were initially identified on sesame seed LDs as a putative calcium-binding protein (Chen *et al.*, 1999) and a putative sterol-binding dehydrogenase (L.,-J., Lin *et al.*, 2002) , respectively. Plant LD proteomes are now available of *Arabidopsis thaliana* seeds, seedlings, and infected and aging leaves (Jolivet *et al.*, 2004; Brocard *et al.*, 2017; Kretzschmar *et al.*, 2020; Fernández-Santos *et al.*, 2020), *Brassica napus* (rapeseed) mature seeds (Katavic *et*

al., 2006a; Jolivet *et al.*, 2009), *Persea americana* (avocado) mesocarp (Horn *et al.*, 2013), *Helianthus annuus* (sunflower) developing seeds (Thakur and Bhatla, 2016), *Zea mays* (maize) embryos (Tnani *et al.*, 2011), *Sesamum indicum* (sesame) seeds (Hamada *et al.*, 2020), *Nicotiana tabacum* (Tobacco) pollen tubes (Kretzschmar *et al.*, 2018), *Triadica sebifera* (Chinese tallow) mesocarp and seed tissues (Zhi *et al.*, 2017), *Jatropha curcas* (physic nut) seeds (Popluechai *et al.*, 2011; Liu *et al.*, 2015), peanut (Zaaboul *et al.*, 2018) and hazelnut (Zuidmeer-Jongejan *et al.*, 2014; Lamberti *et al.*, 2020). Proteomes of plastidial LDs, so called plastoglobuli are e.g. available for Arabidopsis leaves (Lundquist *et al.*, 2012), but the focus of the present thesis lies on cytosolic LDs.

Intriguingly, some proteins not expected to localise to LDs have repeatedly been reported in LD proteome analyses, e.g. heat shock proteins (HSPs) (Horn *et al.*, 2013; Liu *et al.*, 2015; Zhi *et al.*, 2017; Hamada *et al.*, 2020). Based on their functions in e.g. protein folding, they would rather be expected in the ER or the cytosol (Li and Srivastava, 2003), but not on LDs. Results like these could suggest that these proteins are either true LD-localised proteins, interacting with LD-localised proteins or that they might be co-purifying in LD fractions as alleged contaminants because of membrane contact sites (MCS) of LDs with other organelles. In total, many proteins have been suggested to localise to LDs by proteomic analyses, but LD-association is often not confirmed by localisation studies and contaminants could be mistakenly believed to be LD-associated. Moreover, while high-confidence LD-associated proteins in mammals are reported to be around 100-150 in a prototypical mammalian cell and 35–40 in yeast (reviewed in Olzmann and Carvalho, 2019), the numbers in plants are even lower. Table 1 shows an overview of high-confidence LD-localised protein families in plants.
In conclusion, LD proteome data show that the LD-protein coat is highly dynamic and dependent not only on tissue-type and developmental state, but also influenced by stress, such as infection.

Table 1: Selection of high-confidence plant LD protein families. An overview of high-confidence LD-localised protein families in plants, based on proteomic studies and/or imaging techniques. Also given is the plant and tissue where LD-association was originally identified as well as protein functions/putative protein functions.

Protein family	originally detected on LDs in	(putative) function
oleosin (OLE, OLEO)	maize scutella (Qu *et al.*, 1986)	LD biogenesis, LD size, biotic stress/emulgator
lipoxygenase (LOX)	cucumber and soybean cotyledons (Feußner and Kindl, 1992)	oxylipin metabolism/signalling
caleosin (CLO)	sesame seeds (Chen *et al.*, 1999)	oxylipin metabolism/biotic and abiotic stress
steroleosin (HSD)	sesame seeds (L.,-J., Lin *et al.*, 2002)	sterol metabolism
oil body-associated lipase (OBL)	castor bean (Eastmond, 2004)	TAG degradation/biotic stress

9/13-hydroperoxide lyase (HPLF)	*Medicago truncatula* (De Domenico *et al.*, 2007)	oxylipin metabolism/signalling
LD associated protein (LDAP)	avocado mesocarp tissue (Horn *et al.*, 2013)	LD biogenesis? abiotic stress
α-Dioxygenase (α-DOX)	Arabidopsis leaves (Shimada *et al.*, 2014)	oxylipin metabolism/biotic stress
MAG lipase (MAGL8)	Arabidopsis germinating seeds and leaves (R., J., Kim *et al.*, 2016)	metabolism
LDAP interacting protein (LDIP)	Arabidopsis cDNA library (Pyc *et al.*, 2017)	LD biogenesis? abiotic stress
cycloarthenol synthase (CAS1)	Tobacco pollen tubes (Kretzschmar *et al.*, 2018)	sterol metabolism
sterol methyltransferase (SMT1)	Tobacco pollen tubes (Kretzschmar *et al.*, 2018)	sterol metabolism
pollen Tube LD protein (PTLD2)	Tobacco pollen tubes (Kretzschmar *et al.*, 2018)	unknown
plant UBX domain-containing protein 10 (PUX10)	Tobacco pollen tubes (Kretzschmar *et al.*, 2018)	protein degradation
phospholipid:sterol acyltransferases (PSAT1)	Tomato (Lara *et al.*, 2018)	sterol metabolism
LD associated lipase (LIDL1)	Arabidopsis seeds and seedlings (Kretzschmar *et al.*, 2020)	metabolism
LD methyltransferase (LIME1)	Arabidopsis seeds and seedlings (Kretzschmar *et al.*, 2020)	metabolism
LD dehydrogenase (LDDH1)	Arabidopsis seeds and seedlings (Kretzschmar *et al.*, 2020)	metabolism
LD-associated hydrolase (LDAH1)	Arabidopsis seeds and seedlings (Kretzschmar *et al.*, 2020)	metabolism
LD protein of seeds (LDPS1)	Arabidopsis seeds and seedlings (Kretzschmar *et al.*, 2020)	unknown
seed LD protein (SLDP)	Arabidopsis seeds and seedlings (Kretzschmar *et al.*, 2020)	unknown
glycerol- 3-phosphate acyltransferase (GPAT4 and 8)	Arabidopsis leaves (Fernández-Santos *et al.*, 2020)	Wax synthesis
phytoalexin-deficient (PAD3)	Arabidopsis leaves (Fernández-Santos *et al.*, 2020)	biotic stress, phytoalexin production

1.1.3 LD functions

With their lipid storing capacity and their variable protein coat, LDs are involved in a wealth of processes, including energy and lipid homeostasis, hormone synthesis, detoxification, stress responses, pathogen/defence responses and signalling. Although a lot of research on these functions has been conducted in yeast or mammals and less in plants, some examples will be described here to convey the idea of LDs as highly versatile and diverse organelles. To understand the cellular roles of the conserved organelle also in other organisms is important to find and understand putative functions and implications of LDs in plants. An overview of the described functions of LDs can be found in Figure 5.

Lipid storage and homeostasis – balancing the lipidome

One of the main functions of LDs, especially in fat-accumulating tissues such as adipocytes or seeds, is storage of lipids as energy supply. TAGs stored in LDs can be used to fuel membrane biosynthesis and/or metabolic processes during cellular growth/membrane expansion or starvation (reviewed in Olzmann and Carvalho, 2019; Ischebeck *et al.*, 2020). In oilseed species such as Arabidopsis, LDs are still best known for their functions in seeds and seedlings, where they are the main storage organelle for stored lipids. TAG accumulation already starts during embryogenesis. Then, during germination and seedling establishment, stored TAG is converted to sugars and fuels heterotrophic growth of the establishing seedling until it achieves photosynthetic competence (Graham, 2008; Yang and Benning, 2018).

LDs are not just involved in cellular energy homeostasis, but also in maintaining lipid homeostasis. They are e.g. involved in the balance of lipid storage versus membrane expansion. In yeast, PA is converted to DAG by the conserved phosphatidate phosphatase (Pah1p). Upon nutrient stress, Pah1p relocates from the cytosol to a nuclear membrane subdomain in contact with growing LDs to convert PA to DAG for TAG synthesis and has thus been proposed to be a metabolic switch for rechannelling lipid fluxes from membrane synthesis to TAG storage. In yeast mutant strains lacking LDs, Pah1 is still relocated to nuclear membranes upon starvation, but lipid precursors are used for phospholipid synthesis and not channelled into TAG, causing nuclear deformation and proliferation of ER membranes (Barbosa, Sembongi, *et al.*, 2015).

This example reinforces the importance of LDs in maintaining cellular lipid homeostasis but also highlights another peculiarity of LDs: instead of drawing on LD stores upon starvation, LDs are often observed to accumulate upon nutrient starvation or other stresses (reviewed in Nguyen and Olzmann, 2017; Ischebeck *et al.*, 2020). LD-stored TAGs here play a role as a transitory FA depot. Starvation induces autophagic processes for quick mobilisation and recycling of resources and thereby often leads to the bulk release of FAs or other cytotoxic lipid species such as acylcarnitine, DAG or ceramides (reviewed in Olzmann and Carvalho, 2019; Nguyen and Olzmann, 2017). In this context, LDs can serve as a buffering system, protecting the cell or certain compartments from lipotoxicity of free FAs or other lipotoxic components. In starving yeast cells, for example, LDs are crucial for ER homeostasis and buffering of FAs during autophagy, and it was excluded that their role is just to provide a source for autophagosome membrane lipids (Barbosa, Sembongi, *et al.*, 2015; Velázquez *et al.*, 2016). In mammals, lipids released by starvation-induced autophagy were shown to be first channelled into LD-stored TAG in a DGAT1-dependent manner, before they were delivered to mitochondria for degradation. By this, LDs prevent lipotoxicity of accumulating acylcarnitines (transport form of FAs for mitochondrial import, lipotoxic in large amounts) (Nguyen *et al.*,

2017). A similar notion is observed in plants after prolonged dark treatment. Prolonged dark treatment causes carbon starvation, as carbon fixation is inactive and starch reserves are used up. Membrane lipids released by starvation-induced degradation after the dark treatment were here shown to be channelled into TAGs prior to their degradation by β-oxidation in peroxisomes. This channelling was found to act as a buffer for cytotoxic lipid intermediates, but intriguingly also protected against reactive oxygen species (ROS) (Fan *et al.*, 2017).
These mechanisms highlight the important role of LDs in providing a transitory depot for lipids, thereby buffering excess or cytotoxic lipids.

LDs during heat stress – remodelling of lipids

Free FAs are not only generated during autophagic processes but can also be released from membranes of the endomembrane system and other organelles by lipases. During senescence or stress-induced lipid remodelling, free FAs can accumulate (reviewed in Yang and Benning, 2018). LD-stored TAGs as a transitory FA depot are likely important during these processes and have been shown to accumulate in response to different abiotic or biotic stresses and during senescence (reviewed in Yang and Benning, 2018; Higashi and Saito, 2019; Lu *et al.*, 2020).

During senescence, β-oxidation rates are reported to be increased and due to the concomitant increase of LDs, it was suggested that membranes are degraded, leading to free FA release and these are channelled through TAG prior to β-oxidation to prevent accumulation of toxic lipid species (reviewed in Masclaux-Daubresse *et al.*, 2020). However, some stresses, such as e.g. temperature-induced stress, require membrane remodelling rather than degradation. High temperature for example can cause membrane hyperfluidity and subsequent bilayer disintegration and also poses an increased risk of peroxidation of unsaturated FAs by ROS (reviewed in Higashi and Saito, 2019). Organisms can circumvent this by altering the physicochemical properties of their membranes. The main constituents of membranes such as the PM are phospholipids, consisting of two fatty acyl chains esterified to a glycerol backbone and a variable, polar head group (Fahy *et al.*, 2005). Physicochemical properties, such as melting points, are mainly determined by the phospholipids' fatty acyl chains: The number of C-C bonds as well as chain lengths have an impact on melting points of the respective FA. While unsaturated FAs e.g. tend to have lower melting points, saturated FAs have a higher melting point (Knothe and Dunn, 2009). The phospholipids' head groups have less impact on melting points, however regarding the membrane as a whole, lipid composition and especially asymmetry in the distribution of different phospholipid classes, e.g. between the two membrane leaflets, present another important membrane property. By altering the saturation status and lengths of phospholipid acyl chains or changing overall phospholipid composition, membrane properties can be adapted to changing environments (reviewed in Niu and Xiang,

2018). Accordingly, in plant leaves it is generally observed that the amount of phospholipids containing saturated acyl chains increases, while poly-unsaturated acyl chains are removed from the phospholipid pool. Concomitant increases in TAGs have frequently been observed in leaves (reviewed in Higashi and Saito, 2019). Increases of TAG levels upon heat stress were not just reported in leaves but also in e.g. Arabidopsis seedlings or tomato fruits (Mueller *et al.*, 2015; Higashi *et al.*, 2015; Shiva *et al.*, 2020; Almeida *et al.*, 2020), as well as in several algal species (Converti *et al.*, 2009; Yang *et al.*, 2013; Allen *et al.*, 2018). A study on *Chlamydomonas reinhardtii* observed that neither total FA content, nor total FA composition changed upon heat-stress. However, lipid class analyses revealed an increase of TAG at the expense of other lipid classes, suggesting the channelling of membrane lipids into TAGs (Légeret *et al.*, 2016). What is more, Arabidopsis *pdat1* mutants are unable to accumulate TAGs upon heat stress, further indicating that increased TAG levels upon heat stress are due to lipid remodelling via the PC-pool rather than due to *de novo* DAG synthesis (see also section 1.1.1) (Mueller *et al.*, 2017). These data hint at an important role of LDs during stress-induced lipid remodelling. Also, levels of sterol derivatives were reported to increase upon heat stress in Arabidopsis leaves (Shiva *et al.*, 2020). Sterols in membranes can regulate permeability, fluidity and also raft formation and the adaptation of sterol compositions in membranes is another possibility to react to external stimuli and stresses (Valitova *et al.*, 2016).

LDs in sterol metabolism

Regarding LD-stored SEs, again, LDs do not simply serve as a passive storage site. SEs, fatty acid-esterified sterols, are important for membrane sterol homeostasis and serve as a storage pool for maintaining and recycling free sterol levels in cell membranes (Ferrer *et al.*, 2017). Sterols are main constituents of membranes in animals, fungi and plants. In contrast to animals, where cholesterol is the predominant sterol species, fungi and plants synthesise a broader and more diversified range of sterols (reviewed in Zhang *et al.*, 2020). The importance of LDs in sterol homeostasis is for example highlighted by an increase of SEs in Arabidopsis plants, when sterol synthesis is upregulated (Shimada *et al*., 2019). Moreover, in proteomic and cell biological analyses of *Nicotiana tabacum* pollen tube LDs, the steroidogenic enzymes CAS1 and SMT1 were found to localise to LDs (Kretzschmar *et al.*, 2018). In addition, subcellular localisation studies of tomato (*Solanum lycopersicum)* PHOSPHOLIPID:STEROL ACYLTRANSFERASE 1 (PSAT1), a type of sterol acyltransferase, revealed LD-localisation of the enzyme (Lara *et al.*, 2018). All these data hint at an involvement of LDs in sterol metabolism.

In steroidogenic cells, especially in mammalian endocrine gonad cells, cholesteryl esters stored in LDs are also used for the synthesis of several steroid hormones (Kraemer *et al.*, 2013). Interestingly, LD-proteome analysis of a steroidogenic mouse tumour cell line revealed

an association of steroidogenic enzymes with LDs: not just two steroleosins were co-purified, but also CYP11A1 and CYP17 and thus all enzymes that are needed for testosterone synthesis (Yamaguchi *et al.*, 2015), suggesting an involvement of LDs in steroid hormone synthesis in mammals. In plants, LDs and LD-localised steroleosins are suggested to be involved in metabolism of brassinosteroids, a class of plant polyhydroxysteroid hormones (L., J., Lin *et al.*, 2002; Ischebeck *et al.*, 2020).

These data might suggest that LDs do not simply store SEs but are actively involved in steroidogenesis and synthesis of steroid hormones (and potentially their regulation).

Other stored components

Apart from TAGs and SEs, yet to a lesser but often physiological relevant extent, other lipid-derived components are also stored in LDs. One example are lipophilic vitamins. Plastoglobuli (LDs inside plastids) in plants and cyanobacteria, as well as LDs in human adipocytes, for example store Vitamin E (tocopherol) (Traber and Kayden, 1987; Peramuna and Summers, 2014; Spicher and Kessler, 2015; Welte and Gould, 2017). Vitamin A (retinol) can be stored as retinyl esters inside LDs, e.g. in human hepatic stellate cells (a type of fat-storing cell in the liver) (Senoo *et al.*, 2007; Welte and Gould, 2017). Also, hydrocarbons such as alkanes, alkenes or isoprenoids are lipophilic and thus likely partition to LDs. Some plants use LDs as a depot for natural rubber (cis-1,4-polyisoprene) in specialised LDs called rubber particles (Laibach *et al.*, 2014) and the filamentous cyanobacterium *Nostoc punctiforme* sequesters heptadecane into LDs (Peramuna *et al.*, 2015). In yeast, the sterol synthesis intermediate squalene ($C_{30}H_{50}$) was shown to be stored in LDs to prevent toxicity (Valachovic *et al.*, 2015), again highlighting the involvement of LDs in preventing lipotoxicity. Not only toxic lipid species or excess FAs can be stored away in LDs for detoxification. It was also shown that an endolichenic fungus can trap endo- and exogenic toxic compounds in LDs as a (self-) resistance mechanism (Chang *et al.*, 2015). In addition, as an ecological remediation strategy, date palm (*Phoenix dactylifera*) seed LDs have been analysed for their capacity to extract dioxins from aquatic systems. It has been shown that exposure to a highly toxic dioxin (2,3,7,8-tetrachlorodibenzo-p-dioxin) resulted in upregulation of several caleosin and steroleosin genes and increased LD formation, although effective partitioning of the dioxin into LDs was independent from LD proteins (Hanano *et al.*, 2016). Apart from these, toxic polycyclic aromatic hydrocarbons and polychlorinated biphenyls were also confirmed to be LD-associated (reviewed in Welte and Gould, 2017).

LDs and proteostasis

An often underestimated component of LDs besides their lipid core is their protein coat. LDs have been implicated in various steps of the life cycle of proteins, as has been reviewed by Welte and Gould (2017). First of all, LDs can be involved in protein assembly, as several

viruses, e.g. Hepatitis C or Dengue, highjack LDs not only for energy supply but also to promote viral assembly. It remains unresolved, however, how exactly LD-association helps in viral protein maturation (reviewed in Welte and Gould, 2017).

LDs can also store proteins. This was e.g. shown for histones in *Drosophila melanogaster* eggs. Eggs contain abundant LDs provided by the mother during oogenesis and several histones associate with these LDs. The presence of histones on LDs was also demonstrated in mammals, e.g. in mouse oocytes. Regarding functionality, it was suggested that histones can either be long-term stored on LDs to be readily available for chromatin assembly, short-term stored to balance newly synthesised histone amounts or serve as antibacterial agents (reviewed in Welte and Gould, 2017).

LDs have also been shown to mitigate ER stress, for one thing by removing excess lipids and maintaining membrane lipid composition (Fuchs *et al.*, 2012; Bosma *et al.*, 2014; Velázquez *et al.*, 2016; Chitraju *et al.*, 2017), for another thing a study on yeast speculated that LDs are involved in the removal of ubiquitination-marked misfolded or damaged proteins from the ER. Supposedly, LDs deliver these proteins to the vacuole via microlipophagy for degradation (Vevea *et al.*, 2015). It has also been suggested that LDs act as a storage for misfolded proteins in the ER, operating along with the ER-associated degradation (ERAD) pathway (Vevea *et al.*, 2015). However, other studies in yeast and mammals clearly showed that LDs are dispensable for ERAD and that at least certain misfolded proteins can still dislocate from the ER and be targeted to the proteasome for degradation, also in the absence of LDs (Olzmann and Kopito, 2011; To *et al.*, 2017). It was therefore suggested, that LDs are only needed for a subset of ERAD substrates, while other ERAD substrates can be degraded LD-independently (Welte and Gould, 2017).

On the other hand, parts of the ERAD machinery are also used for a process termed LD-associated degradation, as was e.g. shown for Arabidopsis plant UBX-domain containing protein 10 (PUX10). LD-localised PUX10 recruits Cell Division Cycle 48 (CDC48) to LDs and interacts with ubiquitin and a mechanism was suggested, where PUX10 recruits CDC48 to ubiquitinated LD-proteins, mainly oleosins, to remove them from LDs for degradation via the 26-S proteasome (Kretzschmar *et al.*, 2018; Deruyffelaere *et al.*, 2018).

LDs and signalling

Another process LDs are involved in is signalling. The TAG precursors DAG and PA both can serve as signalling molecules and as described, their levels can quickly change upon stress, thereby influencing the stress responses (Henne *et al.*, 2018). LDs also play a role in signalling through other lipid-derived signalling molecules. One class of these lipid-derived signalling molecules are oxylipins. Oxylipins are generally not stored, but synthesised *de novo* upon need through oxidation of polyunsaturated fatty acids (PUFAs) and often play a role in intra- or extra-

cellular signalling processes. In animals, cyclooxygenases (COX), lipoxygenases (LOX), or the cytochrome P450 epoxygenases catalyse oxylipin formation, while plants mainly rely on LOX-dependant synthesis, although plant LD-localised α-dioxygenase (α-DOX) shows homology to mammalian COX enzymes. Well-known oxylipins in plants include the hormone jasmonic acid (JA) (reviewed in Wasternack and Feussner, 2018). LDs are likely implicated in oxylipin production. One of the major plant LD-localised proteins, caleosin, has peroxygenase activity and is involved in epoxy fatty acid biosynthesis, which represents a step in oxylipin metabolism (reviewed in Rahman *et al.*, 2018). Also, LOX enzymes, as well as α-DOX have been found associated to plant LDs (Feußner and Kindl, 1992; Shimada *et al.*, 2014). Arabidopsis LDs have been identified as a site for synthesis of the oxylipin 2-hydroxyoctadecatrienoic acid (2-HOT) via CLO3 and α-DOX1 upon fungal infection and senescence. 2-HOT has antifungal activity and thus acts as a phytoalexin (Shimada *et al.*, 2014). Intriguingly, the *Medicago truncatula* hydroperoxide lyase (HPL) 9/13-HPL (HPLF), a CYP74C enzyme that catalyses the cleavage of PUFA hydroperoxides produced by LOX enzymes to generate volatile aldehydes and oxo acids, also shows dual localisation to LDs and the cytosol. The produced aldehyde volatiles are believed to play a role in inter- and intra-organismal plant signalling, as well as in molecular cross-talk with surrounding non-plant organisms (De Domenico *et al.*, 2007). Also, exogenous application of certain oxylipins in mammalian adipocytes was shown to reduce or even block TAG accumulation in LDs, suggesting a putative feedback regulation (Zahradka *et al.*, 2017). All in all, there are not many reports on LD-produced oxylipins, but localisation of precursors as well as enzymes involved in oxylipin metabolism suggests a role of LDs in oxylipin signalling and regulation.

LDs have also been implicated in nuclear signalling mechanisms in mammals. One example is the PLIN5-mediated LD-nuclear signalling: upon β-adrenergic receptor stimulation, LD-localised PLIN5 is phosphorylated and subsequently translocated to the nucleus. Monounsaturated FAs derived from ATGL (adipose tag lipase) activity bind to PLIN5 and are trafficked along. In the nucleus, they allosterically activate sirtuin1 (SIRT1) and promote SIRT1-mediated deacetylation of target genes that eventually leads to an increase in mitochondrial biogenesis and FA oxidation (reviewed in Seibert *et al.*, 2020). However, so far, no such mechanisms have been described in plants.

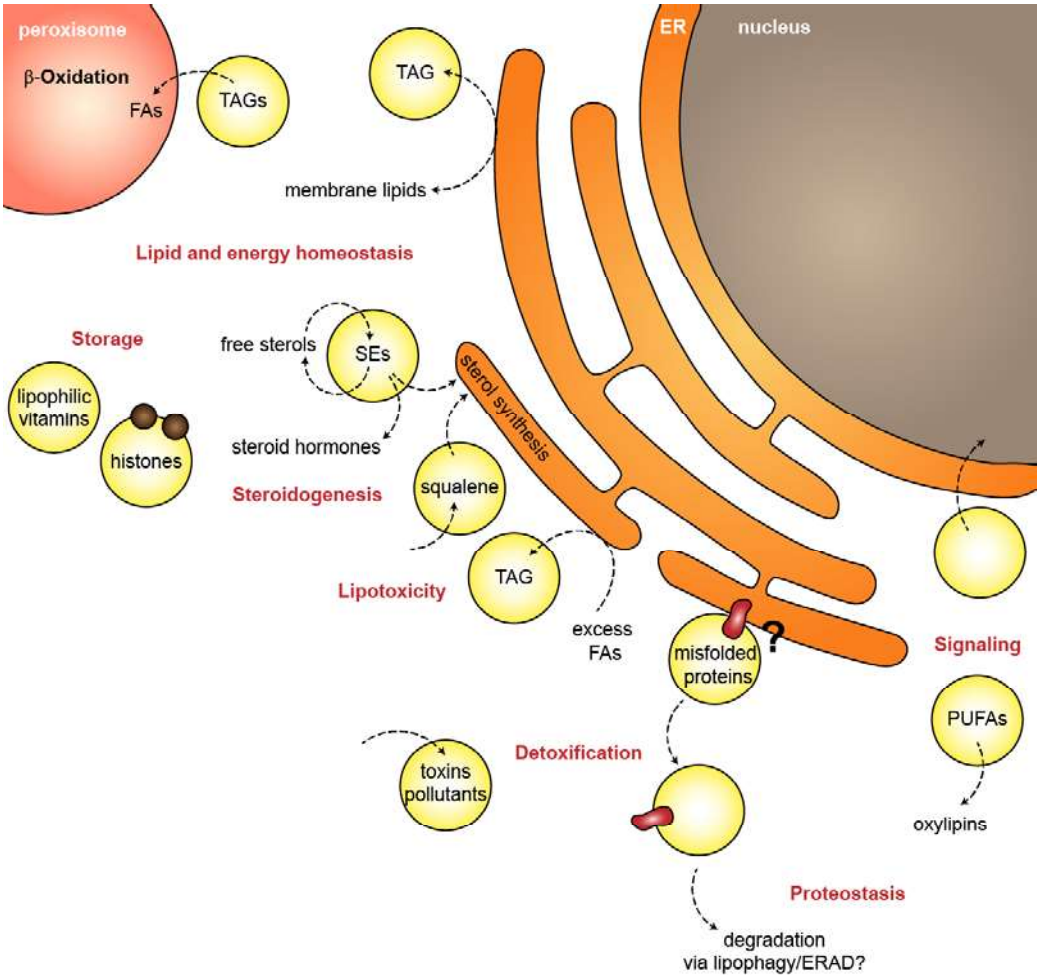

Figure 5: Overview of varying LD functions from different organisms. LDs have various, partly overlapping functions, a selection of which is depicted here. Processes LDs are involved in include energy homeostasis, stress responses, signalling and pathogen defence. The best known function of LDs is the storage and provision of energy in form of TAG. By transitory storing and providing FAs as required, LDs actively participate in cellular and organellar lipid homeostasis. LDs might also be involved in homeostasis of free sterol levels in membranes and provide enzymes and precursors for sterol synthesis and steroid hormone synthesis. Other LD-stored components include e.g. lipophilic vitamins, but also proteins, as e.g. histones, can be stored on LDs. Another important function of LDs is detoxification. Not only excess and toxic lipids, but also other lipophilic toxins and pollutants can be detoxified by buffering and storing them away. It was also suggested that LDs are involved in detoxification of misfolded proteins from the ER by transferring them to the vacuole via lipophagy, putatively also with an involvement of ERAD, however this function was questioned. Lastly, LDs provide precursors as well as enzymes for the synthesis of lipid-derived oxylipins. They have also been implicated in direct LD to nucleus signalling, influencing gene regulation. Reviewed in Welte and Gould, 2017; Nguyen and Olzmann, 2017; Thiam and Dugail, 2019; Olzmann and Carvalho, 2019; Ischebeck *et al.*, 2020).

1.2 Membrane Contact sites (MCS)

Membrane contact sites (MCS) present a topic of increasing interest. MCS are transient physical contacts between organelles without fusion of their membranes. They are established through proteins that span the usually 10-30 nm between the interacting organelles and pose an alternative, non-vesicular route for the exchange of molecules or signals (mostly Ca^{2+}, ROS or lipid signals) through the cytosol. Moreover, they are involved in autophagy and plasmodesmata formation, as well as plant virus infection via plasmodesmata. Also, they have been implicated in lipid metabolism, stress response and organelle trafficking and biogenesis (reviewed in Prinz *et al.*, 2020; Prinz, 2014). Although initially believed to only occur between the ER and the PM or the ER and mitochondria, the last decades showed that MCS occur ubiquitously between all organelles in the cell (Eisenberg-Bord *et al.*, 2016; Valm *et al.*, 2017; Scorrano *et al.*, 2019; Baillie *et al.*, 2020; Prinz *et al.*, 2020; Rossini *et al.*, 2020).

1.2.1 Functions of MCS

MCS function in connecting two organelles, thereby allowing for molecular exchange. With their role in interorganellar transport of molecules such as lipids or Ca^{2+}, they are e.g. involved in signalling and metabolic channelling, thereby also regulating membrane dynamics and homeostasis. By tethering organelles they are also involved in e.g. organelle trafficking (reviewed in Prinz *et al.*, 2020). As is true for LD research, also MCS research in the last years in great parts focused on mammals and yeast, while plant MCS research is lagging behind. To understand the impact of MCS on trafficking or signalling mechanisms, again also some non-plant MCS functions will be highlighted here.

Lipid transport

Molecular mechanisms of lipid transport at MCS are not fully understood and the functions of non-vesicular transport, as opposed to vesicular transport, in general are not entirely clear. Organelles that are not part of the secretory pathway, thus not receiving vesicles, must receive lipids in a vesicle-independent way (reviewed in Wong *et al.*, 2019). Also, loss of the secretory pathway for bulk transport of lipids can obviously be compensated by cells, as genetic or chemical inhibition of vesicle transport has little effect on lipid transfer capacity (Vance *et al.*, 1991; Baumann *et al.*, 2005). There are hints from yeast and mammals that an ER-Golgi tether-mediated transport of ceramides between the ER and the Golgi is upregulated, when vesicular transport is inhibited. These data suggest that non-vesicular transport can overtake transport functions when vesicle transport is impaired (Funato and Riezman, 2001; Hanada *et al.*, 2003; Liu *et al.*, 2017; Prinz *et al.*, 2020). Moreover, non-vesicular lipid trafficking was proposed to be faster than vesicular trafficking, enabling rapid adaptations of membrane lipid compositions to adjust for changing environmental conditions such as heat or cold stress. Another advantage

of lipid transfer via MCS might be that in contrast to vesicular trafficking, no proteins are carried along with the lipids (reviewed in Wong *et al.*, 2019).

Mostly, lipid transfer at MCS occurs via lipid transfer proteins (LTPs). LTPs are found in all species and all of the identified LTPs have a common feature: they provide a hydrophobic environment that allows for the transport of lipids (reviewed in Wong *et al.*, 2019). Often (but not exclusively), LTPs localise to MCS, e.g. through binding other MCS-localised proteins such as VESICLE ASSOCIATED PROTEINs (VAPs, reviewed in Wong *et al.*, 2019; Prinz *et al.*, 2020). Most LTPs form a cavity and move lipids, one by one, from the donor to the acceptor compartment. Sometimes, one lipid species is exchanged for another (reviewed in Wong *et al.*, 2019). This is also called 'counter transport' and often occurs when lipids are transported against a gradient: LTPs, such as oxysterol-binding proteins, then often use phosphatidylinositol 4-phosphates (PI4P) concentration differences between two membranes to drive the transport of another lipid (reviewed in Prinz *et al.*, 2020). Interestingly, the large group of non-specific LTPs, which occur only in land plants but not in algae or any other species, have been suggested to be key proteins in the conquest of terrestrial habitats (reviewed in Edqvist *et al.*, 2018).

An example for lipid transport at MCS is the transport of phosphatidylserine (PS) from the ER (where it is synthesised) to mitochondria (where it is e.g. needed to maintain proper PE levels) via MCS in yeast, channelling of which is driven by its own production (Kannan *et al.*, 2017). The transport of lipids to mitochondria is especially important for mitochondrial membrane synthesis and signalling, as lipid exchange with mitochondria occurs mostly non-vesicular. In addition, transport from outer to inner mitochondrial membranes occurs via MCS, in plants for example via TIM, TOM or MICOS complexes (reviewed in Michaud *et al.*, 2017). Another example are ceramides, which are produced at the ER and are transported to the Golgi for further sphingolipid synthesis via a ceramide transport protein (CERT)-mediated MCS in mammalian cells (Kumagai and Hanada, 2019). In plants, no CERT or CERT-like proteins have been identified, although also in plants, ceramides and sphingolipids in general have to be transported form the ER to other destinations (Hurlock *et al.*, 2014).

By their functions in lipid trafficking, MCS are also implicated in lipid signalling mechanisms, e.g. through transport of phosphatidylinositol (PI). PI is synthesised at the ER and a precursor for phosphoinositides, such as PI4Ps, which are lipid signalling molecules. Different kinases, not residing at the ER, convert PI to phosphoinositides and thus require transport of PI to the site of phosphoinositide synthesis. This transport is partly mediated via MCS (Dickson and Hille, 2019). Phosphorylation of PI or hydrolysis of phosphoinositides was also suggested to occur via a process called signalling '*in trans*'. Signalling *in trans* describes the action of an enzyme localised in one compartment on a substrate localised in another compartment and

presents a form of an MCS. In yeast, the ER-localised phosphoinositide phosphatase Sac1p might hydrolyse PM- or Golgi-localised PI4P to PI *in trans*, however this is still under debate (reviewed in Prinz *et al.*, 2020). In tomato, e.g. the PM-localised ACYL-COA:STEROL ACYLTRANSFERASE (*Sl*ASAT) was suggested to catalytically act *in trans* on its ER-embedded sterol substrate (Lara *et al.*, 2018). Signalling *in trans* can also occur lipid-independently, e.g. by the ER-localised protein tyrosine phosphatase 1b (PTP1b) that dephosphorylates PM- or endosome-localised receptor tyrosine kinases (RTKs) in mammals (reviewed in Haj *et al.*, 2012; Prinz *et al.*, 2020).

Metabolic Channelling and signalling of non-lipidic molecules

As described above, one important function of MCS in metabolite channelling is the channelling of lipids through the hydrophilic cytosol, but also other molecules are exchanged. MCS also facilitate the efficient vesicle-independent transport of Ca^{2+}. The entry of Ca^{2+} through the PM into the cell for example requires a MCS between the PM and the ER to allow for a direct flux of Ca^{2+} into the ER, without increasing cytosolic Ca^{2+} concentrations (reviewed in Prinz *et al.*, 2020). By transporting Ca^{2+}, MCS are again involved in signalling mechanisms: Ca^{2+} and ROS signalling often occur at ER-mitochondria MCS. In mammals for example, a protein tether between the ER and mitochondria is formed by the mitochondrial localised voltage-dependent anion-selective channel protein (VDAC), the mitochondrial localised chaperone 75-kDa glucose-regulated (GRP75; also mitochondrial stress-70 protein) and the ER-localised inositol-1,4,5-trisphosphate receptors (IP3Rs). This complex influences e.g. cell death signalling (Szabadkai *et al.*, 2006). Generally, there is a close interplay of Ca^{2+} and ROS signalling at ER-mitochondria contacts, as e.g. Ca^{2+}-induced ROS mobilisation from mitochondrial cristae in human cell cultures creates dynamic H_2O_2 nanodomains at the ER-mitochondrion interface that in turn regulate Ca^{2+} channels (Booth *et al.*, 2016). This way, MCS can also influence ROS signalling.

Apart from Ca^{2+} and lipids, other small molecules can probably also be exchanged at MCS, e.g. iron, that is directly transferred between mitochondria and endosomes in erythroid cells. MCS might even enable the direct exchange of metabolites between enzymes, thereby increasing reaction rates and also preventing intermediates from being channelled to other metabolic pathways (reviewed in Prinz *et al.*, 2020).

Regulation of organellar membrane dynamics

Another important function of MCS is the regulation of organellar membrane dynamics. MCS play a role in organelle fission and fusion, autophagosome formation, diffusion barriers, endosomal cargo sorting, organelle trafficking and positioning, and organelle subpopulations (reviewed in Prinz *et al.*, 2020).

Of special interest for the present thesis is the proposed function of MCS in organelle trafficking and positioning, as well as in the establishment of organelle subpopulations. One way MCS can influence organelle trafficking is when an organelle hitchhikes another organelle that is transported in a motor-based way. This hitchhiking is made possible by MCS that connect the two organelles. Peroxisomes in *Aspergillus nidulans* hitchhike early endosomes this way to reach their proper cellular destination (Salogiannis *et al.*, 2016). On the other hand, vesicles can be prevented from being transported through the cell by anchoring them to immobile organelles via MCS (Jongsma *et al.*, 2016; Prinz *et al.*, 2020). Some MCS proteins can switch between anchoring an organelle to another organelle or to motor proteins. The human cholesterol sensor ORP1L for example connects endosomes and dynactin motor complexes when cholesterol levels are sufficient. When cholesterol levels decrease, ORP1L releases dynactin and starts to interact with ER-localised VAPs, anchoring endosomes to the ER instead (reviewed in Prinz *et al.*, 2020).

In budding yeast cells, another implication of MCS in organelle trafficking can be observed. Here, MCS are involved in the inheritance of organelles from mother to daughter cells. Peroxisomes in budding yeast divide asymmetrically, creating a peroxisome subpopulation containing an ER-anchor and a subpopulation lacking the anchor. Peroxisomes lacking the anchor are transferred to daughter cells during budding. Peroxisomes containing the anchor are retained in the mother cell by forming an MCS with the ER, thereby ensuring stable peroxisome transfer over generations (Knoblach *et al.*, 2013). A similar mechanism is observed for LDs: a subset is transferred to daughter cells while another subset is retained at the perinuclear ER through an MCS (Knoblach and Rachubinski, 2015). Likewise, inheritance of mitochondria in budding yeast is regulated by at least three different tethers with the PM and ER (reviewed in Prinz *et al.*, 2020).

Lastly, MCS can also create subpopulations of organelles: functionally distinct subpopulations of organelles can form contacts with other membranes. However, this has so far only been described for functionally distinct LDs that are in contact with certain ER subdomains in yeast and functionally distinct mitochondria in contact with LDs in mammalian brown adipose tissue (reviewed in Prinz *et al.*, 2020).

1.2.2 Specialised plant MCS

Many MCS are conserved among eukaryotes, but generally data on plant MCS is scarce. However, some known MCS are specific to plants. Among the plant-specific MCS, there are stress-inducible MCS formed e.g. by stromules or plasmodesmata (PD), which pose a special form of MCS allowing for intercellular communication (reviewed in Pérez-Sancho *et al.*, 2016).

Chloroplast and stress-inducible MCS

As plastids are unique features of plants and algae (reviewed in Sadali *et al.*, 2019), MCS between plastids, such as the chloroplast, and other organelles are unique to these species. The transport of lipids from the ER to plastids is believed to be facilitated by non-vesicular transport and ER-plastid MCS have indeed been microscopically observed (reviewed in Michaud and Jouhet, 2019). The part of the ER that is in close association to plastids is characterised by a specific lipid and protein composition – it for example contains PC synthase activity. PC is the main precursor of plastidial galactoglycerolipids, such as monogalactosyldiacylglycerol (MGDG) or digalactosyldiacylglycerol (DGDG), both of which are synthesised in the plastid envelope (Benning, 2008). MGDG synthase 1 (MGD1) in the inner envelope uses PC-derived DAG as substrate for MGDG synthesis, however it is not resolved yet which lipid is transferred from the ER to the plastid. PC, lyso-PC, PA and/or DAG have been proposed as candidates, evidence for all three are reviewed and discussed in Michaud and Jouhet (2019). What is more, plastids are able to grow stroma-filled protrusions, called stromules, which can interact with other organelles such as the ER, the nucleus or the PM. These stromules are stress-inducible and it is believed that stress-induced stromules establish contact sites e.g. with the nucleus to directly transfer plastidial proteins and chloroplast-localised transcription factors (reviewed in Pérez-Sancho *et al.*, 2016). Likewise, also peroxisomes are able to grow protrusions, called peroxules. Peroxules, too, are inducible by changing redox-status and aid in detoxifying ROS. They can form contacts with chloroplasts or mitochondria and also tri-organellar contacts of these organelles have been observed after high light stress (reviewed in Pérez-Sancho *et al.*, 2016). Furthermore, peroxules can form contacts with LDs for TAG breakdown, which will be described in section 1.2.3. Stress-induced protrusions that form contacts with plastids can also be produced by mitochondria. DGDG was shown to be relocated from plastid membranes to mitochondrial membranes upon phosphate starvation, putatively via a large mitochondrial transmembrane lipoprotein complex (MTL) (reviewed in Pérez-Sancho *et al.*, 2016).

Plasmodesmata

Another example for unique plant MCS are plasmodesmata (PD). PD are specialised ER-PM contact sites only occurring in plants (reviewed in Pérez-Sancho *et al.*, 2016). PDs are cytoplasmic pores connecting neighbouring cells through the cell wall and are important for intercellular signalling and molecule exchange. Both the PM and the ER run through PDs forming membrane tubules. Intriguingly, along the PD's whole length, the ER is in contact with the PM through unidentified proteinaceous elements (Ding *et al.*, 1992; Pérez-Sancho *et al.*, 2016). In Arabidopsis, the two proteins SYNAPTOTAGMIN 1 (SYT1) and VAP27-1, that are involved in a ER-PM MCS, have been identified in PD, though, and are putative tethering candidates (Levy *et al.*, 2015; Wang *et al.*, 2016; Levy and Tilsner, 2020).

Generally, research on plant MCS is still in its infancy. It is expected that within the next years, basic questions on plant MCS will be tackled and also e.g. the influence of MCS on delivering lipidic cell wall components or release of vacuolar content to the apoplast will be elucidated (reviewed in Pérez-Sancho *et al.*, 2016). A recent overview of identified plant MCS can be found in Baillie *et al.* (2020).

1.2.3 MCS of LDs

Several recent reviews focus on MCS between LDs and other organelles (reviewed in Barbosa, Savage, *et al.*, 2015; Barbosa and Siniossoglou, 2017; Schuldiner and Bohnert, 2017; Thiam and Dugail, 2019; Bohnert, 2019; Bohnert, 2020). It is well established that LDs engage in contact sites with nearly all other organelles. However, focus of these reviews is mostly put on yeast or animals, whereas data on plant LD-MCS (as is true for plant MCS in general) is scarce. To date, only LD-peroxisome and LD-ER contact sites have been described in plants. It is likely however, that LDs in plants, too, interact with many more organelles. An overview of the described MCS, putatively also occurring in plants, is shown in Figure 6.

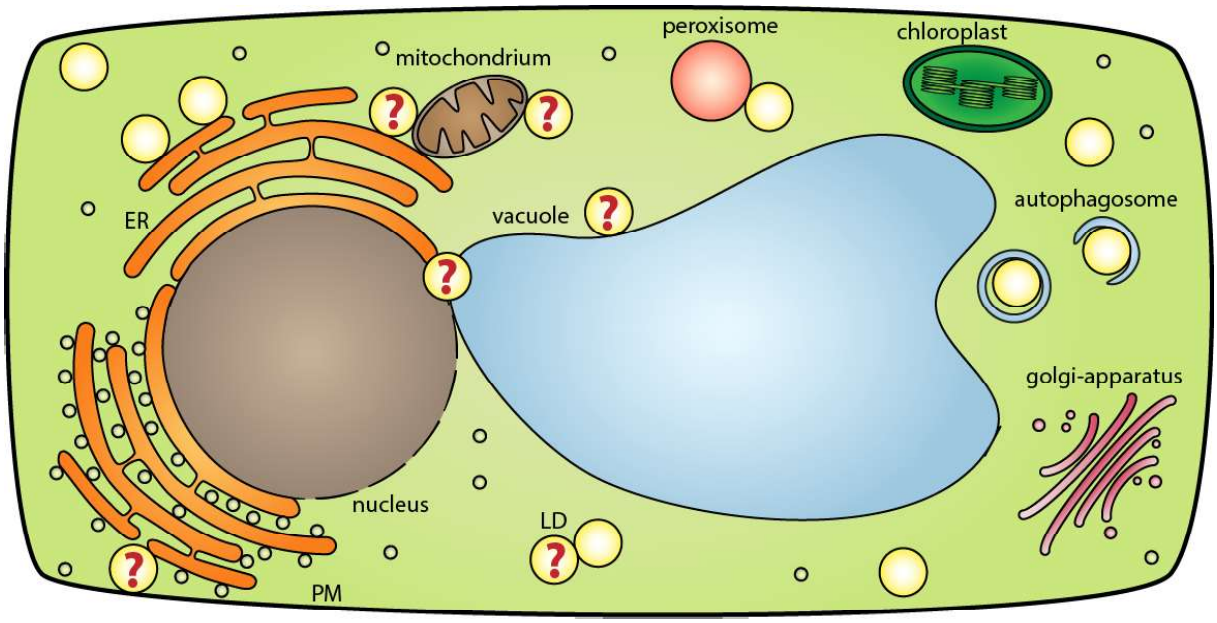

Figure 6: Depiction of confirmed and putative LD contact sites in plants. Plant LDs are believed to be in contact with most other cellular compartments. However, so far, only LD-ER and LD-peroxisome MCS have been characterised on the molecular level. From what is known in mammals and yeast, connections of LDs with the vacuole, mitochondria, the nucleus, the PM and other LDs are likely, have however not been experimentally validated or characterised so far.

LD-ER

LD-ER contact sites have extensively been reviewed by Hugenroth and Bohnert (2020) and are probably one of the best described LD contacts – and a contact that has also been described in plants. The number of proteins known to be involved in LD-ER contacts is

constantly increasing (Gross *et al.*, 2011; Cai *et al.*, 2015; Grippa *et al.*, 2015; Xu *et al.*, 2018; Hariri *et al.*, 2019; Ugrankar *et al.*, 2019; Greer *et al.*, 2020).

Apart from the already mentioned Seipins, which are involved in LD biogenesis at LD-ER contact sites, several other proteins have been described, e.g. yeast Mdm1 (human Snx14) (Hariri *et al.*, 2019; Datta *et al.*, 2019) or the mammalian SNARE-interacting Rab18 (Xu *et al.*, 2018). Mdm1, an ER-anchored protein that was originally discovered as a tether for nucleus-vacuole-junctions, is also involved in the biogenesis of LDs (Henne *et al.*, 2015; Hariri *et al.*, 2018; Hariri *et al.*, 2019). Mdm1 likely facilitates a tri-organellar connection between the ER, the vacuole and LDs. As for many LD proteins, Mdm1/Snx14 does not have any sequence homologues in plants. Described plant LD-ER tethers are limited to Seipins and their interactor VAP27-1, which are important for LD biogenesis and proliferation (Cai *et al.*, 2015; Greer *et al.*, 2020).

Generally, LD-ER contacts present a special case of MCS and not only true protein-mediated MCS are found. LDs are connected to the ER via lipidic bridges of the LD phospholipid monolayer and the outer ER membrane leaflet during their formation. Yeast LDs have been described to permanently stay connected to the ER, but the extent of this connection in other organisms is less clear (reviewed in Hugenroth and Bohnert, 2020). It is known, however, that LDs can also re-attach to the ER, likely in a COP I-dependent manner (Thiam *et al.*, 2013; Wilfling *et al.*, 2014; Hugenroth and Bohnert, 2020). The lipidic continuities are unique to LD contacts and do not necessarily meet the criteria for a true MCS, since membranes are fused. Per definition, true MCS differ from other organelle contacts in that physical integrity of both organelles is sustained (in contrast to e.g. vesicle fusion, which ultimately results in disintegration of the vesicle and mixing of contents). The connection of the monolayer-bound LD with the outer leaflet of the bilayer-bound ER is thus a special case, as membranes fuse, but content mixing of the organelles cannot occur when a monolayer fuses with a bilayer. (reviewed in Hugenroth and Bohnert, 2020).

The functions of the different LD-ER contact sites, apart from the obvious function in LD biogenesis and lipid exchange is protein exchange. Some proteins exhibiting a hydrophobic hairpin/helix topology, are able to insert into bi- or monolayers and can be exchanged between LDs and ER via the lipidic bridges, as was e.g. shown for GPAT4 (Wilfling *et al.*, 2013; Kory *et al.*, 2016). How this process is regulated remains to be elucidated.

LD-peroxisome

Contacts between LDs and peroxisomes have long been described and are, regarding peroxisomes' central roles in lipid metabolism, not surprising (Schrader, 2001; Binns *et al.*, 2006; Valm *et al.*, 2017). Molecular tethering machineries however long remained unknown (reviewed in Bohnert, 2020).

In plants and yeast, the peroxisome is considered the major site of β-oxidation (reviewed in Poirier *et al.*, 2006), while in mammals most β-oxidation takes place in mitochondria and only very-long-chain fatty acids and branched fatty acids are degraded in peroxisomes (reviewed in Olzmann and Carvalho, 2019). Concomitantly, there are also striking differences in the formation of MCS between LDs and peroxisomes in animals, plants and yeast. Contact sites in plants are established by the already mentioned peroxules, tubular protrusions from the peroxisome that wrap around the LD. Yeast cells form so called pexopodia, which are subdomains of peroxisomes specialised in β-oxidation that penetrate into LDs. Animal peroxisomes do not form peroxules or pexopodia but instead the LD membrane probably grows a tubule (reviewed in Esnay *et al.*, 2020).

In plants, SDP1 catalyses the hydrolysis of TAG and releases FAs that can be transported to peroxisomes (Eastmond, 2006). The lipase is described to be delivered to LDs (in a not entirely understood process) by growing peroxules, requiring the activity of VPS29, a core component of the retromer protein complex (Thazar-Poulot *et al.*, 2015). True localisation of SDP1 during this process is unclear and while it might be delivered to LDs, it might also stay on the peroxule and establish the MCS from there. In any case, access of SDP1 to TAG and subsequent transport of FAs to peroxisomes via the peroxisomal membrane-bound ATP-binding cassette (ABC) transporter PXA1 (also called PED3) is enabled (Thazar-Poulot *et al.*, 2015). In the peroxisome, FAs are then degraded by β-oxidation and fed into the glyoxylate cycle to fuel e.g. sucrose production (reviewed in Michaud and Jouhet, 2019; Esnay *et al.*, 2020). Knockout of *SDP1* increases physical interaction between peroxisomes and LDs, this effect can be counteracted by exogenous application of sucrose. Genetic blocking of β-oxidation has the same effect, suggesting that LDs and peroxisomes disengage in a sucrose-dependant manner (Cui *et al.*, 2016). Proteins directly involved in the formation of the contact site have not yet been identified. It was however suggested, that PXA1, that contains a putative VAP-interacting FFAT-like motif, might form a tethering complex with VAPs (Mikitova and Levine, 2012; Esnay *et al.*, 2020). As already touched upon in previous sections, VAPs are proteins engaging in contacts of the ER with other cellular components such as vesicles or the PM (Wang *et al.*, 2016; Siao *et al.*, 2016; Stefano *et al.*, 2018; Greer *et al.*, 2020). They are ER-localised, tail-anchored proteins and characterised by a major sperm domain that interacts with FFAT-motifs. In mammals, VAPs are often described to stabilise MCS, especially those involved in lipid transfer (reviewed in Esnay *et al.*, 2020). Based on the major sperm domain, the Arabidopsis genome harbours 10 VAP isoforms, VAP27-1 to 27-10, most of which remain uncharacterised. VAP27-1, VAP27-3 and VAP27-4 in Arabidopsis have been described to localise to PM-ER contacts (Wang *et al.*, 2016); VAP 27-1 is also involved in LD-ER tethering (Greer *et al.*, 2020). Taken these data together, it was therefore suggested – although direct evidence is lacking –

that VAPs might also play a role in LD-peroxisome contacts in plants (reviewed in Esnay *et al.*, 2020).

Interestingly, studies on budding yeast found that LD biogenesis and biogenesis of pre-peroxisomal vesicles occur at the same ER subdomains, including cooperation of Seipin and PEX30, and authors proposed a correlation between LD and peroxisome biogenesis (Joshi *et al.*, 2018; Wang *et al.*, 2018).

LD-mitochondria

As is true for LD-peroxisome contacts, LD-mitochondria contacts also serve in the direct handover of fatty acids for energy release, as mammalian β-oxidation takes place predominantly in mitochondria (reviewed in Olzmann and Carvalho, 2019). Contacts of mitochondria and LDs in mammals increase upon nutrient deprivation, as is expected for using the stored energy reserves (reviewed in Bohnert, 2020). Contrarily, a study on an LD-bound subpopulation of mitochondria in brown adipose tissue found reduced β-oxidation rates and increased ATP synthesis, and this ATP was suggested to fuel FA activation that is needed prior to TAG synthesis (Benador *et al.*, 2018). As already described in the section on LD functions (see 1.1.3), mitochondria-LD contacts were shown to protect mitochondria from lipotoxicity by accumulating acylcarnitines after autophagy-derived bulk lipid release (Nguyen and Olzmann, 2017). Recently, also a tri-organellar contact site between mitochondria, LDs and the ER in white adipose tissue was described. Mitoguardian 2 (MIGA2) is anchored in the mitochondrial outer membrane via its N-terminal transmembrane segments and associates to LDs via a C-terminal amphipathic helix. It also contains a FFAT-motif in its middle domain, interacting with ER-localised VAPs, thereby connecting the three organelles (Freyre *et al.*, 2019). Overexpression of MIGA2 results in increased contacts between mitochondria and LDs as well as mitochondria and the ER, and knockout of MIGA2 causes defects in TAG synthesis and LD expansion. Knockout also renders cells unable to convert glucose to TAG (Freyre *et al.*, 2019).

Other candidates for mediating LD-mitochondria contacts in mammals are LD-localised PLINs, e.g. PLIN5. The C-terminus of PLIN5 was shown to recruit mitochondria in mammals (Wang *et al.*, 2011). Another described mammalian MCS is mediated by LD-localised PLIN1 and mitochondrial mitofusin 2 (MFN2) (reviewed in Olzmann and Carvalho, 2019). As mentioned, plant genomes do not harbour sequence homologues of *PLINs*. Overall, MCS of mitochondria with other organelles are well described in yeast and mammals, but information on plant mitochondria-MCS in general and mitochondria-LD contacts in specific are scarce (reviewed in Michaud *et al.*, 2017). Contacts are likely, though, as also yeast mitochondria, which in contrast to mammalian mitochondria do not perform β-oxidation, were found in contact with LDs (Shai *et al.*, 2018). Some proteomic analyses on plant LD proteins also suggested

connections of LDs and mitochondria, based on co-purified mitochondrial proteins in LD-fractions (Zhi *et al.*, 2017; Hamada *et al.*, 2020).

In conclusion, LD-mitochondrial contacts can serve as sites for lipogenesis (as a mean of detoxification) as well as lipolysis (for energy supply), according to tissue type and environmental conditions (Olzmann and Carvalho, 2019; Bohnert, 2020).

LD-vacuole

Contacts of LDs and the vacuole in yeast (or LDs and lysosomes in mammals) have been well described, especially regarding their role in lipophagy. LDs can be degraded via two pathways: lipolysis, involving lipases, or lipophagy, involving the degradation of LDs in the vacuole (or lysosomes). For lipophagy, again two distinctions exist: microlipophagy, describing the direct, autophagosome-independent engulfment of LDs into invaginations of the vacuole or lysosome lumen; and macrolipophagy, describing the uptake of LDs into double membrane-bound autophagosomes and subsequent delivery to the vacuole (reviewed in Huang *et al.*, 2019). All of the described processes likely require the presence of MCS. In yeast, proteins of the highly conserved endosomal sorting complexes required for transport (ESCRT) machinery have been shown to be involved in LD turnover during microlipophagy, independently of the core autophagy-related gene (ATG) proteins (Oku *et al.*, 2017). It was suggested that the ESCRT machinery induces the invagination of LDs during microlipophagy (reviewed in Huang *et al.*, 2019). Arabidopsis ESCRT homologues are known to play a role in regulating autophagosome-vacuole fusion and also vacuole biogenesis, however their direct role in LD turnover and in LD-MCS in plants remains unclear (reviewed in Huang *et al.*, 2019). In a study on dark-induced starvation in Arabidopsis leaves, LDs were reported to be found inside the vacuole and a lipophagic mechanism morphologically resembling microlipophagy was proposed (Fan *et al.*, 2019). Tonoplast-surrounded LDs have also been observed during germination in Arabidopsis and here, too, an internalisation into the vacuole was suggested (Poxleitner *et al.*, 2006). Data are however not conclusive as to whether LDs are truly completely internalised or just appear so in 2D images and are actually just pushed into the vacuole from several sides.

In yeast, also the existence of a tri-organellar LD-ER-vacuole tether mediated by Mdm1 has been reported. It promotes locally confined LD biogenesis at the nucleus-vacuole junctions (NVJ), a well-studied yeast MCS, at the beginning of yeast stationary growth phases (Hariri *et al.*, 2019). For this, also the yeast LD organisation (Ldo) machinery is needed, which is also known to interact with Seipin (Teixeira *et al.*, 2018; Eisenberg-Bord *et al.*, 2018; reviewed in Bohnert, 2020). Interestingly, upon progression into the late stationary growth phase, LDs in yeast move from NVJs to the vacuole surface, where they stay in contact with the vacuole membrane until they are taken up for degradation via microlipophagy. Concomitantly to LD movement across the vacuole membrane, liquid-ordered membrane domains rich in sterols

develop in the vacuole membrane. LDs were shown to be attached to these sterol-rich membrane domains and also are needed for formation of these domains, so that a mutual correlation was suggested. Proteins involved in this tether are to date unknown and it is also unknown if these contacts serve a physiological function except microlipophagy (reviewed in Olzmann and Carvalho, 2019; Bohnert, 2020).

LD-LD

MCS can also occur between LDs themselves. In mammals, these contacts are mediated by the cell death-inducing DFFA-like effector (CIDE) proteins CIDEA, CIDEB and CIDEC (also called fat-specific protein 27, FSP27), which form trans-organelle oligomers. Through this mechanism, LDs can fuse and thus grow (Gao *et al.*, 2017). By forming oligomers, CIDE proteins establish a pore through which TAGs – but not proteins – can be exchanged, always from the smaller to the larger LD (Gong *et al.*, 2011; Jambunathan *et al.*, 2011). To date, it is not known what happens to remaining proteins and phospholipids, as the smaller LD shrinks during fusion (Olzmann and Carvalho, 2019). It is however believed that the contacts serve additional functions, apart from complete LD fusion, like e.g. modulating accessibility of cytosolic lipases to stored TAGs by altering surface-to-volume ratios (Schuldiner and Bohnert, 2017; Olzmann and Carvalho, 2019). Depletion or knockout of CIDE leads to accumulation of numerous small LDs, however LD-LD contacts are still observed, indicating that additional LD-LD tethers exist (reviewed in Olzmann and Carvalho, 2019).

In plants, as in any other clade except vertebrates, again no sequence homologues of CIDE proteins are found. A study however tested stable ectopic expression of mouse FSP27 (CIDEC) in Arabidopsis and found that it does stably localise to LDs and accumulate at LD-LD contact sites. Also, number and size of LDs as well as LD fusion and clustering were increased, indicating that expression of CIDEC alone is sufficient to induce LD-LD contacts, also in non-native species (Price *et al.*, 2020). Moreover, fusion of LDs *in vivo* does occur in plants, as is e.g. observable during germination (Miquel *et al.*, 2014; Kretzschmar *et al.*, 2018), however it is not clear if this is a passive process where LDs without protein coat coalesce and fuse or whether it is actively protein-mediated.

Apart from CIDE protein, little is known about tethering machineries connecting LDs and it remains to be verified, if these contacts exist without ultimately resulting in complete LD fusion (which would per definition not be a true MCS) (reviewed in Schuldiner and Bohnert, 2017).

1.3 Aims

LDs barely received attention of cell biologists for the first decades after their discovery. Consequently, not only knowledge on detailed mechanisms of LD biology is lacking, but also basic questions are still not resolved, including fundamental processes like biogenesis, degradation, interactions with other organelles or protein targeting. The overall aim of this work was to contribute to a general understanding of LDs and processes they are involved in. Two projects were pursued: (i) Identification and functional characterisation of a family of so far unknown LD-associated proteins in the model plant *Arabidopsis thaliana* and (ii) elucidation of the role of LDs in heat stress adaptation of *Nicotiana tabacum* pollen tubes.

A prerequisite for the first part was to confirm the LD-localisation of candidate proteins from an already existing proteome screen. For this, fluorophore-tagged protein candidates were cloned, transiently transformed into *Nicotiana tabacum* pollen tubes and protein localisation determined via confocal laser scanning microscopy. The verification of two homologous LD-associated proteins, SLDP1 and SLDP2, led to their molecular characterisation *in planta*. This was based on cell biology and proteome analyses of transient expression and/or mutant lines obtained through forward genetics (T-DNA insertion, CRISPR/Cas9). Loss of SLDP1 and SLDP2 revealed a putative interaction partner, LIPA, which was likewise investigated to ultimately unravel potential recruitment mechanisms between the proteins in question, LDs and other cellular compartments.

For the second part, a more functional approach was chosen. Pollen and pollen tubes are tissues very sensitive to abiotic stresses such as heat or drought stress and naturally harbour many LDs. Three major objectives aimed at elucidating the involvement of LDs in heat-induced lipid remodelling and thermotolerance in pollen tubes. A lipidome analysis by LC-MS/MS and GC-MS of heat stressed pollen tubes in comparison to non-stressed tubes was performed to establish a potential role of LDs as sink for unsaturated fatty acids and/or hub for fatty acid shuffling. A complementary transcriptome analysis was conducted to understand heat stress adaptation in pollen tubes and support a predicted involvement of LDs. Lastly, changes in central metabolites were analysed by GC-MS to obtain a more complete picture of the pollen tube response to high temperatures.

2 Article I: Lipid droplets in plants and algae: Distribution, formation, turnover and function

This review was published online in the journal Seminars in Cell and Developmental Biology in February 2020. The full article can also be found online:

https://doi.org/ 10.1016/j.semcdb.2020.02.014

Author contribution

H. E. Krawczyk wrote a paragraph for chapter 2. She concepted and created the figures. and critically read and revised the manuscript.

Seminars in Cell and Developmental Biology xxx (xxxx) xxx–xxx

Contents lists available at ScienceDirect

Seminars in Cell & Developmental Biology

journal homepage: www.elsevier.com/locate/semcdb

Lipid droplets in plants and algae: Distribution, formation, turnover and function

Till Ischebeck[a,*], Hannah E. Krawczyk[a], Robert T. Mullen[b], John M. Dyer[c], Kent D. Chapman[d]

[a] University of Göttingen, Albrecht-von-Haller-Institute for Plant Sciences and Göttingen Center for Molecular Biosciences (GZMB), Department of Plant Biochemistry, 37077, Göttingen, Germany
[b] University of Guelph, Department of Molecular Cell Biology, Guelph, Ontario, N1G 2W1, Canada
[c] United States Department of Agriculture, Agriculture Research Service, US Arid-Land Agricultural Research Center, Maricopa, AZ, 85138, USA
[d] University of North Texas, BioDiscovery Institute, Department of Biological Sciences, Denton, TX, 76203, USA

ARTICLE INFO

Keywords:
Lipid droplets
Plants
Arabidopsis
Algae
Triacylglycerol

ABSTRACT

Plant oils represent an energy-rich and carbon-dense group of hydrophobic compounds. These oils are not only of economic interest, but also play important, fundamental roles in plant and algal growth and development. The subcellular storage compartments of plant lipids, referred to as lipid droplets (LDs), have long been considered relatively inert oil vessels. However, research in the last decade has revealed that LDs play far more dynamic roles in plant biology than previously appreciated, including transient neutral lipid storage, membrane remodeling, lipid signaling, and stress responses. Here we discuss recent developments in the understanding of LD formation, turnover and function in land plants and algae.

1. Introduction

Lipid droplets (LDs) are spherical subcellular structures that occur in all eukaryotes, as well as some prokaryotes [1–4]. In eukaryotes, LDs are formed at the endoplasmic reticulum (ER) [3,5] and may detach into the cytoplasm or remain connected to the ER membrane. Regardless of the nature of their connection with the ER, LDs have highly unique lipid and protein compositions and have been associated with an increasing number of cellular functions [2,6–8]. Therefore, LDs are increasingly recognized as *bona fide* organelles rather than inert ER-derived storage particles.

In plants and algae, LDs have been historically referred to as lipid bodies, oil bodies, oleosomes or spherosomes. However, more recently, the plant community has adopted the term LD as used in the mammalian and yeast literature, taking into account that these fundamental hydrophobic compartments are evolutionarily conserved across eukaryotes [2]. In plants, there are also LDs formed inside plastids, called plastoglobuli, that are similar in their architecture to cytoplasmic LDs. These structures will not be discussed here, but have been described in detail elsewhere [9–12].

LDs are found throughout all photosynthetic organisms [2]. In land plants, they are generally observed in all cell types [8,13], but are especially prominent in certain organs, tissues and cell types, including the spores of mosses [4] and the seeds and pollen of vascular plants [14]. They are also highly abundant in the mesocarp tissues of oil palm fruits [15], olives, and avocado [16], as well as in tubers of yellow nutsedge [17]. In addition, many single-celled algae accumulate high amounts of neutral lipids and LDs, particularly during stress conditions [18–20].

2. Plant LD composition varies among plant species and within different cell types

In comparison to other organelles, LDs have a unique structure, as

Abbreviations: α-DOX, α-dioxygenase; ATG, autophagy-related protein; CDC48, cell division cycle 48; CLO, caleosin; CPK, Ca^{2+}-dependent protein kinase; DAG, 1,2-diacylglycerol; DGAT, diacylglycerol acyltransferase; ER, endoplasmic reticulum; ERAD, ER-associated protein degradation; 2-HOT, 2-hydroxy-octadecatrienoic acid; LACS, long-chain acyl-CoA synthetase; LD, lipid droplet; LDAP, LD-associated protein; LDIP, LDAP-interacting protein; LEC2, leafy cotyledon 2; MAG, monoacylglycerol; MLDP, major LD protein; OBL, oil body lipase; PA, phosphatidic acid; PC, phosphatidylcholine; PDAT, phospholipid:diacylglycerol acyltransferase; PE, phosphatidylethanolamine; PI, phosphatidylinositol; PS, phosphatidylserine; PUX, plant UBX domain-containing protein; PXA1, peroxisomal ABC-transporter 1; SDP1, sugar-dependent 1; TAG, triacylglycerol; UBA, ubiquitin-associated; UBX, ubiquitin regulatory X; WRI1, wrinkled 1

* Corresponding author at: Till Ischebeck, Department of Plant Biochemistry, Georg-August-Universität Göttingen, Justus-von-Liebig Weg 11, 37077, Göttingen, Germany.
E-mail address: tischeb@uni-goettingen.de (T. Ischebeck).

https://doi.org/10.1016/j.semcdb.2020.02.014
Received 15 November 2019; Received in revised form 28 January 2020; Accepted 29 February 2020

they are not composed of a phospholipid bilayer surrounding an aqueous compartment, but rather a monolayer that separates the hydrophobic core from the cytoplasm. Isolated LDs from seeds of several plant species such as rape, sesame and maize have a monolayer that contributes 1–2 % of the total lipid content and is composed primarily of phosphatidylcholine (PC, 41–64 % w/w), phosphatidylserine (PS, ~18-33 % w/w), phosphatidylethanolamine (PE, ~3-18 % w/w) and phosphatidylinositol (PI, ~7-21 % w/w) [21]. Similar ranges of phospholipid classes and proportions were reported for LDs isolated from cotton seeds [22].

The hydrophobic core of LDs in most plant species and cell types examined consists primarily of triacylglycerols (TAGs). These TAGs can vary considerably in fatty acid composition, including their position on the three stereo-specific carbons of the glycerol headgroup, as well as the number of carbon atoms and presence and position of double bonds in the fatty acyl chains. While the fatty acid composition of seed oils from most domesticated oilseed crops includes just five common fatty acids (i.e., palmitic, stearic, oleic, linoleic, and linolenic acids), the seeds of other plants are known to accumulate high amounts of so-called unusual fatty acids; examples include the hydroxylated fatty acids in castor bean (*Ricinus communis)* [23], cyclic fatty acids in cotton and the tree *Sterculia foetida* [24], and fatty acids containing conjugated double bonds in the tung tree Vernicia fordii [25]. In addition to TAGs, LDs may also contain sterol esters, including the esters of phytosterols and fatty acids, which contribute 0.3 % to the seed oil of Arabidopsis [26] and 24 % to the neutral lipids of tobacco pollen [27].

In some plant species, other types of hydrophobic compounds are found within LDs. These include carotenoids in algae [28], wax esters (esters of fatty acids and fatty alcohols) in seeds of jojoba (*Simmondsia chinensis*) [29], and polyterpene poly(cis-1,4-isoprene) in the latex of rubber-producing plants, such as the rubber tree (*Hevea brasiliensis*) [30] or dandelion (*Taraxacum brevicorniculatum*) [31]. The latter LDs containing polyisoprenes are referred to as rubber particles, and they share similarities to other cytoplasmic LDs based on their physical properties [30] and homology of some of their LD surface-associated or so-called LD ‘coat’ proteins [32,33]. However, rubber particles and cytoplasmic LDs differ in terms of the mechanisms underlying the biosynthesis of their hydrophobic storage molecules [34].

LDs in various organs of land-plant species appear to vary considerably in their protein composition, both on a qualitative and quantitative basis [35]. Oleosins, for example, are the most abundant LD coat proteins in seeds of many angiosperms, such as Arabidopsis, rapeseed, maize and rice, and gymnosperms, including pine [36]. Oleosins are also enriched in LDs in pollen [37,38] and the tapetum [39], but so far have not been detected in high abundance in LDs of most vegetative cell types [40]. Oleosin transcripts, however, are induced during desiccation in the grass *Oropetium thomaeum* [41], suggesting a common role for oleosins during seed development and the plant stress response to dehydration. Other LD protein families, including caleosins and steroleosins, are also commonly found in seed LD proteomes, but additional protein isoforms may be expressed in vegetative tissues [42]. Another prominent family of LD proteins are the LDAPs (LD-associated proteins), which appear to be among the most abundant coat proteins on LDs in vegetative cell types [32]. These proteins, along with the LDAP-interacting protein (LDIP), have been detected in seedlings [43], as well as in pollen tubes [38], and leaves [44].

Several LD proteins, including LDAPs and LDIP, are conserved among land plants, but obvious homologs are not found in the unicellular green alga *Chlamydomonas reinhardtii* or non-photosynthetic eukaryotes. For other LD proteins, like steroleosins, homologs exist not only in algae, but also in fungi and animals [2].

The LD proteome of unicellular algae is quite different from that of land plants [45]. *C. reinhardtii*, for example, has a homolog of oleosin [46], but this protein was not detected on LDs [47]. Instead, the main LD protein of *C. reinhardtii*, based on proteomic analysis, is MLDP (major LD protein) [48,49], a protein not found in land plants. However, more recent cell biology data suggest that this protein is not directly associated with LDs [47]. Nonetheless, MLDP was also identified as a major structural protein associated with LDs in other algae, such as *Lobosphaera incisa* [50] and *Chromochloris zofingiensis* [51]. And while no oleosin, steroleosin, caleosin or LDAP homologs were detected in the *L. incisa* genome [50], in *C. zofingiensis*, four of the five encoded caleosins were found in LD proteome fractions, and two of them were confirmed by microscopy to be localized to LDs. Hence, together with MLDP, caleosins are likely major structural LD proteins in the freshwater green alga [51]. Moreover, in *L. incisa*, a small protein of unknown function, as well as a highly abundant putative lipase, were confirmed to localize to LDs [50]. In *C. zonfingiensis*, a total of 163 proteins were discovered by proteomics to be associated to LDs, nine of which were confirmed by microscopy, including the two aforementioned caleosins, two lipases, and an L-gulonolactone oxidase that potentially catalyzes the conversion of L-gulono-1,4-lactone to ascorbic acid [51]. In the diatome *Phaeodactylum tricornutum* [52], 54 proteins were identified in LD-enriched fractions, but it remains to be elucidated which of these proteins are localized to LDs or play a role in LD function.

Despite recent efforts, the overall number of *bona fide* LD protein families in plants and algae is relatively meager (Table 1), but modern, bottom-up proteomics approaches, combined with cell-biological analyses, continue to increase their numbers [35,45]. Undoubtedly, these studies will further expand the inventory of LD proteins in plants and algae and continue to point to the variation in protein composition of LDs that reflects the differences in cellular and metabolic functions of this organelle across species, tissues and cell types.

3. TAG synthesis and LD biogenesis in plants is concerted and involves both plastids and the ER

The formation of LDs is closely linked to the synthesis of their hydrophobic (core) constituents. Therefore, an increase in TAG synthesis regularly leads to an increase in the number and/or size of LDs (reviewed by Vanhercke et al. [61]). In plants, fatty acids, the building blocks of TAGs, sterol esters and wax esters, are synthesized in the plastid stroma [62]. Briefly, during the initial synthesis by the fatty acid synthase complex, fatty acids are elongated up to 16 or 18 carbons in length [63]. The first double bond can be inserted at the Δ9 position while the fatty acyl chain is still connected to the acyl carrier protein. Further desaturations can take place in the plastid after incorporation of the monounsaturated fatty acid into galactolipids, or at the ER after export from the plastid and incorporation into PC. The synthesis of fatty acids in the plastids stands in contrast to other non-plant eukaryotes, where fatty acids are synthesized in the cytoplasm [64,65].

The synthesis of TAGs in plants has been best characterized in Arabidopsis, but probably is similar in most land plant species. In Arabidopsis, and as depicted in Fig. 1, TAG is predominantly synthesized by either DIACYLGLYCEROL ACYLTRANSFERASE 1 (DGAT1) or PHOSPHOLIPID:DIACYLGLYCEROL ACYLTRANSFERASE 1 (PDAT1) [66], which are localized in the ER [67,68]. While both enzymes use 1,2-diacylglycerol (DAG) as the acceptor of the third fatty acyl group, their acyl donors differ. In the case of DGAT1, the acyl donor is a fatty acyl-CoA, while for PDAT1, it is PC. There is a second, unrelated DGAT enzyme called DGAT2 that also contributes to TAG synthesis in plants and has been associated in several cases with the preferential incorporation of unusual fatty acids into TAG [69]. The DAG acceptor is predominantly formed by dephosphorylation of phosphatidic acid (PA) [70], which can be synthesized by the removal of the head group from a phospholipid such as PC by a phospholipase D. A more familiar means to generate PA is the *de novo* synthesis by the Kennedy pathway enzymes glycerol-3-phosphate acyltransferase and lysophosphatidic acid acyltransferase [67,71]. In addition, DAG can also be directly synthesized from membrane phospholipids by the action of phospholipases C

Table 1
Selection of LD proteins of vascular plants and the algae *C.reinhardtii* and *Nannochloropsis*.

Protein family	Function(s)[a]	Homologs in animals and/or fungi[b]	Reference[c]
Oleosin	Influences LD size; important for LD stability and freezing tolerance	No	[53]
Caleosin	Peroxygenase; involved in phytoalexin production	Fungi	[54]
Steroleosin	Possible role in brassinosteroid metabolism, but substrates and products unknown	Animals, Fungi	[55]
LD-associated protein (LDAP)	Involved in LD formation and turnover; induced by abiotic stress	No	[32]
LDAP-interacting protein (LDIP)	Influences LD number and size	No	[43]
Plant UBX domain-containing protein 10 (PUX10)	LD protein degradation	Animals, Fungi	[38] [56]
Cycloartenolsynthase	Phytosterol synthesis	Animals, Fungi (Lanosterol-synthase)	[38]
α-Dioxygenase	Phytoalexine production	Animals, Fungi	[57]
Oil body lipase	Volatile production in tomato; pollen tube growth in Arabidopsis	Fungi	[58]
Seed lipid droplet protein	Unknown	No	[59]
Lipid droplet protein in seeds	Unknown	No	[59]
Lipid droplet lipase	Unknown; homolog in yeast has lipase and sterol esterase activity	Fungi	[59]
Lipid droplet methyltransferase	Unknown; homologs in poppy are involved in alkaloid metabolism	Animals, Fungi	[59]
Major lipid droplet protein (MLDP)	Influences LD size in *C.reinhardtii*	No	[47]
LD surface protein	Influences LD size in *Nannochloropsis sp.*	No	[60]

[a] Protein functional annotation according to publications described in main text.
[b] Candidate homologs identified using the NCBI Blast search tool.
[c] Publication of first description of protein's association with LDs in plants/algae.

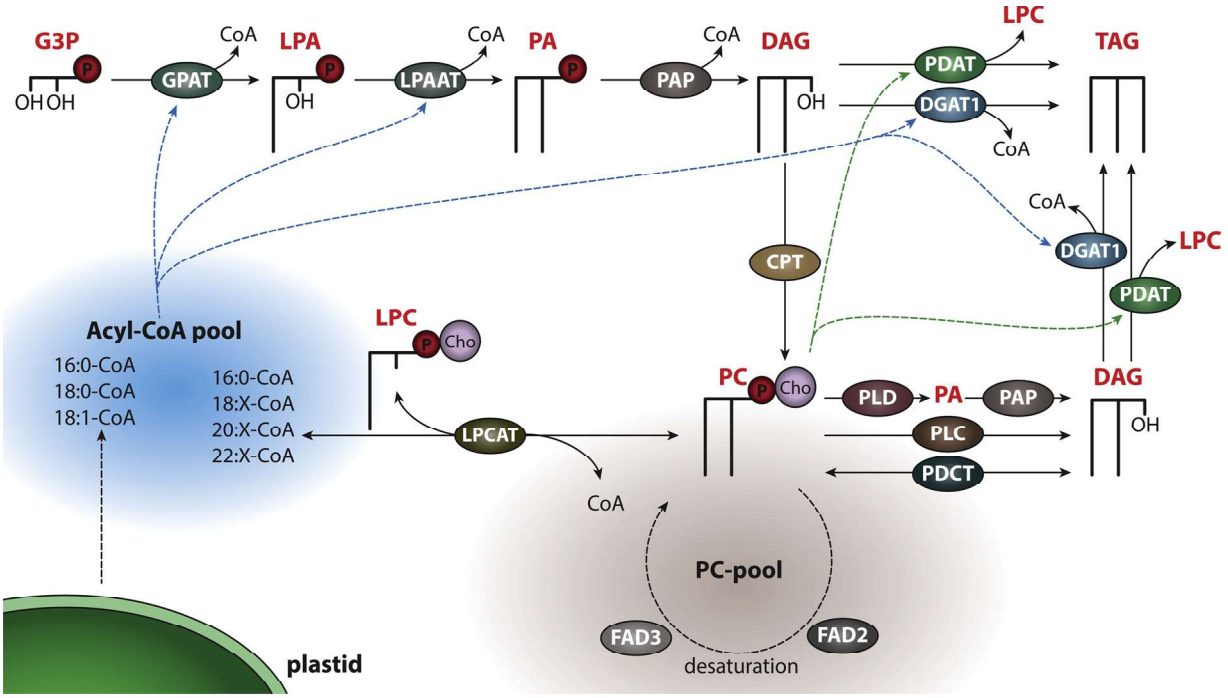

Fig. 1. Several pathways lead to the synthesis of TAG in Arabidopsis seeds. The final step in triacylglycerol (TAG) biosynthesis in Arabidopsis seeds is catalyzed primarily by overlapping functions of DIACYLGLYCEROL ACYLTRANSFERASE 1 (DGAT1) or PHOSPHOLIPID:DIACYLGLYCEROL ACYLTRANSFERASE 1 (PDAT1). Both enzymes transfer a fatty acyl chain to the *sn*-3 position of diacylglycerol (DAG), but DGAT1 uses acyl-Coenzyme A (acyl-CoA) as the acyl donor while PDAT1 uses phosphatidylcholine (PC), which is synthesized from CDP-Choline and DAG by choline phosphotransferase (CPT), and releases lysophosphatidylcholine (LPC). 1,2-DAG can be derived from either *de novo* biosynthetic pathways or membrane lipids such as PC. During *de novo* synthesis, phosphatidic acid (PA) is formed via lysophosphatidic acid (LPA) by the consecutive actions of glycerol-3-phosphate acyltransferase (GPAT) and lysophosphatidic acid acyltransferase (LPAAT) from acyl-CoAs and glycerol-3-phosphate (G3P). PA is then dephosphorylated to DAG by PA phosphatase (PAP). 1,2-DAG synthesis from membrane lipids requires either a phospholipase C (PLC) or the concerted action of a phospholipase D (PLD) and PAP. Alternatively, the head group of PC can be transferred to DAG creating again PC and DAG, but potentially with different acyl chains. This latter reaction is catalyzed by diacylglycerol cholinephosphotransferase (PDCT). The acyl-CoA pool is filled either from *de novo* synthesis of fatty acids (16:0, 18:0 and 18:1, where the first number represents the total number of carbon atoms in the fatty acyl chain and the second number represents the number of double bonds) in the plastids or also from recycling of membrane lipids (18:X, 20:X and 22:X, where X typically represents up to three double bonds in 18:X and up to one in 20:X and 22:X). As *de novo* synthesized fatty acids only have a maximum of one double bond at the Δ9 position, acyl groups have to go through the PC pool to obtain additional double bonds at the Δ12 and/or Δ15 positions by fatty acid desaturases 2 and 3 (FAD2 and FAD3), or to be elongated. Figure based on Bates (2016) [67], which contains additional details of these biosynthetic pathways.

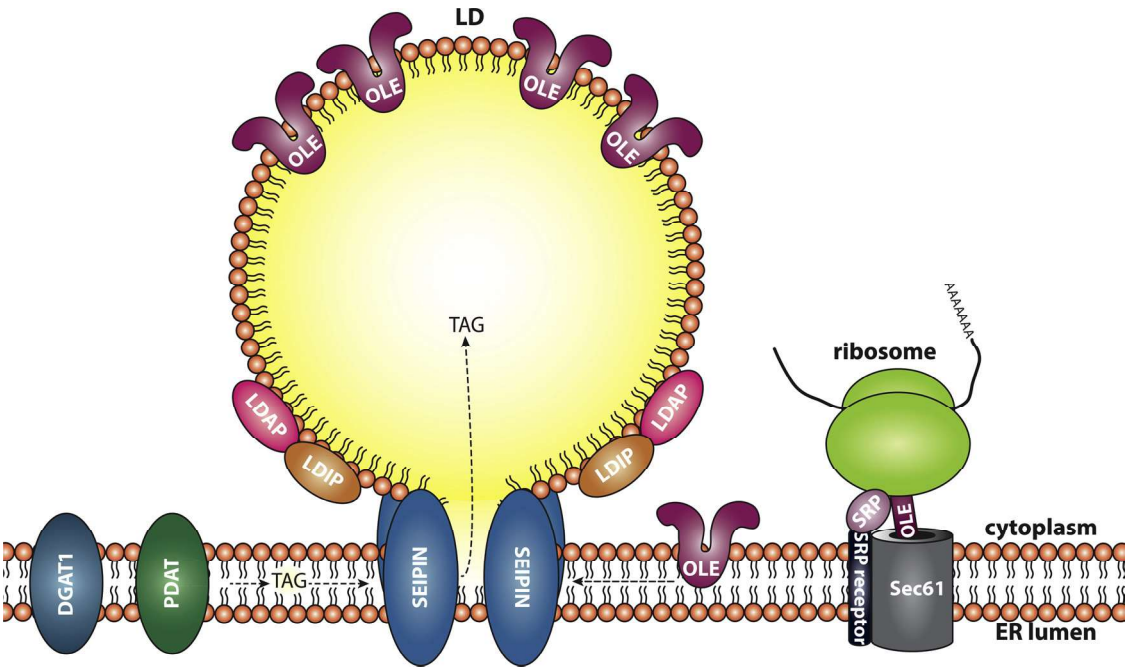

Fig. 2. Working model of LD biogenesis in Arabidopsis. Triacylglycerols (TAG) are synthesized at the ER by DIACYLGLYCEROL ACYLTRANSFERASES 1 (DGAT1) and/or PHOSPHOLIPID:DIACYLGLYCEROL ACYLTRANSFEASE 1 (PDAT1), and are then channeled into the growing, nascent LD. SEIPIN proteins are localized at the ER-LD junction and regulate LD formation, a process that also includes various LD surface-associated 'coat' proteins such as oleosin (OLE), LD-associated proteins (LDAPs), and LDIP (LDAP-interacting protein). Oleosins are first co-translationally synthesized on ER membranes in an SRP/SEC61-dependent manner then traffic to the growing LD; other proteins, such as LDAP and LDIP, appear to target directly from their sites of synthesis in cytoplasm to the LD surface. After reaching an appropriate size, LDs bud off the ER (via a yet-to-be discovered mechanism) and are released into the cytoplasm. Figure based on Pyc et al. (2017) [8], which contains additional details on LD biogenesis in plants.

[72]. The acyl-CoA pool is fueled by several pathways, but in principle, the acyl chains can be derived from either the *de novo* synthesis pathway of the plastid or from recycling of membrane phospholipids via the Land's cycle [73]. In the latter case, the acyl chains may carry additional double bonds at the Δ12 and Δ15 position (for a more in-depth review of TAG synthesis in plants refer to [67]).

Sterols and wax esters are also synthesized in the ER in plant cells. In Arabidopsis, the enzyme primarily responsible for sterol ester synthesis is a phosopholipid:sterol acyltransferase (PSAT) [74]. Wax esters are the main neutral lipids in jojoba seeds and synthesized by a wax ester synthase that uses acyl-CoA and an acyl-CoA-derived fatty alcohol as substrates [75].

In terms of the coordination of neutral lipid synthesis and LD biogenesis in plants, it remains an open question whether LD-stored neutral lipids are synthesized in close proximity to a growing LD, or if these lipids migrate in between the two leaflets of the ER membrane to reach their destination. It is also not known how the sites of LD formation are defined within the ER. Furthermore, few studies have investigated how nascent LD-associated proteins are properly targeted in plant cells and how they become associated with the LD monolayer. All of these processes likely require proteins not directly involved in lipid metabolism but, rather, possess non-enzymatic functions, some of which have recently been identified and characterized (summarized in Fig. 2).

One important, non-enzymatic player in LD formation is SEIPIN, which is a protein that is conserved across eukaryotes and whose name is derived from the Berardinelli-Seip syndrome that leads to severe lipodystrophy in humans [76]. SEIPINs are localized at ER-LD junction sites, where they regulate the proper size and formation of LDs [77–79]. They also help to stabilize ER-LD connections [80–82]. Unlike in yeast, insects and humans, which only contain a single *SEIPIN* gene, three *SEIPIN* genes exist in Arabidopsis, suggesting that the protein family has expanded in order to participate in both conserved and plant-specific functions. In Arabidopsis, the disruption of two of the three *SEIPIN* genes leads to the formation of aberrant, enlarged LDs in seeds and pollen, and although the overall TAG levels in *seipin* mutant plants are not strongly affected, there is a reduction of pollen fertility and seed germination, possibly due to misfunctioning of the enlarged LDs [83]. On the other hand, the overexpression of SEIPIN in Arabidopsis leaves and seeds results in an increase in TAG formation and a proliferation of small and/or large LDs, depending on the individual or combination of ectopically-expressed SEIPINs [78]. More recently, it was also shown that the LDAPs and their interacting partner LDIP are involved in the proper compartmentation of LDs [55,84,85], but the underlying mechanisms, as well as those involved in SEIPIN function in plants, are not yet known.

Another protein family involved in the proper formation of LDs are oleosins [52,86–88], which, as mentioned above, are the major coat proteins on LDs in seeds and pollen grains. Oleosins are relatively small proteins (~20 kDa) that are anchored to the LD surface by a hydrophobic hairpin structure [89,90]. Oleosins are co-translationally inserted into ER membranes then sequestered into nascent LDs, where they are thought to play a role in their budding from the ER [87,91–93]. Oleosins are also considered to be important in shielding LDs from each other and preventing aberrant LD-LD fusions. In support of this premise, a reduction in the abundance of oleosins resulted in the formation of enlarged LDs in seeds and seedlings [94–96] and an increase in susceptibility of seeds to freezing stress [94].

The proper formation and function of LDs depends on the correct targeting of proteins to the LD surface. For many subcellular compartments, specific amino acid sequences have been identified that mediate the proper targeting of proteins to their respective subcellular compartments [97]. These targeting pathways often involve recognition of discrete targeting signals by cognate receptor proteins that helps shuttle the proteins to the correct intracellular destination(s). In contrast, no canonical targeting sequence(s) has been identified for LD proteins. In plants, however, insights to the targeting information for some individual protein families, especially oleosins, have been gained. It was shown that *in vitro*-synthesized oleosin is incorporated into microsomes

that derive from the endomembrane system [98] and heterologous expression experiments in yeast revealed that oleosins rely on the signal recognition particle and the SEC61 complex for their correct targeting to LDs [99]. These results imply that oleosins are first incorporated into the ER before they reach the LDs. It is also known that the anchoring of oleosins to the LD surface is mediated by a long hydrophobic stretch of amino acids that is thought to form a hairpin structure that penetrates into the LD core [87]. A hydrophobic stretch was also identified as part of the LD targeting signal in the LD coat protein PLANT UBX-DOMAIN – CONTAINING PROTEIN 10 (PUX10) [38].

In addition to targeting to LDs indirectly via the ER, many LD proteins are thought to target directly to the LD surface from the cytoplasm [100]. While this process has yet to be characterized extensively in plants, studies in other organisms have shown that LD-associated proteins often employ amphipathic helices that recognize "packing defects" present on the LD monolayer [101,102]. These packing defects occur when the neutral lipids of the LD core become exposed through the phospholipid monolayer, which creates hydrophobic "pockets" that are recognized (and stabilized) by large, hydrophobic amino acids in the amphipathic helix. Consistent with this premise, the LDIP protein in plants has been shown to contain a discrete amphipathic helix-like sequence that is necessary and sufficient for LD targeting [55]. LDAP might also target LDs via amphipathic helices, given that the protein is predicted to contain several of these sequences. The targeting of LDAP to LDs, however, requires the full-length protein sequence [84], suggesting that the putative amphipathic helices might function in concert, analogous to the targeting of the perilipin LD proteins in animals [103].

The abundance of proteins involved in lipid metabolism and LD formation in plants is dynamically regulated in order to adjust neutral lipid synthesis and LD formation to the cellular needs during plant growth, development and/or environmental changes. For instance, the transcription factors WRINKLED1 (WRI1) and LEAFY COTYLEDON2 (LEC2) play important roles in regulating genes associated with TAG formation during Arabidopsis seed embryo development, whereby a disruption of either gene leads to a strong reduction of TAG in seeds [104–108]. On the other hand, ectopic overexpression of either *WRI1* or *LEC2* leads to increases in fatty acid and TAG synthesis, as well as concomitant increases in LD abundance [61], particularly in vegetative tissues, such as in tobacco leaves [109] or potato tubers [110]. Notably, LEC2 and WRI1 do not only control genes involved fatty acid synthesis, but also the expression of seed-specific LD coat proteins [108], including oleosins, caleosins, steroleosins, and the TAG lipase OIL BODY LIPASE 1 (OBL1). Similarly, in Arabidopsis leaves, it was recently shown that the transcription factor MYB96 is important for the accumulation of TAG and LDs under drought stress [111], suggesting that, in addition to LEC2 and WRI1, multiple transcription factors are involved in the proper synthesis and compartmentalization of TAG in LDs in plants.

4. Turnover of LDs in plants

In plants and algae, LD lipids, such as TAGs, represent not only an energy source, but also a precursor for the synthesis of organic compounds, such as organic acids and sugars. The molecular features of TAG breakdown and utilization have been elucidated primarily from studies of Arabidopsis seed germination and seedling establishment [112] (Fig. 3). Once an oilseed has germinated, TAGs are rapidly broken down and converted to sugars, which provide the carbon and energy required for heterotrophic growth prior to photosynthetic establishment. Seeds harboring mutations in TAG and/or fatty acid breakdown pathways are often capable of germinating (i.e., radicle emergence from the seed coat), but are unable to grow any further. The requirement for TAG breakdown during seedling establishment can be bypassed, however, by providing an exogenous source of carbohydrate, such as sucrose [113,114]. This sucrose-dependent feature has allowed for the identification of many mutants involved in the process of TAG mobilization, including the major TAG lipase and the fatty acid transporter in peroxisomes [112].

The lipase primarily responsible for TAG breakdown in germinated Arabidopsis seeds is the patatin-like lipase SUGAR-DEPENDENT1 (SDP1) [113]. SDP1-deficient plants are severely hampered in seedling establishment [113] and degrade TAG slower than wild type, especially when the homolog of SDP1, referred to as SDP1-LIKE, is also disrupted [114]. Both lipases are important also for TAG degradation in vegetative tissues, since TAG accumulates in leaves of *sdp1/sdp1-like* double knockout plants [115]. Further, biochemical characterization of SDP1 showed that it catalyzes the release of two fatty acids from TAG, at least *in vitro* [113]. The enzyme subsequently responsible for the hydrolysis of the remaining monoacylglycerol (MAG) is considered to be a MAG lipase associated with LDs [116].

While SDP1 was initially proposed to be directly associated with LDs [113], akin to its TAG lipase counterparts in mammals, it was later shown that the protein is localized first on peroxisomes (or glyoxysomes as they are called in germinating seedlings). The protein then becomes associated with LDs via peroxisomal membrane extensions called peroxules, which form intimate connections with LDs [117,118]. As a result of these peroxisomal membrane-LD contact sites, fatty acids released by SDP1 are readily taken up into peroxisomes for their subsequent degradation by β-oxidation. In germinated seedlings, the products of β-oxidation are used for synthesis of succinate via the glyoxylate cycle, which is subsequently converted to carbohydrate and transported throughout the seedling to help fuel post-germinative growth [119].

Prior to their import into peroxisomes, fatty acids released by SDP1 first have to be activated to their acyl-CoA esters by a long-chain acyl-CoA synthetase (LACS) [120]. The PEROXISOMAL ABC-TRANSPORTER1 (PXA1) then imports the acyl-CoAs [121–124] into the peroxisomal matrix and apparently cleaves the acyl-CoA thioester bond during this process [125]. Free fatty acids are once again activated to acyl-CoAs by the peroxisomal-matrix-localized LACS6 and LACS7 enzymes, and then degraded by β-oxidation [120].

TAG degradation in green algae appears to be similar to vascular plants, and species like *C. reinhardtii* harbor homologs to the proteins involved in TAG and fatty acid breakdown as those in Arabidopsis [126]. However, an additional lipase was identified in algae (i.e., *C. reinhardtii* LIP1) that was shown to be important for TAG breakdown, although it acts directly on DAG and polar lipids instead of TAG [127].

The breakdown of other LD-derived neutral lipids in plants, such as sterol or wax esters, is less explored and the enzymes responsible for their hydrolysis are not known. Also, little is known about the breakdown of the LD monolayer phospholipids, although phospholipases and phospholipase activities have been detected in the LD fraction of several plant species [128–130]. As an alternative to hydrolysis, it has also been proposed that the phospholipids from LDs contribute to the expansion of peroxisome membranes during lipid mobilization [22], although the mechanism for this lipid transfer process is also unknown.

Apart from lipids, the proteins associated with LDs also have to be degraded during LD turnover. While LD protein degradation in vegetative cell types has not been well studied, some insights have been gained from recent studies of Arabidopsis seedlings. During Arabidopsis seed germination, oleosins, caleosins and steroleosins are ubiquitinated [38,56,131,132]. Further, for oleosins, polyubiquitinations of lysine residues 48 and 63 were detected [56], suggesting that ubiquitination serves as a signal for the degradation of oleosins by the proteasome [133]. Proteasomal degradation also requires that substrate proteins are removed from organellar membranes. For ER-localized proteins, the so-called ER-associated protein degradation (ERAD) pathway is known to remove proteins from the ER lumen and membrane [134]. This pathway, including many of the proteins involved in the overall process, is conserved across eukaryotes and probably best studied in the yeast *Saccharomyces cerevisiae* [135]. One key protein in the pathway is

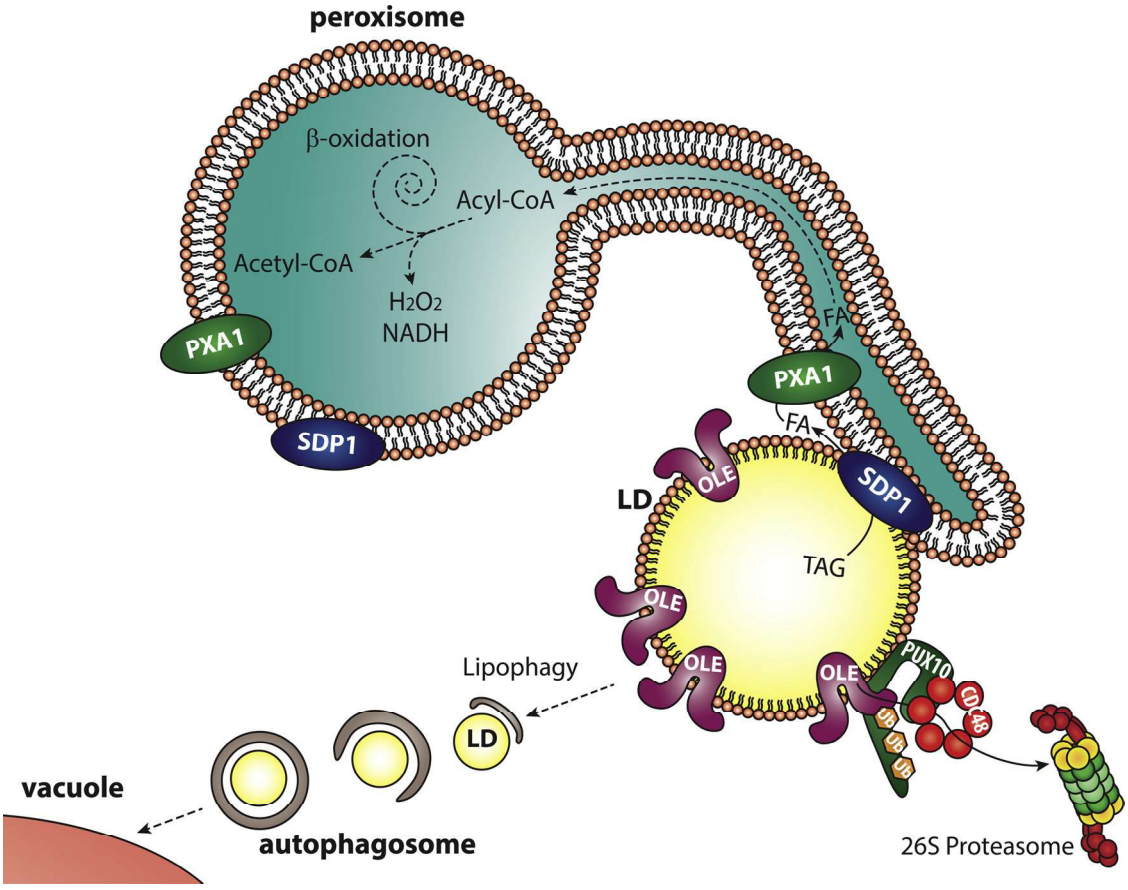

Fig. 3. LD turnover in plants. During periods of rapid TAG breakdown, such as post-germinative seedling growth, peroxisomes become associated with LDs via peroxisome membrane extensions called peroxules, which forms an intimate connection that allows the peroxisomal-surface-associated TAG lipase SUGAR DEPENDENT1 (SDP1) to come in contact with the TAGs in LDs. Fatty acids (FAs) released by SDP1 are transported into the peroxisomal matrix via the peroxisomal ABC-transporter 1 (PXA1). The FAs are subsequently activated (i.e., converted to acyl-CoA esters) and undergo β-oxidation, which results in the production of acetyl-CoA, H_2O_2 and NADH. One mechanism by which LD coat proteins such as oleosins (OLE) are degraded is via the ubiquitin (Ub)-proteasomal pathway. The plant UBX-domain-containing protein 10 (PUX10) interacts with ubiquitinated oleosins and recruits the CELL DIVISION CYCLE 48 (CDC48) protein, which uses ATP to unfold and removes oleosin from the LD for its subsequent degradation by the proteasome. Additional evidence suggests that whole LDs can be degraded also by macroautophagy (lipophagy), which begins by formation of autophagosomes (see text for details). Figure based in part on models presented in Pyc et al. (2017) [8], Deruyffelaere et al., (2018) [56] and Kretzschmar et al. (2018) [38].

Ubx2p, which acts as a scaffold to bring together ubiquitinated target proteins and other proteins associated with the proteasomal machinery [136]. The ubiquitin-associated (UBA) domain of Ubx2p can interact with ubiquitinated proteins, while the protein's ubiquitin regulatory X (UBX) domain recruits the ATPase cell division cycle 48 (CDC48) [137]. In doing so, CDC48 comes into close proximity with the ubiquitinated protein and, in an ATP-dependent manner, unfolds the protein and makes it accessible for proteasomal degradation [138].

The closest homolog to Ubx2p in plants is PUX10, which is predominantly localized at LDs in pollen tubes, developing embryos, and seedlings [38,56]. PUX10 was shown to recruit CDC48 [38,56], and loss of PUX10 activity leads to a decrease in oleosin and steroleosin breakdown [38], as well as an accumulation of ubiquitinated oleosin proteins [56]. However, the degradation of LD proteins in *pux10* mutants is merely slowed, not blocked, suggesting that either the ubiquitin proteasome pathway is partially active without PUX10 or that another breakdown pathway exists for the turnover of LD proteins in plants when the PUX10/ubiquitin-mediated process is disrupted.

The second mechanism for LD protein degradation in eukaryotic cells is autophagy, whereby proteins, complexes, or whole organelles are selectively delivered to the vacuole for turnover [139]. During this process, lipids can also be degraded and recycled. One component of autophagy, termed macroautophagy, features the uptake *en bulk* of protein complexes or organelles into autophagosomes prior to their fusion with the vacuole. The formation of these double-membrane structures requires autophagy-related (ATG) proteins, which are highly conserved across eukaryotes [140]. When LDs are degraded by macroautophagy, the process is referred to as lipophagy [141]. Overall, lipophagy has not been well explored in plants. However, there have been a few electron-microscopy-based observations indicative of the process, namely LDs within vacuoles in Arabidopsis seedlings [142], mature Arabidopsis leaves [143], and lily pollen tubes [37]. Nonetheless, the extent that lipophagy degrades LDs and hydrolyzes TAGs in plants is not clear.

As mentioned above, during seedling establishment in Arabidopsis, when there is rapid TAG breakdown, almost no TAG degradation is observed when the SDP1 and SDP1-LIKE lipases are disrupted [114]. These observations suggest that lipophagy does not contribute significantly to TAG breakdown during seedling establishment. However, disruption of the autophagy-related gene *ATG5* also hampered seedling establishment, and this could be overcome by the addition of exogenous sugar [144]. Further, the TAG content in the *atg5* mutant seedlings remained significantly elevated compared to wild-type seedlings. In a conflicting study, however, TAG content was decreased in seedlings of the same *atg5* mutant line [143]. Undoubtedly, further experiments, such as time-course analysis of TAG degradation in autophagy-affected plants, are required before overall conclusions about the contribution(s) of lipophagy to LD degradation can be made. Three-dimensional

reconstructions of cells should also help reveal if and to what extent LDs are taken up into vacuoles and if they are indeed engulfed prior to that by autophagosomes. Likewise, the role of autophagy (lipophagy) in algae remains an open question, although recent studies have shown that this process is important in algal lipid metabolism and influences algal growth [141], since a knockout mutant of ATG8, a key initiator of autophagy, in C. reinhardtii displayed reduced TAG degradation [145].

5. Physiological functions of plant LDs

While the mechanisms of LD formation and turnover are likely similar in most plant species, tissues and cell types, the physiological function of these organelles can vary greatly, as described here for seeds and seedlings, pollen, leaves, and algae.

5.1. Seeds and seedlings

The earliest physiological function assigned to LDs in plants was as a storage depot for carbon and energy in seeds, especially in the cotyledons and embryonic axis and, to some extent in some species, the endosperm [146]. During seed development, the embryonic tissue, when still nourished by the maternal tissue, accumulates large amounts of storage lipids that are packaged into LDs [147]. TAG, for example, can account for up to ~40 % of the dry weight of mature Arabidopsis seeds. After seed filling, the seeds of most plants desiccate and undergo a quiescent state that can survive extended periods of suboptimal conditions, e.g., drought, heat, cold, etc. [148]. During this phase, proteins and membranes have to be protected so that cells and their organelle constituents retain functionality once they are rehydrated and prior to germination [149]. Apart from oleosins being important for LD integrity during cold stress of seeds [94], it is not known which other LD proteins specifically contribute to the stabilization of LDs. Also, the LDs of castor bean, which contain TAG with hydroxy fatty acids, possess proteins similar to those found in Arabidopsis LDs [58], suggesting that distinct proteins are not needed for the compartmentalization of LDs containing unusual fatty acids. However, it is also possible that not all LD-related proteins in castor bean have been identified. Likewise, the proteome of LDs from jojoba cotyledons, which contain mostly wax esters instead of TAG, is similar to that of Arabidopsis, albeit there appears to be higher proportions of specific LDAP isoforms in jojoba that may be selectively associated with wax-ester-containing LDs [150].

After rehydration, TAG is consumed during post-germinative growth and most of the TAG is depleted once the plant becomes photoautotrophic [113]. In comparison to TAG, the importance of sterol esters during this developmental stage is less clear. It is presumed that these compounds are cleaved to release sterols for membrane biogenesis, but the knockout mutants of the major sterol ester-forming enzymes, PSAT1 and ASAT1, show no obvious deficiencies in seed germination or seedling establishment, despite strong reductions in sterol esters [26].

Apart from providing a source of carbon and energy, LDs might also be involved in other physiological processes in seeds and seedlings. One role could be the steroleosin-dependent synthesis of brassinosteroids, which are plant hormones important for a variety of developmental processes in plants [151]. In seeds, overexpression of the steroleosin *HYDROXYSTEROID DEHYDROGENASE 1* led to a reduction of primary seed dormancy [152,153], a process that prevents the germination of seeds under favorable conditions for some time after seed desiccation. The exact substrates and products of steroleosin enzymes remain to be elucidated.

Recently, additional LD proteins were identified in the seeds and seedlings of Arabidopsis [59]. Several of these LD proteins emerged only after the seedlings turned green following germination, indicating that these proteins might have a role(s) specific to seedling establishment or in green leaves in general.

5.2. Pollen and pollen tubes

Pollen grains contain the male gametophytic cells and play an essential role in the fertilization process of flowering plants, where pollen tubes grow from the stigma surface towards the ovules and can reach several centimeters in length [154]. Similar to seeds, pollen grains accumulate LDs during their maturation, which might serve as a source of carbon and energy that drives pollen germination and pollen tube growth. In olive, for example, LDs are turned over during pollen germination and tube growth [130]. On the other hand, pollen often contains a relatively small amount of TAG (e.g., 2% of dry weight in tobacco [27] and 4% in rapeseed [155]), which is considered insufficient to generate the energy and/or membrane lipids necessary to fully support pollen tube growth and fertilization [154]. In addition, pollen tubes are nourished by the female tissue and are not entirely dependent on their own reserves [156]. Nevertheless, mutants defective in SEIPIN proteins produce enlarged LDs that are not able to enter the pollen tube and are severely impaired in male fertility in Arabidopsis [83]. The potential importance of LDs in pollen tubes is supported also by the observations that pollen fertility is reduced in Arabidopsis mutants impaired in fatty acid import into peroxisomes, their subsequent activation to acyl-CoAs, or the β-oxidation pathway [122]. The enzyme primarily responsible for degradation of TAGs during pollen tube growth might be SDP1-LIKE, given that the corresponding gene is strongly expressed in pollen tubes in Arabidopsis [114]. Furthermore, the OBL1 lipase in tobacco was recently shown to be important for pollen tube growth [157]. Interestingly, a homolog of OBL1 in tomato is involved in the generation of oxylipin-derived volatiles in leaves [158], suggesting that OBL1 might perform a similar function in oxylipin metabolism in pollen tubes by providing free fatty acids for their production. Further evidence for an LD-based oxylipin production in pollen tubes comes from an LD-associated lipoxygenase found in pollen tubes of olive [130].

5.3. Leaves

The amount of TAG and the number of LDs in leaves are generally much lower than that in seeds and pollen, however they increase and decrease regularly during the day-night (diurnal) cycle and are strongly increased during abiotic stress conditions [84,159–161]. Heat stress, for example [161], results in a ~10-fold increase in TAG levels, albeit the amount formed (i.e., 0.25 mg g fresh weight, which represents ~0.3 % of the dry mass) is still significantly lower in comparison to the amount of TAG in seeds and pollen. Similar increases in TAG in leaves were observed during drought stress [159,161] and also during desiccation stress in the resurrection grass *O. thomaeum* [41]. Under these stress conditions, TAGs are thought to serve as a sink for free fatty acids released due to membrane breakdown and/or remodeling [35,162]. Once the stress is removed, the TAGs can then be potentially rechanneled into membrane lipids, as indicated by lipidomic analysis of Arabidopsis leaves subjected to heat stress [161]. Alternatively, the free fatty acids can also be directed into peroxisomes for β-oxidation, as shown under extended dark conditions; when plants are kept in the dark for 24 h [163], endogenous starch becomes depleted and cells begin to breakdown plastidial membrane lipids as a source of carbon and energy [164]. Notably, plants harboring mutations in the primary transporter involved in uptake of fatty acids into peroxisomes (i.e., *pxa1* mutants) were especially sensitive to extended dark treatment, showing a rapid accumulation of TAG and cytotoxic free fatty acids [164,165]. However, these plants survived if, in addition to loss of the peroxisomal transporter function, the TAG lipase SDP1 was also disrupted [163]. These observations suggest that fatty acids generated by membrane breakdown are first channeled into TAG and then released from TAG for subsequent import into peroxisomes for β-oxidation.

The importance of LDs during abiotic stress is also readily apparent from studies of double-knockout-mutant *ldap1/ldap3* plants, which are

more susceptible to drought stress than wild-type plants [166]. LDAPs are required for the proper compartmentation of LDs in leaves [84] and are also upregulated during drought stress [166]. Interestingly, the ectopic overexpression of LDAPs from either Arabidopsis [166] or dandelion (*T. brevicorniculatum)* [167] in Arabidopsis results in an increase in drought resistance, indicating that these proteins are not merely required for LD compartmentation, but are also capable of inducing processes that increase drought tolerance in plants.

Apart from acting as a sink for free fatty acids and participating in the plant's response to abiotic stress, LDs and their associated proteins appear to play several other roles in leaves. The overexpression of steroleosins, for example, enhances plant growth and development and increases resistance to salt stress, possibly due to the influence of steroleosins on brassinosteroid metabolism [152]. LDs also appear to be involved in biotic stress responses, i.e., when a plant is infected with a pathogen. For example, the Arabidopsis Ca^{2+}-dependent protein kinase1 (CPK1) localizes to LDs and is important for defense against *Fusarium oxysporum*, *Botrytis cinerea* and *Pseudomonas syringae*; *cpk1* mutant plants are more susceptible to infection by these pathogens, while *CPK1*-overexpressing lines are more resistant [168]. The functional role (s) of CPK1 and purpose for its association with LDs, however, are not known. By contrast, considerable insight has been gained on the coordinated roles of two other LD proteins, CALEOSIN3 (CLO3) and α-DIOXYGENASE1 (α-DOX1), during the infection of Arabidopsis plants with the fungal pathogen *Colletotrichum higginsianum* [169]. α-DOX1 uses free α-linolenic acid as a substrate to produce unstable 2-hydroperoxy-octadecatrienoic, which is quickly converted to stable 2-hydroxy-octadecatrienoic (2−HOT) by the peroxygenase activity of CLO3. 2−HOT subsequently acts as a phytoalexin against *C. higginsianum* in the perilesional region of infected leaves, and, thereby, prevents any further spreading of the pathogen. CLO3 and α-DOX1 were later identified in a proteomic analysis of LDs in senescent leaves, which also revealed several other proteins associated with the production of plant defense compounds [43]. However, LD localization of these other proteins was not validated by additional methods, leaving their intracellular localization unconfirmed.

5.4. Microalgae

Similar to leaves, the accumulation of TAG and LDs under stress has been shown for a variety of microalgae, including green algae and diatoms [18–20]. These stress conditions include heat [170,171] and salt stress [172,173], as well as nutrient deprivation [18]. Cultivation of microalgae in nitrogen-limiting conditions [174–177] leads to significant increases in TAG and LDs [20]. In comparison to leaves, the increase in TAG levels in algae subjected to stress is much higher and can reach up to 45 % and 37 % of dry weight in *Chlorella vulgaris* and *Nannochloropsis*, respectively [176].

One role for LDs and TAG in algae could be again to act as a sink for membrane-derived fatty acids [170], including the plastidial lipids that are degraded under nitrogen-depletion conditions [177–179]. Additionally, TAG in algal LDs might serve as a carbon sink, in addition to starch. For instance, upon stress, the energy-consuming process of cell division comes to a halt and alga enter a quiescent stage [180]. It has been speculated that during this transition, photosynthesis is still active, which requires that algal cells dispose of the excess reducing equivalents. Aside from starch, TAG synthesis represents one way to consume these reducing equivalents. Notably, in a starchless mutant of *C. reinhardtii*, the amount of TAG synthesized under nitrogen deprivation was nearly doubled in comparison to that the control strain, indicating that TAG can act as an alternate sink for excess carbon and reducing equivalents [175].

After stress has been removed or nutrient conditions restored, LD-compartmentalized TAGs in algae can act as a source of lipids for rebuilding the photosynthetic machinery and as a source of energy to help restart cell division [126]. Upon nitrogen repletion, for instance, TAG levels are quickly reduced and cell growth is enhanced, while cells disrupted for TAG degradation grow much more slowly [18,181]. However, no clear connection has been established between TAG breakdown and algal cell division [180]. Overall, there is paucity of studies from the algal field that describe the process of TAG breakdown, in general, and one reason for this is that only a few lipases have been well characterized [18].

An intriguing phenomenon involving lipid remodeling within marine algal cells following viral infection has been reported in cells of *Emiliania huxleyi* [182]. Here, viral infection stimulates lipid remodeling of the algal host to induce cell death and lysis, and to produce LD-compartmentalized TAGs with predominantly saturated and monounsaturated fatty acids [183]. The fatty acid composition of virus-induced TAGs was distinctly different from TAGs produced by these algae during nutrient deprivation. The LDs only accumulated in infected algal cells and became enriched in virions upon lytic release from the alga [183]. Based on these and other data, the buoyant LDs in the virions may support the infection cycle of the virus by facilitating their distribution in the water column. In addition, the LDs in the algal cells were required for compartmentalization of viral components during viral replication and assembly in the host. This intriguing algal-biotic interaction further demonstrates the versatile roles for LDs beyond a mere storage compartment.

6. Conclusion

Research into the biology of LDs in plant cells is a rapidly growing field that has increased the visibility of this highly versatile organelle. Recent work has also highlighted similarities as well as striking differences between LDs in plants and in other eukaryotes. For the most part, the fundamental understanding of LD biology in plants has been enhanced by research over the past few years to increase the inventory of proteins that participate in the formation and turnover of these hydrophobic compartments. However, many gaps persist. For example, how is the intracellular formation of LDs in plants regulated at a mechanistic level? What is the interaction between autophagy-independent and autophagy-dependent pathways for plant LD turnover? The physiological function(s) of LDs in plant cells also needs more investigation. What is the purpose for the transient formation of plant LDs diurnally or in response to environmental stressors? What is the role of LDs in plant metabolism apart from TAG synthesis and breakdown? Regardless of these open questions, a solid foundation is being laid down for future functional studies and for biotechnology approaches that aim to increase the amount of tailor-made plant oils needed for nutritional and industrial purposes.

Funding

Support for LD research in the author's labs was provided by the German research foundation DFG (IS 273/2-2 and IS 273/7-1) to TI and the U.S. Department of Energy, BER Division (DE-SC0000797) and, more recently, the BES-Physical Biosciences program (DE-SC0016536) to KDC, RTM and JMD. Funding was also provided by the Natural Sciences and Engineering Research Council of Canada (RGPIN-2018-04629) to RTM. Mention of trade names or commercial products in this article is solely for the purpose of providing specific information and does not imply recommendation or endorsement by the U. S. Department of Agriculture. USDA is an equal opportunity provider and employer.

Acknowledgements

We apologize to those researchers whose work was not cited because of space limitations.

References

[1] D. Murphy, The dynamic roles of intracellular lipid droplets: from archaea to mammals, Protoplasma 249 (3) (2012) 541–585, https://doi.org/10.1007/s00709-011-0329-7.

[2] K.D. Chapman, J.M. Dyer, R.T. Mullen, Biogenesis and functions of lipid droplets in plants, J. Lipid Res. 53 (2) (2012) 215–226, https://doi.org/10.1194/jlr.R021436.

[3] T.C. Walther, R.V. Farese Jr., Lipid droplets and cellular lipid metabolism, Annu. Rev. Biochem. 81 (1) (2012) 687–714, https://doi.org/10.1146/annurev-biochem-061009-102430.

[4] C.-Y. Huang, C.-I. Chung, Y.-C. Lin, Y.-I.C. Hsing, A.H.C. Huang, Oil bodies and Oleosins in Physcomitrella possess characteristics representative of early trends in evolution, Plant Physiol. 150 (3) (2009) 1192–1203, https://doi.org/10.1104/pp.109.138123.

[5] K.D. Chapman, M. Aziz, J.M. Dyer, R.T. Mullen, Mechanisms of lipid droplet biogenesis, Biochem. J. 476 (13) (2019) 1929–1942, https://doi.org/10.1042/BCJ20180021.

[6] R.V. Farese Jr., T.C. Walther, Lipid droplets finally get a little R-E-S-P-E-C-T, Cell 139 (5) (2009) 855–860, https://doi.org/10.1016/j.cell.2009.11.005.

[7] J.A. Olzmann, P. Carvalho, Dynamics and functions of lipid droplets, Nat. Rev. Mol. Cell Biol. 20 (3) (2019) 137–155, https://doi.org/10.1038/s41580-018-0085-z.

[8] M. Pyc, Y. Cai, M.S. Greer, O. Yurchenko, K.D. Chapman, J.M. Dyer, R.T. Mullen, Turning over a new leaf in lipid droplet biology, Trends Plant Sci. 22 (7) (2017) 596–609, https://doi.org/10.1016/j.tplants.2017.03.012.

[9] L. Spicher, F. Kessler, Unexpected roles of plastoglobules (plastid lipid droplets) in vitamin K1 and E metabolism, Curr. Opin. Plant Biol. 25 (2015) 123–129, https://doi.org/10.1016/j.pbi.2015.05.005.

[10] S. Rottet, C. Besagni, F. Kessler, The role of plastoglobules in thylakoid lipid remodeling during plant development, Biochim. Biophys. Acta 1847 (9) (2015) 889–899, https://doi.org/10.1016/j.bbabio.2015.02.002.

[11] C. Brehelin, F. Kessler, K.J. van Wijk, Plastoglobules: versatile lipoprotein particles in plastids, Trends Plant Sci. 12 (6) (2007) 260–266, https://doi.org/10.1016/j.tplants.2007.04.003.

[12] K.J. van Wijk, F. Kessler, Plastoglobuli: Plastid microcompartments with integrated functions in metabolism, plastid developmental transitions, and environmental adaptation, Annu. Rev. Plant Biol. 68 (2017) 253–289, https://doi.org/10.1146/annurev-arplant-043015-111737.

[13] T.L. Shimada, M. Hayashi, I. Hara-Nishimura, Membrane dynamics and multiple functions of oil bodies in seeds and leaves, Plant Physiol. 176 (1) (2018) 199–207, https://doi.org/10.1104/pp.17.01522.

[14] A.H.C. Huang, Oleosins and oil bodies in seeds and other organs, Plant Physiol. 110 (4) (1996) 1055–1061, https://doi.org/10.1104/pp.110.4.1055.

[15] T.J. Tranbarger, S. Dussert, T. JoÃ«t, X. Argout, M. Summo, A. Champion, D. Cros, A. Omore, B. Nouy, F. Morcillo, Regulatory mechanisms underlying oil palm fruit mesocarp maturation, ripening, and functional specialization in lipid and carotenoid metabolism, Plant Physiol. 156 (2) (2011) 564–584, https://doi.org/10.1104/pp.111.175141.

[16] J.H.E. Ross, J. Sanchez, F. Millan, D.J. Murphy, Differential presence of oleosins in oleogenic seed and mesocarp tissues in olive (*Olea europaea*) and avocado (*Persea americana*), Plant Sci. 93 (1–2) (1993) 203–210.

[17] Z. Yang, H. Ji, D. Liu, Oil biosynthesis in underground oil-rich storage vegetative tissue: comparison of *Cyperus esculentus* tuber with oil seeds and fruits, Plant Cell Physiol. 57 (12) (2016) 2519–2540, https://doi.org/10.1093/pcp/pcw165.

[18] Y. Li-Beisson, J.J. Thelen, E. Fedosejevs, J.L. Harwood, The lipid biochemistry of eukaryotic algae, Prog. Lipid Res. 74 (2019) 31–68, https://doi.org/10.1016/j.plipres.2019.01.003.

[19] Z.-Y. Du, C. Benning, Triacylglycerol accumulation in photosynthetic cells in plants and algae, in: Y. Nakamura, Y. Li-Beisson (Eds.), Lipids in Plant and Algae Development, Springer International Publishing, Cham, 2016, pp. 179–205.

[20] S.S. Merchant, J. Kropat, B. Liu, J. Shaw, J. Warakanont, TAG, You're it! Chlamydomonas as a reference organism for understanding algal triacylglycerol accumulation, Curr. Opin. Biotechnol. 23 (3) (2012) 352–363, https://doi.org/10.1016/j.copbio.2011.12.001.

[21] J.T.C. Tzen, Y. Cao, P. Laurent, C. Ratnayake, A.H.C. Huang, Lipids, proteins, and structure of seed oil bodies from diverse species, Plant Physiol. 101 (1993) 267–276, https://doi.org/10.1104/pp.101.1.267.

[22] K.D. Chapman, R.N. Trelease, Acquisition of membrane lipids by differentiating glyoxysomes - role of lipid bodies, J. Cell Biol. 115 (4) (1991) 995–1007, https://doi.org/10.1083/jcb.115.4.995.

[23] C. Borch-Jensen, B. Jensen, K. Mathiasen, J. Mollerup, Analysis of seed oil from *Ricinus communis* and *Dimorphoteca pluvialis* by gas and supercritical fluid chromatography, J. Am. Oil Chem. Soc. 74 (3) (1997) 277–284, https://doi.org/10.1007/s11746-997-0136-7.

[24] K.M. Schmid, G.W. Patterson, Distribution of cyclopropenoid fatty acids in malvaceous plant parts, Phytochemistry 27 (9) (1988) 2831–2834, https://doi.org/10.1016/0031-9422(88)80672-1.

[25] J. Smith, C.R, Occurrence of unusual fatty acids in plants, in: R.T. Holman (Ed.), Progress in the Chemistry of Fats and Other Lipids, Pergamon Press, Oxford, 1970, pp. 137–177.

[26] P. Bouvier-Nave, A. Berna, A. Noiriel, V. Compagnon, A.S. Carlsson, A. Banas, S. Stymne, H. Schaller, Involvement of the phospholipid sterol acyltransferase1 in plant sterol homeostasis and leaf senescence, Plant Physiol. 152 (1) (2010) 107–119, https://doi.org/10.1104/pp.109.145672.

[27] A.H. Rotsch, J. Kopka, I. Feussner, T. Ischebeck, Central metabolite and sterol profiling divides tobacco male gametophyte development and pollen tube growth into eight metabolic phases, Plant J. 92 (1) (2017) 129–146, https://doi.org/10.1111/tpj.13633.

[28] A.E. Solovchenko, Physiological role of neutral lipid accumulation in eukaryotic microalgae under stresses, Russ. J. Plant Physiol. 59 (2) (2012) 167–176, https://doi.org/10.1134/s1021443712020161.

[29] T.K. Miwa, Jojoba oil wax esters and derived fatty acids and alcohols - Gas chromatographic analyses, J. Am. Oil Chem. Soc. 48 (6) (1971) 259–264, https://doi.org/10.1007/BF02638458.

[30] K. Berthelot, S. Lecomte, Y. Estevez, F. Peruch, *Hevea brasiliensis* REF (Hev b 1) and SRPP (Hev b 3): an overview on rubber particle proteins, Biochimie 106 (2014) 1–9, https://doi.org/10.1016/j.biochi.2014.07.002.

[31] N. Laibach, A. Hillebrand, R.M. Twyman, D. Prüfer, C. Schulze Gronover, Identification of a *Taraxacum brevicorniculatum* rubber elongation factor protein that is localized on rubber particles and promotes rubber biosynthesis, Plant J. 82 (4) (2015) 609–620, https://doi.org/10.1111/tpj.12836.

[32] P.J. Horn, C.N. James, S.K. Gidda, A. Kilaru, J.M. Dyer, R.T. Mullen, J.B. Ohlrogge, K.D. Chapman, Identification of a new class of lipid droplet-associated proteins in plants, Plant Physiol. 162 (4) (2013) 1926–1936, https://doi.org/10.1104/pp.113.222455.

[33] Q. Xiang, K. Xia, L. Dai, G. Kang, Y. Li, Z. Nie, C. Duan, R. Zeng, Proteome analysis of the large and the small rubber particles of Hevea brasiliensis using 2D-DIGE, Plant Physiol. Biochem. 60 (2012) 207–213, https://doi.org/10.1016/j.plaphy.2012.08.010.

[34] S. Yamashita, H. Yamaguchi, T. Waki, Y. Aoki, M. Mizuno, F. Yanbe, T. Ishii, A. Funaki, Y. Tozawa, Y. Miyagi-Inoue, Identification and reconstitution of the rubber biosynthetic machinery on rubber particles from *Hevea brasiliensis*, Elife 5 (2016) e19022, , https://doi.org/10.7554/eLife.19022.

[35] A.H.C. Huang, Plant lipid droplets and their associated proteins: potential for rapid advances, Plant Physiol. 176 (3) (2018) 1894–1918, https://doi.org/10.1104/pp.17.01677.

[36] L.S.H. Wu, G.H.H. Hong, R.F. Hou, J.T.C. Tzen, Classification of the single oleosin isoform and characterization of seed oil bodies in gymnosperms, Plant Cell Physiol. 40 (3) (1999) 326–334, https://doi.org/10.1093/oxfordjournals.pcp.a029545.

[37] P.-L. Jiang, C.-S. Wang, C.-M. Hsu, G.-Y. Jauh, J.T.C. Tzen, Stable oil bodies sheltered by a unique oleosin in lily pollen, Plant Cell Physiol. 48 (6) (2007) 812–821, https://doi.org/10.1093/pcp/pcm051.

[38] F.K. Kretzschmar, L.F. Mengel, A. Müller, K. Schmitt, K.F. Blersch, O. Valerius, G. Braus, T. Ischebeck, PUX10 is a lipid droplet-localized scaffold protein that interacts with CDC48 and is involved in the degradation of lipid droplet proteins, Plant Cell 30 (2018) 2137–2160, https://doi.org/10.1105/tpc.18.00276.

[39] J.H.E. Ross, D.J. Murphy, Characterization of anther-expressed genes encoding a major class of extracellular oleosin-like proteins in the pollen coat of Brassicaceae, Plant J. 9 (5) (1996) 625–637, https://doi.org/10.1046/j.1365-313X.1996.9050625.x.

[40] Y. Fang, R.L. Zhu, B.D. Mishler, Evolution of oleosin in land plants, PLoS One 9 (8) (2014), https://doi.org/10.1371/journal.pone.0103806.

[41] R. VanBuren, M. Wai Ching, Q. Zhang, X. Song, P.P. Edger, D. Bryant, T.P. Michael, T.C. Mockler, D. Bartels, Seed desiccation mechanisms co-opted for vegetative desiccation in the resurrection grass *Oropetium thomaeum*, Plant Cell Environ. 40 (10) (2017) 2292–2306, https://doi.org/10.1111/pce.13027.

[42] A.V. Klepikova, A.S. Kasianov, E.S. Gerasimov, M.D. Logacheva, A.A. Penin, A high resolution map of the *Arabidopsis thaliana* developmental transcriptome based on RNA-seq profiling, Plant J. 88 (6) (2016) 1058–1070, https://doi.org/10.1111/tpj.13312.

[43] M. Pyc, Y. Cai, S.K. Gidda, O. Yurchenko, S. Park, F.K. Kretzschmar, T. Ischebeck, O. Valerius, G.H. Braus, K.D. Chapman, J.M. Dyer, R.T. Mullen, Arabidopsis lipid drop-associated protein (LDAP) - interacting protein (LDIP) influences lipid droplet size and neutral lipid homeostasis in both leaves and seeds, Plant J. 92 (6) (2017) 1182–1201, https://doi.org/10.1111/tpj.13754.

[44] L. Brocard, F. Immel, D. Coulon, N. Esnay, K. Tuphile, S. Pascal, S. Claverol, L. Fouillen, J.J. Bessoule, C. Brehelin, Proteomic analysis of lipid droplets from Arabidopsis aging leaves brings new insight into their biogenesis and functions, Front. Plant Sci. 8 (2017) 894, https://doi.org/10.3389/fpls.2017.00894.

[45] H. Goold, F. Beisson, G. Peltier, Y. Li-Beisson, Microalgal lipid droplets: composition, diversity, biogenesis and functions, Plant Cell Rep. 34 (4) (2015) 545–555, https://doi.org/10.1007/s00299-014-1711-7.

[46] M.-D. Huang, A.H.C. Huang, Bioinformatics reveal five lineages of Oleosins and the mechanism of lineage evolution related to Structure/Function from green algae to seed plants, Plant Physiol. 169 (1) (2015) 453–470, https://doi.org/10.1104/pp.15.00634.

[47] N.-L. Huang, M.-D. Huang, T.-L.L. Chen, A.H.C. Huang, Oleosin of subcellular lipid droplets evolved in green algae, Plant Physiol. 161 (4) (2013) 1862–1874, https://doi.org/10.1104/pp.112.212514.

[48] E.R. Moellering, C. Benning, RNA interference silencing of a major lipid droplet protein affects lipid droplet size in *Chlamydomonas reinhardtii*, Eukaryot. Cell 9 (1) (2010) 97–106, https://doi.org/10.1128/ec.00203-09.

[49] H.M. Nguyen, M. Baudet, S. Cuine, J.M. Adriano, D. Barthe, E. Billon, C. Bruley, F. Beisson, G. Peltier, M. Ferro, Y. Li-Beisson, Proteomic profiling of oil bodies isolated from the unicellular green microalga *Chlamydomonas reinhardtii*: with focus on proteins involved in lipid metabolism, Proteomics 11 (21) (2011) 4266–4273, https://doi.org/10.1002/pmic.201100114.

[50] H. Siegler, O. Valerius, T. Ischebeck, J. Popko, N.J. Tourasse, O. Vallon, I. Khozin-Goldberg, G.H. Braus, I. Feussner, Analysis of the lipid body proteome of the

oleaginous alga *Lobosphaera incisa*, BMC Plant Biol. 17 (1) (2017) 98, https://doi.org/10.1186/s12870-017-1042-2.
[51] X. Wang, H. Wei, X. Mao, J. Liu, Proteomics analysis of lipid droplets from the oleaginous alga *Chromochloris zofingiensis* reveals novel proteins for lipid metabolism, Genomics Proteomics Bioinformatics (2019), https://doi.org/10.1016/j.gpb.2019.01.003.
[52] J. Lupette, A. Jaussaud, K. Seddiki, C. Morabito, S. Brugière, H. Schaller, M. Kuntz, J.-L. Putaux, P.-H. Jouneau, F. Rébeillé, D. Falconet, Y. Coute, J. Jouhet, M. Tardif, J. Salvaing, E. Marechal, The architecture of lipid droplets in the diatom *Phaeodactylum tricornutum*, Algal Research - Biomass, Biofuels Bioprod. Biorefining 38 (2019) 101415, , https://doi.org/10.1016/j.algal.2019.101415.
[53] R. Qu, S. Wang, Y. Lin, V.B. Vance, A.H.C. Huang, Characteristics and biosynthesis of membrane proteins of lipid bodies in the scutella of maize (*Zea mays* L.), Biochem. J. 235 (1986) 57–65, https://doi.org/10.1042/bj2350057.
[54] J.C.F. Chen, C.C.Y. Tsai, J.T.C. Tzen, Cloning and secondary structure analysis of caleosin, a unique calcium-binding protein in oil bodies of plant seeds, Plant Cell Physiol. 40 (10) (1999) 1079–1086, https://doi.org/10.1093/oxfordjournals.pcp.a029490.
[55] L.J. Lin, S.S. Tai, C.C. Peng, J.T. Tzen, Steroleosin, a sterol-binding dehydrogenase in seed oil bodies, Plant Physiol. 128 (4) (2002) 1200–1211, https://doi.org/10.1104/pp.010928.
[56] C. Deruyffelaere, Z. Purkrtova, I. Bouchez, B. Collet, J.L. Cacas, T. Chardot, J.L. Gallois, S. D'Andrea, PUX10 associates with CDC48A and regulates the dislocation of ubiquitinated oleosins from seed lipid droplets, Plant Cell 30 (9) (2018) 2116–2136, https://doi.org/10.1105/tpc.18.00275.
[57] T.L. Shimada, Y. Takano, T. Shimada, M. Fujiwara, Y. Fukao, M. Mori, Y. Okazaki, K. Saito, R. Sasaki, K. Aoki, I. Hara-Nishimura, Leaf oil body functions as a subcellular factory for the production of a phytoalexin in Arabidopsis, Plant Physiol. 164 (1) (2014) 105–118, https://doi.org/10.1104/pp.113.230185.
[58] P.J. Eastmond, Cloning and characterization of the acid lipase from castor beans, J. Biol. Chem. 279 (44) (2004) 45540–45545, https://doi.org/10.1074/jbc.M408686200.
[59] F.K. Kretzschmar, N. Doner, H.E. Krawczyk, P. Scholz, K. Schmitt, O. Valerius, G. Braus, R.T. Mullen, T. Ischebeck, Identification of low-abundant lipid droplet proteins in seeds and seedlings, Plant Physiol. (2020), https://doi.org/10.1104/pp.19.01255 pp.01255.2019.
[60] A. Vieler, S.B. Brubaker, B. Vick, C. Benning, A lipid droplet protein of *Nannochloropsis* with functions partially analogous to plant oleosins, Plant Physiol. 158 (4) (2012) 1562–1569, https://doi.org/10.1104/pp.111.193029.
[61] T. Vanhercke, J.M. Dyer, R.T. Mulle, A. Kilaru, M.M. Rahman, J.R. Petrie, A.G. Green, O. Yurchenko, S.P. Singh, Metabolic engineering for enhanced oil in biomass, Prog. Lipid Res. 74 (2019) 103–129, https://doi.org/10.1016/j.plipres.2019.02.002.
[62] N.M. Packter, P.K. Stumpf, Fat metabolism in higher plants. Production of short- and medium-chain acyl-acyl carrier protein by spinach stroma preparations treated with cerulenin, Biochim. Biophys. Acta 409 (3) (1975) 274–282.
[63] Y. Li-Beisson, B. Shorrosh, F. Beisson, M.X. Andersson, V. Arondel, P.D. Bates, S. Baud, D. Bird, A. DeBono, T.P. Durrett, R.B. Franke, I.A. Graham, K. Katayama, A.A. Kelly, T. Larson, J.E. Markham, M. Miquel, I. Molina, I. Nishida, O. Rowland, L. Samuels, K.M. Schmid, H. Wada, R. Welti, C. Xu, R. Zallot, J. Ohlrogge, Acyl-lipid metabolism, The Arabidopsis Book, The American Society of Plant Biologists, 2013 p. e0161.
[64] H.P. Klein, C.M. Volkmann, F.C. Chao, Fatty acid synthetase of Saccharomyces cerevisiae, J. Bacteriol. 93 (6) (1967) 1966–1971.
[65] D.E. DeKay, D.E. Bauman, C.L. Davis, Characterization of fatty acid synthesis by cow mammary subcellular fractions, J. Dairy Sci. 59 (8) (1976) 1513–1517, https://doi.org/10.3168/jds.S0022-0302(76)84394-9.
[66] M. Zhang, J. Fan, D.C. Taylor, J.B. Ohlrogge, DGAT1 and PDAT1 acyltransferases have overlapping functions in Arabidopsis triacylglycerol biosynthesis and are essential for normal pollen and seed development, Plant Cell 21 (12) (2009) 3885–3901, https://doi.org/10.1105/tpc.109.071795.
[67] P.D. Bates, Understanding the control of acyl flux through the lipid metabolic network of plant oil biosynthesis, Biochim. Biophys. Acta 1861 (9, Part B) (2016) 1214–1225, https://doi.org/10.1016/j.bbalip.2016.03.021.
[68] J.M. Shockey, S.K. Gidda, D.C. Chapital, J.-C. Kuan, P.K. Dhanoa, J.M. Bland, S.J. Rothstein, R.T. Mullen, J.M. Dyer, Tung tree DGAT1 and DGAT2 have nonredundant functions in triacylglycerol biosynthesis and are localized to different subdomains of the endoplasmic reticulum, Plant Cell 18 (9) (2006) 2294–2313, https://doi.org/10.1105/tpc.106.043695.
[69] R. Li, K. Yu, D. Hildebrand, DGAT1, DGAT2 and PDAT expression in seeds and other tissues of epoxy and hydroxy fatty acid accumulating plants, Lipids 45 (2) (2010) 145–157, https://doi.org/10.1007/s11745-010-3385-4.
[70] P.J. Eastmond, A.-L. Quettier, J.T.M. Kroon, C. Craddock, N. Adams, A.R. Slabas, PHOSPHATIDIC ACID PHOSPHOHYDROLASE1 and 2 regulate phospholipid synthesis at the endoplasmic reticulum in Arabidopsis, Plant Cell 22 (8) (2010) 2796–2811, https://doi.org/10.1105/tpc.109.071423.
[71] J. Shockey, A. Regmi, K. Cotton, N. Adhikari, J. Browse, P.D. Bates, Identification of Arabidopsis GPAT9 (At5g60620) as an essential gene involved in triacylglycerol biosynthesis, Plant Physiol. 170 (1) (2015) 163–179, https://doi.org/10.1104/pp.15.01563.
[72] I. Pokotylo, P. Pejchar, M. Potocký, D. Kocourková, Z. Krcková, E. Ruelland, V. Kravets, J. Martinec, The plant non-specific phospholipase C gene family. Novel competitors in lipid signalling, Prog. Lipid Res. 52 (1) (2013) 62–79, https://doi.org/10.1016/j.plipres.2012.09.001.
[73] K.D. Chapman, J.B. Ohlrogge, Compartmentation of triacylglycerol accumulation in plants, J. Biol. Chem. 287 (4) (2012) 2288–2294, https://doi.org/10.1074/jbc.R111.290072.
[74] A. Banas, A.S. Carlsson, B. Huang, M. Lenman, W. Banas, M. Lee, A. Noiriel, P. Benveniste, H. Schaller, P. Bouvier-Nave, S. Stymne, Cellular sterol ester synthesis in plants is performed by an enzyme (phospholipid:sterol acyltransferase) different from the yeast and mammalian acyl-CoA:sterol acyltransferases, J. Biol. Chem. 280 (41) (2005) 34626–34634, https://doi.org/10.1074/jbc.M504459200.
[75] K.D. Lardizabal, J.G. Metz, T. Sakamoto, W.C. Hutton, M.R. Pollard, M.W. Lassner, Purification of a Jojoba embryo wax synthase, cloning of its cDNA, and production of high levels of wax in seeds of transgenic Arabidopsis, Plant Physiol. 122 (3) (2000) 645–656, https://doi.org/10.1104/pp.122.3.645.
[76] B.R. Cartwright, J.M. Goodman, Seipin: from human disease to molecular mechanism, J. Lipid Res. 53 (6) (2012) 1042–1055, https://doi.org/10.1194/jlr.R023754.
[77] J. Magre, M. Delepine, E. Khallouf, T. Gedde-Dahl Jr., L. Van Maldergem, E. Sobel, J. Papp, M. Meier, A. Megarbane, A. Bachy, A. Verloes, F.H. d'Abronzo, E. Seemanova, R. Assan, N. Baudic, C. Bourut, P. Czernichow, F. Huet, F. Grigorescu, M. de Kerdanet, D. Lacombe, P. Labrune, M. Lanza, H. Loret, F. Matsuda, J. Navarro, A. Nivelon-Chevalier, M. Polak, J.J. Robert, P. Tric, N. Tubiana-Rufi, C. Vigouroux, J. Weissenbach, S. Savasta, J.A. Maassen, O. Trygstad, P. Bogalho, P. Freitas, J.L. Medina, F. Bonnicci, B.I. Joffe, G. Loyson, V.R. Panz, F.J. Raal, S. O'Rahilly, T. Stephenson, C.R. Kahn, M. Lathrop, J. Capeau, B.W. Group, Identification of the gene altered in Berardinelli-Seip congenital lipodystrophy on chromosome 11q13, Nat. Genet. 28 (4) (2001) 365–370, https://doi.org/10.1038/ng585.
[78] Y. Cai, J.M. Goodman, M. Pyc, R.T. Mullen, J.M. Dyer, K.D. Chapman, Arabidopsis SEIPIN proteins modulate triacylglycerol accumulation and influence lipid droplet proliferation, Plant Cell 27 (9) (2015) 2616–2636, https://doi.org/10.1105/tpc.15.00588.
[79] J. Bi, W. Wang, Z. Liu, X. Huang, Q. Jiang, G. Liu, Y. Wang, X. Huang, Seipin promotes adipose tissue fat storage through the ER Ca^{2+}-ATPase SERCA, Cell Metab. 19 (5) (2014) 861–871, https://doi.org/10.1016/j.cmet.2014.03.028.
[80] H. Wang, M. Becuwe, B.E. Housden, C. Chitraju, A.J. Porras, M.M. Graham, X.N. Liu, A.R. Thiam, D.B. Savage, A.K. Agarwal, A. Garg, M.-J. Olarte, Q. Lin, F. Fröhlich, H.K. Hannibal-Bach, S. Upadhyayula, N. Perrimon, T. Kirchhausen, C.S. Ejsing, T.C. Walther, R.V. Farese, Seipin is required for converting nascent to mature lipid droplets, eLife 5 (2016) e16582, , https://doi.org/10.7554/eLife.16582.
[81] V.T. Salo, I. Belevich, S. Li, L. Karhinen, H. Vihinen, C. Vigouroux, J. Magré, C. Thiele, M. Hölttä-Vuori, E. Jokitalo, Seipin regulates ER–lipid droplet contacts and cargo delivery, EMBO J. 35 (24) (2016) 2699–2716, https://doi.org/10.15252/embj.201695170.
[82] A. Grippa, L. Buxó, G. Mora, C. Funaya, F.-Z. Idrissi, F. Mancuso, R. Gomez, J. Muntanyà, E. Sabidó, P. Carvalho, The seipin complex Fld1/Ldb16 stabilizes ER–lipid droplet contact sites, J. Cell Biol. 211 (4) (2015) 829–844, https://doi.org/10.1083/jcb.201502070.
[83] M. Taurino, S. Costantini, S. De Domenico, F. Stefanelli, G. Ruano, M.O. Delgadillo, J.J. Sanchez-Serrano, M. Sanmartín, A. Santino, E. Rojo, SEIPIN proteins mediate lipid droplet biogenesis to promote pollen transmission and reduce seed dormancy, Plant Physiol. 176 (2) (2017) 1531–1546, https://doi.org/10.1104/pp.17.01430.
[84] S.K. Gidda, S. Park, M. Pyc, O. Yurchenko, Y. Cai, P. Wu, D.W. Andrews, K.D. Chapman, J.M. Dyer, R.T. Mullen, Lipid droplet-associated proteins (LDAPs) are required for the dynamic regulation of neutral lipid compartmentation in plant cells, Plant Physiol. 170 (4) (2016) 2052–2071, https://doi.org/10.1104/pp.15.01977.
[85] D. Coulon, L. Brocard, K. Tuphile, C. Brehelin, Arabidopsis LDIP protein locates at a confined area within the lipid droplet surface and favors lipid droplet formation, Biochimie (2019), https://doi.org/10.1016/j.biochi.2019.09.018.
[86] M. Miquel, G. Trigui, S. d'Andrea, Z. Kelemen, Sb. Baud, A. Berger, C. Deruyffelaere, A. Trubuil, Lc. Lepiniec, B. Dubreucq, Specialization of oleosins in oil body dynamics during seed development in Arabidopsis seeds, Plant Physiol. 164 (4) (2014) 1866–1878, https://doi.org/10.1104/pp.113.233262.
[87] C.Y. Huang, A.H.C. Huang, Unique motifs and length of hairpin in oleosin target the cytosolic side of endoplasmic reticulum and budding lipid droplet, Plant Physiol. 174 (4) (2017) 2248–2260, https://doi.org/10.1104/pp.17.00366.
[88] V.B. Vance, A.H.C. Huang, The major protein from lipid bodies of maize. Characterization and structure based on cDNA cloning, J. Biol. Chem. 262 (1987) 11275–11279.
[89] B.M. Abell, L.A. Holbrook, M. Abenes, D.J. Murphy, M.J. Hills, M.M. Moloney, Role of the proline knot motif in oleosin endoplasmic reticulum topology and oil body targeting, Plant Cell 9 (8) (1997) 1481–1493, https://doi.org/10.1105/tpc.9.8.1481.
[90] P. Jolivet, L. Ayme, A. Giuliani, F. Wien, T. Chardot, Y. Gohon, Structural proteomics: topology and relative accessibility of plant lipid droplet associated proteins, J. Proteomics 169 (2017) 87–98, https://doi.org/10.1016/j.jprot.2017.09.005.
[91] R. Qu, A.H.C. Huang, Oleosin KD 18 on the surface of oil bodies in maize, J. Biol. Chem. 265 (4) (1990) 2238–2243.
[92] J.T.C. Tzen, Integral proteins in plant oil bodies, Isrn Bot. 2012 (2012) 16, https://doi.org/10.5402/2012/173954.
[93] J.T.C. Tzen, Y.K. Lai, K.L. Chan, A.H.C. Huang, Oleosin isoforms of high and low molecular weights are present in the oil bodies of diverse seed species, Plant Physiol. 94 (3) (1990) 1282–1289, https://doi.org/10.1104/pp.94.3.1282.
[94] T.L. Shimada, T. Shimada, T. Hideyuki, F. Yoichiro, I. Hara-Nishimura, A novel role for oleosins in freezing tolerance of oilseeds in *Arabidopsis thaliana*, Plant J. 55

(5) (2008) 798–809, https://doi.org/10.1111/j.1365-313X.2008.03553.x.
[95] J.T.L. Ting, A.H.C. Huang, Oils-to-oleosins ratio determines the size and shape of oil bodies in maize kernels, in: J.P. Williams, M.U. Khan, N.W. Lem (Eds.), Physiology, Biochemistry and Molecular Biology of Plant Lipids, Kluwer Academic Publ, PO Box 17/3300 AA Dordrecht, Netherlands, 1997, pp. 295–297.
[96] R.M.P. Siloto, K. Findlay, A. Lopez-Villalobos, E.C. Yeung, C.L. Nykiforuk, M.M. Moloney, The accumulation of oleosins determines the size of seed oilbodies in Arabidopsis, Plant Cell 18 (8) (2006) 1961–1974, https://doi.org/10.1105/tpc.106.041269.
[97] S.A. Mackenzie, Plant organellar protein targeting: a traffic plan still under construction, Trends Cell Biol. 15 (10) (2005) 548–554, https://doi.org/10.1016/j.tcb.2005.08.007.
[98] M.J. Hills, M.D. Watson, D.J. Murphy, Targeting of oleosins to the oil bodies of oilseed rape (*Brassica napus* L.), Planta 189 (1993) 24–29, https://doi.org/10.1007/bf00201339.
[99] F. Beaudoin, B.M. Wilkinson, C.J. Stirling, J.A. Napier, *In vivo* targeting of a sunflower oil body protein in yeast secretory (*sec*) mutants, Plant J. 23 (2) (2000) 159–170, https://doi.org/10.1046/j.1365-313x.2000.00769.x.
[100] N. Kory, R.V. Farese Jr., T.C. Walther, Targeting fat: Mechanisms of protein localization to lipid droplets, Trends Cell Biol. 26 (7) (2016) 535–546, https://doi.org/10.1016/j.tcb.2016.02.007.
[101] A. Čopič, S. Antoine-Bally, M. Giménez-Andrés, C.L.T. Garay, B. Antonny, M.M. Manni, S. Pagnotta, J. Guihot, C.L. Jackson, A giant amphipathic helix from a perilipin that is adapted for coating lipid droplets, Nat. Commun. 9 (1) (2018) 1332, https://doi.org/10.1038/s41467-018-03717-8.
[102] C. Prévost, M.E. Sharp, N. Kory, Q. Lin, G.A. Voth, R.V. Farese Jr., T.C. Walther, Mechanism and determinants of amphipathic helix-containing protein targeting to lipid droplets, Dev. Cell 44 (1) (2018) 73–86, https://doi.org/10.1016/j.devcel.2017.12.011 e4.
[103] D. Ajjaji, K. Ben M'barek, M.L. Mimmack, C. England, H. Herscovitz, L. Dong, R.G. Kay, S. Patel, V. Saudek, D.M. Small, D.B. Savage, A.R. Thiam, Dual binding motifs underpin the hierarchical association of perilipins1-3 with lipid droplets, Mol. Biol. Cell 30 (5) (2019) 703–716, https://doi.org/10.1091/mbc.E18-08-0534.
[104] S. Baud, M.S. Mendoza, A. To, E. Harscoet, L. Lepiniec, B. Dubreucq, WRINKLED1 specifies the regulatory action of LEAFY COTYLEDON2 towards fatty acid metabolism during seed maturation in Arabidopsis, Plant J. 50 (5) (2007) 825–838, https://doi.org/10.1111/j.1365-313X.2007.03092.x.
[105] J.G. Angeles-Núñez, A. Tiessen, Mutation of the transcription factor LEAFY COTYLEDON 2 alters the chemical composition of Arabidopsis seeds, decreasing oil and protein content, while maintaining high levels of starch and sucrose in mature seeds, J. Plant Physiol. 168 (16) (2011) 1891–1900, https://doi.org/10.1016/j.jplph.2011.05.003.
[106] N. Focks, C. Benning, *wrinkled1*: a novel, low-seed-oil mutant of Arabidopsis with a deficiency in the seed-specific regulation of carbohydrate metabolism, Plant Physiol. 118 (1) (1998) 91–101, https://doi.org/10.1104/pp.118.1.91.
[107] A. Cernac, C. Andre, S. Hoffmann-Benning, C. Benning, WRI1 is required for seed germination and seedling establishment, Plant Physiol. 141 (2) (2006) 745–757, https://doi.org/10.1104/pp.106.079574.
[108] J. Mu, H. Tan, Q. Zheng, F. Fu, Y. Liang, J. Zhang, X. Yang, T. Wang, K. Chong, X.-J. Wang, J. Zuo, LEAFY COTYLEDON1 is a key regulator of fatty acid biosynthesis in Arabidopsis, Plant Physiol. 148 (2) (2008) 1042–1054, https://doi.org/10.1104/pp.108.126342.
[109] T. Vanhercke, U.K. Divi, A. El Tahchy, Q. Liu, M. Mitchell, M.C. Taylor, P.J. Eastmond, F. Bryant, A. Mechanicos, C. Blundell, Y. Zhi, S. Belide, P. Shrestha, X.R. Zhou, J.P. Ral, R.G. White, A. Green, S.P. Singh, J.R. Petrie, Step changes in leaf oil accumulation via iterative metabolic engineering, Metab. Eng. 39 (2017) 237–246, https://doi.org/10.1016/j.ymben.2016.12.007.
[110] P. Hofvander, T. Ischebeck, H. Turesson, S.K. Kushwaha, I. Feussner, A.S. Carlsson, M. Andersson, Potato tuber expression of Arabidopsis WRINKLED1 increase triacylglycerol and membrane lipids while affecting central carbohydrate metabolism, Plant Biotechnol. J. 14 (9) (2016) 1883–1898, https://doi.org/10.1111/pbi.12550.
[111] H.G. Lee, M.E. Park, B.Y. Park, H.U. Kim, P.J. Seo, The Arabidopsis MYB96 transcription factor mediates ABA-dependent triacylglycerol accumulation in vegetative tissues under drought stress conditions, Plants (Basel) 8 (9) (2019), https://doi.org/10.3390/plants8090296.
[112] I.A. Graham, Seed storage oil mobilization, Annu. Rev. Plant Biol. 59 (1) (2008) 115–142, https://doi.org/10.1146/annurev.arplant.59.032607.092938.
[113] P.J. Eastmond, SUGAR-DEPENDENT1 encodes a patatin domain triacylglycerol lipase that initiates storage oil breakdown in germinating *Arabidopsis* seeds, Plant Cell 18 (3) (2006) 665–675, https://doi.org/10.1105/tpc.105.040543.
[114] A.A. Kelly, A.-L. Quettier, E. Shaw, P.J. Eastmond, Seed storage oil mobilization is important but not essential for germination or seedling establishment in Arabidopsis, Plant Physiol. 157 (2) (2011) 866–875, https://doi.org/10.1104/pp.111.181784.
[115] A.A. Kelly, H. van Erp, A.-L. Quettier, E. Shaw, G. Menard, S. Kurup, P.J. Eastmond, The SUGAR-DEPENDENT1 lipase limits triacylglycerol accumulation in vegetative tissues of Arabidopsis, Plant Physiol. 162 (3) (2013) 1282–1289, https://doi.org/10.1104/pp.113.219840.
[116] R.J. Kim, H.J. Kim, D. Shim, M.C. Suh, Molecular and biochemical characterizations of the monoacylglycerol lipase gene family of *Arabidopsis thaliana*, Plant J. 85 (6) (2016) 758–771, https://doi.org/10.1111/tpj.13146.
[117] S. Cui, Y. Hayashi, M. Otomo, S. Mano, K. Oikawa, M. Hayashi, M. Nishimura, Sucrose production mediated by lipid metabolism suppresses the physical interaction of peroxisomes and oil bodies during germination of *Arabidopsis thaliana*, J. Biol. Chem. 291 (38) (2016) 19734–19745, https://doi.org/10.1074/jbc.M116.748814.
[118] N. Thazar-Poulot, M. Miquel, I. Fobis-Loisy, T. Gaude, Peroxisome extensions deliver the Arabidopsis SDP1 lipase to oil bodies, Proc. Natl. Acad. Sci. 112 (13) (2015) 4158–4163, https://doi.org/10.1073/pnas.1403322112.
[119] S. Goepfert, Y. Poirier, ß-Oxidation in fatty acid degradation and beyond, Curr. Opin. Plant Biol. 10 (3) (2007) 245–251, https://doi.org/10.1016/j.pbi.2007.04.007.
[120] M. Fulda, J. Schnurr, A. Abbadi, E. Heinz, J. Browse, Peroxisomal acyl-CoA synthetase activity is essential for seedling development in *Arabidopsis thaliana*, Plant Cell 16 (2004) 394–405, https://doi.org/10.1105/tpc.019646.
[121] B.K. Zolman, I.D. Silva, B. Bartel, The Arabidopsis *pxa1* mutant is defective in an ATP-binding cassette transporter-like protein required for peroxisomal fatty acid beta-oxidation, Plant Physiol. 127 (3) (2001) 1266–1278.
[122] S. Footitt, D. Dietrich, A. Fait, A.R. Fernie, M.J. Holdsworth, A. Baker, F.L. Theodoulou, The COMATOSE ATP-Binding cassette transporter is required for full fertility in Arabidopsis, Plant Physiol. 144 (3) (2007) 1467–1480, https://doi.org/10.1104/pp.107.099903.
[123] H. Hayashi, L. De Bellis, Y. Hayashi, K. Nito, A. Kato, M. Hayashi, I. Hara-Nishimura, M. Nishimura, Molecular characterization of an Arabidopsis acyl-coenzyme A synthetase localized on glyoxysomal membranes, Plant Physiol. 130 (4) (2002) 2019–2026, https://doi.org/10.1104/pp.012955.
[124] A. Baker, D.J. Carrier, T. Schaedler, Hans R. Waterham, Carlo W. van Roermund, Frederica L. Theodoulou, Peroxisomal ABC transporters: functions and mechanism, Biochem. Soc. Trans. 43 (5) (2015) 959–965, https://doi.org/10.1042/bst20150127.
[125] C. De Marcos Lousa, C.W.T. van Roermund, V.L.G. Postis, D. Dietrich, I.D. Kerr, R.J.A. Wanders, S.A. Baldwin, A. Baker, F.L. Theodoulou, Intrinsic acyl-CoA thioesterase activity of a peroxisomal ATP binding cassette transporter is required for transport and metabolism of fatty acids, Proc. Natl. Acad. Sci. 110 (4) (2013) 1279–1284, https://doi.org/10.1073/pnas.1218034110.
[126] F. Kong, I.T. Romero, J. Warakanont, Y. Li-Beisson, Lipid catabolism in microalgae, New Phytol. 218 (4) (2018) 1340–1348, https://doi.org/10.1111/nph.15047.
[127] X. Li, C. Benning, M.-H. Kuo, Rapid triacylglycerol turnover in Chlamydomonas reinhardtii requires a lipase with broad substrate specificity, Eukaryot. Cell 11 (12) (2012) 1451–1462, https://doi.org/10.1128/ec.00268-12.
[128] M. Rudolph, A. Schlereth, M. Körner, K. Feussner, E. Berndt, M. Melzer, E. Hornung, I. Feussner, The lipoxygenase-dependent oxygenation of lipid body membranes is promoted by a patatin-type phospholipase in cucumber cotyledons, J. Exp. Bot. 62 (2) (2011) 749–760, https://doi.org/10.1093/jxb/erq310.
[129] A. Gupta, S.C. Bhatla, Preferential phospholipase A_2 activity on the oil bodies in cotyledons during seed germination in *Helianthus annuus* L. Cv, Morden, Plant Science 172 (3) (2007) 535–543, https://doi.org/10.1016/j.plantsci.2006.11.008.
[130] A. Zienkiewicz, K. Zienkiewicz, J.D. Rejon, M.I. Rodriguez-Garcia, A.J. Castro, New insights into the early steps of oil body mobilization during pollen germination, J. Exp. Bot. 64 (1) (2013) 293–302, https://doi.org/10.1093/jxb/ers332.
[131] C. Deruyffelaere, I. Bouchez, H. Morin, A. Guillot, M. Miquel, M. Froissard, T. Chardot, S. D'Andrea, Ubiquitin-mediated proteasomal degradation of oleosins is involved in oil body mobilization during post-germinative seedling growth in Arabidopsis, Plant Cell Physiol. 56 (7) (2015) 1374–1387, https://doi.org/10.1093/pcp/pcv056.
[132] E.S.L. Hsiao, J.T.C. Tzen, Ubiquitination of oleosin-H and caleosin in sesame oil bodies after seed germination, Plant Physiol. Biochem. 49 (1) (2011) 77–81, https://doi.org/10.1016/j.plaphy.2010.10.001.
[133] B. Sharma, D. Joshi, P.K. Yadav, A.K. Gupta, T.K. Bhatt, Role of ubiquitin-mediated degradation system in plant biology, Front. Plant Sci. 7 (2016) 806, https://doi.org/10.3389/fpls.2016.00806.
[134] Y. Liu, J. Li, Endoplasmic reticulum-mediated protein quality control in Arabidopsis, Front. Plant Sci. 5 (2014), https://doi.org/10.3389/fpls.2014.00162.
[135] X. Wu, T.A. Rapoport, Mechanistic insights into ER-associated protein degradation, Curr. Opin. Cell Biol. 53 (2018) 22–28, https://doi.org/10.1016/j.ceb.2018.04.004.
[136] J.D. Wilson, Y. Liu, C.M. Bentivoglio, C. Barlowe, Sel1p/Ubx2p participates in a distinct Cdc48p-dependent endoplasmic reticulum-associated degradation pathway, Traffic 7 (9) (2006) 1213–1223, https://doi.org/10.1111/j.1600-0854.2006.00460.x.
[137] J.M. Lord, L.M. Roberts, C.J. Stirling, Quality control: another player joins the ERAD cast, Curr. Biol. 15 (23) (2005) R963–R964, https://doi.org/10.1016/j.cub.2005.11.013.
[138] G.H. Baek, H. Cheng, V. Choe, X. Bao, J. Shao, S. Luo, H. Rao, Cdc48: a swiss army knife of cell biology, J. Amino Acids 2013 (2013) 183421, , https://doi.org/10.1155/2013/183421.
[139] S. Michaeli, G. Galili, P. Genschik, A.R. Fernie, T. Avin-Wittenberg, Autophagy in Plants–What's New on the Menu? Trends Plant Sci. 21 (2) (2016) 134–144, https://doi.org/10.1016/j.tplants.2015.10.008.
[140] Y. Ohsumi, Historical landmarks of autophagy research, Cell Res. 24 (1) (2014) 9, https://doi.org/10.1038/cr.2013.169.
[141] Y. Yoshitake, H. Ohta, M. Shimojima, Autophagy-mediated regulation of lipid metabolism and its impact on the growth in algae and seed plants, Front. Plant Sci. 10 (2019) 709, https://doi.org/10.3389/fpls.2019.00709.
[142] M. Poxleitner, S.W. Rogers, A. Lacey Samuels, J. Browse, J.C. Rogers, A role for caleosin in degradation of oil-body storage lipid during seed germination, Plant J. 47 (6) (2006) 917–933, https://doi.org/10.1111/j.1365-313X.2006.02845.x.
[143] J. Fan, L. Yu, C. Xu, Dual role for autophagy in lipid metabolism in Arabidopsis, Plant Cell 31 (7) (2019) 1598–1613, https://doi.org/10.1105/tpc.19.00170.

[144] T. Avin-Wittenberg, K. Bajdzienko, G. Wittenberg, S. Alseekh, T. Tohge, R. Bock, P. Giavalisco, A.R. Fernie, Global analysis of the role of autophagy in cellular metabolism and energy homeostasis in Arabidopsis seedlings under carbon starvation, Plant Cell 27 (2) (2015) 306–322, https://doi.org/10.1105/tpc.114.134205.
[145] M. Kajikawa, M. Yamauchi, H. Shinkawa, M. Tanaka, K. Hatano, Y. Nishimura, M. Kato, H. Fukuzawa, Isolation and characterization of Chlamydomonas autophagy-related mutants in nutrient-deficient conditions, Plant Cell Physiol. 60 (1) (2019) 126–138, https://doi.org/10.1093/pcp/pcy193.
[146] A.H.C. Huang, Oil bodies and oleosins in seeds, Annu. Rev. Plant Physiol. Plant Mol. Biol. 43 (1992) 177–200.
[147] S. Baud, B. Dubreucq, M. Miquel, C. Rochat, L. Lepiniec, Storage reserve accumulation in Arabidopsis: metabolic and developmental control of seed filling, Arabidopsis Book (2008).
[148] W.M. Waterworth, C.M. Bray, C.E. West, Seeds and the art of genome maintenance, Front. Plant Sci. 10 (2019) 706, https://doi.org/10.3389/fpls.2019.00706.
[149] D.K. Hincha, A. Thalhammer, LEA proteins: IDPs with versatile functions in cellular dehydration tolerance, Biochem. Soc. Trans. 40 (5) (2012) 1000–1003, https://doi.org/10.1042/BST20120109.
[150] D. Sturtevant, S. Lu, Z.-W. Zhou, Y. Shen, S. Wang, J.-M. Song, J. Zhong, D.J. Burks, Z.-Q. Yang, Q.-Y. Yang, A.E. Cannon, C. Herrfurth, I. Feussner, L. Borisjuk, E. Munz, G.F. Verbeck, X. Wang, R.K. Azad, B. Singleton, J.M. Dyer, L.-L. Chen, K.D. Chapman, L. Guo, The genome of jojoba (Simmondsia chinensis): a taxonomically-isolated species that directs wax-ester accumulation in its seeds, Sci. Adv. 6 (eaay3240) (2020).
[151] A.P. Singh, S. Savaldi-Goldstein, Growth control: brassinosteroid activity gets context, J. Exp. Bot. 66 (4) (2015) 1123–1132, https://doi.org/10.1093/jxb/erv026.
[152] F. Li, T. Asami, X. Wu, E.W. Tsang, A.J. Cutler, A putative hydroxysteroid dehydrogenase involved in regulating plant growth and development, Plant Physiol. 145 (1) (2007) 87–97, https://doi.org/10.1104/pp.107.100560.
[153] S. Baud, N.R. Dichow, Z. Kelemen, S. d'Andrea, A. To, N. Berger, M. Canonge, J. Kronenberger, D. Viterbo, B. Dubreucq, L. Lepiniec, T. Chardot, M. Miquel, Regulation of HSD1 in seeds of Arabidopsis thaliana, Plant Cell Physiol. 50 (8) (2009) 1463–1478, https://doi.org/10.1093/pcp/pcp092.
[154] T. Ischebeck, Lipids in pollen — they are different, Biochim. Biophys. Acta 1861 (9, Part B) (2016) 1315–1328, https://doi.org/10.1016/j.bbalip.2016.03.023.
[155] P. Piffanelli, J.H.E. Ross, D.J. Murphy, Intra- and extracellular lipid composition and associated gene expression patterns during pollen development in Brassica napus, Plant J. 11 (3) (1997) 549–562, https://doi.org/10.1046/j.1365-313x.1997.11030549.x.
[156] J. Selinski, R. Scheibe, Pollen tube growth: Where does the energy come from? Plant Signal. Behav. 9 (12) (2014) e977200, https://doi.org/10.4161/15592324.2014.977200.
[157] A.O. Müller, T. Ischebeck, Characterization of the enzymatic activity and physiological function of the lipid droplet-associated triacylglycerol lipase AtOBL1, New Phytol. 217 (3) (2018) 1062–1076, https://doi.org/10.1111/nph.14902.
[158] K. Garbowicz, Z. Liu, S. Alseekh, D. Tieman, M. Taylor, A. Kuhalskaya, I. Ofner, D. Zamir, H.J. Klee, A.R. Fernie, Y. Brotman, Quantitative trait loci analysis identifies a prominent gene involved in the production of fatty-acid-derived flavor volatiles in tomato, Mol. Plant 11 (2018) 1147–1165, https://doi.org/10.1016/j.molp.2018.06.003.
[159] F. Gasulla, K. Vom Dorp, I. Dombrink, U. Zahringer, N. Gisch, P. Dormann, D. Bartels, The role of lipid metabolism in the acquisition of desiccation tolerance in *Craterostigma plantagineum*: a comparative approach, Plant J. 75 (5) (2013) 726–741, https://doi.org/10.1111/tpj.12241.
[160] Y. Higashi, Y. Okazaki, F. Myouga, K. Shinozaki, K. Saito, Landscape of the lipidome and transcriptome under heat stress in *Arabidopsis thaliana*, Sci. Rep. 5 (2015) 10533, https://doi.org/10.1038/srep10533.
[161] S.P. Mueller, D.M. Krause, M.J. Mueller, A. Fekete, Accumulation of extra-chloroplastic triacylglycerols in *Arabidopsis* seedlings during heat acclimation, J. Exp. Bot. 66 (15) (2015) 4517–4526, https://doi.org/10.1093/jxb/erv226.
[162] Y. Yang, C. Benning, Functions of triacylglycerols during plant development and stress, Curr. Opin. Biotechnol. 49 (2018) 191–198, https://doi.org/10.1016/j.copbio.2017.09.003.
[163] J. Fan, L. Yu, C. Xu, A central role for triacylglycerol in membrane lipid breakdown, fatty acid beta-oxidation, and plant survival under extended darkness, Plant Physiol. 174 (3) (2017) 1517–1530, https://doi.org/10.1104/pp.17.00653.
[164] S.P. Slocombe, J. Cornah, H. Pinfield-Wells, K. Soady, Q.Y. Zhang, A. Gilday, J.M. Dyer, I.A. Graham, Oil accumulation in leaves directed by modification of fatty acid breakdown and lipid synthesis pathways, Plant Biotechnol. J. 7 (7) (2009) 694–703, https://doi.org/10.1111/j.1467-7652.2009.00435.x.
[165] H.-H. Kunz, M. Scharnewski, K. Feussner, I. Feussner, U.-I. Flügge, M. Fulda, M. Gierth, The ABC transporter PXA1 and peroxisomal b-oxidation are vital for metabolism in mature leaves of Arabidopsis during extended darkness, Plant Cell 21 (2009) 2733–2749, https://doi.org/10.1105/tpc.108.064857.
[166] E.Y. Kim, K.Y. Park, Y.S. Seo, W.T. Kim, Arabidopsis small rubber particle protein homolog SRPs play dual roles as positive factors for tissue growth and development and in drought stress responses, Plant Physiol. 170 (4) (2016) 2494–2510, https://doi.org/10.1104/pp.16.00165.
[167] N. Laibach, S. Schmidl, B. Müller, M. Bergmann, D. Prüfer, C. Schulze Gronover, Small rubber particle proteins from *Taraxacum brevicorniculatum* promote stress tolerance and influence the size and distribution of lipid droplets and artificial poly (cis-1, 4-isoprene) bodies, Plant J. 93 (6) (2018) 1045–1061, https://doi.org/10.1111/tpj.13829.
[168] M. Coca, B. San Segundo, AtCPK1 calcium-dependent protein kinase mediates pathogen resistance in Arabidopsis, Plant J. 63 (3) (2010) 526–540, https://doi.org/10.1111/j.1365-313X.2010.04255.x.
[169] T.L. Shimada, I. Hara-Nishimura, Leaf oil bodies are subcellular factories producing antifungal oxylipins, Curr. Opin. Plant Biol. 25 (0) (2015) 145–150, https://doi.org/10.1016/j.pbi.2015.05.019.
[170] B. Légeret, M. Schulz-Raffelt, H.M. Nguyen, P. Auroy, F. Beisson, G. Peltier, G. Blanc, Y. Li-Beisson, Lipidomic and transcriptomic analyses of *Chlamydomonas reinhardtii* under heat stress unveil a direct route for the conversion of membrane lipids into storage lipids, Plant Cell Environ. 39 (4) (2016) 834–847, https://doi.org/10.1111/pce.12656.
[171] A. Converti, A.A. Casazza, E.Y. Ortiz, P. Perego, M. Del Borghi, Effect of temperature and nitrogen concentration on the growth and lipid content of *Nannochloropsis oculata* and *Chlorella vulgaris* for biodiesel production, Chem. Eng. Process. Process. Intensif. 48 (6) (2009) 1146–1151, https://doi.org/10.1016/j.cep.2009.03.006.
[172] J. Fan, L. Zheng, Acclimation to NaCl and light stress of heterotrophic *Chlamydomonas reinhardtii* for lipid accumulation, J. Biosci. Bioeng. 124 (3) (2017) 302–308, https://doi.org/10.1016/j.jbiosc.2017.04.009.
[173] D. Pal, I. Khozin-Goldberg, Z. Cohen, S. Boussiba, The effect of light, salinity, and nitrogen availability on lipid production by *Nannochloropsis* sp, Appl. Microbiol. Biotechnol. (2011) 1–13, https://doi.org/10.1007/s00253-011-3170-1.
[174] G. Breuer, P.P. Lamers, D.E. Martens, R.B. Draaisma, R.H. Wijffels, The impact of nitrogen starvation on the dynamics of triacylglycerol accumulation in nine microalgae strains, Bioresour. Technol. 124 (2012) 217–226, https://doi.org/10.1016/j.biortech.2012.08.003.
[175] I.K. Blaby, A.G. Glaesener, T. Mettler, S.T. Fitz-Gibbon, S.D. Gallaher, B. Liu, N.R. Boyle, J. Kropat, M. Stitt, S. Johnson, C. Benning, M. Pellegrini, D. Casero, S.S. Merchant, Systems-level analysis of nitrogen starvation-induced modifications of carbon metabolism in a *Chlamydomonas reinhardtii* starchless mutant, Plant Cell 25 (11) (2013) 4305–4323, https://doi.org/10.1105/tpc.113.117580.
[176] A. Taleb, J. Pruvost, J. Legrand, H. Marec, B. Le-Gouic, B. Mirabella, B. Legeret, S. Bouvet, G. Peltier, Y. Li-Beisson, S. Taha, H. Takache, Development and validation of a screening procedure of microalgae for biodiesel production: application to the genus of marine microalgae Nannochloropsis, Bioresour. Technol. 177 (2015) 224–232, https://doi.org/10.1016/j.biortech.2014.11.068.
[177] J. Popko, C. Herrfurth, K. Feussner, T. Ischebeck, T. Iven, R. Haslam, M. Hamilton, O. Sayanova, J. Napier, I. Khozin-Goldberg, I. Feussner, Metabolome analysis reveals betaine lipids as major source for triglyceride formation, and the accumulation of sedoheptulose during nitrogen-starvation of Phaeodactylum tricornutum, PLoS One 11 (10) (2016) e0164673, , https://doi.org/10.1371/journal.pone.0164673.
[178] J. Jia, D. Han, H.G. Gerken, Y. Li, M. Sommerfeld, Q. Hu, J. Xu, Molecular mechanisms for photosynthetic carbon partitioning into storage neutral lipids in *Nannochloropsis oceanica* under nitrogen-depletion conditions, Algal Res. 7 (2015) 66–77, https://doi.org/10.1016/j.algal.2014.11.005.
[179] H. Abida, L.-J. Dolch, C. Mei, V. Villanova, M. Conte, M.A. Block, G. Finazzi, O. Bastien, L. Tirichine, C. Bowler, F. Rébeillé, D. Petroutsos, J. Jouhet, E. Maréchal, Membrane glycerolipid remodeling triggered by nitrogen and phosphorus starvation in *Phaeodactylum tricornutum*, Plant Physiol. 167 (2015) 118–136, https://doi.org/10.1104/pp.114.252395.
[180] C.-H. Tsai, J. Warakanont, T. Takeuchi, B.B. Sears, E.R. Moellering, C. Benning, The protein compromised Hydrolysis of Triacylglycerols 7 (CHT7) acts as a repressor of cellular quiescence in Chlamydomonas, Proc. Natl. Acad. Sci. 111 (44) (2014) 15833–15838, https://doi.org/10.1073/pnas.1414567111.
[181] M. Siaut, S. Cuine, C. Cagnon, B. Fessler, M. Nguyen, P. Carrier, A. Beyly, F. Beisson, C. Triantaphylides, Y. Li-Beisson, G. Peltier, Oil accumulation in the model green alga *Chlamydomonas reinhardtii*: characterization, variability between common laboratory strains and relationship with starch reserves, BMC Biotechnol. 11 (1) (2011) 7, https://doi.org/10.1186/1472-6750-11-7.
[182] A. Vardi, B.A.S. Van Mooy, H.F. Fredricks, K.J. Popendorf, J.E. Ossolinski, L. Haramaty, K.D. Bidle, Viral glycosphingolipids induce lytic infection and cell death in marine phytoplankton, Science 326 (5954) (2009) 861–865, https://doi.org/10.1126/science.1177322.
[183] S. Malitsky, C. Ziv, S. Rosenwasser, S. Zheng, D. Schatz, Z. Porat, S. Ben-Dor, A. Aharoni, A. Vardi, Viral infection of the marine alga *Emiliania huxleyi* triggers lipidome remodeling and induces the production of highly saturated triacylglycerol, New Phytol. 210 (1) (2016) 88–96, https://doi.org/10.1111/nph.13852.

3 Article II: Identification of Low-Abundance Lipid Droplet Proteins in Seeds and Seedlings

This research article was published online in the journal Plant Physiology in March 2020. Supplementary figures and Supplementary datasets can be found online together with the full article:

https://doi.org/10.1104/pp.19.01255

Author contribution

H. E. Krawczyk cloned and microscopically screened several of the identified putative LD-localised proteins to confirm their LD-localisation. She identified SLDP1, presented in Figure 5F, to be an LD-localised protein.

Identification of Low-Abundance Lipid Droplet Proteins in Seeds and Seedlings[1][OPEN]

Franziska K. Kretzschmar,[a,2] Nathan M. Doner,[b,2] Hannah E. Krawczyk,[a] Patricia Scholz,[a] Kerstin Schmitt,[c] Oliver Valerius,[c] Gerhard H. Braus,[c] Robert T. Mullen,[b] and Till Ischebeck[a,3,4]

[a]University of Göttingen, Albrecht-von-Haller-Institute for Plant Sciences and Göttingen Center for Molecular Biosciences (GZMB), Department of Plant Biochemistry, 37077 Göttingen, Germany
[b]University of Guelph, Department of Molecular and Cellular Biology, Guelph, ON N1G 2W1, Canada
[c]University of Göttingen, Institute for Microbiology and Genetics and Göttingen Center for Molecular Biosciences (GZMB), Department of Molecular Microbiology and Genetics, 37077 Göttingen, Germany

ORCID IDs: 0000-0001-8875-6336 (F.K.K.); 0000-0002-5941-6399 (N.M.D.); 0000-0003-0323-7591 (H.E.K.); 0000-0003-0761-9175 (P.S.); 0000-0001-9627-031X (K.S.); 0000-0003-4430-819X (O.V.); 0000-0002-3117-5626 (G.H.B.); 0000-0002-6915-7407 (R.T.M.); 0000-0003-0737-3822 (T.I.).

The developmental program of seed formation, germination, and early seedling growth requires not only tight regulation of cell division and metabolism, but also concerted control of the structure and function of organelles, which relies on specific changes in their protein composition. Of particular interest is the switch from heterotrophic to photoautotrophic seedling growth, for which cytoplasmic lipid droplets (LDs) play a critical role as depots for energy-rich storage lipids. Here, we present the results of a bottom-up proteomics study analyzing the total protein fractions and LD-enriched fractions in eight different developmental phases during silique (seed) development, seed germination, and seedling establishment in Arabidopsis (*Arabidopsis thaliana*). The quantitative analysis of the LD proteome using LD-enrichment factors led to the identification of six previously unidentified and comparably low-abundance LD proteins, each of which was confirmed by intracellular localization studies with fluorescent protein fusions. In addition to these advances in LD protein discovery and the potential insights provided to as yet unexplored aspects in plant LD functions, our data set allowed for a comparative analysis of the LD protein composition throughout the various developmental phases examined. Among the most notable of the alterations in the LD proteome were those during seedling establishment, indicating a switch in the physiological function(s) of LDs after greening of the cotyledons. This work highlights LDs as dynamic organelles with functions beyond lipid storage.

While the sporophyte of angiosperms is photoautotrophic during most of its life cycle, it is largely heterotrophic during its initial formation, including embryo development and early seedling establishment. Toward that end, the growing embryo is protected during seed formation by the mother plant, which provides it with nutrients for embryo growth and the accumulation of storage compounds needed later for seed germination and seedling establishment. In Arabidopsis (*Arabidopsis thaliana*) seeds, a combination of storage proteins and lipids accumulates in the embryo, with a minor proportion also being deposited in the endosperm (Penfield et al., 2005). This leads to seeds that contain up to 40% of their dry weight in lipids (Baud et al., 2002), most of which are in the form of neutral lipids, such as triacylglycerols (TAGs) and sterol esters, and that are compartmentalized and stored in cytoplasmic lipid droplets (LDs). LDs in seeds typically range in size from 0.5 to 2 μm and comprise up to ~60% of the volume of a mature embryonic cell, making them, along with storage vacuoles, the most abundant organelles (Mansfield and Briarty, 1992; Tzen et al., 1993; Kretzschmar et al., 2018). The proper mobilization of these storage lipids within LDs during germination and seedling establishment is essential for providing the growing plant with carbon and energy. However, while the major function of LDs in seeds is related to energy storage, which is relatively well understood in terms of the

[1]This work was supported by the Deutsche Forschungsgemeinschaft (DFG; IS 273/2-2 to T.I., INST1525/16-1 FUGG to Jörg Großhans, and DFG-GZ: INST 186/1230-1 FUGG to Stefanie Pöggeler), the Studienstiftung des Deutschen Volkes (to F.K.K. and P.S.), the U.S. Department of Energy, Office of Science, BES-Physical Biosciences Program (DE-SC0016536, in part to R.T.M.) to support *N. benthamiana* experiments, and the Natural Sciences and Engineering Research Council of Canada (RGPIN-2018-04629 to R.T.M.).

[2]These authors contributed equally to the article.
[3]Author for contact: tischeb@uni-goettingen.de.
[4]Senior author.
The author responsible for distribution of materials integral to the findings presented in this article in accordance with the policy described in the Instructions for Authors (www.plantphysiol.org) is: Till Ischebeck (tischeb@uni-goettingen.de).

F.K.K., G.H.B., R.T.M., and T.I. designed the work, F.K.K., N.M.D., H.E.K., P.S., K.S., O.V., and T.I. performed research, F.K.K., H.E.K., P.S., K.S., G.H.B., and T.I. analyzed data, and F.K.K., N.M.D., R.T.M., and T.I. wrote the manuscript. All authors critically read and revised the manuscript and approved the final version.
[OPEN]Articles can be viewed without a subscription.
www.plantphysiol.org/cgi/doi/10.1104/pp.19.01255

metabolic pathways involved, the roles of LDs after seedling establishment, and later in development in vegetative tissues (i.e. leaves, roots, and stems), are far less understood.

A variety of proteins are known to be associated with the surface of LDs in plant cells and to carry out specific structural and/or enzymatic functions (Chapman et al., 2019). Among these so-called LD proteins, three major families, oleosins, steroleosins, and caleosins, have been relatively well characterized in terms of their association with LDs and participation in LD biology. Oleosins, for instance, were the first family of plant LD proteins discovered (Qu et al., 1986; Vance and Huang, 1987) and are predominantly expressed in the seeds and pollen, where they are the most abundant proteins on LDs (Huang, 2017). The functions of oleosins include roles in the formation of nascent LDs at the endoplasmic reticulum (ER), as well as preventing the fusion and coalescence of mature LDs (Siloto et al., 2006; Shimada et al., 2008). Steroleosins (also referred to as HYDROXYSTEROID DEHYDROGENASES [HSDs]) are homologs of metazoan sterol dehydrogenases (Lin et al., 2002), which mediate the homeostasis of steroid-derived hormones (Chapman et al., 2012). While the substrates and products of steroleosins remain to be determined, they are thought to play a role in brassinosteroid metabolism (Li et al., 2007; Baud et al., 2009). Caleosins are calcium-binding and heme-containing peroxygenases that, like oleosins, accumulate primarily in seeds (Naested et al., 2000; Hanano et al., 2006), although their function is not known. In leaves, however, caleosins appear to work in close coordination with another LD protein, α-dioxygenase (α-DOX), to produce 2-hydroxy-octadecatrienoic acid that can act as a phytoalexin, indicating that LDs serve as a production site for antimicrobial compounds within the plant cell (Shimada et al., 2014). Other LD proteins involved in the generation of oxylipins are lipoxygenases in cucumber (*Cucumis sativus*; Rudolph et al., 2011) and a lipase from tomato (*Solanum lycopersicum*; Garbowicz et al., 2018). Homologs of the latter in castor bean (*Ricinus communis*) and Arabidopsis localize to LDs and catalyze the hydrolysis of lipids, including TAG (Eastmond, 2004; Müller and Ischebeck, 2018).

With ongoing advances in proteomic techniques, it is becoming increasingly easier to detect proteins that are of relatively low abundance. This has facilitated the discovery of LD proteins in recent years, and in doing so has presented an increasingly complex picture of the functional roles of LDs in plants (Pyc et al., 2017b). For instance, the identification of the LD-ASSOCIATED PROTEIN (LDAP) family has provided insights into the function of LDs in vegetative tissues. Originally identified in the LD proteome of the mesocarp of avocado (*Persea americana*; Horn et al., 2013), LDAPs were subsequently shown to be ubiquitously expressed in Arabidopsis and to influence LD abundance in leaves (Gidda et al., 2016), as well as conferring resistance to drought stress (Kim et al., 2016). Additionally, an interacting protein of the LDAPs, referred to as LDIP (LDAP-INTERACTING PROTEIN) has since been identified (Pyc et al., 2017a). While the physiological role of LDIP remains to be determined, its ubiquitous expression, LD localization, and unique LD phenotype in the leaves of mutant plants (i.e. enlarged LDs) suggest that it is important in LD biogenesis and/or turnover. Another recently discovered plant LD protein is a member of the UBX domain-containing (PUX) protein family, PUX10, which was shown to localize to LDs in the tobacco (*Nicotiana tabacum*) pollen tube and Arabidopsis seeds, and appears to play a role in the polyubiquitination pathway for degradation of other LD proteins (Deruyffelaere et al., 2018; Kretzschmar et al., 2018). Evidence for this latter conclusion include a delay in the turnover of LD proteins, including the oleosins, during seed germination in the *pux10* mutant, which is consistent with the oleosins being a substrate for the ubiquitin-proteasomal pathway (Hsiao and Tzen, 2011; Deruyffelaere et al., 2015).

Despite the above-mentioned examples, only a few other plant LD proteins have been identified, which is conspicuous considering the relatively large number of LD proteins that have been found in other evolutionarily diverse organisms, such as yeast and animals, and the correspondingly wide range of cellular functions ascribed to these proteins (Du et al., 2013; Bersuker et al., 2018; Zhang and Liu, 2019). Moreover, given the general conservation that appears to exist in LD functioning and biogenesis/turnover among different organisms (Chapman et al., 2019), including plant versus nonplant species, there are likely many as yet unidentified plant LD proteins that carry out comparable, as well as plant-specific, functions.

Proteomic approaches have been used with a variety of plant species as a means to inventory proteins involved in specific processes during growth and development, in certain organs and tissues, and/or in response to an environmental cue (Eldakak et al., 2013). Also, seeds of several plant species have been the focus of previous proteomics-based studies (Hajduch et al., 2005; Li et al., 2016; Wang et al., 2016). In studies on Arabidopsis seeds, for example, often two or more conditions are compared to each other, such as the influence of different hormones (Chibani et al., 2006; Yin et al., 2015; Li et al., 2016) or stress (Lee et al., 2015; Fercha et al., 2016; Xu et al., 2017). Similarly, proteomics approaches have been used to study Arabidopsis seed dormancy, ripening, and aging (Gallardo et al., 2001; Chibani et al., 2006; Kubala et al., 2015; Nguyen et al., 2015; Yin et al., 2015), seed development (Hajduch et al., 2010; Lorenz et al., 2018), germination (Quan et al., 2013; Durand et al., 2019), and seedling establishment. However, none of these latter studies provided a comparative analysis of proteomes from these different developmental stages, nor a proteome of any specific organelle(s), such as LDs.

Here, we present the results of a study using a state-of-the-art proteomics platform to survey tissues from two stages during Arabidopsis silique development and six stages during seed germination and early

seedling establishment. Additionally, we analyzed the proteome of an LD-enriched fraction for each developmental stage and discovered six proteins that localize to LDs, as confirmed by fluorescence microscopy. Our proteomics survey also allowed us to follow the dynamics of LD protein composition through silique development, germination, and seedling establishment, which will undoubtedly serve to help inform further research aimed at understanding the molecular mechanisms underlying LD (protein) biology in plants and will provide a better understanding of these developmental stages in Arabidopsis in general.

RESULTS

A Proteomic Analysis of Arabidopsis Tissues from Silique Development to Seedling Establishment

In order to gain more insight into the proteins mediating the processes underlying silique development, seed germination, and seedling establishment in Arabidopsis, we investigated the proteome at each of these stages using label-free tandem mass spectrometry (MS/MS). More specifically, proteins were isolated from two phases of silique growth, corresponding roughly to seed maturation (referred to as Phase I siliques, 7–14 d after fertilization [DAF]) and desiccation (i.e. Phase II siliques, 14–21 DAF), as previously defined (Fig. 1A; Baud et al., 2002). Additionally, proteomes during seed germination and seedling establishment were monitored using rehydrated mature seeds, stratified seeds, and seedlings at 24, 36, 48, and 60 h after stratification (Fig. 1A). In the latter experiments, seeds had completed germination, as defined by radicle emergence after 24 h in long-daylight conditions at 22°C. By 48 h, seedling cotyledons had emerged and opened, and by 60 h, they were dark green.

For each developmental stage examined, total cellular extracts and LD-enriched fractions were generated in five biological replicates. As described in more detail in the "Materials and Methods" section, peptides derived from both fractions were analyzed by liquid chromatography (LC)-MS/MS, and the MS raw data files were processed using MaxQuant software to identify proteins (Supplemental Datasets S1–S4). Protein intensities were determined by both the intensity-based absolute quantification (iBAQ) and the label-free quantification (LFQ) algorithms (Cox and Mann, 2008; Cox et al., 2014). iBAQ and LFQ values were then calculated as per mille of all intensities in each sample to obtain relative iBAQ (riBAQ) and relative LFQ (rLFQ) values. When calculating enrichment factors for protein identification (i.e. the relative protein abundance in the LD-enriched fraction divided by the relative abundance in the total fraction), riBAQ values were used.

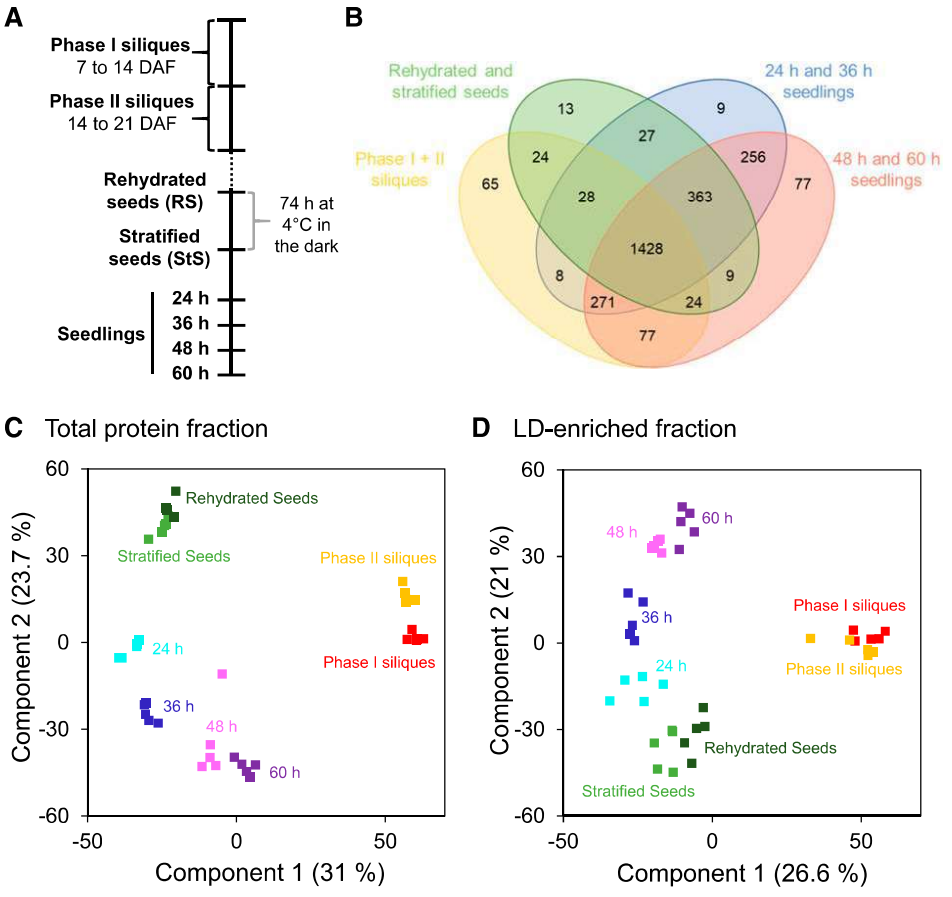

Figure 1. Graphical representation of proteomic data derived from Arabidopsis siliques, seeds, and seedlings. A, Tissues were collected from two developmental stages of silique development (phase I, 7–14 DAF; phase II, 14–21 DAF) and six stages of seed germination and seedling establishment (rehydrated seeds, stratified seeds, and seedlings from 24 to 60 h of growth). B, Venn diagram of the distribution of all detected proteins from each of the different developmental stages examined. Proteins identified with at least two peptides using the iBAQ algorithm were grouped into four groups, as depicted. Common proteins were identified via InteractiVenn (Heberle et al., 2015). C and D, PCA was performed to compare the distribution of the five biological replicates at each developmental stage for both the total protein and LD-enriched fractions. Numbers in brackets give the percentage of the total variance represented by Components 1 and 2, respectively.

For quantitative comparison of the total proteome of different stages (i.e. protein dynamics), rLFQ values were used. In total, we detected 2,696 protein groups identified by at least two peptides, based on the iBAQ data processing algorithm (Table 1). The number of protein groups was lowest in older (Phase II) siliques and rehydrated seeds and highest during the late stages of seedling establishment.

As shown in Figure 1B, more than half of the total protein groups detected (i.e. 1,428 of 2,696) were shared between all of the developmental stages examined, while a wide range of other proteins were unique for certain stages. In principal component analysis (PCA) plots, the total protein and LD-enriched protein groups from the five biological replicates of each stage clustered closely together (Fig. 1, C and D; Supplemental Datasets S5–S10), indicating good reproducibility of protein sampling and processing. The PCA plots also reflected the unique proteome of siliques compared to the other tissues, based on their separation in component 1 for both the total protein and LD-enriched protein fractions (Fig. 1, C and D). This unique proteome is likely based, in part, on the inclusion of silique wall material in these samples. Further, the distribution along component 2 indicated in both total and LD-enriched protein fractions that the younger siliques (Phase I) are more similar to older (60 h) green seedlings, while the older siliques (Phase II) are more similar to rehydrated or stratified seeds. The fact that siliques are more similar to seedlings than seeds in component 2 may be because of the high content of silique wall cells in addition to developing seed cells. Likewise, along component 2, the seeds and seedlings are distributed in a stage-dependent manner, with rehydrated seeds and 60 h seedlings being the most distinct (Fig. 1, C and D).

Unique Proteins Exist in the Seed and Early Seedling Total Protein Proteomes

One objective for generating an extensive proteomics dataset for Arabidopsis during seed development, germination, and post-germinative growth was to identify developmental-stage-specific proteins potentially involved in distinct cellular processes during these time points in the plant's life cycle, such as during seed desiccation and the switch in the seedling from hetero- to photoautotrophic growth. Toward that end, we performed hierarchical clustering after data normalization to analyze our total proteome datasets for proteins that were increased in abundance during these developmental phases (Supplemental Datasets S11 and S12). In total, 40 clusters were defined, and clusters containing >20 proteins are presented as a heat map in Figure 2A. Notably, four of the clusters contain proteins that are highest in abundance during either the two seed stages (i.e. Fig. 2, A and B, RS and StS, Clusters 1 and 2) or the two earliest stages of seedling establishment (i.e. 24 and 36 h after stratification; Clusters 11 and 12; Fig. 2, A and C). In Clusters 1 and 2, for instance, we found 71 proteins (Supplemental Dataset S12), including several late-embryogenesis-abundant proteins, two cell wall-modifying enzymes, and several proteins of unknown function. While seed storage proteins like CRUCIFERIN2 and CRUCIFERIN3 also have their highest intensities during the seed stages, their degradation is slower than that of the proteins present in Clusters 1 and 2. Clusters 11 and 12 contained 70 proteins (Supplemental Dataset S12), including several involved in either β-oxidation, such as LONG-CHAIN ACYL-COA SYNTHETASE7 (LACS7), ACYL-COA OXIDASE1 (ACX1), and enoyl-CoA hydratase ABNORMAL INFLORESCENCE MERISTEM1 (AIM1), or lipid metabolism, such as CYCLOARTENOL SYNTHASE (CAS) and OIL BODY LIPASE1 (OBL1). On the other hand, glyoxylate cycle enzymes, such as the peroxisomal NAD-MALATE DEHYDROGENASE1 or MALATE SYNTHASE, were grouped in Cluster 10, which, like Clusters 11 and 12, was also highest in abundance at 36 h after stratification, but remained so during later stages of seedling establishment.

We also applied a gene ontology (GO) term analysis of our proteomics datasets (Fig. 3; Supplemental Datasets S13–S15) by assigning all of the associated GO terms to every protein identified in the total protein fractions for each developmental stage. Thereafter, rLFQ intensities of all proteins assigned to each GO term were summed. As presented in Figure 3, the GO

Table 1. *Summary of proteins identified in the total protein and LD-enriched protein fractions derived from Arabidopsis siliques, seeds, and seedlings, and the percentage of LD proteins within all samples*

iBAQ-processed proteomic data of both the total protein fraction and the LD-enriched fraction was filtered for at least two peptides per protein group. Then, the relative abundance of LD-associated proteins in the LD-enriched fraction was calculated based on their iBAQ scores. LD proteins were chosen taking into account protein families known and identified in this work.

Developmental Stage	Total Protein Fraction	LD-Enriched Fraction	% of LD Proteins in LD-Enriched Fraction
Phase I siliques	1,723	1,266	16.8 ± 4.4
Phase II siliques	1,417	1,337	17.5 ± 1.1
Rehydrated seeds	1,425	1,353	31.8 ± 1.5
Stratified seeds	1,511	1,024	31.8 ± 8
24 h seedlings	2,004	1,158	24.3 ± 7.9
36 h seedlings	2,197	1,368	25.9 ± 5.1
48 h seedlings	2,218	1,478	28.5 ± 4.5
60 h seedlings	2,198	1,723	34.1 ± 12.2

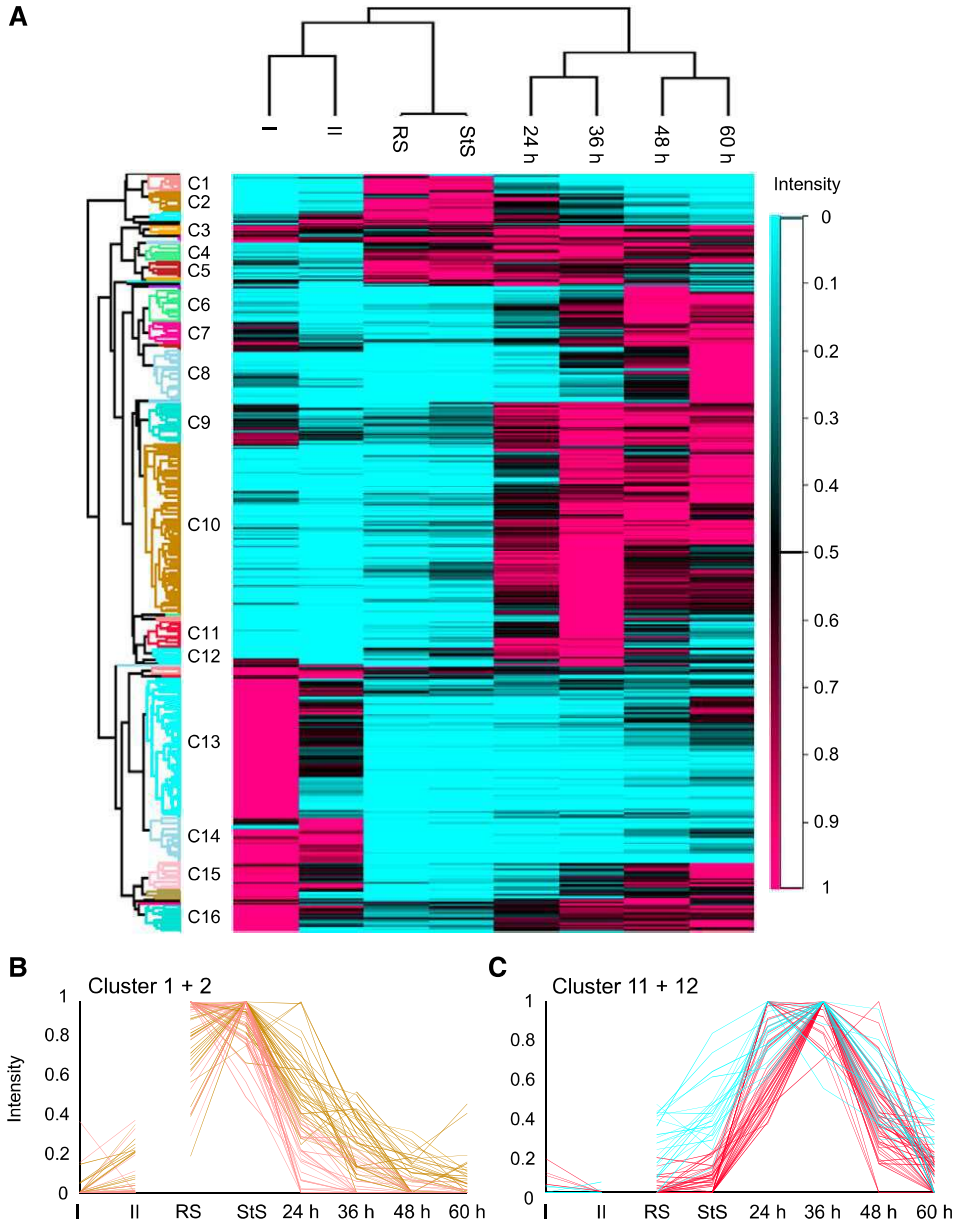

Figure 2. Identification of protein abundance clusters in total protein fractions derived from Arabidopsis siliques, seeds, and seedlings. A, Hierarchical clustering analysis of the normalized protein abundance over each of the developmental stages examined. In total, 40 row clusters were defined. Clusters harboring >20 proteins are labeled C1–C16. B and C, The expression profiles of all proteins in Clusters 1 and 2 (B; pink and brown lines; seed-specific proteins) and Clusters 11 and 12 (C; red and blue lines; early seedling establishment proteins) are shown. As silique samples also contain proteins derived from the silique wall, they should not necessarily be considered seed precursors, as indicated by the interrupted line between the II and RS samples. I, Phase I siliques; II, phase II siliques; RS, rehydrated seeds; StS, stratified seeds; 24 to 60 h, seedlings 24 to 60 h after stratification.

term analysis revealed some important general trends. For instance, proteins involved in the "fatty acid biosynthesis process" were more abundant during silique (seed) development, and proteins associated with "nutrient reservoir activity" were of highest abundance during the seed stages. Further, proteins involved in GO-term-defined processes related to seedling establishment were upregulated during this phase (i.e. 24- to 60-h seedlings). These include proteins involved in "Fatty acid β-oxidation" and the "Glyoxylate cycle," as well as the "Proteasome-mediated ubiquitin-dependent protein catabolic process," which, as mentioned in the the first section. reflects, at least in part, the proteasomal degradation of LD proteins but also of other proteins. There was also a higher abundance of proteins with GO terms associated with photoautotrophic growth (e.g. "Chlorophyll biosynthetic process" and "Reductive pentose-phosphate cycle") at the later stages of seedling establishment (i.e. 48- and 60-h seedlings).

We next analyzed the subcellular localization of the proteins. For this, we used the proteomics-confirmed annotation dataset at the Plant Proteome Database (Sun et al., 2009). This dataset contains 78 different subcellular annotations that we summed up to 10 different localizations: plastid, ER, vacuole, peroxisome, Golgi apparatus, mitochondrion, nucleus, cytoplasm, plasma membrane, and plastoglobule. The LD annotation was performed by us based on previous studies and taking into account LD proteins identified in this study (see later). Overall, the largest changes in abundance were observed for the proteins annotated as plastidial (Table 2; Supplemental Datasets S16–S18), with their abundance changing ~10-fold between

GO term		n TF	n total	Phase I silique	Phase II siliques	Stratified seeds	Imbibed seeds	24 h seedlings	36 h seedlings	48 h seedlings	60 h seedlings
Biological process:											
Cell wall organization	GO:0071555	24	288	3.4	1.7	1.3	1.5	3.0	4.9	3.2	2.3
Chlorophyll biosynthetic process	GO:0015995	30	43	1.4	0.4	0.1	0.1	2.2	8.8	14.6	16.4
Endocytosis	GO:0006897	5	56	0.0	0.0	0.0	0.1	1.1	1.4	0.4	0.2
Fatty acid beta-oxidation	GO:0006635	18	40	0.9	0.4	2.3	2.1	7.8	8.8	8.2	6.2
Fatty acid biosynthetic process	GO:0006633	33	94	4.7	2.6	2.2	1.9	1.9	2.5	2.7	2.8
Gluconeogenesis	GO:0006094	19	22	65.2	37.5	15.5	16.4	24.6	33.1	40.0	41.1
Glycolytic process	GO:0006096	46	69	97.6	56.3	20.0	21.0	28.5	39.5	55.4	60.7
Glyoxylate cycle	GO:0006097	6	7	1.5	0.9	2.9	5.9	36.7	49.6	31.7	20.0
Intracellular protein transport	GO:0006886	51	244	4.7	2.2	0.7	0.9	3.6	4.3	2.4	3.2
Lipid storage	GO:0019915	9	27	4.7	12.1	10.7	12.5	7.3	4.6	2.5	1.2
Lipid transport	GO:0006869	22	147	7.0	9.4	4.6	4.7	2.0	1.1	1.4	0.3
Mitotic cell cycle	GO:0000278	12	85	2.0	0.4	0.4	0.3	5.2	9.7	9.8	10.1
mRNA processing	GO:0006397	18	174	1.1	0.4	0.3	0.3	1.5	2.5	2.2	4.1
Photosynthesis	GO:0015979	65	124	130.6	87.2	1.0	1.1	4.5	14.2	36.4	67.2
Proteasome-mediated ubiquitin-dependent protein catabolic process	GO:0043161	35	97	3.7	1.8	0.8	2.4	4.2	4.9	3.3	3.2
Protein catabolic process	GO:0030163	27	96	9.1	7.7	5.1	7.2	7.9	7.1	5.6	6.8
Reductive pentose-phosphate cycle	GO:0019253	15	19	137.8	81.5	6.3	5.9	15.8	65.4	166.6	207.5
Starch biosynthetic process	GO:0019252	12	33	5.2	2.4	0.2	0.4	0.7	1.3	1.8	2.7
Tricarboxylic acid cycle	GO:0006099	34	54	6.6	3.9	7.5	10.6	47.5	63.5	44.3	31.6
Cellular component:											
Cul4-RING E3 ubiquitin ligase complex	GO:0080008	7	124	0.0	0.0	0.0	0.0	0.6	0.8	0.4	0.4
Cytosolic ribosome	GO:0022626	146	194	133.2	75.7	18.0	24.5	81.5	157.6	263.7	287.4
Proteasome complex	GO:0000502	45	81	4.2	1.9	1.0	3.2	6.1	7.3	4.9	4.8
Molecular function:											
Nutrient reservoir activity	GO:0045735	25	68	96.7	302.2	520.8	503.3	370.2	233.7	127.4	65.7

Figure 3. Changes in protein intensity of functional groups, based on GO terms, in the total protein fractions derived from Arabidopsis siliques, seeds, and seedlings. Proteins were assigned to GO terms and the relative abundance (rLFQ) of all proteins within a GO term is shown for each stage examined. "*n* total" corresponds to the total number of genes assigned to one GO term, "*n* TF" to the number of proteins detected in the total cellular fraction assigned to this GO term. Darker red represents higher total intensities compared to the other growth stages. Shown are selected GO terms.

siliques and seeds, and between seeds and 60-h seedlings. On the other hand, the abundance of LD proteins nearly triples from younger to older siliques, is highest in rehydrated and stratified seeds, and decreases progressively in seedlings (Table 2; Supplemental Fig. S1).

Calculation of Enrichment Factors Enables the Identification of Low-Abundant LD Proteins in Arabidopsis

The second main objective of this work was to identify previously unidentified proteins associated with plant LDs, since further characterization of these proteins would undoubtedly aid in our understanding of LD functions and/or biogenesis, maintenance, and turnover. Our LD enrichment protocol (see "Materials and Methods" for details) avoided the use of harsh chemicals or extensive washing of the LDs in an effort to preserve weaker protein associations to the LDs and, thus, allowing us to potentially identify new, low-abundant LD proteins, albeit at the cost of perhaps including non-LD protein contaminants.

As shown in Table 1, >1,000 proteins were identified in each of the LD-enriched fractions from the different developmental stages examined. Known LD proteins (and those proteins described in this study) constituted between ~17% (in the siliques) and >30% (in seeds and 60-h seedlings) of the total protein content in the LD-enriched fractions (Table 1). To distinguish putative LD proteins from contaminating proteins, we calculated the LD-enrichment factor for each protein, i.e. the ratio of the protein's relative intensity in the LD-enriched fraction to its relative intensity in the total protein fraction (Supplemental Dataset S19). Further, in order to ensure that no other subcellular compartment(s) copurified with LDs, we also calculated the enrichment factors of proteins from different subcellular compartments (Supplemental Fig. S2). Overall, the LD-enrichment factors indicated that while occasionally some organelles copurified with LDs (i.e. enrichment factor >1), most had enrichment factors <1, and the enrichment factors were consistently the highest for LDs (ranging from 4.7 to 122.7; Supplemental Fig. S2). As LDs are ER derived (Chapman et al., 2019), our data could help to identify ER proteins that are localized at ER-LD junction sites. On the other hand, it is important to rule out ER proteins that are simply copurifying with LDs. We believe this to be unlikely, as the overall enrichment factors of previously annotated ER proteins

Table 2. *Annotation of subcellular localization of proteins in the total protein fractions derived from Arabidopsis siliques, seeds, and seedlings*

All proteins were annotated with 78 subcellular localizations obtained from the Plant Proteome Database and combined into 11 groups. The riBAQ intensities (in per mille) of the proteins were added up for 11 different subcellular compartments.

Localization	Phase I Siliques	Phase II Siliques	Rehydrated Seeds	Stratified Seeds	24 h Seedlings	36 h Seedlings	48 h Seedlings	60 h Seedlings
Plastid	571.3	392.3	44.1	40.0	52.4	154.0	334.3	477.5
ER	8.0	5.1	2.2	2.6	8.8	13.2	13.1	15.9
Vacuole	14.8	16.1	4.8	5.5	7.1	9.9	12.1	23.6
Peroxisome	15.1	9.8	9.6	10.0	22.7	26.6	26.4	21.2
Golgi apparatus	0.3	0.2	0.5	0.6	1.1	1.4	0.7	0.5
Mitochondrion	22.8	13.5	9.0	10.7	32.0	39.5	33.9	34.5
Nucleus	29.1	18.7	17.3	19.3	29.2	34.3	35.8	26.8
Cytoplasm	67.8	28.3	40.3	48.3	148.1	195.7	205.9	183.5
Plastoglobule	12.3	14.1	0.8	0.8	0.9	2.0	5.1	6.4
Plasma membrane	15.4	9.1	2.5	3.0	6.3	8.9	9.3	9.2
LD	9.1	25.3	57.4	69.8	37.9	18.8	8.3	4.8

only reached a highest value of 2.1 in 60-h seedlings, while LD proteins had an overall enrichment factor of 122.7 in this stage (Supplemental Fig. S2). Also, none of the annotated ER proteins showed large enrichment factors that would make them strong candidates to be LD proteins (Supplemental Fig. S3).

To narrow down candidate LD proteins from the extensive proteome of the LD-enriched fraction(s), we calculated enrichment factors for each protein and tested whether this enrichment was statistically significant. In doing so, we obtained a *P*-value based on on a two-sided *t* test (Supplemental Dataset 19). For each protein, we chose the stage where its abundance was relatively highest, only considering proteins that were identified in at least four of the five replicates in this stage, and had a riBAQ of at least 0.1 ‰. These data were used to generate the volcano plot shown in Figure 4. In total, 291 proteins significantly enriched in the LD-enriched fraction were found (refer to proteins on the right side of the plot in Fig. 4). Among these were most previously known LD proteins, including oleosin, steroleosin, and caleosin family members, as well as the LDAPs. Also prevalent in the LD-enriched fraction were several promising candidate LD proteins, which were chosen based on their strong enrichment and high *P*-value. On the other hand, overall abundance was less of a factor for selection, and several of the candidate LD proteins had a riBAQ of <0.4 ‰ in the LD-enriched fraction (Table 3) and were not among the top 100 most abundant proteins therein (based on data included in Supplemental Dataset S4).

The subcellular localization of the candidate LD proteins was subsequently assessed using two independent plant cell systems that are both well established for the study of protein trafficking and localization, including to LDs: *N. tabacum* pollen tubes transformed by particle bombardment (Fig. 5; Supplemental Fig. S4; Müller et al., 2017) and *Nicotiana benthamiana* leaves transformed by *Agrobacterium tumefaciens* infiltration (Fig. 6; Cai et al., 2015; Gidda et al., 2016). In both cases, full-length open reading frames (ORFs) encoding candidate LD proteins were cloned as mVenus or mCherry fluorescent protein fusions and transiently expressed, and subcellular localization then was assessed by confocal laser-scanning microscopy. LD localization of fusion proteins was determined by staining of LDs with the neutral lipid stains Nile red (Greenspan et al., 1985) or BODIPY493/503 (Listenberger and Brown, 2007).

In total, the LD localization of six proteins was confirmed using both plant cell systems (Figs. 5 and 6). We termed these proteins LD-ASSOCIATED LIPASE1 (LIDL1), LD METHYLTRANSFERASE1 (LIME1), LD PROTEIN OF SEEDS (LDPS), SEED LD PROTEIN1 (SLDP1), LD-ASSOCIATED HYDROLASE1 (LDAH1), and LD DEHYDROGENASE1 (LDDH1), taking into account their functional annotations at The Arabidopsis Information Resource (TAIR) and their expression patterns based on the Arabidopsis eFP Browser tool at the Bio-Analytic Resource for Plant Biology

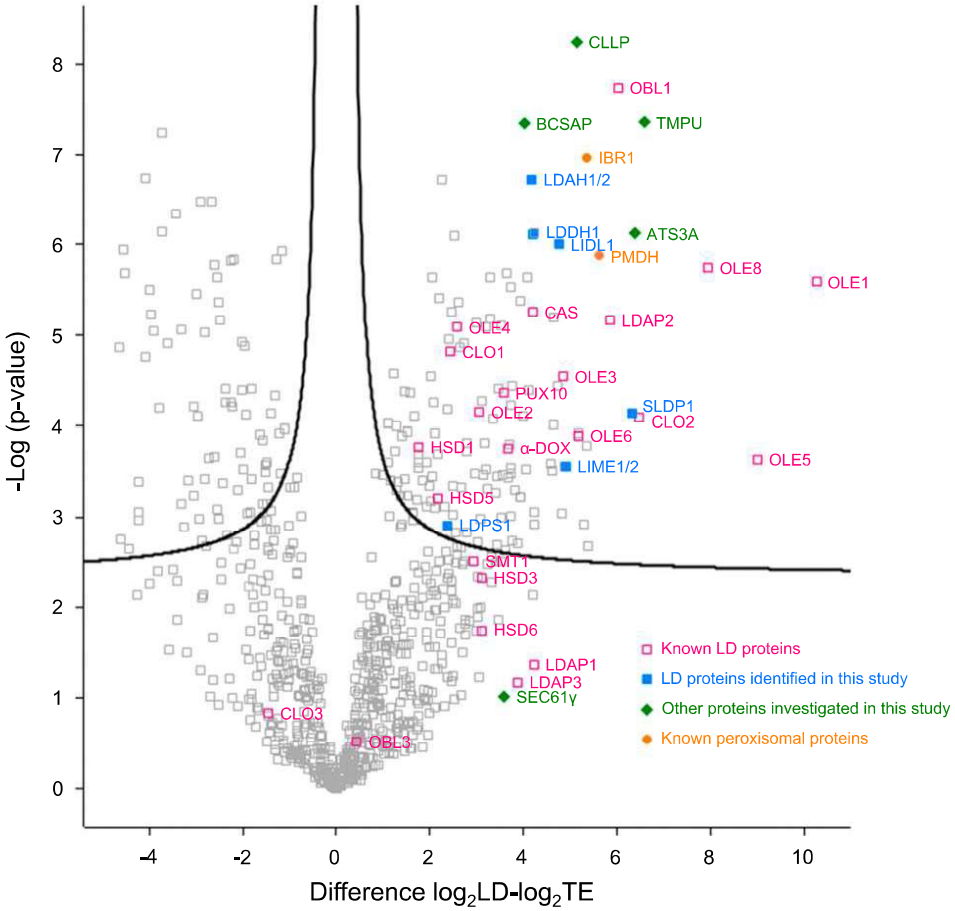

Figure 4. Enrichment analysis of proteins in the LD-enriched fractions derived from Arabidopsis siliques, seeds, and seedlings. A volcano plot was constructed to visualize proteins that are significantly LD enriched (upper right). The developmental stage (siliques, seeds, and seedlings) with the highest abundance (riBAQ) was chosen for each protein and the $\log_2$-transformed values and *P*-values were calculated at this stage. Only proteins detected in four of the five replicates and with an riBAQ >0.1 are included in this figure. As depicted in the legend, known LD and peroxisomal proteins are indicated in blue and orange, respectively, and the proteins chosen for further study that did or did not localize to LDs in pollen tubes and tobacco leaves are shown in blue and green, respectively. Black lines indicate a false discovery rate of 0.001. Abbreviations: ATS3A, EMBRYO-SPECIFIC PROTEIN; BCSAP, BRISC COMPLEX SUBUNIT ABRO1-LIKE PROTEIN; CCLP, CURCULIN-LIKE LECTIN FAMILY PROTEIN; SMT, STEROL METHYLTRANSFERASE; TMPU, TRANSMEMBRANE PROTEIN OF UNKNOWN FUNCTION.

(https://bar.utoronto.ca/efp/cgi-bin/efpWeb.cgi). Other proteins, although initially selected as promising candidates due to their highly significant, strong enrichment in LD-enriched fractions (Fig. 4), did not localize to LDs, based on experiments in pollen tubes (Supplemental Fig. S4), although at least one of these proteins, SEC61γ, which is a subunit of the Sec translocon at the ER membrane (Spiess et al., 2019), appeared to localize to regions of the ER that in some instances were in close proximity to or encircled LDs (Fig. 7). These results with SEC61γ are intriguing because they are reminiscent of the localization of SEIPIN in plant cells, an ER membrane protein involved in the formation of nascent LDs (Cai et al., 2015), suggesting that SEC61γ might also function at ER-LD junctions.

Another candidate protein assessed in terms of its subcellular localization was the OIL BODY-ASSOCIATED PROTEIN1A (OBAP1A). OBAPs were described previously to be localized to LDs, based on studies with a maize (*Zea mays*) protein isoform (López-Ribera et al., 2014). However, all three Arabidopsis OBAPs identified in this study (i.e. OBAP1A, OBAP2, and OBAP3) were only slightly enriched in the LD-enriched fraction during the silique stage and were strongly depleted in LDs during all other phases examined, including those stages where their abundance in total protein fractions was highest (i.e. rehydrated and stratified seeds; Supplemental Fig. S4A; refer also to Fig. 4). These results are consistent with our previous reported Arabidopsis seedling LD proteomes (Pyc et al., 2017a; Kretzschmar et al., 2018), in which OBAPs were not enriched. Consistent with these observations, when transiently expressed as either C- or N-terminal-tagged mVenus fusion proteins in tobacco pollen tubes, OBAP1A displayed exclusively a diffuse fluorescence, indicative of its localization to the cytoplasm, and there were no obvious associations with any distinct subcellular compartment(s) (Supplemental Fig. S4B). Similarly, OBAP1A-mCherry transiently expressed in *N. benthamiana* leaf cells localized throughout the cell (i.e. cytoplasm) and did not appear to localize to BODIPY-stained LDs (Supplemental Fig. S4C).

The LD Proteome Changes during Seedling Establishment

In addition to the discovery of LD proteins (Figs. 5 and 6), we analyzed the dynamics of LD proteins in general, in terms of their relative abundance throughout the various stages of seed development, germination, and post-germinative growth. As presented in Table 1 and Supplemental Figure S1, the abundance of both previously known and newly identified LD proteins in the total proteome increased during seed development (i.e. in siliques), was relatively high in

Table 3. *Arabidopsis proteins chosen as LD protein candidates*

In part, proteins were named in this study. ATS3A, EMBRYO-SPECIFIC PROTEIN; BCSAP, BRISC COMPLEX SUBUNIT ABRO1-LIKE PROTEIN; CCLP, CURCULIN-LIKE LECTIN FAMILY PROTEIN; TMPU, TRANSMEMBRANE PROTEIN OF UNKNOWN FUNCTION.

Protein Name	AGI Code[a]	Homolog	Description[b]	Stage with Highest Abundance in LD Fraction	Abundance at Highest Stage (riBAQ ‰)	Enrichment Factor[c]	*P*-Value (−Log)[c]	Subcellular Localization[d]
ATS3A	AT2G41475.1	AT5G62200	Embryo-specific protein 3	48 h seedlings	1.17 ± 0.54	84.4	6.12	Non-LD foci
BCSAP	AT3G08780.1	–	BRISC complex subunit Abro1-like protein	60 h seedlings	0.17 ± 0.05	16.3	7.34	Cytoplasm
CCLP	AT1G78830.1	–	Curculin-like lectin family protein	60 h seedlings	0.36 ± 0.1	35.0	8.24	Non-LD foci
LDAH1	AT1G10740.1*	AT1G23330*	α/β-hydrolase	60 h seedlings	0.19 ± 0.07	19.1	6.72	LD
LDDH1	AT1G75180.1	AT1G19400	Dehydrogenase	60 h seedlings	0.26 ± 0.04	18.4	6.11	LD
LDPS	AT3G19920.1	AT5G64230	Unknown	Stratified seeds	0.31 ± 0.19	7.4	2.36	LD
LIDL1	AT1G18460.1	AT1G19360	Lipase family protein	60 h seedlings	0.31 ± 0.15	26.9	6.01	LD
LIME1	AT4G33110.1	AT4G33120	Coclaurine methyltransferase	48 h seedlings	1.12 ± 0.62	30.3	3.55	LD
OBAP1A	AT1G05510.1	AT5G45690	Oil body-associated protein	Rehydrated seeds	1.95 ± 1.19	0.22	2.65	Cytoplasm
SEC61γ	AT5G50460.1*	AT4G24920*	Subunit of SEC61 translocon	Stratified seeds	0.96 ± 1.2	11.9	1.02	ER/LD
SLDP1	AT1G65090.3	AT5G36100	Unknown	60 h seedlings	2.1 ± 0.45	17.5	6.31	LD
TMPU	AT1G27290.1	–	Transmembrane protein of unknown function	60 h seedlings	1.12 ± 0.47	97.0	7.36	ER subdomains

[a]Gene locus identifier according to the Arabidopsis Genome Initiative. The given splice variant corresponds to the one tested for subcellular localization. Arabidopsis Genome Initiative codes marked with an asterisk were not identified unambiguously. [b]Description based on TAIR10 annotation. [c]Enrichment factors and *P*-values were calculated from the given developmental stages at which the protein had the highest riBAQ intensity value in the LD-enriched fraction. Missing values were imputed with a value of 0.01. [d]Subcellular localizations found in this study

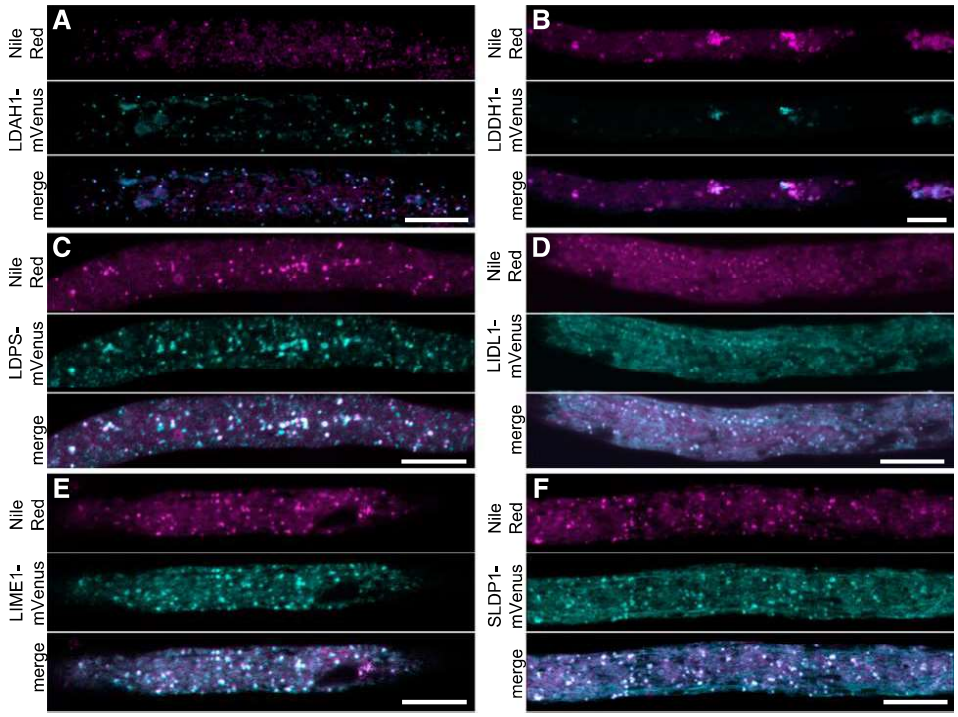

Figure 5. Subcellular localization of selected candidate LD proteins in *N. tabacum* pollen tubes. A to F, Candidate proteins fused to mVenus at their C termini were transiently expressed in *N. tabacum* pollen tubes (cyan channel). LDs were stained with Nile red (magenta channel). In the merge channel, colocalization appears white. Note, in B, that expression of LDDH1-mVenus led to clustering of LDs. Bars = 10 μm.

seeds (rehydrated and stratified seeds), and then progressively decreased in seedlings after germination, until 60 h after stratification when it was highest. Next, in order to further assess changes in the composition of the LD proteome during development, the abundance of all LD proteins was added in each stage, and the individual fraction for each protein was calculated (Supplemental Dataset S20).

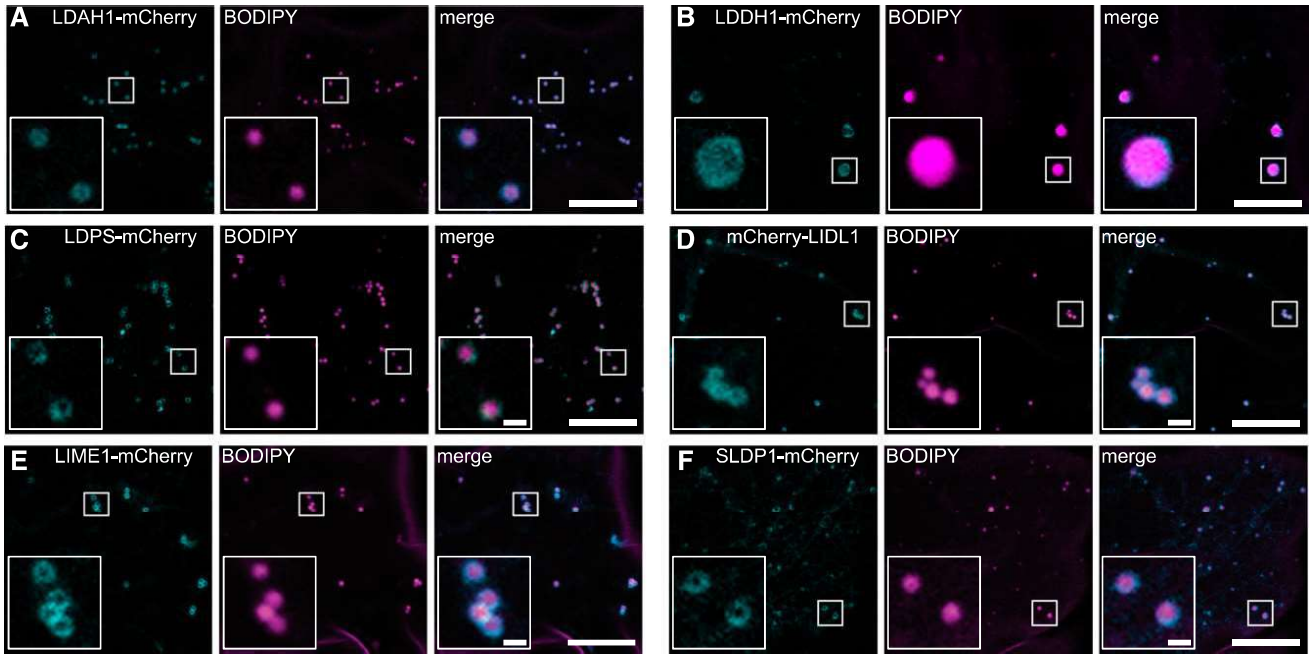

Figure 6. Subcellular localization of selected LD protein candidates in *N. benthamiana* leaves. A to F, Candidate proteins fused to mCherry at their N or C termini were transiently expressed in *N. benthamiana* leaves (cyan channel). LDs were stained with BODIPY 493/503 (magenta channel). In the corresponding merge channel, note that a torus fluorescence pattern attributable to the expressed fusion protein encircles the BODIPY-stained LDs. Boxes denote portions of the cells shown at higher magnification in the insets. Bars = 10 μm (1 μm in insets).

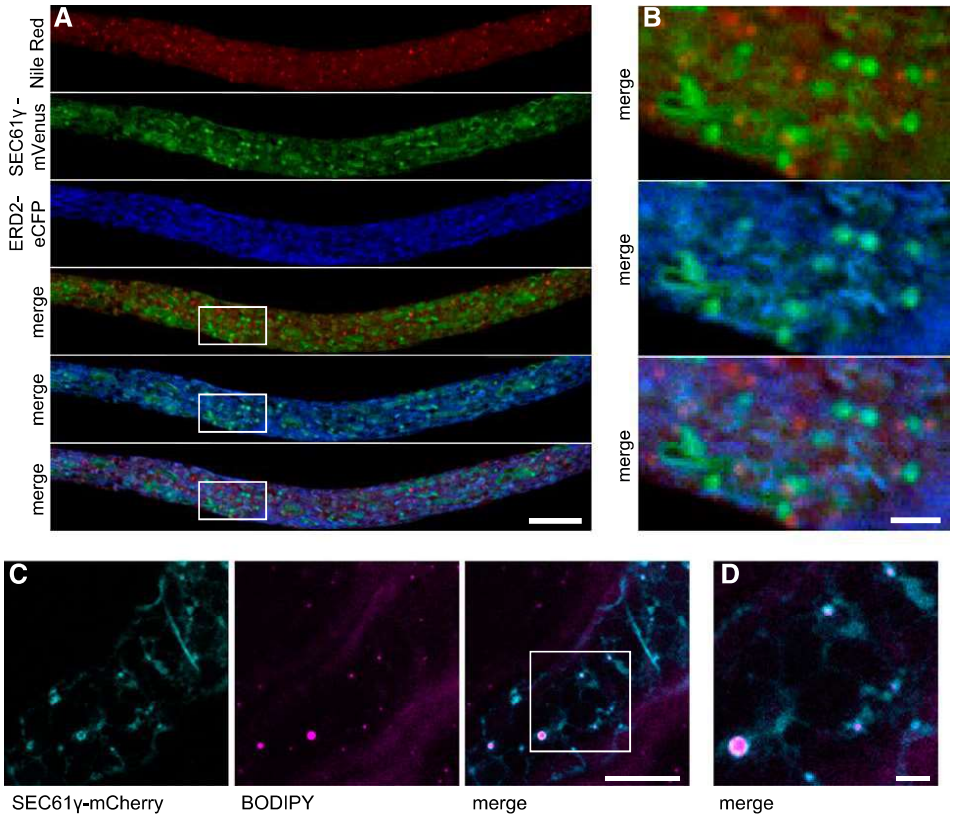

Figure 7. Subcellular localization of SEC61γ in tobacco pollen tubes and *N. benthamiana* leaves. SEC61γ fused at its C terminus to mVenus or mCherry was transiently expressed in *N. tabacum* pollen tubes (A and B) or in *N. benthamiana* leaves (C). LDs were stained with Nile red (A and B) or BODIPY 493/503 (C and D). SEC61γ was cotransformed with the ER marker ERD2-CFP (A and B) and partially colocalizes with the ER. SEC61γ also accumulates at potential ER-LD contact sites (B–D). The box in C indicates the area of the cells shown at higher magnification in D. Bars = 10 μm (A and C) or 2 μm (B and D).

Collectively, the most abundant oleosin protein family members (i.e. OLE1, OLE2, OLE4, and OLE5) contributed a relatively constant proportion of proteins in the LD proteome throughout seedling establishment (Fig. 8). By contrast, the prevalence of the most abundant caleosin, CLO1, and steroleosin, HSD1, continuously decreased during the same time period, while CLO2 and HSD2/3 increased. In general, >85% of the LD proteome during all of the developmental stages examined consisted of six proteins: OLE1, OLE2, OLE4, OLE5, CLO1, and HSD1. Less abundant LD proteins, on the other hand, displayed a wide range of dynamics (Fig. 8). For instance, while some of these proteins, such as LDIP, SLDP1, LDPS, and OBL1, were detected in the LD proteomes at most or all time points, their relative abundance varied considerably. The proportion of OBL1, for example, increases steadily over the course of seedling establishment, while that of LDPS decreases (Fig. 8). Several other proteins, e.g. LIDL1 and LIDL2, LIME1/2, LDAH1/2, and LDDH1/2, contribute only to the seedling LD proteomes, but not those of seeds or siliques. None of the LDAP protein isoforms, LDAP1–LDAH3, were detected in the seed LD proteomes, but were most abundant in siliques (LDAP1 and LDAP3) and seedlings (LDAP2; Fig. 8). Interestingly, α-DIOXYGENASE1, which was previously described to be specifically enriched at LDs during senescence (Brocard et al., 2017) and pathogen attack (Shimada et al., 2014), was present in the seedling LD proteome at 36 h and onward, suggesting that it might also have functions during early plant growth.

Phosphorylation and Ubiquitination of LD Proteins

It is well established that posttranslational modifications can influence the activity, localization, and/or fate (e.g. turnover) of a protein (Arsova et al., 2018). Two such modifications, phosphorylation and ubiquitination, have previously been identified on oleosins, caleosins, and steroleosins, and their ubiquitination has been implicated in their degradation (Hsiao and Tzen, 2011; Deruyffelaere et al., 2015; Kretzschmar et al., 2018). To assess whether other LD proteins are targets of similar posttranslational modifications, possibly as a means of (protein) regulation in the cell, we analyzed our proteomic dataset for peptides with appended phosphate and/or ubiquitin moieties. Overall, modifications were detected on 182 proteins, including the LD proteins CLO1, HSD1, LDAP2, OLE2, and OLE4 (Table 4; Supplemental Datasets S21–S30).

DISCUSSION

Growth Stage-Specific Proteomes Provide Extensive and Useful Data

We present here a quantitative proteomic dataset, generated with an Orbitrap MS, for Arabidopsis silique development, seed germination, and seedling establishment. Previous works investigating Arabidopsis seed germination (Gallardo et al., 2001; Galland et al., 2014) identified 67 and 475 proteins, respectively. Our data are consistent with those studies, but offer

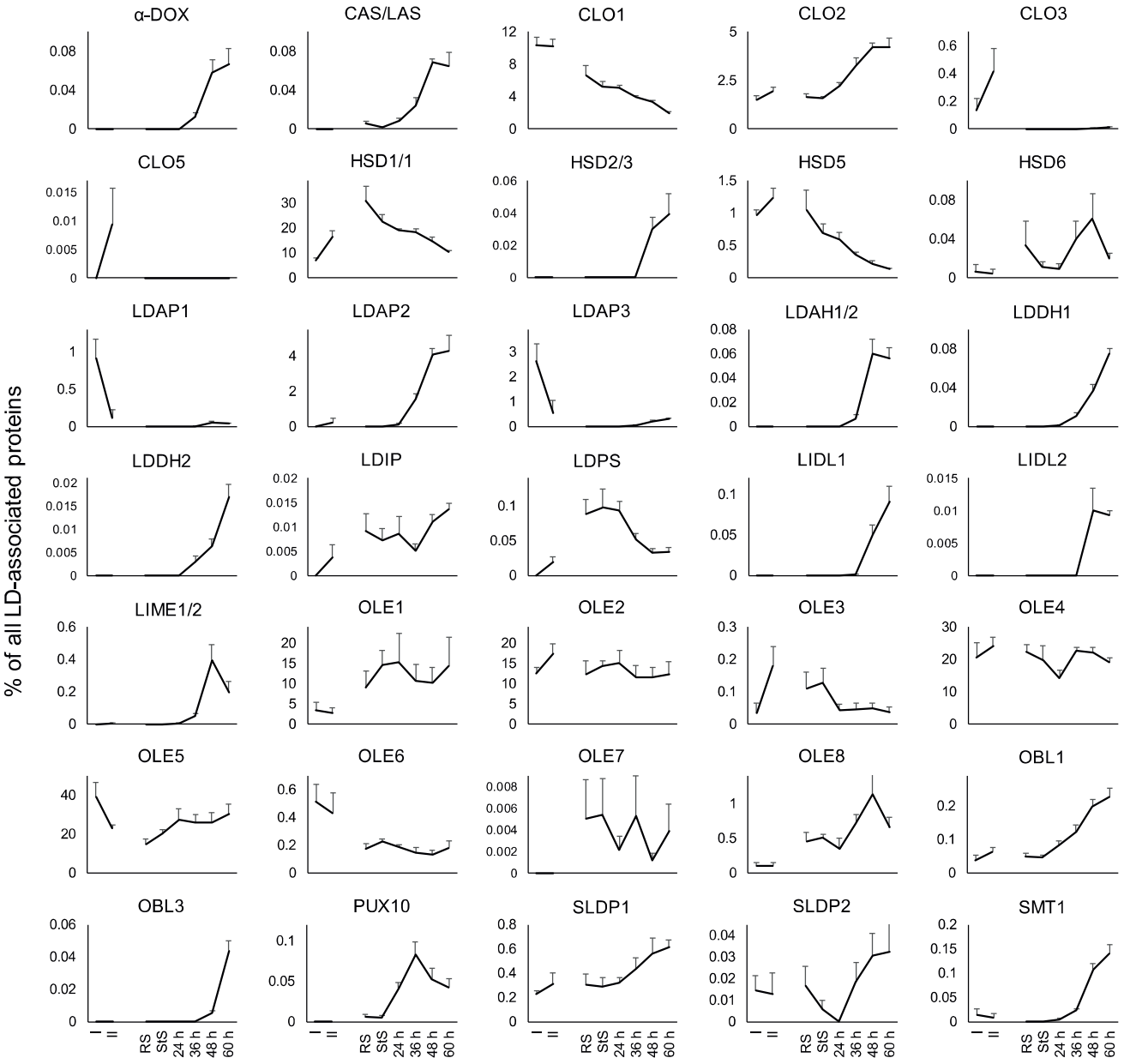

Figure 8. Dynamic composition of the LD proteome derived from Arabidopsis siliques, seeds, and seedlings. The riBAQ intensities of LD-associated proteins in the LD-enriched fraction were calculated as a percentage of the riBAQ of all known LD-associated proteins. This way, the contribution of each protein to the complete LD proteome and the dynamic changes in the abundance of the LD proteins can be observed. Protein isoform numbers separated by a slash indicate that these proteins could not be distinguished based on the proteomic data. Two highly similar genes of the steroleosin family are both annotated as HSD1. I, Phase I siliques; II, phase II siliques; RS, rehydrated seeds; StS, stratified seeds; 24 to 60 h, seedlings 24 to 60 h after stratification. As silique samples also contain proteins derived from silique wall, they should not necessarily be considered to be seed precursors, as indicated by the interrupted line between the II and RS samples. $n = 5$ per stage. Error bars represent the SD.

coverage of a relatively larger number of proteins across various developmental stages, including seedling establishment. In another recent study on the seed proteome of Arabidopsis seeds, 3,243 proteins were identified (Li et al., 2019). While the number of proteins in our study is lower, we also used more stringent criteria for protein selection (such as a minimum of two peptides per protein instead of one peptide) and focused on changes in protein abundance throughout several developmental phases. More specifically, in order to detect relative differences in abundance of individual proteins between different samples, the corresponding MS raw datasets were analyzed with the MaxQuant software (https://www.maxquant.org/). MaxQuant integrates and compares the area of peptide peaks within MS1 spectra and considers the

Table 4. *Posttranslational modifications detected on LD proteins and ubiquitin*

Sites marked with an asterisk were not identified unambiguously. For a complete list of modified proteins and modification sites, see Supplemental Datasets 21–30. RS, rehydrated seeds; StS, stratified seeds.

Protein	Ubiquitination						Phosphorylation					
	RS	StS	24-h Seedlings	36-h Seedlings	48-h Seedlings	60-h Seedlings	RS	StS	24-h Seedlings	36-h Seedlings	48-h Seedlings	60-h Seedlings
OLE2	–	–	–	–	K146	–	S18	–	–	–	–	–
OLE4	K157*	K157*	K43	K157*	K157*	K157*	Y153	Y153	S40	–	–	–
	K159*	K159*	K157*	K159*	K159*	K159*	Y164	–	Y42	–	–	–
	K168	–	K159*	K168	K168	K168	–	–	–	–	–	–
	–	–	K168	–	–	–	–	–	–	–	–	–
CLO1	–	K4	–	–	–	–	–	–	–	–	–	–
HSD1	–	–	–	K289	–	–	S340	S348	–	T283	–	–
	–	–	–	K295	–	–	T343	–	–	–	–	–
	–	–	–	–	–	–	S348	–	–	–	–	–
LDAP2	–	–	–	K108	–	–	–	–	–	T118	–	S128
	–	–	–	K125	–	–	–	–	–	S122	–	–
UBQ13	–	–	K48	K6	K48	–	–	–	S246	T7	S246	–
	–	–	K63	K11	K63	–	–	–	S247	T9	S247	–
	–	–	–	K48	–	–	–	–	–	S246	T249	–
	–	–	–	K63	–	–	–	–	–	S247	–	–

monoisotopic peak, as well as isotopic peaks. This integration is considered more accurate than peptide-count-based quantification (Cox et al., 2014; Wang et al., 2019a). Isotope labeling-based methods have advantages in relative and absolute quantification of proteins in comparison to label-free quantification, as used in this study, as peptides from different samples can be mixed and analyzed in a single run. However, the number of isotope tags that can be used to differentiate between peptides from different samples is usually ≤10 (Wang et al., 2019a), limiting the number of comparable conditions (in this study, for example, 16 conditions were analyzed).

MaxQuant implies two quantification algorithms. In the simpler iBAQ algorithm, the sum of the MS1 intensities of peptides from one protein is divided by the number of theoretically possible peptides of reasonable length, thereby giving protein intensities normalized to the theoretical peptide number. The intensities of a given protein can be also compared between samples (Krey et al., 2014). By contrast, the LFQ algorithm uses elaborated normalization strategies between samples on the level of peptide intensities within and across MS1 chromatograms (Cox et al., 2014). It leads to smaller variations of relative quantifications between biological replicates in general, as well as in our samples (Supplemental Datasets S2 and S4).

While the coverage of our proteomics dataset is relatively lower than that of datasets derived using transcriptomic-based techniques (Narsai et al., 2011), transcript abundance does not necessarily correlate with protein abundance, especially during developmental processes when transcripts can exist before they are actually translated. For example, one of the proteins we identified, AT4G27450, which is annotated (by TAIR) to be of unknown function, is present at the transcript level during seed maturation (based on eFP Browser; Nakabayashi et al., 2005; Schmid et al., 2005), but is not detectable at the protein level. Instead, AT4G27450 protein abundance increases sharply in seedlings 24 h after stratification and decreases thereafter (Fig. 2, Cluster 11; Supplemental Datasets S11 and S12). Since AT4G27450 transcripts are not present in vegetative tissues, except during anoxia stress (based on the eFP Browser), it is also a good candidate to play a distinct role(s) during seed germination, which could be further addressed by studying knockout lines. Other proteins from Clusters 11 and 12 that increased transiently during seedling establishment could also play important roles during seed germination. Examples of proteins from Clusters 1 and 2 (Fig. 2; Supplemental Datasets S11 and S12) that are almost exclusively present in imbibed seeds and then decrease in abundance include putative oxidoreductase (At1g54870) and β-glucosidase (AT3G21370) enzymes (Supplemental Datasets S11 and S12), which are highly abundant (18.5‰ and 7.3‰, respectively (Supplemental Datasets S11 and S12), indicative of important roles during seed desiccation or germination that could be further studied.

Proteomics Combined with a Cell-Biological Approach Was Used to Identify Low-Abundance LD Proteins

The number of studies to date investigating the protein composition of LDs in plants, including senescent Arabidopsis leaves (Brocard et al., 2017) and a variety of algal species (Moellering and Benning, 2010; Siegler et al., 2017; Lupette et al., 2019; Wang et al., 2019b), has increased concomitantly with the use of MS-based proteomic techniques in general. However, in those studies, as well as in this one, not all proteins detected in LD-enriched fractions are necessarily bona fide LD proteins, as other proteins may copurify with LDs or are just not sufficiently depleted, which is an intrinsic

shortcoming of MS-based analysis of LDs. To address this important potential caveat, we employed several measures of "quality control" in order to minimize false-positive LD proteins. First, in addition to sampling the LD-enriched fraction, we took a sample of the total cellular protein extract prior to LD enrichment. With both the LD-enriched proteome and the total cellular proteome we were able to calculate LD-enrichment factors. We then used the iBAQ algorithm for candidate discovery, since the LFQ algorithm, as discussed above, leads to a larger number of missing values, causing low-abundance proteins to be missing from the total cellular extracts and disallowing calculation of an enrichment factor.

Using enrichment factors, we could identify contaminants in the LD-enriched fractions that were abundant therein, but did not have a high enrichment factor. On the other hand, we were also able to identify proteins of relatively low abundance (e.g. LDAH1 is only the 283rd most abundant protein in the LD fraction in 60-h seedlings) as good candidates for a cell-biological verification. These latter studies were carried out using two different model plant cell systems (Figs. 5 and 6) that have been successfully used elsewhere to assess the subcellular localization of fluorescent protein-tagged LD proteins, tobacco pollen tubes and *N. benthamiana* leaves (Cai et al., 2017; Müller et al., 2017; Pyc et al., 2017a; Siegler et al., 2017; Kretzschmar et al., 2018).

Overall, we confirmed six candidate LD proteins (Fig. 5 and 6), and we also presented the subcellular localization of several proteins that did not localize to LDs (Supplemental Fig. S4) despite being excellent candidates based on their prevalence in the LD-enriched fractions (Fig. 4). This indicates that candidate protein selection based on enrichment factors can still yield false positives, probably caused by noise and/or artificial protein coenrichment. Importantly, apparent non-LD localization could also occur because these candidate proteins need specific binding partners for LD association that are either present in insufficient amounts or absent in pollen tubes and leaves. Furthermore, the interaction of proteins with LDs might be more transient, yielding an enrichment in isolated LD fractions, but not readily apparent (via microscopy) in plant cell-based expression studies. We also provided evidence that proteins previously annotated as being localized to LDs, based on their homology to proteins in other species, might not in fact be associated with LDs in Arabidopsis. A pertinent example is OBAP1A, a transiently expressed (fusion) protein that was not enriched in the LD fractions of seeds and seedlings and did not localize to LDs in pollen tubes or leaves (Supplemental Fig. S5). These observations are in contrast to the reported LD localization of maize OBAP1 in *N. benthamiana* leaves, which shares ~64% amino acid sequence identity with Arabidopsis OBAP1A (López-Ribera et al., 2014), suggesting that the two proteins have diverged in terms of their ability to target to LDs.

The LD Proteome Varies Across Developmental Stages and Tissues

The considerable changes in the protein composition of LDs over the time frame of seed formation and maturation, germination, and seedling establishment (Fig. 8) highlights the organelle's dynamic nature in terms of its functioning throughout these various stages of growth and development. The main role of LDs during seed development, for instance, is to serve as cellular depots for newly synthesized storage lipids (e.g. TAGs), which, during germination, are subsequently mobilized via β-oxidation and used as an energy source for early seedling growth. Thereafter, during greening of the cotyledons in seedlings and the onset of photoautotrophic growth (i.e. in 48- and 60-h seedlings), LDs are no longer primarily required for the compartmentalization of stored lipids for heterotrophic growth and thus likely play roles in other cellular processes. Consistent with the latter notion, the LD proteome in the 48- and 60-h seedlings underwent among some of the most rapid and pronounced changes (Fig. 8), and many of the 35 LD proteins identified are only found in these two stages. Indeed, this diversification possibly represents a transition from seed-type LDs to vegetative-type LDs, wherein functions other than energy storage are carried out. One such previously described function for LDs in vegetative tissues is pathogen defense, which is mediated, in part, by CLO3 and α-DOX (Shimada et al., 2014; Brocard et al., 2017). Further, RNA sequencing data indicate that the newly identified LD proteins LIDLs, LDAHs, LDDHs, and LIME1 are all ubiquitously expressed in vegetative tissues, while LIME2 is expressed primarily in roots (Supplemental Dataset S31; data based on trava.org; Klepikova et al., 2016). Further research on these and other LD proteins will undoubtedly add to the growing list of functions related to vegetative-type LDs.

The changes in the LD proteome observed across the different stages of growth and development that we examined (Fig. 8) may require not only the synthesis of proteins, but also their degradation. For instance, during germination and seedling establishment, the overall amount of LD proteins decreases (Supplemental Fig. S1) and the bulk of the proteins is degraded within the first 36 h after stratification. During these time points, the LD protein PUX10, which is known to be involved in the degradation of other LD proteins via the ubiquitin-proteasome degradation pathway, shows the highest relative abundance on LDs (Fig. 8; Deruyffelaere et al., 2018; Kretzschmar et al., 2018). Our data also show that several LD proteins harbor ubiquitination sites (Table 3). Furthermore, on ubiquitin itself, we detected ubiquitinations on lysines 48 and 63 (K48 and K63), which is indicative of polyubiquitin chains associated with protein degradation (Komander and Rape, 2012) only during the earlier stages of seedling establishment (i.e. 24- to 48-h seedlings; Table 3).

The Identification of LD Proteins Inspires Future Investigation into the Roles of Plant LDs

We successfully identified members of six protein families that have not been described previously as localized to LDs in plant cells or been studied with respect to their physiological function. Five of these proteins, namely LIDL1, LIME1, LDDH1, LDAH1, and SLDP1, each have one homolog (45% to 90% identity at the amino acid sequence level) that was either found separately in our proteomics dataset enriched in the LD fraction or was indistinguishable from its counterpart based on the detected peptide sequences (Supplemental Dataset S4). The function of the six identified proteins can in part be hypothesized by considering their homology to other related and characterized proteins, including those with known or putative enzymatic function(s).

The LIME1/LIME2 proteins, for example, share homology with a protoberberine methyltransferase (Liscombe and Facchini, 2007) and a coclaurine N-methyltransferase from poppy (*Papaver somniferum*), which catalyzes the synthesis of methylate coclaurine, an intermediate in the morphine biosynthetic pathway (Onoyovwe et al., 2013). Morphine is a hydrophobic compound found in the latex of the opium poppy, and latex particles are a class of LDs that contain polyisoprenoids instead of TAGs and sterol esters (Nawamawat et al., 2011). Thus, the LIME1/LIME2 proteins in Arabidopsis might catalyze a step in the synthesis of secondary metabolites, which are stored within LDs due to their high hydrophobicity. Similarly, the LD protein LDPS may also participate in plant secondary metabolism. LDPS is annotated as a BTB/POZ-domain-containing protein, the domain of which is thought to mediate protein-protein interactions (Collins et al., 2001). The homolog of LDPS, AT5G64230.1, which shares 33% identity at the protein level, is annotated as a 1,8-cineole synthase but has not been studied in terms of whether it actually functions in the monoterpene biosynthetic pathway. Nonetheless, this sequence similarity suggests that LDPS is also involved in monoterpene metabolism in plant cells, perhaps serving in the proper compartmentalization of hydrophobic monoterpenes in LDs.

The yeast (*Saccharomyces cerevisiae*) homolog of Arabidopsis LIDL1 and LIDL2, which are putative lipases, has been shown to have sterol esterase activity, and loss-of-function yeast mutants accumulate sterol esters (Athenstaedt et al., 1999; Jandrositz et al., 2005), suggesting that LIDL1 and LIDL2 may be LD-specific sterol esterases. This latter hypothesis is notable because sterol esters are also present in the LD core, where they are found in minor amounts in Arabidopsis seed LDs (Bouvier-Navé et al., 2010) but can make up a much higher proportion of the stored neutral lipid in other tissues in plants or in other organisms (Onal et al., 2017; Rotsch et al., 2017). Whether LIDL1 and LIDL2 are responsible for the metabolism of stored sterol esters in Arabidopsis is an open question. It also remains to be determined whether LDAH1 and LDDH1 participate in plant metabolism, as indicated by their annotation as an α/β-hydrolase and a putative erythronate-4-phosphate dehydrogenase, respectively. Interestingly, LDDH1 was found previously to be associated with plastids (Teresinski et al., 2019) and we detected it only after the greening of the (60 h) seedling cotyledons. This could indicate that LDDH1 is associated with plastid-LD contact sites. LDDH1 may also act in concert with LDAH1, as these two genes are coexpressed based on ATTED-II version 9.2 (Obayashi et al., 2018) and GENEVESTIGATOR 7.2.6 (Hruz et al., 2008).

SLDPs are uncharacterized proteins, and with the exception of a hydrophobic domain near their N termini that might serve as a membrane anchor, they possess no conserved domains/motifs or significant sequence similarity to other characterized proteins in plants or in nonplant species, such as yeast and mammals. SLDP2, like SLDP1, was found enriched in the LD fraction, but was much less abundant and therefore did not meet the criteria to be considered a strong candidate LD protein (Fig. 4).

While some of the candidate proteins investigated did not localize to LDs (Supplemental Fig. S4), despite being excellent candidates based on their prevalence in the LD-enriched fractions (Fig. 4), it is still possible that these proteins are important for LD biology. One such protein is SEC61γ, which was enriched in the LD proteome and localized to regions of the ER that were often in close contact with LDs (Fig. 7). The SEC61 complex is important for both the incorporation of nascent proteins into the ER (Spiess et al., 2019) and also their retrotranslocation (Scott and Schekman, 2008). Therefore, it is plausible that this complex is also involved in the targeting and/or degradation of LD proteins, as was previously discussed in a study where oleosin was ectopically expressed in yeast (Beaudoin et al., 2000).

In conclusion, the discovery of LD proteins in this study opens up the possibility for uncovering new aspects of plant LD function, biogenesis, and turnover. The existence of several proteins conserved across kingdoms implies that at least some aspects of LD biology are conserved, yet on the other hand, there are also plant-specific LD proteins, suggesting that plant LDs serve additional, unique roles not found in other organisms (Chapman et al., 2019). Undoubtedly, insights into such functions will be gained by identifying and confirming additional LD proteins in plants, and the combined MS-based proteomics and cell-biological approach used here will continue to serve toward that end. Furthermore, our understanding of LDs will increase as these proteins are investigated further.

MATERIALS AND METHODS

Plant Materials

Tobacco (*Nicotiana tabacum*) and Arabidopsis (*Arabidopsis thaliana*, ecotype Columbia) plants were grown as described previously (Kretzschmar et al., 2018). For the two silique development phases (I and II), complete siliques were harvested, and 2 g of the older siliques, or 3 g of the younger siliques, were

pooled for one biological replicate. For rehydrated seeds, stratified seeds, and seedlings 24 and 36 h post-stratification, 100 mg of dry seed material per biological replicate was used. For 48- and 60-h seedlings, dry seed starting material was increased to 160 mg per biological replicate. Rehydrated seeds were incubated in water for 30 min without surface sterilization. For stratified seeds and post-stratification seedling time points, surface-sterilized seeds (sterilized with 6% [w/v] sodium hypochlorite and 0.1% [v/v] Triton X-100) were spread on half-strength Murashige and Skoog media (Murashige and Skoog, 1962) and incubated in the dark at 4°C for 74 h. Then, stratified seed samples were harvested, and all other plants were transferred into a 22°C 16-h light/8-h dark cycle growth chamber with 150 μmol photons m^{-2} s^{-1} daytime light strength; post-stratification seed/seedling time points (24–60 h) indicate the time spent in this condition.

Isolation of Total and LD-Enriched Protein Fractions

After harvesting, each sample was mixed with appropriate amounts (2 mL for rehydrated seeds, 3 mL for stratified seeds – 48 h samples, 3.5 mL for 60 h, 15 mL for younger siliques, 20 mL for older siliques) of grinding buffer [10 mM sodium phosphate buffer, pH 7.4, 200 μM phenylmethylsulfonyl fluoride, 0.5 mM dithiobis (succinimidyl propionate)] and ground with sand to homogeneity with a precooled (on ice) mortar and pestle. The homogenates were centrifuged for 1 min at 100*g*. For the total protein sample, 100 μL of the homogenate was mixed with 900 μL 96% (v/v) ethanol to precipitate proteins. For enrichment of LDs, the homogenate was subjected to three consecutive 20,000*g* centrifugations for 15 min at 4°C. After each centrifugation step, the resulting fat pad was taken off the aqueous phase and transferred into a fresh aliquot of grinding buffer, where it was resuspended. After the third centrifugation step, the fat pad was resuspended in 1 mL 96% (v/v) ethanol.

Proteomic Sample Preparation and LC-MS/MS Analysis of Peptides

Proteins were isolated and their concentrations were determined. They were then subjected to in-gel tryptic-digestion as described previously (Kretzschmar et al., 2018), but with 20 μg of protein digested per replicate. Peptides were then subjected to LC-MS/MS analysis modified from what was described previously (Schmitt et al., 2017). First, 2 μL peptide samples were separated by nano-flow LC on a RSLCnano Ultimate 3000 system (Thermo Fisher Scientific). The peptides were loaded with 0.07% (v/v) trifluoroacetic acid on an Acclaim PepMap 100 precolumn (100 μm × 2 cm, C18, 3 μm, 100 Å; Thermo Fisher Scientific) with a flow rate of 20 μL/min for 3 min. Then, peptides were separated by reverse-phase chromatography on an Acclaim PepMan RSLC column (75 μm × 50 cm, C18, 3 μm, 100 Å; Thermo Fisher Chemical) with a flow rate of 300 nL/min. The peptides were eluted with the following gradient: 96% solvent A (0.1% [v/v] formic acid) and 4% solvent B (80% [v/v] acetonitrile and 0.1% [v/v] formic acid) to 10% solvent B over 2 min, to 30% solvent B over 58 min, to 45% solvent B over 22 min, and to 90% solvent B over 12 min. All solvents and acids were of Optima LC-MS quality and purchased from Thermo Fisher Scientific. Eluted peptides were ionized online by nano-electrospray ionization with a Nanospray Flex Ion Source (Thermo Fisher Scientific) at 1.5 kV (liquid junction) and analyzed with a Q Exactive HF mass spectrometer (Thermo Fisher Scientific). Full scans were recorded in a mass range of 300–1,650 *m/z* at a resolution of 30,000 followed by data-dependent top 10 higher-energy collisional dissociation fragmentation (dynamic exclusion enabled). LC-MS method programming and data acquisition were performed with XCalibur 4.0 software (Thermo Fisher Scientific).

MS Data Processing

MS and MS/MS raw data were processed for feature detection, peptide identification, and protein group assembly with the MaxLFQ algorithm in MaxQuant software version 1.6.2.10 (Cox and Mann, 2008; Cox et al., 2014). Default settings were used and are specified in the metadata file (Supplemental Table S1). Additionally, label-free quantification was enabled in group-specific parameter settings. In global parameter settings, "match between runs" and iBAQ were enabled. The TAIR10 protein database was used as reference. Only proteins identified by at least two peptides were considered. When comparing and relating LD-enriched fractions to total protein fractions, riBAQ values were used, as this algorithm picks up smaller values more often. Enrichment factors were calculated by dividing the average riBAQ value of the LD-enriched fraction by the riBAQ value of the total cellular extract. For quantitative comparison of the total proteome of different time points, rLFQ values are shown, as these display smaller variations between replicates in our hands.

To identify posttranslational modifications, the data were searched for phosphorylation of Ser, Thr, and Tyr, and for ubiquitination of Lys. Settings are specified in the metadata file (Supplemental Table S2). Data analysis was performed in Perseus 1.6.2.2 (Tyanova et al., 2016) and in Excel 2016 (Microsoft).

The Venn diagram was created with InteractiVenn (Heberle et al., 2015). For PCA, proteins were only taken into account if they were found in all replicates of at least one of the stages. The rLFQ values were $\log_2$-transformed. After imputation of missing values by normal distribution (width, 0.9; down shift, 1.8 for total cellular extracts and 2.1 for LD-enriched fractions), PCA was performed with Perseus using default settings. Projections were exported and the data were graphed in Excel 2016.

For cluster analysis, LFQ-processed data were filtered for at least four valid values in at least one of the eight time points. For each protein, the maximum value was set to 1, and the remaining time points were calculated as fractions of this value. The resulting data matrix was used for hierarchical clustering in Perseus 1.6.2.2, with Euclidean distances and preprocessing with k-means.

GO terms were assigned based on the annotation of the TAIR homepage as of December 13, 2018. Annotations of protein localization were obtained from the Plant Proteome Database (Sun et al., 2009) as of February 26, 2019. LD localization was reassigned based on results of this study and Kretzschmar et al. (2018). The volcano plot was created with Perseus. Proteins were included if the average riBAQ intensity was >0.1 in at least one stage and if the protein was detected in at least four of the five biological replicates of at least one stage. Missing values were imputed by 0.01 before $\log_2$ transformation and calculation of *P*-values and false discovery rate using the following settings: Test, *t* test; side, both; number of randomizations, 250; s0 (artificial within groups variance), 0.1; and false discovery rate, 0.001.

Molecular Cloning and Plasmid Construction

Complementary DNA was prepared from RNA extracted from 10 mg mature (dry) seeds, 50 mg 7-d-old seedlings, or 50 mg inflorescences using a Spectrum Plant Total RNA Kit (Sigma-Aldrich). All constructs were amplified using Phusion High-Fidelity DNA Polymerase (Thermo Fisher Scientific) according to the manufacturer's protocol. Molecular cloning into the Gateway vectors pUC-LAT52-mVenusC-GW and pUC-LAT52-mVenusN-GW (Müller et al., 2017), as well as the vector pMDC32-ChC, was performed as depicted in Müller et al. (2017). The use of CFP-SKL for marking peroxisomes (Müller et al., 2017) and the use of ERD2-CFP (ARABIDOPSIS ENDOPLASMIC RETICULUM RETENTION DEFECTIVE2) for marking the ER (Kretzschmar et al., 2018) has been described previously.

The pMDC32-ChC plant expression binary vector, encoding the monomeric Cherry fluorescent protein ORF adjacent to a 5′ recombination site that allows for mCherry to be translationally fused to the C terminus protein of interest, was constructed in the following manner. First the mCherry ORF was amplified using the mCherry-FP-*Pac*I and mCherry-RP-*Sac*I primers (Supplemental Table S3) and pRTL2-Cherry (Gidda et al., 2011) as template DNA. The resulting PCR products were then digested with *Pac*I and *Sac*I and inserted into similarly digested pMDC32 (Curtis and Grossniklaus, 2003), yielding pMDC32-ChC1. Thereafter, the Cm^r/ccdB region of pMDC32-ChC1 was amplified using the primers *ccdB*-FP-*Kpn*I and *ccdB*-RP-*Pac*I (Supplemental Table S3), which resulted in the removal of a stop codon upstream of the Cherry ORF and reinsertion into *Kpn*I-*Pac*I-digested pMDC32-ChC1, yielding pMDC32-ChC.

Custom oligonucleotide primers were synthesized by Sigma-Aldrich; a complete list of all primers is given in Supplemental Table S3. All plasmids constructed in this study, including their promoter and cloning regions and any fusion protein ORFs, were verified by automated sequencing performed at Microsynth AG or the University of Guelph Advanced Analysis Centre Genomics Facility.

Particle Bombardment and Microscopy of *N. tabacum* Pollen Tubes

Pollen grains were transformed by particle bombardment, in vitro cultivated on microscope slides, stained with Nile red (Sigma-Aldrich), and analyzed by confocal laser-scanning microscopy as described by Müller et al. (2017) and Kretzschmar et al. (2018), or with a Zeiss LSM780 (Carl Zeiss) using similar settings. For each construct, at least 10 pollen tubes were imaged.

Transient Transformation and Microscopy of *Nicotiana benthamiana* Leaves

N. benthamiana plants were grown in soil with a 16-h light/8-h dark day/night cycle at 22°C. Leaves of ~4-week-old plants were infiltrated with *Agrobacterium tumefaciens* (strain LBA4404) harboring the selected expression vector as described in Pyc et al. (2017b). All infiltrations were performed with pORE04-35S:p19 containing the tomato bushy stunt virus gene *P19* in order to enhance transgene expression (Petrie et al., 2010).

A. tumefaciens-infiltrated leaves were processed for confocal laser scanning microscopy imaging, including staining of LDs with BODIPY 493/503 (Invitrogen), as previously described (Gidda et al., 2016). Micrographs of leaves were acquired using a Leica SP5 confocal laser scanning microscope (Leica Microsystems). Excitations and emission signals for fluorescent proteins and BODIPY were collected sequentially as single optical sections in double-labeling experiments like those described in Gidda et al. (2016); single-labeling experiments showed no detectable crossover at the settings used for data collection. All fluorescence images of cells shown are representative of at least two separate experiments, including at least three separate transformations of leaf cells.

Accession Numbers

Sequence data from this article can be found in the GenBank/EMBL data libraries under accession numbers AT3G01420 (αDOX); AT2G41475 (ATS3A); AT3G08780 (BCSAP); AT2G07050 (CAS); AT1G78830 (CCLP); AT4G26740 (CLO1); AT5G55240 (CLO2); AT2G33380 (CLO3); AT1G70680 (CLO5); AT1G29330 (ERD2); At5G50600/AT5G50700 (HSD1/1); AT3G47350 (HSD2); AT3G47360 (HSD3); AT4G10020 (HSD5); AT5G50770 (HSD6); AT3G45130 (LAS); AT1G10740 (LDAH1); AT1G23330 (LDAH2); AT1G67360 (LDAP1); AT2G47780 (LDAP2); AT3G05500 (LDAP3); AT1G75180 (LDDH1); AT1G19400 (LDDH2); AT5G16550 (LDIP); AT1G18460 (LIDL1); AT1G73920 (LIDL2); AT3G19920 (LDPS); AT4G33110 (LIME1); AT4G33120 (LIME2); AT3G20820 (LRR); AT1G05510 (OBAP1A); AT3G14360 (OBL1); AT1G45201 (OBL3);. AT4G25140 (OLE1); AT5G40420 (OLE2); AT5G51210 (OLE3); AT3G27660 (OLE4); AT3G01570 (OLE5); AT1G48990 (OLE6); AT2G25890 (OLE7); AT3G18570 (OLE8); AT4G10790 (PUX10); AT5G50460 (SEC61γ); AT1G65090 (SLDP1); AT5G36100 (SLDP2); AT5G13710 (SMT1); and AT1G27290 (TMPU).

Supplemental Data

The following supplemental materials are available.

Supplemental Figure S1. Abundance of LD proteins within the total protein fraction from Arabidopsis siliques, seeds, and seedlings.

Supplemental Figure S2. Enrichment of organelle-specific proteins in the LD-enriched fractions from Arabidopsis siliques, seeds, and seedlings.

Supplemental Figure S3. Enrichment analysis of proteins in the LD-enriched fractions derived from Arabidopsis siliques, seeds, and seedlings with highlighted LD and ER proteins.

Supplemental Figure S4. Subcellular localization of other selected, candidate proteins in *N. tabacum* pollen tubes.

Supplemental Figure S5. Abundance in total and LD-enriched protein fractions and subcellular localization of the Arabidopsis OBAP1A protein.

Supplemental Table S1. Metadata file for LC-MS/MS data processing with MaxQuant.

Supplemental Table S2. Metadata file for LC-MS/MS data processing with MaxQuant checking for posttranslational modifications.

Supplemental Table S3. Primers used for Gateway molecular cloning and sequencing.

Supplemental Dataset S1. Proteins found in siliques and seedlings—Raw LFQ values.

Supplemental Dataset S2. Proteins found in siliques and seedlings—Normalized and sorted LFQ values.

Supplemental Dataset S3. Proteins found in siliques and seedlings—Raw iBAQ values.

Supplemental Dataset S4. Proteins found in siliques and seedlings—Normalized and sorted iBAQ values.

Supplemental Dataset S5. Proteins found in siliques and seedlings—Imputed $\log_2$-transformed LFQ values of total protein fraction.

Supplemental Dataset S6. Loadings of PCA plot created with Supplemental Dataset 5 (total fraction).

Supplemental Dataset S7. Projections of PCA plot created with Supplemental Dataset 5 (total fraction).

Supplemental Dataset S8. Proteins found in siliques and seedlings—Imputed $\log_2$-transformed LFQ values of lipid droplet-enriched fractions.

Supplemental Dataset S9. Loadings of PCA plot created with Supplemental Dataset 8 (lipid droplet-enriched fraction).

Supplemental Dataset S10. Projections of PCA plot created with Supplemental Dataset 8 (lipid droplet-enriched fraction).

Supplemental Dataset S11. Proteins found in the total protein fraction of siliques and seedlings—Normalized and sorted LFQs with at least four valid values in at least one condition.

Supplemental Dataset S12. Data set used to create the heat map presented in Figure 2.

Supplemental Dataset S13. Sums of rLFQ values of proteins associated with the same GO ID.

Supplemental Dataset S14. Phase-dependent averages of sums of rLFQ values of proteins associated with the same GO ID.

Supplemental Dataset S15. Selected GO ID sums.

Supplemental Dataset S16. Subcellular localization of proteins.

Supplemental Dataset S17. Sums of riBAQ values of proteins with the same subcellular localization.

Supplemental Dataset S18. List of curated subcellular localization acquired from the Plant Proteome Data Base.

Supplemental Dataset S19. Results matrix from the enrichment analysis.

Supplemental Dataset S20. Contribution of LD proteins to the total LD proteome.

Supplemental Dataset S21. Modified proteins identified in Phase I silique samples.

Supplemental Dataset S22. Modified proteins identified in Phase II silique samples.

Supplemental Dataset S23. Modified proteins identified in rehydrated seed samples.

Supplemental Dataset S24. Modified proteins identified in stratified seed samples.

Supplemental Dataset S25. Modified proteins identified in 24-h seedling samples.

Supplemental Dataset S26. Modified proteins identified in 36-h seedling samples.

Supplemental Dataset S27. Modified proteins identified in 48-h seedling samples.

Supplemental Dataset S28. Modified proteins identified in 60-h seedling samples.

Supplemental Dataset S29. All modified proteins identified across samples, including their modified sites.

Supplemental Dataset S30. All modified LD proteins identified across samples, including their modified sites.

Supplemental Dataset S31. Gene expression levels of LD proteins identified in this study.

ACKNOWLEDGMENTS

We thank Ivo Feussner for all his support and many helpful discussions, Dr. Christiane Gatz and Dr. Alexander Stein for their valuable advice, and Dr. Kent Chapman and Dr. John Dyer for their insightful discussions about

this work. We are grateful also to Dr. Jörg Großhans and Dr. Steven Johnsen for granting access to their confocal microscopes, Dr. Florian Wegwitz and Johannes Sattmann for their assistance, Dr. Leonie Steinhorst and Dr. Jörg Kudla for generating and providing plasmids, and Dr. Ivo Feussner, Dr. Jennifer Popko, and Dr. Frederike Ruhe for providing the plasmid pCambia33.1Gs mCherry-LIDL1. Technical assistance was provided by Siqi Sun and Antony Grüness.

Received October 9, 2019; accepted November 24, 2019; published December 11, 2019.

LITERATURE CITED

Arsova B, Watt M, Usadel B (2018) Monitoring of plant protein post-translational modifications using targeted proteomics. Front Plant Sci **9:** 1168

Athenstaedt K, Zweytick D, Jandrositz A, Kohlwein SD, Daum G (1999) Identification and characterization of major lipid particle proteins of the yeast *Saccharomyces cerevisiae*. J Bacteriol **181:** 6441–6448

Baud S, Boutin JP, Miquel M, Lepiniec L, Rochat C (2002) An integrated overview of seed development in *Arabidopsis thaliana* ecotype WS. Plant Physiol Biochem **40:** 151–160

Baud S, Dichow NR, Kelemen Z, d'Andréa S, To A, Berger N, Canonge M, Kronenberger J, Viterbo D, Dubreucq B, et al (2009) Regulation of HSD1 in seeds of *Arabidopsis thaliana*. Plant Cell Physiol **50:** 1463–1478

Beaudoin F, Wilkinson BM, Stirling CJ, Napier JA (2000) In vivo targeting of a sunflower oil body protein in yeast secretory (sec) mutants. Plant J **23:** 159–170

Bersuker K, Peterson CWH, To M, Sahl SJ, Savikhin V, Grossman EA, Nomura DK, Olzmann JA (2018) A proximity labeling strategy provides insights into the composition and dynamics of lipid droplet proteomes. Dev Cell **44:** 97–112

Bouvier-Navé P, Berna A, Noiriel A, Compagnon V, Carlsson AS, Banas A, Stymne S, Schaller H (2010) Involvement of the phospholipid sterol acyltransferase1 in plant sterol homeostasis and leaf senescence. Plant Physiol **152:** 107–119

Brocard L, Immel F, Coulon D, Esnay N, Tuphile K, Pascal S, Claverol S, Fouillen L, Bessoule J-J, Bréhélin C (2017) Proteomic analysis of lipid droplets from Arabidopsis aging leaves brings new insight into their biogenesis and functions. Front Plant Sci **8:** 894

Cai Y, Goodman JM, Pyc M, Mullen RT, Dyer JM, Chapman KD (2015) Arabidopsis SEIPIN proteins modulate triacylglycerol accumulation and influence lipid droplet proliferation. Plant Cell **27:** 2616–2636

Cai Y, McClinchie E, Price A, Nguyen TN, Gidda SK, Watt SC, Yurchenko O, Park S, Sturtevant D, Mullen RT, et al (2017) Mouse fat storage-inducing transmembrane protein 2 (FIT2) promotes lipid droplet accumulation in plants. Plant Biotechnol J **15:** 824–836

Chapman KD, Aziz M, Dyer JM, Mullen RT (2019) Mechanisms of lipid droplet biogenesis. Biochem J **476:** 1929–1942

Chapman KD, Dyer JM, Mullen RT (2012) Biogenesis and functions of lipid droplets in plants. J Lipid Res **53:** 215–226

Chibani K, Ali-Rachedi S, Job C, Job D, Jullien M, Grappin P (2006) Proteomic analysis of seed dormancy in Arabidopsis. Plant Physiol **142:** 1493–1510

Collins T, Stone JR, Williams AJ (2001) All in the family: The BTB/POZ, KRAB, and SCAN domains. Mol Cell Biol **21:** 3609–3615

Cox J, Hein MY, Luber CA, Paron I, Nagaraj N, Mann M (2014) Accurate proteome-wide label-free quantification by delayed normalization and maximal peptide ratio extraction, termed MaxLFQ. Mol Cell Proteomics **13:** 2513–2526

Cox J, Mann M (2008) MaxQuant enables high peptide identification rates, individualized p.p.b.-range mass accuracies and proteome-wide protein quantification. Nat Biotechnol **26:** 1367–1372

Curtis MD, Grossniklaus U (2003) A gateway cloning vector set for high-throughput functional analysis of genes in planta. Plant Physiol **133:** 462–469

Deruyffelaere C, Bouchez I, Morin H, Guillot A, Miquel M, Froissard M, Chardot T, D'Andrea S (2015) Ubiquitin-mediated proteasomal degradation of oleosins is involved in oil body mobilization during post-germinative seedling growth in Arabidopsis. Plant Cell Physiol **56:** 1374–1387

Deruyffelaere C, Purkrtova Z, Bouchez I, Collet B, Cacas J-L, Chardot T, Gallois J-L, D'Andrea S (2018) PUX10 is a CDC48A adaptor protein that regulates the extraction of ubiquitinated oleosins from seed lipid droplets in Arabidopsis. Plant Cell **30:** 2116–2136

Du X, Barisch C, Paschke P, Herrfurth C, Bertinetti O, Pawolleck N, Otto H, Rühling H, Feussner I, Herberg FW, Maniak M (2013) Dictyostelium lipid droplets host novel proteins. Eukaryot Cell **12:** 1517–1529

Durand TC, Cueff G, Godin B, Valot B, Clément G, Gaude T, Rajjou L (2019) Combined proteomic and metabolomic profiling of the *Arabidopsis thaliana vps29* mutant reveals pleiotropic functions of the retromer in seed development. Int J Mol Sci **20:** 1–22

Eastmond PJ (2004) Cloning and characterization of the acid lipase from castor beans. J Biol Chem **279:** 45540–45545

Eldakak M, Milad SIM, Nawar AI, Rohila JS (2013) Proteomics: A biotechnology tool for crop improvement. Front Plant Sci **4:** 35

Fercha A, Capriotti AL, Caruso G, Cavaliere C, Stampachiacchiere S, Zenezini Chiozzi R, Laganà A (2016) Shotgun proteomic analysis of soybean embryonic axes during germination under salt stress. Proteomics **16:** 1537–1546

Galland M, Huguet R, Arc E, Cueff G, Job D, Rajjou L (2014) Dynamic proteomics emphasizes the importance of selective mRNA translation and protein turnover during *Arabidopsis* seed germination. Mol Cell Proteomics **13:** 252–268

Gallardo K, Job C, Groot SPC, Puype M, Demol H, Vandekerckhove J, Job D (2001) Proteomic analysis of arabidopsis seed germination and priming. Plant Physiol **126:** 835–848

Garbowicz K, Liu Z, Alseekh S, Tieman D, Taylor M, Kuhalskaya A, Ofner I, Zamir D, Klee HJ, Fernie AR, et al (2018) Quantitative trait loci analysis identifies a prominent gene involved in the production of fatty acid-derived flavor volatiles in tomato. Mol Plant **11:** 1147–1165

Gidda SK, Park S, Pyc M, Yurchenko O, Cai Y, Wu P, Andrews DW, Chapman KD, Dyer JM, Mullen RT (2016) Lipid droplet-associated proteins (LDAPs) are required for the dynamic regulation of neutral lipid compartmentation in plant cells. Plant Physiol **170:** 2052–2071

Gidda SK, Shockey JM, Falcone M, Kim PK, Rothstein SJ, Andrews DW, Dyer JM, Mullen RT (2011) Hydrophobic-domain-dependent protein-protein interactions mediate the localization of GPAT enzymes to ER subdomains. Traffic **12:** 452–472

Greenspan P, Mayer EP, Fowler SD (1985) Nile red: A selective fluorescent stain for intracellular lipid droplets. J Cell Biol **100:** 965–973

Hajduch M, Ganapathy A, Stein JW, Thelen JJ (2005) A systematic proteomic study of seed filling in soybean. Establishment of high-resolution two-dimensional reference maps, expression profiles, and an interactive proteome database. Plant Physiology **137:** 1397–1419

Hajduch M, Hearne LB, Miernyk JA, Casteel JE, Joshi T, Agrawal GK, Song Z, Zhou M, Xu D, Thelen JJ (2010) Systems analysis of seed filling in Arabidopsis: Using general linear modeling to assess concordance of transcript and protein expression. Plant Physiol **152:** 2078–2087

Hanano A, Burcklen M, Flenet M, Ivancich A, Louwagie M, Garin J, Blée E (2006) Plant seed peroxygenase is an original heme-oxygenase with an EF-hand calcium binding motif. J Biol Chem **281:** 33140–33151

Heberle H, Meirelles GV, da Silva FR, Telles GP, Minghim R (2015) InteractiVenn: A web-based tool for the analysis of sets through Venn diagrams. BMC Bioinformatics **16:** 169

Horn PJ, James CN, Gidda SK, Kilaru A, Dyer JM, Mullen RT, Ohlrogge JB, Chapman KD (2013) Identification of a new class of lipid droplet-associated proteins in plants. Plant Physiol **162:** 1926–1936

Hruz T, Laule O, Szabo G, Wessendorp F, Bleuler S, Oertle L, Widmayer P, Gruissem W, Zimmermann P (2008) Genevestigator v3: A reference expression database for the meta-analysis of transcriptomes. Adv Bioinforma **2008:** 420747

Hsiao ESL, Tzen JTC (2011) Ubiquitination of oleosin-H and caleosin in sesame oil bodies after seed germination. Plant Physiol Biochem **49:** 77–81

Huang AHC (2017) Plant lipid droplets and their associated oleosin and other proteins: Potential for rapid advances. Plant Physiol **176:** 1894–1918

Jandrositz A, Petschnigg J, Zimmermann R, Natter K, Scholze H, Hermetter A, Kohlwein SD, Leber R (2005) The lipid droplet enzyme Tgl1p hydrolyzes both steryl esters and triglycerides in the yeast, *Saccharomyces cerevisiae*. Biochim Biophys Acta **1735:** 50–58

Kim EY, Park KY, Seo YS, Kim WT (2016) Arabidopsis small rubber particle protein homolog SRPs play dual roles as positive factors for

tissue growth and development and in drought stress responses. Plant Physiol **170:** 2494–2510

Klepikova AV, Kasianov AS, Gerasimov ES, Logacheva MD, Penin AA (2016) A high resolution map of the *Arabidopsis thaliana* developmental transcriptome based on RNA-seq profiling. Plant J **88:** 1058–1070

Komander D, Rape M (2012) The ubiquitin code. Annu Rev Biochem **81:** 203–229

Kretzschmar FK, Mengel LA, Müller AO, Schmitt K, Blersch KF, Valerius O, Braus GH, Ischebeck T (2018) PUX10 is a lipid droplet-localized scaffold protein that interacts with CELL DIVISION CYCLE48 and is involved in the degradation of lipid droplet proteins. Plant Cell **30:** 2137–2160

Krey JF, Wilmarth PA, Shin JB, Klimek J, Sherman NE, Jeffery ED, Choi D, David LL, Barr-Gillespie PG (2014) Accurate label-free protein quantitation with high- and low-resolution mass spectrometers. J Proteome Res **13:** 1034–1044

Kubala S, Garnczarska M, Wojtyla Ł, Clippe A, Kosmala A, Żmieńko A, Lutts S, Quinet M (2015) Deciphering priming-induced improvement of rapeseed (*Brassica napus* L.) germination through an integrated transcriptomic and proteomic approach. Plant Sci **231:** 94–113

Lee J, Lee W, Kwon SW (2015) A quantitative shotgun proteomics analysis of germinated rice embryos and coleoptiles under low-temperature conditions. Proteome Sci **13:** 27

Li F, Asami T, Wu X, Tsang EWT, Cutler AJ (2007) A putative hydroxysteroid dehydrogenase involved in regulating plant growth and development. Plant Physiol **145:** 87–97

Li P-C, Ma J-J, Zhou X-M, Li G-H, Zhao C-Z, Xia H, Fan S-J, Wang X-J (2019) *Arabidopsis* MDN1 is involved in the establishment of a normal seed proteome and seed germination. Front Plant Sci **10:** 1118

Li Q-F, Xiong M, Xu P, Huang L-C, Zhang C-Q, Liu Q-Q (2016) Dissection of brassinosteroid-regulated proteins in rice embryos during germination by quantitative proteomics. Sci Rep **6:** 34583

Lin L-J, Tai SSK, Peng C-C, Tzen JTC (2002) Steroleosin, a sterol-binding dehydrogenase in seed oil bodies. Plant Physiol **128:** 1200–1211

Liscombe DK, Facchini PJ (2007) Molecular cloning and characterization of tetrahydroprotoberberine *cis-N*-methyltransferase, an enzyme involved in alkaloid biosynthesis in opium poppy. J Biol Chem **282:** 14741–14751

Listenberger LL, Brown DA (2007) Fluorescent detection of lipid droplets and associated proteins. Curr Protoc Cell Biol **35:** 24.2.1-24.2.11

López-Ribera I, La Paz JL, Repiso C, García N, Miquel M, Hernández ML, Martínez-Rivas JM, Vicient CM (2014) The evolutionary conserved oil body associated protein OBAP1 participates in the regulation of oil body size. Plant Physiol **164:** 1237–1249

Lorenz C, Brandt S, Borisjuk L, Rolletschek H, Heinzel N, Tohge T, Fernie AR, Braun H-P, Hildebrandt TM (2018) The role of persulfide metabolism during Arabidopsis seed development under light and dark conditions. Front Plant Sci **9:** 1381

Lupette J, Jaussaud A, Seddiki K, Morabito C, Brugière S, Schaller H, Kuntz M, Putaux JL, Jouneau PH, Rébeillé F, et al (2019) The architecture of lipid droplets in the diatom *Phaeodactylum tricornutum*. Algal Res **38:** 101415

Mansfield SG, Briarty LG (1992) Cotyledon cell development in *Arabidopsis thaliana* during reserve deposition. Can J Bot **70:** 151–164

Moellering ER, Benning C (2010) RNA interference silencing of a major lipid droplet protein affects lipid droplet size in *Chlamydomonas reinhardtii*. Eukaryot Cell **9:** 97–106

Müller AO, Blersch KF, Gippert AL, Ischebeck T (2017) Tobacco pollen tubes—A fast and easy tool for studying lipid droplet association of plant proteins. Plant J **89:** 1055–1064

Müller AO, Ischebeck T (2018) Characterization of the enzymatic activity and physiological function of the lipid droplet-associated triacylglycerol lipase AtOBL1. New Phytol **217:** 1062–1076

Murashige T, Skoog F (1962) A revised medium for rapid growth and bio assays with tobacco tissue cultures. Physiol Plant **15:** 473–497

Naested H, Frandsen GI, Jauh GY, Hernandez-Pinzon I, Nielsen HB, Murphy DJ, Rogers JC, Mundy J (2000) Caleosins: Ca^{2+}-binding proteins associated with lipid bodies. Plant Mol Biol **44:** 463–476

Nakabayashi K, Okamoto M, Koshiba T, Kamiya Y, Nambara E (2005) Genome-wide profiling of stored mRNA in *Arabidopsis thaliana* seed germination: Epigenetic and genetic regulation of transcription in seed. Plant J **41:** 697–709

Narsai R, Law SR, Carrie C, Xu L, Whelan J (2011) In-depth temporal transcriptome profiling reveals a crucial developmental switch with roles for RNA processing and organelle metabolism that are essential for germination in Arabidopsis. Plant Physiol **157:** 1342–1362

Nawamawat K, Sakdapipanich JT, Ho CC, Ma Y, Song J, Vancso JG (2011) Surface nanostructure of *Hevea brasiliensis* natural rubber latex particles. Colloids Surf A Physicochem Eng Asp **390:** 157–166

Nguyen T-P, Cueff G, Hegedus DD, Rajjou L, Bentsink L (2015) A role for seed storage proteins in *Arabidopsis* seed longevity. J Exp Bot **66:** 6399–6413

Obayashi T, Aoki Y, Tadaka S, Kagaya Y, Kinoshita K (2018) ATTED-II in 2018: A plant coexpression database based on investigation of the statistical property of the mutual rank index. Plant Cell Physiol **59:** e3

Onal G, Kutlu O, Gozuacik D, Dokmeci Emre S (2017) Lipid droplets in health and disease. Lipids Health Dis **16:** 128

Onoyovwe A, Hagel JM, Chen X, Khan MF, Schriemer DC, Facchini PJ (2013) Morphine biosynthesis in opium poppy involves two cell types: Sieve elements and laticifers. Plant Cell **25:** 4110–4122

Penfield S, Graham S, Graham IA (2005) Storage reserve mobilization in germinating oilseeds: *Arabidopsis* as a model system. Biochem Soc Trans **33:** 380–383

Petrie JR, Shrestha P, Liu Q, Mansour MP, Wood CC, Zhou X-R, Nichols PD, Green AG, Singh SP (2010) Rapid expression of transgenes driven by seed-specific constructs in leaf tissue: DHA production. Plant Methods **6:** 8

Pyc M, Cai Y, Gidda SK, Yurchenko O, Park S, Kretzschmar FK, Ischebeck T, Valerius O, Braus GH, Chapman KD, et al (2017a) *Arabidopsis* lipid droplet-associated protein (LDAP)-interacting protein (LDIP) influences lipid droplet size and neutral lipid homeostasis in both leaves and seeds. Plant J **92:** 1182–1201

Pyc M, Cai Y, Greer MS, Yurchenko O, Chapman KD, Dyer JM, Mullen RT (2017b) Turning over a new leaf in lipid droplet biology. Trends Plant Sci **22:** 596–609

Qu R, Wang SM, Lin YH, Vance VB, Huang AH (1986) Characteristics and biosynthesis of membrane proteins of lipid bodies in the scutella of maize (*Zea mays* L.). Biochem J **235:** 57–65

Quan S, Yang P, Cassin-Ross G, Kaur N, Switzenberg R, Aung K, Li J, Hu J (2013) Proteome analysis of peroxisomes from etiolated Arabidopsis seedlings identifies a peroxisomal protease involved in β-oxidation and development. Plant Physiol **163:** 1518–1538

Rotsch AH, Kopka J, Feussner I, Ischebeck T (2017) Central metabolite and sterol profiling divides tobacco male gametophyte development and pollen tube growth into eight metabolic phases. Plant J **92:** 129–146

Rudolph M, Schlereth A, Körner M, Feussner K, Berndt E, Melzer M, Hornung E, Feussner I (2011) The lipoxygenase-dependent oxygenation of lipid body membranes is promoted by a patatin-type phospholipase in cucumber cotyledons. J Exp Bot **62:** 749–760

Schmid M, Davison TS, Henz SR, Pape UJ, Demar M, Vingron M, Schölkopf B, Weigel D, Lohmann JU (2005) A gene expression map of *Arabidopsis thaliana* development. Nat Genet **37:** 501–506

Schmitt K, Smolinski N, Neumann P, Schmaul S, Hofer-Pretz V, Braus GH, Valerius O (2017) Asc1p/RACK1 connects ribosomes to eukaryotic phosphosignaling. Mol Cell Biol **37:** e00279-16

Scott DC, Schekman R (2008) Role of Sec61p in the ER-associated degradation of short-lived transmembrane proteins. J Cell Biol **181:** 1095–1105

Shimada TL, Shimada T, Takahashi H, Fukao Y, Hara-Nishimura I (2008) A novel role for oleosins in freezing tolerance of oilseeds in *Arabidopsis thaliana*. Plant J **55:** 798–809

Shimada TL, Takano Y, Shimada T, Fujiwara M, Fukao Y, Mori M, Okazaki Y, Saito K, Sasaki R, Aoki K, et al (2014) Leaf oil body functions as a subcellular factory for the production of a phytoalexin in Arabidopsis. Plant Physiol **164:** 105–118

Siegler H, Valerius O, Ischebeck T, Popko J, Tourasse NJ, Vallon O, Khozin-Goldberg I, Braus GH, Feussner I (2017) Analysis of the lipid body proteome of the oleaginous alga *Lobosphaera incisa*. BMC Plant Biol **17:** 98

Siloto RMP, Findlay K, Lopez-Villalobos A, Yeung EC, Nykiforuk CL, Moloney MM (2006) The accumulation of oleosins determines the size of seed oilbodies in Arabidopsis. Plant Cell **18:** 1961–1974

Spiess M, Junne T, Janoschke M (2019) Membrane protein integration and topogenesis at the ER. Protein J **38:** 306–316

Sun Q, Zybailov B, Majeran W, Friso G, Olinares PDB, van Wijk KJ (2009) PPDB, the plant proteomics database at Cornell. Nucleic Acids Res **37:** D969–D974

Teresinski HJ, Gidda SK, Nguyen TND, Howard NJM, Porter BK, Grimberg N, Smith MD, Andrews DW, Dyer JM, Mullen RT (2019) An RK/ST C-terminal motif is required for targeting of OEP7.2 and a subset of other Arabidopsis tail-anchored proteins to the plastid outer envelope membrane. Plant Cell Physiol **60:** 516–537

Tyanova S, Temu T, Sinitcyn P, Carlson A, Hein MY, Geiger T, Mann M, Cox J (2016) The Perseus computational platform for comprehensive analysis of (prote)omics data. Nat Methods **13:** 731–740

Tzen J, Cao Y, Laurent P, Ratnayake C, Huang A (1993) Lipids, proteins, and structure of seed oil bodies from diverse species. Plant Physiol **101:** 267–276

Vance VB, Huang AH (1987) The major protein from lipid bodies of maize. Characterization and structure based on cDNA cloning. J Biol Chem **262:** 11275–11279

Wang X, Shen S, Rasam SS, Qu J (2019a) MS1 ion current-based quantitative proteomics: A promising solution for reliable analysis of large biological cohorts. Mass Spectrom Rev **38:** 461–482

Wang X, Wei H, Mao X, Liu J (2019b) Proteomics analysis of lipid droplets from the oleaginous alga *Chromochloris zofingiensis* reveals novel proteins for lipid metabolism. Genomics Proteomics Bioinformatics **17:** 260–272

Wang Y, Ma X, Zhang X, He X, Li H, Cui D, Yin D (2016) ITRAQ-based proteomic analysis of the metabolic mechanisms behind lipid accumulation and degradation during peanut seed development and post-germination. J Proteome Res **15:** 4277–4289

Xu E, Chen M, He H, Zhan C, Cheng Y, Zhang H, Wang Z (2017) Proteomic analysis reveals proteins involved in seed imbibition under salt stress in rice. Front Plant Sci **7:** 2006

Yin X, He D, Gupta R, Yang P (2015) Physiological and proteomic analyses on artificially aged *Brassica napus* seed. Front Plant Sci **6:** 112

Zhang C, Liu P (2019) The new face of the lipid droplet: Lipid droplet proteins. Proteomics **19:** e1700223

4 Manuscript I: Identification of a putative lipid droplet-plasma membrane tethering complex

The manuscript is being prepared for submission. Supplementary figures are attached to the main part. Supplementary tables containing raw and processed proteomics data are available on the data drive included in this thesis and will be available online after publication.

Supplementary Material

Supplementary Material: Sequences
Supplementary Dataset S1: Raw LFQs
Supplementary Dataset S2: Normalised and filtered LFQs
Supplementary Dataset S3: Imputations
Supplementary Dataset S4: LD-enriched proteins
Supplementary Movies S1-S6
Supplementary Figures 1-8

Author contribution

H. E. Krawczyk designed experiments. All *in silico* analyses as well as all data analyses were performed by her. She generated CRISPR/Cas9 mutant lines and cloned all constructs (except for leaf transformations). She performed most of the transient transformations and pollen tube microscopy, including quantifications on images. Time course analyses of seedlings were performed by her, as was RNA extraction for qPCR analyses lipid extractions. Proteome data analysis was performed by her. She prepared all figures and supplements and wrote the manuscript.

Other contributions

TI helped designing experiments; NMD did *Nicotiana benthamiana* transformation and microscopy as well as cloning of the respective constructs; PS performed qPCR analysis; SS did protein isolations and prepared samples for proteome analysis; TI and SS helped in acquiring pollen tube images and did pollen tube time series; SH performed electron microscopy. HEK prepared figures; NMD, and TI read and revised the manuscript.

Identification of a putative lipid droplet-plasma membrane tethering complex

Hannah Elisa Krawczyk[1], Siqi Sun[1], Nathan M. Doner[2], Patricia Scholz[1], Kerstin Schmitt[3], Oliver Valerius[3], Stefan Hillmer[4], Gerhard H. Braus[3], Robert T. Mullen[2], Till Ischebeck[1,5]

[1]University of Göttingen, Albrecht-von-Haller-Institute for Plant Sciences and Göttingen Center for Molecular Biosciences (GZMB), Department of Plant Biochemistry, 37077 Göttingen, Germany

[2]University of Guelph, Department of Molecular and Cellular Biology, Guelph, ON N1G 2W1, Canada

[3]University of Göttingen, Institute for Microbiology and Genetics and Göttingen Center for Molecular Biosciences (GZMB), Department for Molecular Microbiology and Genetics, Göttingen, Germany

[4]Heidelberg University, Electron Microscopy Core Facility, Heidelberg, Germany

[5]University of Göttingen, Albrecht-von-Haller-Institute for Plant Sciences, Göttingen Metabolomics/Lipidomics Platform, 37077 Göttingen, Germany

Abstract

Membrane contact sites (MCS) are interorganellar contacts that allow for the direct exchange of molecules such as lipids or Ca^{2+} between organelles, but can also be a mean for tethering of organelles. In mammals and yeast, LDs have been shown to engage in MCS with nearly all organelles in the cell, while in plants only LD-ER and LD-peroxisome contacts have been characterised. We here analyse three proteins of previous unknown function, LD-localised SEED LIPID DROPLET PROTEIN (SLDP) 1 and 2 and PM-localised LIPID DROPLET PLASMA MEMBRANE ADAPTOR. Knockout of SLDP1 and 2, as well as knockout of LIPA lead to aberrant clustering of LDs in seedlings, while ectopic co-expression of SLDP and LIPA in *Nicotiana tabacum* pollen tubes is sufficient to reconstitute LD-PM tethering in this tissue, where LDs normally dynamically float in the cytosol stream. We propose a model, in which SLDP and LIPA interact and thereby form a tether to anchor a subset of LDs to the PM during post-germinative growth in *Arabidopsis thaliana.*

Key words

Arabidopsis, lipid droplets, seed, germination, seedling, TAG, membrane contact sites, tethering complex, plasma membrane

Introduction

As the availability of organelle-specific proteome data increases, it is also the inter-organelle connections via membrane contact sites (MCS) that are increasingly sparking interest (Prinz *et al.*, 2020). MCS facilitate physical interactions and even exchange of molecules between organelles without the need of membrane fusion events. The transient connections are established through tethering proteins connecting the membranes of interacting organelles and allow for direct exchange of lipids, signals (e.g. Ca^{2+}, ROS) or other molecules (Baillie *et al.*, 2020; Prinz *et al.*, 2020; Rossini *et al.*, 2020). It is well-recognised that MCS can form between nearly all organelles (Eisenberg-Bord *et al.*, 2016; Valm *et al.*, 2017; Shai *et al.*, 2018; Baillie *et al.*, 2020). The ER or the peroxisome for example are organelles with comparatively well described interactomes (Shai *et al.*, 2016; Zang *et al.*, 2020). Also, multi-organelle contacts have been described: For instance, the human protein MIGA2 connects mitochondria, the ER and lipid droplets (LDs) to promote *de novo* lipogenesis in adipocytes (Freyre *et al.*, 2019). Although the ER-derived LD is another organelle promiscuously engaging in MCS, its interactome is less well described than others (Bohnert, 2020). The LD consists of a lipophilic core of neutral lipids such as triacylglycerols (TAGs) and sterol esters and is surrounded by a protein-decorated phospholipid monolayer. Long believed to be an inert storage organelle, it is nowadays widely appreciated that LDs actively participate in many cellular processes involving lipids or their derivatives (Thiam and Beller, 2017; Welte and Gould, 2017; Ischebeck *et al.*, 2020). Rather than just providing storage lipids when needed, LDs act as dynamic hubs for cellular lipid fluxes. Excess lipids, especially free fatty acids, are cytotoxic and lipid homeostasis is crucial for the cell (Schaffer, 2003). In this regard, LDs can serve as a sink, effectively reducing cytosolic free fatty acids (Fan *et al.*, 2017; Olzmann and Carvalho, 2019; de Vries and Ischebeck, 2020) and ROS (Muliyil *et al.*, 2020) but also sequestering harmful proteins (Geltinger *et al.*, 2020) or storing histone complexes (Johnson *et al.*, 2018) on the LD surface.

Taking the role of MCS in non-vesicular transport of lipids through the hydrophilic cytosol into account (Cockcroft and Raghu, 2018), it is not surprising that LDs, too, have been described to engage in contact sites with nearly all other organelles in the cell (Gao and Goodman, 2015; Schuldiner and Bohnert, 2017; Valm *et al.*, 2017; Bohnert, 2020). However, most described contact sites have been observed in mammalian or yeast cells. Described LD-MCS in plants are limited to LD-ER contact sites for storage lipid accumulation (Cai *et al.*, 2015; Greer *et al.*, 2020) and LD-peroxisome contact sites for storage lipid breakdown (Eastmond, 2006; Cui *et al.*, 2016). An LD contact site that has so far not been described in plants is between LDs and the plasma membrane (PM) - a connection that has recently been described in *Drosophila melanogaster* (Ugrankar *et al.*, 2019).

SEED LD PROTEIN 1 (SLDP1) was recently described as an LD-localised protein (Kretzschmar *et al.*, 2020). It has a close homologue in *Arabidopsis thaliana*, SLDP2. We have found that double mutants of the corresponding genes display an aberrant positioning of LDs during germination. We have also identified a new LD protein, here termed LIPA, that mis-localises to the PM in the absence of SLDP2 and found that *lipa* mutants phenocopy *sldp1 sldp2* mutants in terms of LD positioning during germination. Moreover, we show that SLDP2 recruits LIPA to LDs and provide evidence that LIPA anchors LDs to the PM via interaction with SLDP2.

Results

SEED LIPID DROPLET PROTEIN (SLDP) 1 and 2 represent an undescribed LD-localised protein family

We described Arabidopsis SLDP1 to be an LD-associated protein in a previous study (Kretzschmar *et al.*, 2020) and a homologue of SLDP1 has also been found in a proteomic screen of LDs isolated from Chinese tallow seeds (Zhi *et al.*, 2017). SLDP1 has a close homologue in Arabidopsis, SLDP2 (AT5G36100). SLDP1 has 3 splice variants and SLDP2 has 2; however SLDP1.3 and SLDP2.1 share the highest homology (43.7 % sequence identity). They share a conserved C-terminus that is missing in SLDP1.1 and SLDP2.2. In addition, SLDP1.1 and SLDP1.2 contain an insertion before the C-terminus that is not found in SLDP2 (Figure 1a, Supplementary Figure 1). We therefore focused on SLDP1.3 and SLDP2.1. Bioinformatic analyses on protein sequences of SLDP1.3 and SLDP2.1 revealed that both proteins contain potential amphipathic helices at their N-termini (Figure 1b), partly overlapping with a following uncharged hydrophobic region of around 40 amino acids (residues 31 – 69/25 – 62 respectively, Supplementary Figure 2). According to the Arabidopsis AtGenExpress, *SLDP1* is only expressed in seeds and expression is highest in stage 9 developing seeds (no data available for *SLDP2*) (Nakabayashi *et al.*, 2005; Schmid *et al.*, 2005; Winter *et al.*, 2007; Waese *et al.*, 2017). According to the Klepikova eFP browser, both *SLDP1* and *SLDP2* are only expressed in seeds and senescing siliques with highest expression in dry seeds (Klepikova *et al.*, 2016; Waese *et al.*, 2017). Protein abundance of SLDP1 and SLDP2 was reported in seeds and up to 60 h old seedlings (Kretzschmar *et al.*, 2020). Transcript analysis of all splice variants in 24 h imbibed seeds by qPCR resulted in very low overall expression levels (relative to the internal standard *UBQ10*), with *SLDP1* showing higher expression than *SLDP2*. Highest expressed splice variants are *SLDP1.1* and *SLDP2.1* (Supplementary Figure 3).

Transient ectopic expression of mVenus-tagged SLDP1.3 and SLDP2.1 in *Nicotiana tabacum* pollen tubes confirmed that both proteins co-localise with stained LDs (Figure 1c). A truncated version of SLDP1.3, containing the amino acid residues 19-81 (including the amphipathic helix

and the hydrophobic stretch until the next proline residue) was sufficient to successfully target SLDP1.3 to LDs. The C-terminus of SLDP1.3, starting at amino acid residue 82 and thereby lacking the putative amphipathic helix and the hydrophobic stretch, is not targeted to LDs but to the cytosol (Figure 1d).

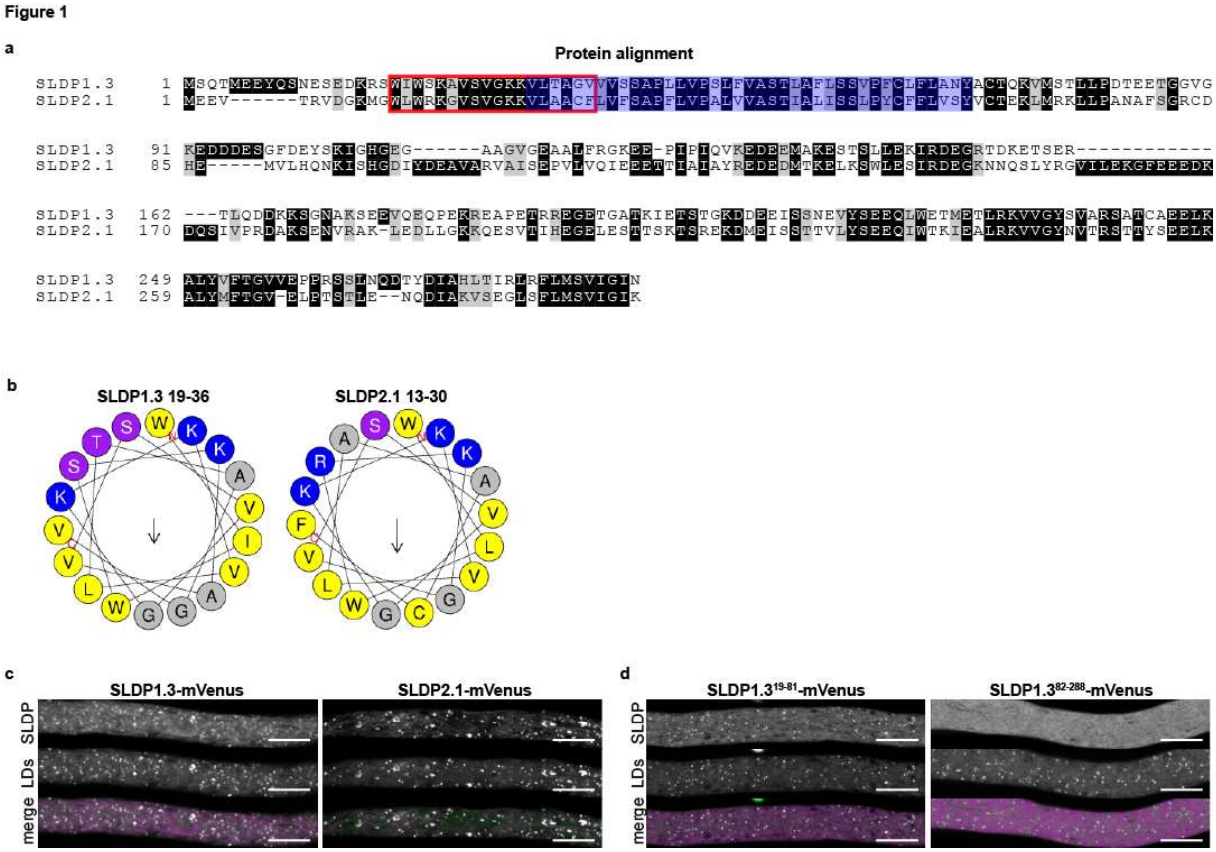

Figure 1: Analysis of SLDP

a Protein alignment of SLDP1.3 and SLDP2.1 (the two major splice variants in seeds), as generated by T-Coffee. In blue, hydrophobic/uncharged regions of SLDP1.3 and SLDP2.1 are highlighted, potential amphipathic helices are highlighted in red. For alignment of all splice variants, see Supplementary Figure 1.

b Helical wheel plots of N-terminal regions of SLDP1.3 (amino acid residues 13-30) and SLDP2.1 (amino acid residues 16-39). Plots were generated with Heliquest (https://heliquest.ipmc.cnrs.fr/cgi-bin/ComputParams.py).

c SLDP-localisation in Tobacco pollen tubes. Transient expression of LAT52::SLDP1.3-mVenus and LAT52::SLDP2.1-mVenus in *Nicotiana tabacum* pollen tubes grown for ~ 5 h. Pollen tubes were fixed in formaldehyde and LDs were stained with Nile red (Sigma-Aldrich). Images are representative of at least 10 observed pollen tubes. In merged channel: Magenta: mVenus-tagged proteins; green: Nile red-stained LDs; white: co-localisation. Bars: 10 mm.

d Truncation constructs of SLDP1.3. An mVenus-tagged LAT52::SLDP1.*3* truncation construct containing the amphipathic helix and the hydrophobic stretch (SLDP1.3 $^{19\text{-}81}$) and another truncation construct containing just the C-terminus without the hydrophobic stretch or the amphipathic helix (SLDP1.3 $^{82\text{-}288}$) were analysed for their localisation in *Nicotiana tabacum* pollen tubes grown for 5 h. Pollen tubes were fixed in formaldehyde and LDs were stained with Nile red (Sigma-Aldrich). Images are representative of at least 10 observed pollen tubes. In merged channel: Magenta: mVenus-tagged proteins; green: Nile red-stained LDs; white: co-localisation. Bars: 10 µm.

Knockout of SLDP severely interferes with cellular organisation during germination

T-DNA and CRISPR/Cas9 mutant lines of SLDP were investigated in this study (Figure 2a, Supplementary Material). While neither single nor double knockout mutants of *SLDP* showed any obvious growth or development phenotypes (Supplementary Figure 4), a phenotype could be observed on the cellular level. Here, Nile red-stained LDs were monitored every 12 h during post-germinative growth over a time course from 12 h until 48 h after stratification in the wild type and mutants. Wild-type seedlings displayed the expected cellular LD distributions: at 12 h, LDs in cotyledon (Figure 2b) as well as hypocotyl (Supplementary Figure 5) cells take up most space in the cell and are still crammed between the protein storage vacuoles and the plasma membrane. In wild-type plants during the course of germination, LDs increase in size and decrease in number, while LDs stay in the cell periphery and accumulate at the PM. In *sldp1 sldp2* knockout seedlings on the other hand, LDs do not evenly distribute along the PM during germination, but instead cluster in the middle of the cell. This phenotype is especially striking from 24 – 36 h. The phenotype is not observed in *sldp1* single knockout mutants, however cotyledon (but not hypocotyl) cells of *sldp2* single knockout seedlings show a light clustering phenotype, too. The described phenotype was observed for both analysed independent mutant lines (T-DNA and CRISPR).

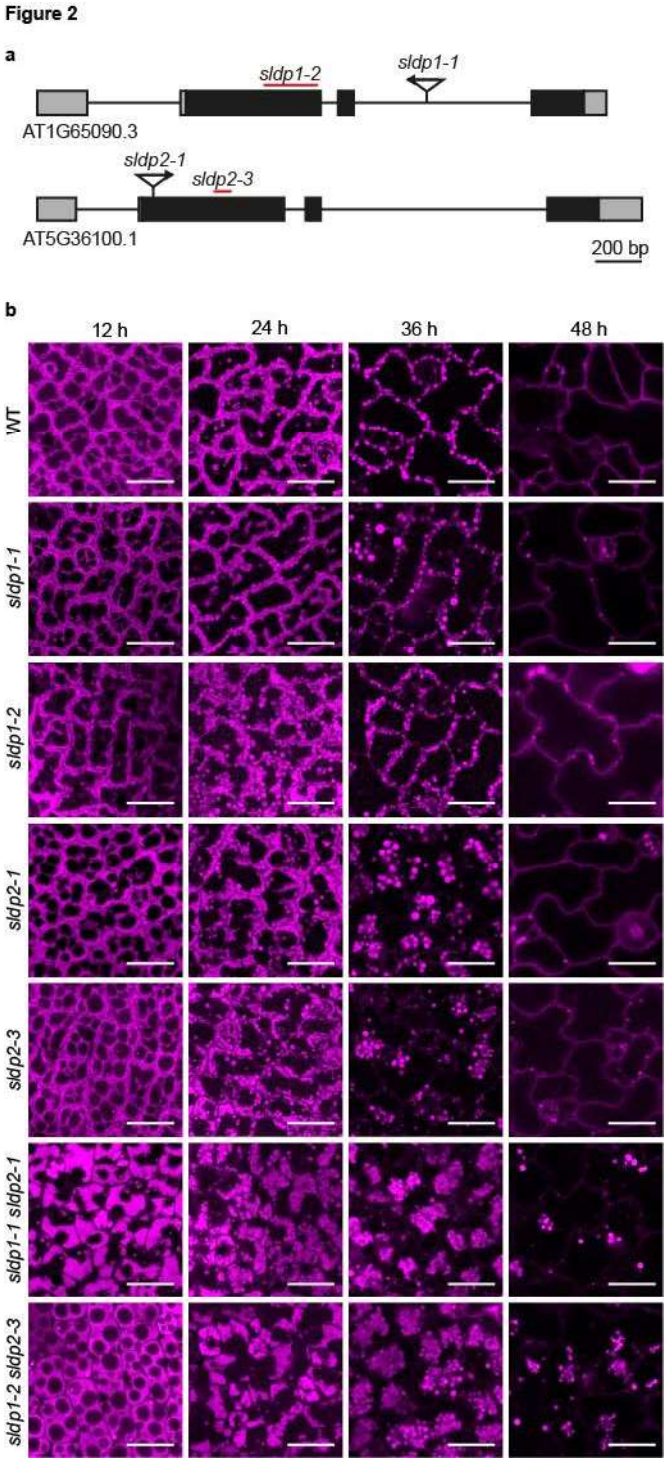

Figure 2: Time-course analysis of SLDP mutant line LDs in cotyledons.
a Schematic depiction of the genomic regions of *SLDP1.3* and *SLDP2.1* with untranslated regions (grey boxes), exons (black boxes), introns (black line), T-DNA insertion sites (triangle, arrow indicating direction of T-DNA) and CRISPR deletion lines (red line). Bar: 200 bp
b Confocal laser scanning microscopy images of germinating wild-type, *sldp1-1, sldp1-3, sldp2-1, sldp2-2*, *sldp1-1 sldp2-1* and *sldp1-3 sldp2-2* seedlings (cotyledons). Surface-sterilised seeds were placed on solid half-strength MS medium supplemented with 1 % sucrose, stratified for 4 days at 4 °C in the dark and LDs were microscopically analysed 12, 24, 36 and 48 h (± 2 h) after stratification. For analysis, LDs were stained with Nile red. Images are single plane images from the middle of the cell (similar planes were chosen for all images). Representative images for each stage and genotype were chosen, at least 5 images were taken. Bars: 10 µm.

Proteomic analyses of wild type and mutant seedlings are mostly unchanged

Proteomic analyses of WT, *sldp1-1*, *sldp2-1* and *sldp1-1 sldp2-1* seedlings (36 h after stratification) was performed. Proteins from total cellular extracts (TE fraction) as well as LD-enriched fractions (LD fraction) were analysed. In total, 2166 proteins were identified. After filtering for proteins detected in all three replicates in at least one group and identified by at least two peptides, a total of 1218 proteins remained, 666 in LD fractions and 1078 in TE fractions (Supplementary Figure 6a,b).

Many of the 666 detected proteins in LD-fractions are likely contamintants co-purifying with LDs and are no *bona fide* LD proteins. To get a set of proteins localising to LDs with high confidence, LD enrichment analysis was performed by comparing protein abundances in TE fractions to protein abundances in LD fractions (Figure 3a). For this, filters (detected at least three times in at least one group and identified by at least two peptides) were applied to the whole data set, including LD and TE fractions (see Supplementary Dataset S1 for raw LFQs and S2 for normalised and filtered LFQs). To present the data in volcano plots, imputations were performed (so that LD enrichment or depletion could also be calculated for proteins absent in one of the fractions) (Supplementary Dataset S3). This way, also proteins with overall low abundance but high enrichment in LD fractions as compared to TE fractions could be detected (see also Kretzschmar *et al.*, 2020). Overall, only minor differences between the lines were observed, only analysis of *sldp2-1* resulted in fewer LD-enriched proteins than the other analyses (Figure 3a, Supplementary Dataset S4). As expected, several oleosins and caleosins were highly enriched and of similar abundance in the wild type and mutant plants analysed. In the wild type, SLDP1 was strongly LD-enriched, but SLDP2 was filtered out in the analysis (it was not detected in three replicates in at least one group). In the *sldp1sldp2* and *sldp1* LD-enrichment analysis, SLDP1 enrichment was much weaker. SLDP1 was however still enriched, because the analysed mutant line is not a knockout but a strong knock-down and abundance was however decreased ~10-fold in both the *sldp1* and *sldp1sldp2* mutants (Supplementary Dataset S1-3).

Comparative proteome analyses reveal LIPID DROPLET PLASMA MEMBRANE ANCHOR (LIPA) as potential interaction partner of SLDP2

Co-purifications of associated membranes and their proteins can give insights on putative MCS. Therefore, also whole LD fractions were analysed and compared between the lines. For this, LD and TE fractions were handled separately and filtering was performed independently for both sets of proteins (Supplementary Dataset S2). Again, imputations were performed to create volcano plots that show proteins enriched or depleted in one of the genotypes (as compared to the wild type), including also proteins completely absent in one of the lines

(Supplementary Dataset S3). In all three analyses (*sldp1* vs. wild type, *sldp2* vs. wild type and *sldp1sldp2* vs. wild type), only two proteins were found (statistically significantly) differentially accumulated (Figure 3b). RING DOMAIN LIGASE2 (RGLG2) was detected and significantly enriched in LD fractions of *sldp1 sldp2* seedlings but was absent in wild-type LD fractions (it was detected in *sldp1* and *sldp2* LD fractions but differential accumulation there was not statistically significant). In contrast, an LD enriched-protein, here called LIPA, was absent on LDs of *sldp2* and *sldp1sldp2* plants. On *sldp1* mutant LDs, LIPA was detected at levels similar to the wild type (Supplementary Dataset S1-3).

The same comparison was performed for TE fractions but did not result in any statistically significant differences between the wild type and the analysed mutants (Supplementary Figure 6d).

Knockout of SLDP2 (but not ~10-fold knock-down of SLDP1) thus seems to be sufficient to lose LIPA in LD fractions and might hint at an interaction of the two proteins.

Figure 3

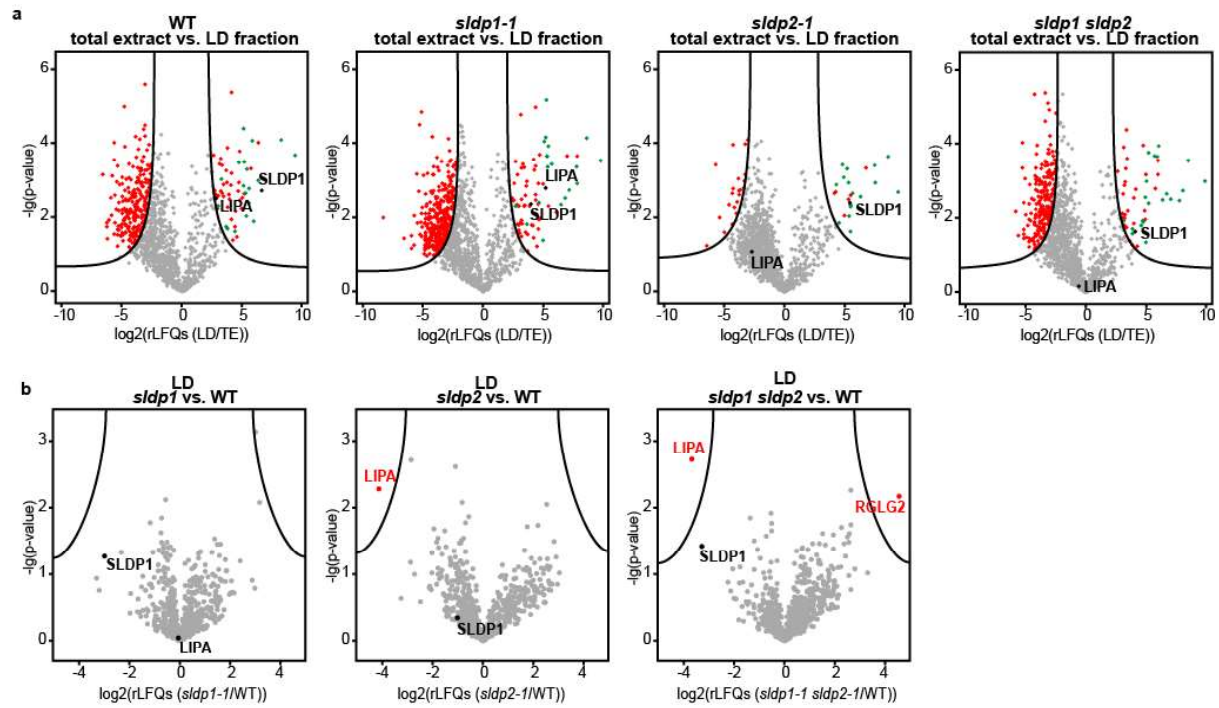

Figure 3: Proteomic Analyses of *sldp* mutants

Proteins were isolated from germinating seedlings 36 h after stratification. Proteins from LD enriched fractions and total protein fractions were analysed by LC-MS/MS after a tryptic in-gel digest (n = 3 replicates).

a Volcano plots of imputed rLFQ values from TE versus LD fractions, to detect proteins enriched at LDs. Proteins in the top right hand corner are significantly enriched at LDs in the respective analysed genotype. SLDP1 and LIPA are marked in black both plots, known LD-proteins among the significantly LD-enriched proteins are marked in green.

b Volcano plots of imputed rLFQ values from LD fractions of the wild type versus mutants, to detect proteins differentially accumulating in the respective genotype. Top left hand corner proteins are significantly depleted in *sldp1 sldp2* LD fractions, top right hand corner proteins are significantly depleted in wild-type LD fractions. SLDP1 and LIPA are marked.

LIPA localises to the PM and the cytosol in pollen tubes and leaves

LIPA is a short, 144 amino acid protein consisting of just one exon and no introns. Several previous Arabidopsis LD proteome studies have found that LIPA is enriched at LDs in siliques, seeds, and seedlings (Pyc *et al.*, 2017; Kretzschmar *et al.*, 2018; Kretzschmar *et al.*, 2020), which is in agreement with our data from wild-type plants (Supplementary Dataset S4). Localisation studies of LIPA in Tobacco pollen tubes and *Nicotiana benthamiana* leaves instead found that LIPA is a PM and/or cytosol-localised protein. In pollen tubes, C-terminally tagged LIPA localises to the cytosol, while N-terminally tagged LIPA partly localises to the cytosol but also shows plasma membrane (PM)-like localisation (Figure 4a). This may suggest that LIPA depends on accessibility of its C-terminus for PM localisation in pollen tubes. Interestingly, in transiently transformed *N. benthamiana* leaves no localisation differences between N- or C-terminally tagged LIPA was observed. Both fusion proteins show localisation to the cytosol and the PM (Figure 4c). The vector used for *N. benthamiana* transformation contains a slightly different and longer linker region (+4 amino acids) between LIPA and the fluorophore (GFP) than the vector used for pollen tube expression (mVenus), which may be responsible for differences in localisation.

When co-expressed, LIPA and SLDP mutually recruit each other

Proteomic analysis hinted at a co-purification of LIPA with SLDP2-decorated LDs, but not with LDs lacking SLDP2. These data suggest that SLDP2 plays a role in LD-localisation of LIPA. According to the Klepikova eFP browser, *SLDP* as well as *LIPA* are seed-specific and the respective genes are not natively expressed in pollen tubes or leaves. To test if SLDP2 is indeed needed for LIPA to localise to LDs, mCherry-tagged SLDP2.1 and mVenus-tagged LIPA were co-transformed in pollen tubes.

The mCherry-tagged SLDPs show the same LD-localisation as mVenus-tagged SLDPs (Figure 1c, Supplementary Figure 7a). Co-expression of LIPA with SLDP2.1 causes some LDs to form agglomerates. More strikingly, co-expression of SLDP2.1-mCherry and LIPA-mVenus (C-terminally tagged) in pollen tubes causes LIPA to re-localise from the cytosol to LDs. Upon co-expression of SLDP2.1-mCherry and mVenus-LIPA (N-terminally tagged), SLDP2.1 changes localisation and shows dual localisation to LDs and partly to the PM (Figure 4a). In re-localising to the PM, SLDP2.1 seems to drag LDs along, which are frequently found in PM-proximity upon co-localisation, suggesting a putative role of LIPA and SLDP2 in LD-PM tethering.

To quantify the PM-anchoring of SLDP and LIPA, LDs in close proximity to the PM were counted manually for all transient expression combinations. Co-expression of SLDP2.1 with N-terminally tagged LIPA significantly increases the number of LDs in proximity to the PM to

around 0.3 LDs per µm pollen tube. Pollen tubes transformed with C-terminally tagged LIPA and SLDP2.1, alone or co-transformed, show on average 0.08 – 0.09 LDs per µm, pollen tubes transformed with N-terminally tagged LIPA alone have 0.18 LDs per µm (Figure 4b).

LIPA immobilises SLDP-decorated LDs at the PM in pollen tubes

To further support the concept of a putative membrane tether, time series imaging of Nile red-stained LDs in LIPA and SLDP co-transformed pollen tubes were performed. Upon co-expression of mVenus-LIPA and SLDP2.1-mVenus, a large amount of LDs is anchored and immobilised at the PM (Figure 4c, Supplementary movie S4, all movies are representative of five recorded videos). In pollen tubes expressing mVenus-LIPA or SLDP2.1-mVenus alone (Figure 4c, Supplementary movie S2-S3), as well as in control pollen tubes expressing just mVenus (Supplementary Figure 7c, Supplementary movie S1), LDs dynamically move through the pollen tube with the cytoplasmic streaming

Similar but weaker results were obtained for SLDP1.3-mCherry: mutual recruitment is possible, but especially videos show that fewer LDs are anchored to the PM than with SLDP2.1 (Supplementary Figure 7b,c, Supplementary movie S5-S6).

Figure 4

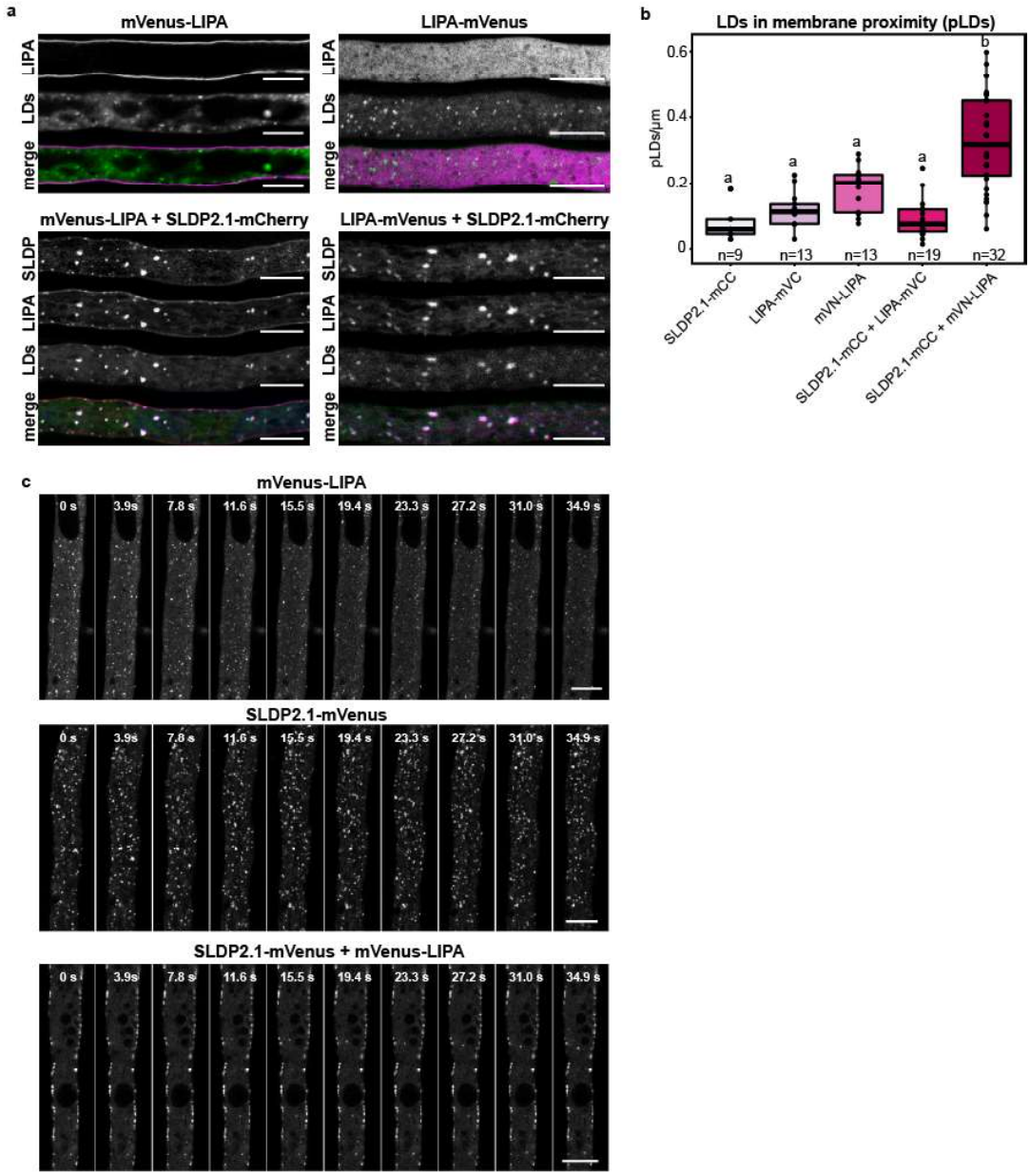

Figure 4: Localisation analysis of LIPA in pollen tubes

a Transient expression of LAT52::mVenus-*LIPA* and LAT52::*LIPA*-mVenus alone and co-expressed with LAT52::*SLDP2.1*-mCherry in *Nicotiana tabacum* pollen tubes grown for ~ 5 h. Pollen tubes were fixed in formaldehyde and LDs were stained with Lipi-Blue. At least 10 pollen tubes were analysed for each transformation, images of at least 5 pollen tubes were taken. For merged image with two channels: magenta: mVenus (LIPA); green: LDs. For merged images with three channels red: mVenus (LIPA), blue: mCherry (SLDP), green: LDs. Bars: 10 µm.

b Analysis of LDs in proximity to the PM (pLDs). LDs close to the PM were counted manually in the Lipi-Blue channel and number of pLDs per mm were calculated. Results are presented as boxplot (displaying lower hinge = 25% quantile, median = 50% quantile, upper hinge = 75% quantile, upper whisker = largest observation less than or equal to upper hinge + 1.5 * IQR, lower whisker = smallest observation greater than or equal to lower hinge - 1.5 * IQR). One-way ANOVA was performed, followed by Tukey post-hoc analysis (F (4,81) = 23.37, p = 7.24e-13, n = as indicated). Results are presented as compact letter display of all pair-wise comparisons in increasing order.

c Pollen tube time series. Transient expression of LAT52::mVenus-*LIPA* and LAT52::*SLDP2.1*-mVenus alone and co-expressed in *Nicotiana tabacum* pollen tubes grown for ~ 5 h. Pollen tubes were fixed in formaldehyde. LDs were stained with Nile red (Sigma Aldrich) and Nile red fluorescence was recorded over the indicated time course. Images for mVenus-LIPA and SLDP2.1-mVenus show LDs moving with the cytoplasmic streaming, while for co-expression of mVenus-LIPA and SLDP2.1-mVenus, LDs are immobilised at the PM. Bars: 10 µm.

Re-localisation of LIPA is also observed in leaves

To further confirm the interaction between SLDP2 and LIPA, transient transformations were performed in *N. benthamiana* leaves. Localisation results were in agreement with the pollen tube localisation data. GFP-tagged LIPA localised to the PM and/or cytosol in leaf cells, but when co-expressed with mCherry-tagged SLDP2, LIPA re-localised to LDs (Figure 5). This shows that the SLDP-induced re-localisation of LIPA is not tissue-specific. Due to the large central vacuole in leaf epidermal cells, most of the cytoplasm (and consequently, LDs) is adjacent to the PM. The LDs that co-localise with SLDP2 and LIPA are found near the PM, but we were not able to determine if they were indeed associated with the PM as in pollen tubes.

LIPA and SLDP thus mutually influence their localisation in pollen tubes and leaves. SLDP can recruit LIPA to LDs, while LIPA can recruit SLDP to the PM, thereby anchoring LDs to the PM.

Figure 5

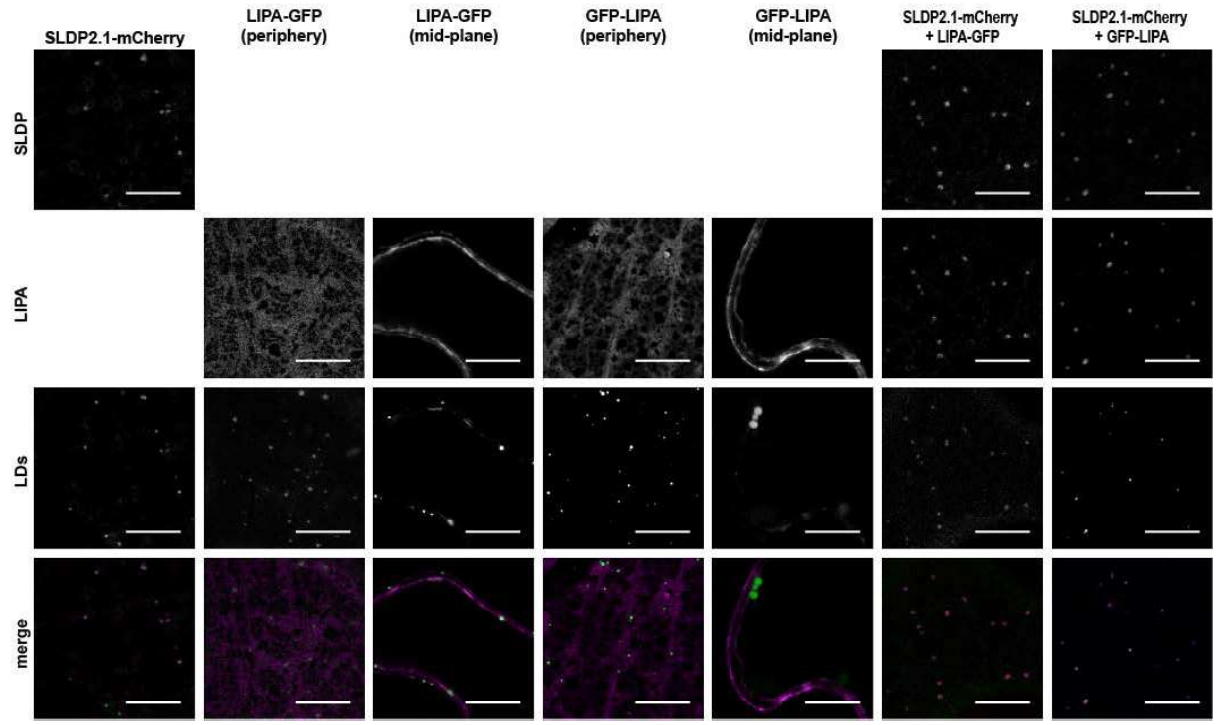

Figure 5: Localisation analysis of LIPA in leaves
Transient expression of pMDC43/LIPA (GFP-LIPA), pMDC32-CGFP/LIPA (LIPA-GFP), and pMDC32-CherryC/SLDP2.1, expressed alone or co-expressed in different combinations in *Nicotiana benthamiana* leaves. LDs were stained with MDH. Images were taken in the cell periphery close to the top of the cell. For single expressions of LIPA-constructs, also images from the mid-plane are shown. For merged image with two channels: magenta: mVenus (LIPA); green: LDs. For merged images with three channels red: mVenus (LIPA), blue: mCherry (SLDP), green: LDs. Bars: 10 µm

Coiled-coil domain of LIPA mediates interaction with SLDP

In silico domain analysis of LIPA did not result in any known domains. Also, no hydrophobic stretches or uncharged regions were detected, neither were transmembrane domains (Supplementary Figure 8a-b). However, analysis with the coiled-coil prediction algorithm COILS (Lupas *et al.*, 1991) revealed a putative coiled-coil domain in the region of amino acid residues 60 – 115 (Supplementary Figure 8c). A truncated version of LIPA, consisting of an N-terminal mVenus and the predicted coiled-coil region of LIPA (amino acid residues 64-113 of 144, LIPA$^{64-113}$), was transformed into pollen tubes, alone and together with SLDP2. LIPA$^{64-113}$ alone shows cytosolic localisation but is recruited to LDs after co-expression of SLDP2.1 (Figure 6a) and is thus sufficient to mediate interaction of SLDP2 and LIPA. To further analyse the importance of the coiled-coil region, two proline residues were introduced in order to disrupt the coiled-coil. Site-directed mutagenesis of a leucine residue at position 80 and a valine residue at position 98 to prolines (LIPA L^{80}P V^{98}P) is predicted to prevent coiled-coil formation (Supplementary Figure 8c). The mutagenesis does not interfere with localisation of full-length N-terminally or C-terminally tagged LIPA in pollen tubes when expressed alone (Supplementary Figure 9). However, interaction of (C- or N-terminally tagged) LIPA L^{80}P V^{98}P and SLDP2.1 in co-transformed pollen tubes is abolished (Figure 6b).

The coiled-coil region of LIPA is thus sufficient and most likely also necessary to mediate interaction of SLDP2 and LIPA.

Figure 6

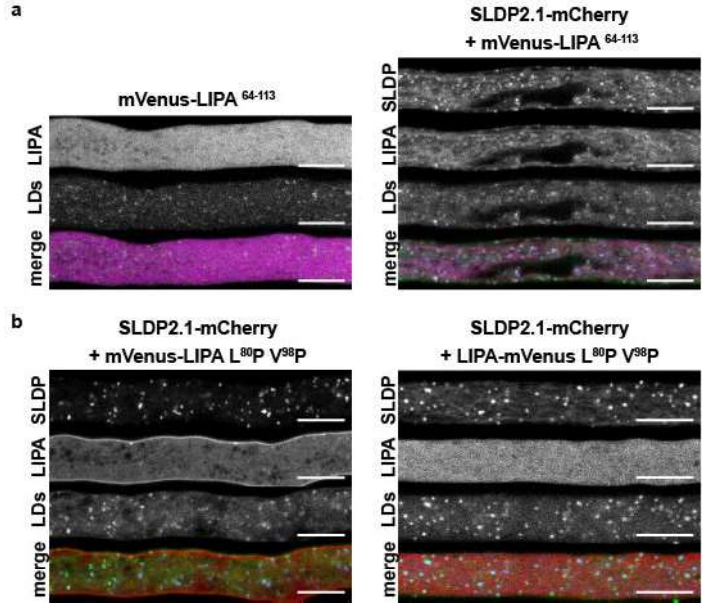

Figure 6: Analysis of LIPA coiled-coil

Transient co-expression of **a** LAT52::mVenus-LIPA$^{64-113}$ and LAT52::SLDP2.1-mCherry and **b** LAT52::mVenus-LIPA L^{80}P V^{98}P or LAT52::LIPA L^{80}P V^{98}P-mVenus and LAT52::SLDP2.1-mCherry in *Nicotiana tabacum* pollen tubes grown for ~ 5 h. Pollen tubes were fixed in formaldehyde and LDs were stained with Lipi-Blue. Images of at least 5 pollen tubes were taken. For merged image with two channels: magenta: mVenus (LIPA); green: LDs. For merged images with three channels red: mVenus (LIPA), blue: mCherry (SLDP), green: LDs. Bars: 10 µm.

Both SLDP proteins as well as LIPA are needed for proper LD distribution during germination

Two knockout lines of *LIPA* were investigated, a T-DNA insertion line and a line created by CRISPR/Cas9 as part of this study. Time-course microscopy of *lipa* knockout seedlings was performed as described before and revealed the same LD clustering phenotype that was observed for *sldp1 sldp2* mutant seedlings (Figure 7). Knockout of LIPA alone thus results in the same phenotype as knockout of SLDP2 or double knockout of SLDP1 and SLDP2 and suggests that all three proteins act together during germination to enable proper LD distribution in the cell.

In wild-type seedlings, always a portion of LDs is always observed in contact with the PM, as is here shown by high-pressure freezing electron microscopy (Figure 8). The presented images show LDs in contact with the PM, most likely not because they are pressed there by other organelles like e.g. the expanding vacuole, but rather because of a true MCS between LDs and the PM. This contact of LDs with the PM is hampered by knockout of either SLDP2 or LIPA.

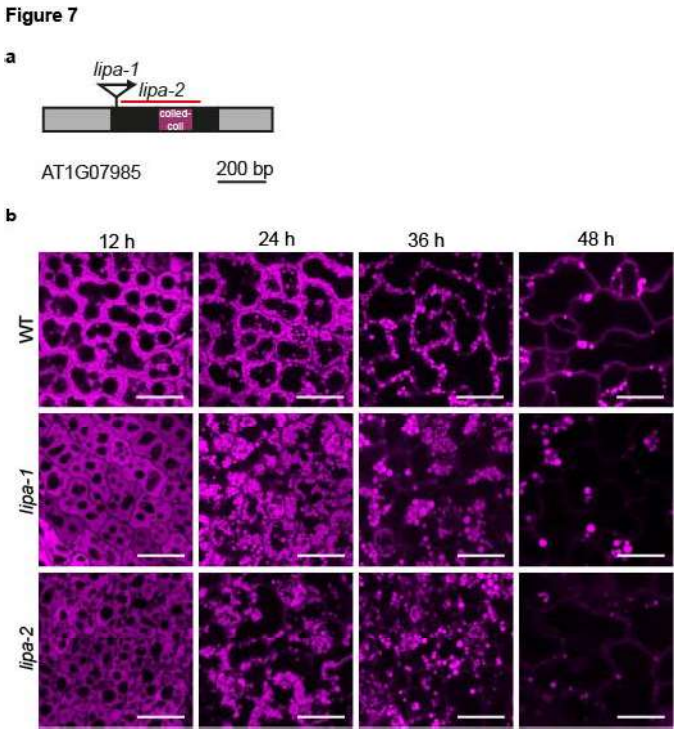

Figure 7: Time-course analysis of LDs in cotyledons

a Schematic depiction of the genomic regions of *LIPA* with untranslated regions (grey boxes), one exon (black boxes), T-DNA insertion sites (triangle, arrow indicating direction of T-DNA) and CRISPR deletion line (red line). Bar: 200 bp

b Confocal laser scanning microscopy images of germinating *lipa-1* and *lipa-2* seedlings (cotyledons). Surface-sterilised seeds were placed on solid half-strength MS medium supplemented with 1 % sucrose, stratified for 4 days at 4 °C in the dark and LDs were microscopically analysed 12, 24, 36 and 48 h (± 2 h) after stratification. For analysis, LDs were stained with Nile red. Images are single plane images from the middle of the cell (similar planes were chosen for all images). Representative images for each stage and genotype were chosen, at least 5 images were taken. Bars: 10 µm.

Figure 8

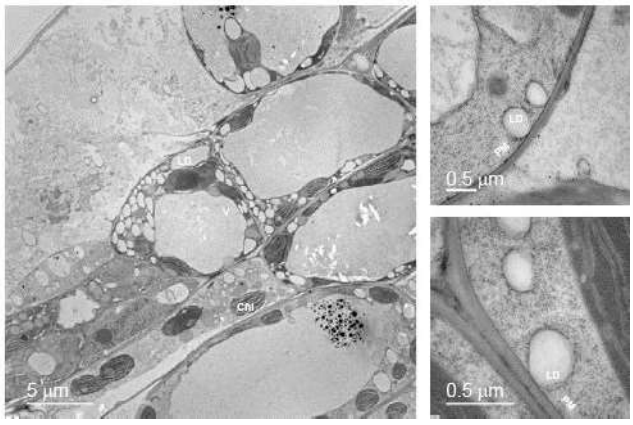

Figure 8: Electron microscopy of LD-PM contacts
High-pressure freezing electron microscopy images of wild-type seedlings after 40 - 48 h of germination. Whole cell overview (large) and close-ups (from different cells) of LDs in contact with the PM. Bars as indicated. Chl – Chloroplast; LD – Lipid Droplet; PM – Plasma Membrane; V – Vacuole.

Discussion

In the present study, plant mutant lines affected in the genes coding for the LD-localised proteins SLDP1 and SLDP2 were analysed. These mutants displayed an aberrant cellular distribution of LDs that were not in contact with the PM during post-germinative growth. Proteomic analyses showed that SLDP2 is needed to recruit LIPA to LDs and further microscopic analyses revealed that upon co-expression of SLDP and LIPA, a portion of LDs was immobilised at the PM. The lack of mobile LDs in co-transformed pollen tubes suggests that we were able to recreate the PM-tethered LDs found in wild-type seedlings by co-expressing SLDP2 and LIPA. Though the LDs in *sldp2*, *sldp1sldp2*, and *lipa* establishing seedlings were not streaming through the cytoplasm, they were improperly positioned in the cotyledon and hypocotyl cells and many were no longer in contact with the PM. Based on these results, we suggest a model where in seedlings, PM-associated LIPA interacts with LD-localised SLDP and forms a MCS to attach LDs to the PM during post-germinative growth (Figure 9).

Figure 9

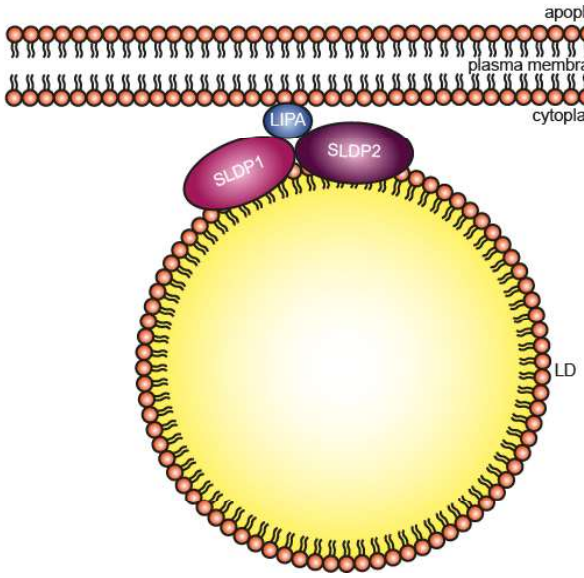

Figure 9: Schematic model of a PM-LD tether formed by SLDP and LIPA
SLDP1 and SLDP2 are bound on LDs and might or might not interact there. LIPA binds to the PM and interacts with SLDP2 and maybe SLDP1 through its coiled-coil region. Thus, LDs might be tethered to the luminal side of the PM.

We show that LD-association of SLDP is mediated by an N-terminal hydrophobic region, similar to what has been reported before for other LD-localised proteins (Wilfling *et al.*, 2013; Kretzschmar *et al.*, 2018). Interaction of LIPA with SLDP is mediated by a coiled-coil region of LIPA. How LIPA is associated to the PM remains unclear, since no transmembrane domains were detected within LIPA protein sequence. LIPA may associate with the PM via binding to an unidentified PM-localised protein. This putative third interaction partner might be present in pollen tubes, but absent in leaves, potentially explaining the differences in localisation of transiently transformed LIPA in the respective organs.

Alternatively, the C-terminal Cys residue of LIPA (IHSKSWR**C***) may be subjected S-palmitoylation, S-farnesylation or S-geranylgeranylation (according to GPS-lipid prediction with high threshold, Xie *et al.*, 2016).

Protein membrane targeting can also be mediated by anionic lipids such as phosphoinositides (PI), phosphatidylserine (PS) or phosphatidic acid (PA). The negatively charged headgroups of these lipids can recruit polybasic stretches of proteins through electrostatic interactions or through lipid-binding domains such as PX or pleckstrin homology domains (Noack and Jaillais, 2020). Indeed, LIPA harbours a polybasic stretch close to its C-terminus (residues 102-123: **RKR**ED**K**TD**K**E**KK**TP**KKKK**GLR**K**) that might mediate PM-association and indeed a variant missing this region no longer localizes to the PM (Figure 5a). Other proteins involved in interorganellar tethers have been described to bind one of the interacting membranes this way, e.g. the phosphoinositide-binding PX domains of Drosophila Snz (localises to ER-PM-LD contacts) (Ugrankar *et al.*, 2019) or yeast Mdm1 (tethering LDs to nucleus-vacuolar junctions

(Henne *et al.*, 2015; Hariri *et al.*, 2018; Hariri *et al.*, 2019). Replacing the yeast Mdm1 vacuole-binding PX domain by a PM-binding one leads to Mdm1 re-localisation to ER-PM contact sites and the accumulation of LDs in the cell periphery (Hariri *et al.*, 2019). Lipid-binding specificity of tethering proteins thus determines location of their interacting LDs in the cell and is sufficient to induce re-localisation of LDs. Loss of this targeting mechanism could reversely lead to the aberrant accumulation of LDs within the cell, as described in the present study.

Another open question is the function of a putative LD-PM contact site in post-germinative growth. Indirect evidence for a putative LD-PM/LD-ER-PM contact sites in plants is already available: It was recently found that ER-LD junction-localised Seipin interacts with ER-PM junction-localised vesicle-associated membrane protein (VAMP)-associated protein 27-1 (VAP27-1) in Arabidopsis (Greer *et al.*, 2020). Seipin is a highly conserved protein that forms large ring-like oligomers in the ER membrane, likely tethering LDs to the ER during LD biogenesis (Sui *et al.*, 2018), while VAP27-1 is an ER-associated protein involved in several functions, including tethering of the ER to the PM through interaction with AtSYT1 (Siao *et al.*, 2016). These findings might indicate that LDs are found in contact with the PM also in other tissues than seedling tissue. Functional implications of a LD-PM tether however remain unclear, as well.

A possible function of LDs at the PM during seedling establishment might be buffering of excess lipids, similar to what has been observed during starvation-induced autophagy. During autophagy, LD biogenesis is a protective mean to prevent lipotoxicity of bulk lipid release and subsequent accumulating acylcarnitines (Nguyen *et al.*, 2017). In a similar way, LDs might be needed as a buffer to prevent toxic lipid accumulation during post-germinative growth. Seedling establishment, especially etiolation when seeds are buried in the soil, requires massive membrane lipid supply for hypocotyl elongation. If membrane lipid synthesis takes place at very high rates, situations of oversupply might arise. Accumulating excess lipids could be sequestered into LDs for detoxification. LDs might also be needed at the PM for membrane repair, either for the same reason as described (to buffer excess lipids produced for membrane repair) or to provide the lipids for membrane repair. More generally spoken, the PM-LD tether might be needed for maintaining PM lipid composition and homeostasis, as has been shown for LD contact sites with e.g. the ER (Velázquez *et al.*, 2016). The importance of this MCS might possibly only come into effect as response to different stresses (e.g. salt stress, freezing stress, mechanical stresses, membrane rupture), which would explain the lack of macroscopic phenotypes observed under laboratory conditions in the present study, despite the striking cellular phenotype.

More studies will have to be conducted in the future to gain mechanistic insights into the localisation, assembly and interaction of the tethering components, analyse the putative

involvement of the ER and/or further proteins and finally to elucidate physiological importance of the LD-PM contact site in seedlings.

Acknowledgement

HEK, OV, KS, GB and TI thank the German research foundation (DFG, Grants IS 273/2-2, IS 273/7-1, IRTG 2172 PRoTECT, BR1502-15-1 and INST 186/1230-1 FUGG to Stefanie Pöggeler).

Experimental Procedures

Plant material and growth conditions

All *Arabidopsis thaliana* (L.) plants employed the ecotype Col-0 or were derived from it in the case of T-DNA and CRISPR mutant lines. They were grown in a climate chamber (York) in 60 % relative humidity, with a constant temperature of 23 °C and under 16-h/8-h day/night cycle with a daytime light intensity of 150 µmol photons m^{-2} s^{-1} (the climate chamber was equipped with LuxLine Plus F36W 830 Warm White de Luxe fluorescent tubes; Osram Silvania). Plants were either grown on soil or on half-strength MS medium (Murashige and Skoog, 1962) supplemented with 0.8 % (w/v) agar with or without 1 % (w/v) sucrose (as indicated) and stratified for four days at 4 °C in the dark. Seeds grown on medium were surface sterilised in 6 % sodium hypochlorite solution for 15 – 20 minutes. For hygromycin-selection, half-strength MS plates were supplemented with 25 µg/ml hygromycin and 1 % (w/v) sucrose, stratified for two days at 4 °C, subjected to light for 4 h and then kept vertically in the dark for three days. Hygromycin-resistant seedlings were transferred to half-strength MS + 1 % (w/v) sucrose without hygromycin for one week prior to transplanting them into soil.

Tobacco (*Nicotiana tabacum* L. cv. Samsun-NN) plants were grown in the greenhouse as previously described (Rotsch *et al.*, 2017). Plants were kept under 14 h of light from mercury-vapor lamps in addition to sunlight. Light intensities reached 150 – 300 µmol m^{-2} sec^{-1} at the flowers and 50 – 100 µmol m^{-2} sec^{-1} at leaves at mid-height. Temperature was set to 16 °C at night and 21 °C during the day with a humidity of 57–68%.

Nicotiana benthamiana plants were grown in soil at 22 °C with a 16-h/8-h day/night cycle and 50 $\mu E \cdot m^{-2} s^{-1}$ light intensity.

Accession Numbers and T-DNA lines

Sequence data from this article can be found in the GenBank/EMBL data libraries under the following accession numbers: AT1G65090 (SLDP1); AT5G36100 (SLDP2); AT1G07985 (LIPA). Sequence analyses and predictions of all analysed mutant lines are also shown in Supplementary Material.

Knockout lines of *SLDP1, SLDP2* and *LIPA* were generated. The commercially available T-DNA insertional lines SALK_204434C (*sldp1-1*, T-DNA inserted in intronic region behind base 1028) and SALK_068917 (*sldp2*-1, T-DNA inserted in first exon behind base 42) and Gabi-KAT 59-K025364-022-723-C08-8409 (*lipa-1*, T-DNA inserted behind base 20) were used, and CRISPR/Cas9 was used to generate *sldp1-2*, *sldp2-3, and lipa-2 (see below)*. Sequence analyses and predictions of all analysed mutant lines are shown in Supplementary Material.

CRISPR/Cas9

To generate CRISPR/Cas9 mutants, sgRNAs were designed using the Cas-Designer and Cas-OFFinder at http://www.rgenome.net/ for a SpCas9 protospacer adjacent motif (PAM) sequence and with a length of 19 bp (without PAM) against the *Arabidopsis thaliana* (TAIR10) genome (Bae *et al.*, 2014; Park *et al.*, 2015). Cloning was performed as described previously (Xing *et al.*, 2014). As template for the sgRNA cassette (including one sgRNA backbone, one U6-26 terminator and one U6-29 promoter), pCBC DT1T2 was used and the generated PCR-product was cloned into pHEE401E via BsaI restriction sites, between a U6-26 promoter on one side and a second sgRNA backbone and a U6-29 terminator on the other side (as described Xing *et al.*, 2014; Wang *et al.*, 2015). This way, a CRISPR/Cas9 construct containing two sgRNAs under two U6 promoters and a Cas9 under the egg-cell specific EC1.2 promoter was obtained. To knock out one gene, two different sgRNAs were targeted at it, aiming at deleting the whole gene stretch between the target sequences. This made it possible to screen for mutant plants via PCR. For this, gDNA was extracted from rosette leaves, the area of interest was amplified via REDTaq®-PCR and screened for the desired smaller PCR-products that indicated a deletion. Homozygous mutants were obtained in the T2 and T1 generation for SLDP1 and SLDP2, respectively. To remove the Cas9-transgene, homozygous mutants were backcrossed to WT plants (and Cas9-loss was confirmed by PCR with U6- and Hygromycin-specific primers).

For *SLDP1*, a mutant line with deletion of bases Δ333-564 in the first exon (resulting in a frameshift and a premature stop codon at position 650-652 for AT1G65090.1 and .2 or at position 686-688 for AT1G65090.3, producing a potential 139 amino acid protein for AT1G65090.1 and .2 or 152 amino acids for AT1G65090.3) was obtained and called *sldp1-2.* For *SLDP2*, a mutant line with deletion of bases Δ304-379 in the first exon (resulting in

frameshift and premature stop codon at position 398-400, producing a potential 107 amino acid protein) was obtained and called *sldp2-3*. For *LIPA* a mutant line with deletion of bases Δ94-214 (resulting in a frameshift and premature stop codon at position 230-232 and a potential 36 amino acid protein) was obtained and called *lipa-2*. Sequence analyses and predictions of all analysed mutant lines are shown in Supplementary Material.

RNA isolation and qPCR

RNA from three replicates was isolated using an RNA extraction kit (Monarch Total RNA Miniprep Kit, NEB). For dry seeds, 5 mg of starting material was used. cDNA synthesis was performed with 900 ng total RNA and 100 pmol oligo(dT) primer using the Maxima Reverse Transcriptase (Thermo Scientific) according to the manufacturer's instructions. Transcript analysis by qPCR was carried out with AT4G05320 (*POLYUBIQUITIN 10*) as reference (Czechowski *et al.*, 2005). Amplification and quantification were performed with the Takyon™ No Rox SYBR® MasterMix dTTP Blue Kit (Eurogentec) in the iCycler System (iQ™5 Real-Time PCR Detection System, Bio-Rad). The amplification mix contained 1x Takyon™ No Rox SYBR® MasterMix dTTP Blue, 2 mM primers and 4 µl cDNA in a final reaction volume of 20 µl. The PCR program consisted of a 3 min denaturation step at 95°C followed by 40 cycles of 10 s at 95°C, 20 s at 58°C, and 40 s at 72°C.
Data analysis was performed using the $2^{-\Delta\Delta CT}$ method that has previously been described (Livak and Schmittgen, 2001).

Plasmid construction

For localisation studies in pollen tubes, coding sequences of the genes of interest were cloned into pLatMVC-GW, pLatMVN-GW or pLatMCC-GW (Müller *et al.*, 2017) via classical or fast Gateway® (Thermo Fisher Scientific) cloning as described before (Müller *et al.*, 2017). All pLat-constructs contain a LAT52 promoter for strong expression in pollen tubes (Twell *et al.*, 1991) and were verified by sequencing.

For localisation studies in leaves, cloning of pMDC32-ChC/SLDP2, encoding SLDP2 appended at its C-terminus to the red fluorescent protein mCherry (SLDP2-mCherry), pMDC32-CGFP/LIPA, encoding LIPA appended at its C-terminus to a monomerised version of GFP (LIPA-mGFP), and pMDC43/LIPA, encoding LIPA appended at its N-terminus to GFP (GFP-LIPA), was performed using Gateway cloning technology (Müller *et al.*, 2017) and the binary vectors pMDC32-ChC (Kretzschmar *et al.*, 2020), pMDC43 (Curtis and Grossniklaus, 2003), and pMDC32-CGFP (described below), respectively. Each binary vector contains the 35S cauliflower mosaic virus promoter and was verified by automated sequencing performed at the University of Guelph Genomics Facility.

The pMDC32-CGFP binary vector contains a Gateway recombination site followed by the full-length mGFP open reading frame, which provides for the expression of a fusion protein with a C-terminal-appended mGFP. To construct pMDC32-CGFP, the mGFP coding sequence was amplified from pRTL2/monoGFP-MCS (Shockey *et al.*, 2006), using primers GFP-FP-PacI (5'-CCGGCCTTAATTAAAATGAGTAAAGGAGAAGAACTTTT-3') and GFP-RP-SacI (5'-CCGGCCGAGCTCTTATTTGTATAGTTCATCCATGCC-3'), which also added 5' PacI and 3' SacI restriction sites. The resulting PCR products were digested with PacI and SacI and ligated into similarly-digested pMDC32-ChC to yield pMDC32-CGFP.

Particle bombardment and pollen tube microscopy

Nicotiana tabacum pollen tubes were transiently transformed using a gene gun. For this, 6 µg of construct DNA was coated onto approx. 0.9 mg gold particles (1 µm), shot onto freshly harvested *N. tabacum* pollen of 5 flowers per transformation. Pollen tubes were grown for 5-7 h in liquid pollen tube medium on a microscope slide in a humid environment (in detail methods on coating and transformation were described before in Müller *et al.*, 2017). For co-transformation, 6 µg DNA of each construct were pre-mixed and then coated onto the gold particles.

For pollen tube microscopy, pollen tubes were fixed in a final concentration of 1.8 % (v/v) formaldehyde in pollen tube medium (modified from Read *et al.*, 1993): 5 % w/v sucrose, 12.5 % w/v PEG-4000, 15 mM MES-KOH pH 5.9, 1 mM CaCl2,1 mM KCl, 0.8 mM MgSO4, 0.01 % H3BO3 v/v, 30 µM CuSO4) and LDs were stained with 0.05 % Nile red (Sigma-Aldrich, St. Louis, Missouri, USA) in DMSO or 0.5 % Lipi-Blue (Dojindo, Molecular Technologies, Rockville, MD, US) in DMSO, as indicated. Micrographs were acquired as single z-sections using a Zeiss LSM 510 or a Zeiss LSM780 confocal microscope (Carl Zeiss). For excitation, 405 nm Diode was used, Lipi-Blue fluorescence was detected from 443 – 475 nm, Nile red was excited with 561 nm and detected at 583-667 nm. Constructs with mCherry were excited with 561 nm and detected at 571 – 614 nm, mVenus was excited with 488 nm and detected at 518 – 550 nm or 497-533 nm when co-imaged with Nile red. HFT 405/ 514/633-nm major beam splitter (MBS) was used.

***N. benthamiana* infiltration and microscopy**

For infiltration, leaves of 4-week-old *N. benthamiana* plants were (co-)infiltrated with *Agrobacterium tumefaciens* (strain LBA4404) harbouring a selected binary vector, as described previously (Kretzschmar *et al.*, 2020). All (co)infiltrations also included *A. tumefaciens* transformed with pORE04-35S::P19, which encodes the tomato bushy stunt virus gene *P19* to enhance transgene expression (Petrie *et al.*, 2010).

(Co-)infiltrated N. benthamiana leaves were prepared for confocal laser scanning microscopy (CLSM) by first fixing with 4% (w/v) formaldehyde, washing with PIPES buffer, and then staining with neutral lipid-specific dye monodansylpentane (MDH) (Abcepta) (Yang *et al.*, 2012) at a working concentration of 0.4 mM, as described previously (Gidda *et al.*, 2016). Micrographs of leaf epidermal cells were acquired as single z-sections using a Leica SP5 CLSM (Leica Microsystems) with the same excitation and emission parameters for mCherry, GFP, and MDH as reported previously (Gidda *et al.*, 2016). All images of cells are representative of at least two independent experiments (i.e., infiltrations), including at least three separate (co-)transformation of leaf epidermal cells.

Seedling preparation and microscopy

For seedling time-course microscopic analyses, wild-type and mutant seedlings were grown and stratified on half-strength MS-medium without sucrose as described above. They were transferred to light at 07.30 am (light period 7 am – 11 pm, 16-h/8-h day/night cycle) and then analysed after 12, 24, 36 and 48 h of germination. Seedlings were harvested into H_2O + 0.1 % Nile red (Sigma Aldrich) in DMSO and directly used for microscopy after removal of seed coats. Micrographs were taken as single z-sections using a Zeiss LSM780 confocal microscope (Carl Zeiss). For Nile Red excitation, 561 nm laser was used, fluorescence was detected at 571-603 nm with a 488/561 MBS. Images of hypocotyl and cotyledon cells are representative of at least two independent experiments (except *lipa-2*, *sldp1-3* and *sldp2-2,* just 1 experiment) including at least 10 observed seedlings. At least 5 images were acquired per genotype and time point.

Proteomic analysis

Arabidopsis thaliana seedlings were surface-sterilised, placed on half-strength MS-medium without sucrose, stratified for 72 h at 4 °C in the dark and then grown at 22°C under 16 h/ 8 h of light-dark regime for 38 h.

Total protein isolation of total extract (TE) and LD fractions, LD-enrichment, proteomics sample preparation including a tryptic in-gel digest, LC/MS analysis and analysis of MS/MS2 raw data was performed for three replicates as previously described (Kretzschmar *et al.*, 2018).

LFQ values were determined using MaxQuant software 1.6.2.10 (Cox and Mann, 2008; Cox *et al.*, 2014). Perseus software (version 1.6.6.2) (Tyanova *et al.*, 2016) was used for data analysis. PCA plots were created from unfiltered raw LFQ values (Supplementary Dataset S1). LFQ values were normalised as ‰ of total sum of all LFQs per replicate and log_2-transformed (rLFQ) for further analyses. For LD-enrichment analysis within one line, all proteins from TE and LD fractions together were filtered for those detected at least three times in at least one group and identified by at least two peptides (Supplementary Dataset S2).

For differential abundance analysis of LD or TE fractions between the lines, LD fraction and TE fraction were analysed separately and filtering was performed independently of the respective other fraction (Supplementary Dataset S2).

For enrichment and differential abundance analyses, rLFQ-values were imputed: missing values were replaced from normal distribution (for total extract: width 0.3, down shift 1.8; for LD fractions: width 0.5, down shift 1.8; for both fractions together: width 0.8, down shift 1.8; Supplementary Dataset S3). To obtain proteins significantly enriched on LDs, LD fractions were compared to TE fractions and analysed for proteins enriched in LD fractions. To find differentially abundant proteins between the different lines, LD fractions of mutants were compared to LD fractions of the wild type, the same was done for TE fractions. Proteins were considered LD-enriched or differentially abundant, respectively, if FDR < 0.01 and S0 > 2 (as determined by two-sided t-test with 250 randomisations). Volcano plots were created to visualise the results.

Electron microscopy

High pressure freezing electron microscopic analysis was performed similarly as described before (Hillmer *et al.*, 2012). Plant material was dissected from hypocotyls or cotyledons of 36-48 h germinated seedlings with a biopsy punch (pfmmedical, Köln; 2mm diameter), submerged in freezing medium (200 mM Suc, 10 mM trehalose, and 10 mM Tris buffer, pH 6.6) transferred into planchettes (Wohlwend, Sennwald, Switzerland; type 241 and 242), and frozen in a high-pressure freezer (HPM010; Bal-Tec, Liechtenstein). Freeze substitution was performed in a Leica EM AFS2 freeze substitution unit in dry acetone supplemented with 0.3% uranyl acetate at −85°C for 16 h before gradually warming up to −50°C over a 5-h period. After washing with 100 % ethanol for 60 min, samples were stepwise infiltrated (intermediate steps of 30 %, 60 % HM20 in ethanol, and twice with 100% HM20 for 1h each), embedded in Lowicryl HM20 at −50 °C and polymerized for 3 d with UV light in the freeze substitution apparatus at -35 °C. Ultrathin sections were cut on a Leica Ultracut S and poststaind with 3 % aqueous uranyl acetate and lead citrate for 3 min each. Micrographs were taken at a Jeol JEM1400 TEM (Jeol Germany, Freising) equipped with a TVIPS TEMCAM F416 digital camera (TVIPS, Gauting) using EMMenue 4 (TVIPS, Gauting).

Bioinformatics

For sequence alignments, T-Coffee (Notredame *et al.*, 2000) (http://tcoffee.crg.cat/apps/tcoffee/do:regular) was used with default settings. Sequence identity was calculated by Needleman-Wunsch global alignment of two sequences (Needleman and Wunsch, 1970) with EMBOSS needle on default settings (https://www.bioinformatics.nl/cgi-bin/emboss/needle). Helical wheel plots were created by

Heliquest (Gautier *et al.*, 2008) (https://heliquest.ipmc.cnrs.fr/cgi-bin/ComputParams.py) with Helix type: alpha and window size: 1_TURN. For hydrophobicity plots, ExPASy ProtScale (https://web.expasy.org/protscale/) was used with a Kyte&Doolittle scale (Kyte and Doolittle, 1982) and a window size of 9. Charge plots were created by EMBOSS explorer charge (http://www.bioinformatics.nl/cgi-bin/emboss/charge?_pref_hide_optional=0) with a window length of 5. TMDprediction was performed with ExPASy TMpred (https://embnet.vital-it.ch/software/TMPRED_form.html). Coiled-coils were predicted by ExPASy COILS (Lupas *et al.*, 1991) (https://embnet.vital-it.ch/software/COILS_form.html) with a window width of 21.

References

Bae, S., Park, J. and Kim, J.S. (2014) Cas-OFFinder: A fast and versatile algorithm that searches for potential off-target sites of Cas9 RNA-guided endonucleases. *Bioinformatics*, **30**, 1473–1475.

Baillie, A.L., Falz, A.L., Müller-Schüssele, S.J. and Sparkes, I. (2020) It started with a kiss: Monitoring organelle interactions and identifying membrane contact site components in plants. *Front. Plant Sci.*, **11**.

Bohnert, M. (2020) Tethering fat: Tethers in lipid droplet contact sites. *Contact*, **3**.

Cai, Y., Goodman, J.M., Pyc, M., Mullen, R.T., Dyer, J.M. and Chapmana, K.D. (2015) Arabidopsis SEIPIN proteins modulate triacylglycerol accumulation and influence lipid droplet proliferation. *Plant Cell*, **27**, 2616–2636.

Cockcroft, S. and Raghu, P. (2018) Phospholipid transport protein function at organelle contact sites. *Curr. Opin. Cell Biol.*, **53**, 52–60.

Cox, J., Hein, M.Y., Luber, C.A., Paron, I., Nagaraj, N. and Mann, M. (2014) Accurate proteome-wide label-free quantification by delayed normalization and maximal peptide ratio extraction, termed MaxLFQ. *Mol. Cell. Proteomics*, **13**, 2513–2526.

Cox, J. and Mann, M. (2008) MaxQuant enables high peptide identification rates, individualized p.p.b.-range mass accuracies and proteome-wide protein quantification. *Nat. Biotechnol.*, **26**, 1367–1372.

Cui, S., Hayashi, Y., Otomo, M., Mano, S., Oikawa, K., Hayashi, M. and Nishimura, M. (2016) Sucrose production mediated by lipid metabolism suppresses the physical interaction of peroxisomes and oil bodies during germination of *Arabidopsis thaliana*. *J. Biol. Chem.*, **291**, 19734–19745.

Curtis, M.D. and Grossniklaus, U. (2003) A gateway cloning vector set for high-throughput functional analysis of genes *in planta*. *Plant Physiol.*, **133**, 462–469.

Czechowski, T., Stitt, M., Altmann, T., Udvardi, M.K. and Scheible, W.R. (2005) Genome-wide identification and testing of superior reference genes for transcript normalization in Arabidopsis. *Plant Physiol.*, **139**, 5–17.

Eastmond, P.J. (2006) SUGAR-DEPENDENT1 encodes a patatin domain triacylglycerol lipase that initiates storage oil breakdown in germinating Arabidopsis seeds. *Plant Cell*, **18**, 665–675.

Eisenberg-Bord, M., Shai, N., Schuldiner, M. and Bohnert, M. (2016) A tether is a tether is a tether: Tethering at membrane contact sites. *Dev. Cell*, **39**, 395–409.

Fan, J., Yu, L. and Xu, C. (2017) A central role for triacylglycerol in membrane lipid breakdown, fatty acid *β*-Oxidation, and plant survival under extended darkness. *Plant Physiol.*, **174**, 1517–1530.

Freyre, C.A.C., Rauher, P.C., Ejsing, C.S. and Klemm, R.W. (2019) MIGA2 links mitochondria, the ER, and lipid droplets and promotes *de novo* lipogenesis in adipocytes. *Mol. Cell*, **76**, 811–825.

Gao, Q. and Goodman, J.M. (2015) The lipid droplet—a well-connected organelle. *Front. Cell Dev. Biol.*, **3**, 1–12.

Gautier, R., Douguet, D., Antonny, B. and Drin, G. (2008) HELIQUEST: A web server to screen sequences with specific α-helical properties. *Bioinformatics*, **24**, 2101–2102.

Geltinger, F., Tevini, J., Briza, P., Geiser, A., Bischof, J., Richter, K., Felder, T. and Rinnerthaler, M. (2020) The transfer of specific mitochondrial lipids and proteins to lipid droplets contributes to proteostasis upon stress and aging in the eukaryotic model system *Saccharomyces cerevisiae*. *GeroScience*, **42**, 19–38.

Gidda, S.K., Park, S., Pyc, M., et al. (2016) Lipid droplet-associated proteins (LDAPs) are required for the dynamic regulation of neutral lipid compartmentation in plant cells. *Plant Physiol.*, **170**, pp.01977.2015.

Greer, M.S., Cai, Y., Gidda, S.K., et al. (2020) SEIPIN isoforms interact with the membrane-tethering protein VAP27-1 for lipid droplet formation. *Plant Cell*, **32**.

Hariri, H., Rogers, S., Ugrankar, R., Liu, Y.L., Feathers, J.R. and Henne, W.M. (2018) Lipid droplet biogenesis is spatially coordinated at ER –vacuole contacts under nutritional stress . *EMBO Rep.*, **19**, 57–72.

Hariri, H., Speer, N., Bowerman, J., et al. (2019) Mdm1 maintains endoplasmic reticulum homeostasis by spatially regulating lipid droplet biogenesis. *J. Cell Biol.*, **218**, 1319–1334.

Henne, W.M., Zhu, L., Balogi, Z., Stefan, C., Pleiss, J.A. and Emr, S.D. (2015) Mdm1/Snx13 is a novel ER-endolysosomal interorganelle tethering protein. *J. Cell Biol.*, **210**, 541–551.

Hillmer, S., Viotti, C. and Robinson, D.G. (2012) An improved procedure for low-temperature embedding of high-pressure frozen and freeze-substituted plant tissues resulting in excellent structural preservation and contrast. *J. Microsc.*, **247**, 43–47.

Ischebeck, T., Krawczyk, H.E., Mullen, R.T., Dyer, J.M. and Chapman, K.D. (2020) Lipid droplets in plants and algae: Distribution, formation, turnover and function. *Semin. Cell Dev. Biol.*

Johnson, M.R., Stephenson, R.A., Ghaemmaghami, S. and Welte, M.A. (2018) Developmentally regulated H2AV buffering via dynamic sequestration to lipid droplets in Drosophila embryos. *Elife*, **7**, 1–28.

Klepikova, A. V., Kasianov, A.S., Gerasimov, E.S., Logacheva, M.D. and Penin, A.A. (2016) A high resolution map of the *Arabidopsis thaliana* developmental transcriptome based on RNA-seq profiling. *Plant J.*, **88**, 1058–1070.

Kretzschmar, F.K., Doner, N.M., Krawczyk, H.E., Scholz, P., Schmitt, K., Valerius, O., Braus, G.H., Mullen, R.T. and Ischebeck, T. (2020) Identification of low-abundance lipid droplet proteins in seeds and seedlings. *Plant Physiol.*, **182**, 1326–1345.

Kretzschmar, F.K., Mengel, L.A., Müller, A.O., Schmitt, K., Blersch, K.F., Valerius, O., Braus, G.H. and Ischebeck, T. (2018) PUX10 Is a lipid droplet-localized scaffold protein that interacts with CELL DIVISION CYCLE48 and is involved in the degradation of lipid droplet proteins. *Plant Cell*, **30**, 2137–2160.

Kyte, J. and Doolittle, R.F. (1982) A simple method for displaying the hydropathic character of a protein. *J. Mol. Biol.*, **157**, 105–132.

Livak, K.J. and Schmittgen, T.D. (2001) Analysis of relative gene expression data using real-time quantitative PCR and the 2-ΔΔCT method. *Methods*, **25**, 402–408.

Lupas, A., Dyke, M. Van and Stock, J. (1991) Predicting coiled coils from protein sequences. *Science*, **252**, 1162–1164.

Muliyil, S., Levet, C., Düsterhöft, S., Dulloo, I., Cowley, S.A. and Freeman, M. (2020) ADAM 17-triggered TNF signalling protects the ageing Drosophila retina from lipid droplet-mediated degeneration . *EMBO J.*, 1–22.

Müller, A.O., Blersch, K.F., Gippert, A.L. and Ischebeck, T. (2017) Tobacco pollen tubes - a fast and easy tool for studying lipid droplet association of plant proteins. *Plant J.*, **89**, 1055–1064.

Murashige, T. and Skoog, F. (1962) A revised medium for rapid growth and bio assays with Tobacco tissue cultures. *Physiol. Plant.*, **15**, 473–497.

Nakabayashi, K., Okamoto, M., Koshiba, T., Kamiya, Y. and Nambara, E. (2005) Genome-wide profiling of stored mRNA in *Arabidopsis thaliana* seed germination: Epigenetic and genetic regulation of transcription in seed. *Plant J.*, **41**, 697–709.

Needleman, S.B. and Wunsch, C.D. (1970) A general method applicable to the search for similarities in the amino acid sequence of two proteins. *J. Mol. Biol.*, **48**, 443–453.

Nguyen, T.B., Louie, S.M., Daniele, J.R., Tran, Q., Dillin, A., Zoncu, R., Nomura, D.K. and Olzmann, J.A. (2017) DGAT1-dependent lipid droplet biogenesis protects mitochondrial function during starvation-induced autophagy. *Dev. Cell*, **42**, 9–21.e5.

Noack, L.C. and Jaillais, Y. (2020) Functions of anionic lipids in plants. *Annu. Rev. Plant Biol.*, **71**, 71–102.

Notredame, C., Higgins, D.G. and Heringa, J. (2000) T-coffee: A novel method for fast and accurate multiple sequence alignment. *J. Mol. Biol.*, **302**, 205–217.

Olzmann, J.A. and Carvalho, P. (2019) Dynamics and functions of lipid droplets. *Nat. Rev. Mol. Cell Biol.*, **20**, 137–155.

Park, J., Bae, S. and Kim, J.S. (2015) Cas-Designer: A web-based tool for choice of CRISPR-Cas9 target sites. *Bioinformatics*, **31**, 4014–4016.

Petrie, J.R., Shrestha, P., Liu, Q., Mansour, M.P., Wood, C.C., Zhou, X.R., Nichols, P.D., Green, A.G. and Singh, S.P. (2010) Rapid expression of transgenes driven by seed-specific constructs in leaf tissue: DHA production. *Plant Methods*, **6**.

Prinz, W.A., Toulmay, A. and Balla, T. (2020) The functional universe of membrane contact sites. *Nat. Rev. Mol. Cell Biol.*, **21**, 7–24.

Pyc, M., Cai, Y., Gidda, S.K., et al. (2017) Arabidopsis LDAP-interacting protein (LDIP) influences lipid droplet size and neutral lipid homeostasis in both leaves and seeds. *Plant J.*, **12**, 3218–3221.

Read, S.M., Clarke, A.E. and Bacic, A. (1993) Stimulation of growth of cultured *Nicotiana tabacum* W 38 pollen tubes by poly(ethylene glycol) and Cu(II) salts. *Protoplasma*, **177**, 1–14.

Rossini, M., Pizzo, P. and Filadi, R. (2020) Better to keep in touch: investigating inter-organelle cross-talk. *FEBS J.*, 1–16.

Rotsch, A.H., Kopka, J., Feussner, I. and Ischebeck, T. (2017) Central metabolite and sterol profiling divides Tobacco male gametophyte development and pollen tube growth into eight metabolic phases. *Plant J.*, **92**, 129–146.

Schaffer, J.E. (2003) Lipotoxicity: when tissues overeat. *Curr. Opin. Lipidol.*, **14**, 281–287.

Schmid, M., Davison, T.S., Henz, S.R., Pape, U.J., Demar, M., Vingron, M., Schölkopf, B., Weigel, D. and Lohmann, J.U. (2005) A gene expression map of *Arabidopsis thaliana* development. *Nat. Genet.*, **37**, 501–6.

Schuldiner, M. and Bohnert, M. (2017) A different kind of love – lipid droplet contact sites. *Biochim. Biophys. Acta - Mol. Cell Biol. Lipids*, **1862**, 1188–1196.

Shai, N., Schuldiner, M. and Zalckvar, E. (2016) No peroxisome is an island - Peroxisome contact sites. *Biochim. Biophys. Acta - Mol. Cell Res.*, **1863**, 1061–1069.

Shai, N., Yifrach, E., Roermund, C.W.T. Van, et al. (2018) Systematic mapping of contact sites reveals tethers and a function for the peroxisome-mitochondria contact. *Nat. Commun.*, **9**.

Shockey, J.M., Gidda, S.K., Chapital, D.C., Kuan, J.C., Dhanoa, P.K., Bland, J.M., Rothstein, S.J., Mullen, R.T. and Dyer, J.M. (2006) Tung tree DGAT1 and DGAT2 have nonredundant functions in triacylglycerol biosynthesis and are localized to different subdomains of the endoplasmic reticulum. *Plant Cell*, **18**, 2294–2313.

Siao, W., Wang, P., Voigt, B., Hussey, P.J. and Baluska, F. (2016) Arabidopsis SYT1 maintains stability of cortical endoplasmic reticulum networks and VAP27-1-enriched endoplasmic reticulum-plasma membrane contact sites. *J. Exp. Bot.*, **67**, 6161–6171.

Sui, X., Arlt, H., Brock, K.P., Lai, Z.W., DiMaio, F., Marks, D.S., Liao, M., Farese, R. V. and Walther, T.C. (2018) Cryo–electron microscopy structure of the lipid droplet–formation protein seipin. *J. Cell Biol.*, **217**.

Thiam, A.R. and Beller, M. (2017) The why, when and how of lipid droplet diversity. *J. Cell Sci.*, **130**, 315-324.

Twell, D., Yamaguchi, J., Wing, R.A., Ushiba, J. and McCormick, S. (1991) Promoter analysis of genes that are coordinately expressed during pollen development reveals pollen-specific enhancer sequences and shared regulatory elements. *Genes Dev.*, **5**, 496–507.

Tyanova, S., Temu, T., Sinitcyn, P., Carlson, A., Hein, M.Y., Geiger, T., Mann, M. and Cox, J. (2016) The Perseus computational platform for comprehensive analysis of (prote)omics data. *Nat. Methods*, **13**, 731–740.

Ugrankar, R., Bowerman, J., Hariri, H., et al. (2019) Drosophila Snazarus regulates a lipid droplet population at plasma membrane-droplet contacts in adipocytes. *Dev. Cell*, **50**, 557–572.

Valm, A.M., Cohen, S., Legant, W.R., et al. (2017) Applying systems-level spectral imaging and analysis to reveal the organelle interactome. *Nature*, **546**, 162–167.

Velázquez, A.P., Tatsuta, T., Ghillebert, R., Drescher, I. and Graef, M. (2016) Lipid droplet-mediated ER homeostasis regulates autophagy and cell survival during starvation. *J. Cell Biol.*, **212**, 621–631.

Vries, J. de and Ischebeck, T. (2020) Ties between stress and lipid droplets pre-date seeds. *Trends Plant Sci.*, **25**, 1203-1214.

Waese, J., Fan, J., Pasha, A., et al. (2017) ePlant: Visualizing and exploring multiple levels of data for hypothesis generation in plant biology. *Plant Cell*, **29**, 1806–1821.

Wang, Z.-P., Xing, H.-L., Dong, L., Zhang, H.-Y., Han, C.-Y., Wang, X.-C. and Chen, Q.-J. (2015) Egg cell-specific promoter-controlled CRISPR/Cas9 efficiently generates homozygous mutants for multiple target genes in Arabidopsis in a single generation. *Genome Biol.*, **16**, 144.

Welte, M.A. and Gould, A.P. (2017) Lipid droplet functions beyond energy storage. *Biochim. Biophys. Acta - Mol. Cell Biol. Lipids*, **1862**, 1260–1272.

Wilfling, F., Wang, H., Haas, J.T., et al. (2013) Triacylglycerol synthesis enzymes mediate lipid droplet growth by relocalizing from the ER to lipid droplets. *Dev. Cell*, **24**, 384–399.

Winter, D., Vinegar, B., Nahal, H., Ammar, R., Wilson, G. V. and Provart, N.J. (2007) An "electronic fluorescent pictograph" browser for exploring and analyzing large-scale biological data sets. *PLoS One*, **2**, 1–12.

Xie, Y., Zheng, Y., Li, H., et al. (2016) GPS-Lipid: A robust tool for the prediction of multiple lipid modification sites. *Sci. Rep.*, **6**, 1–9.

Xing, H.-L., Dong, L., Wang, Z.-P., Zhang, H.-Y., Han, C.-Y., Liu, B., Wang, X.-C. and Chen, Q.-J. (2014) A CRISPR/Cas9 toolkit for multiplex genome editing in plants. *BMC Plant Biol.*, **14**, 327.

Yang, H.J., Hsu, C.L., Yang, J.Y. and Yang, W.Y. (2012) Monodansylpentane as a blue-fluorescent lipid-droplet marker for multi-color live-cell imaging. *PLoS One*, **7**.

Zang, J., Zhang, T., Hussey, P.J. and Wang, P. (2020) Light microscopy of the endoplasmic reticulum–membrane contact sites in plants. *J. Microsc*, **280**, 134-139.

Zhi, Y., Taylor, M.C., Campbell, P.M., et al. (2017) Comparative lipidomics and proteomics of lipid droplets in the mesocarp and seed tissues of Chinese tallow (*Triadica sebifera*). *Front. Plant Sci.*, **8**, 1–20.

Supplementary Figures

Supplementary Figure 1

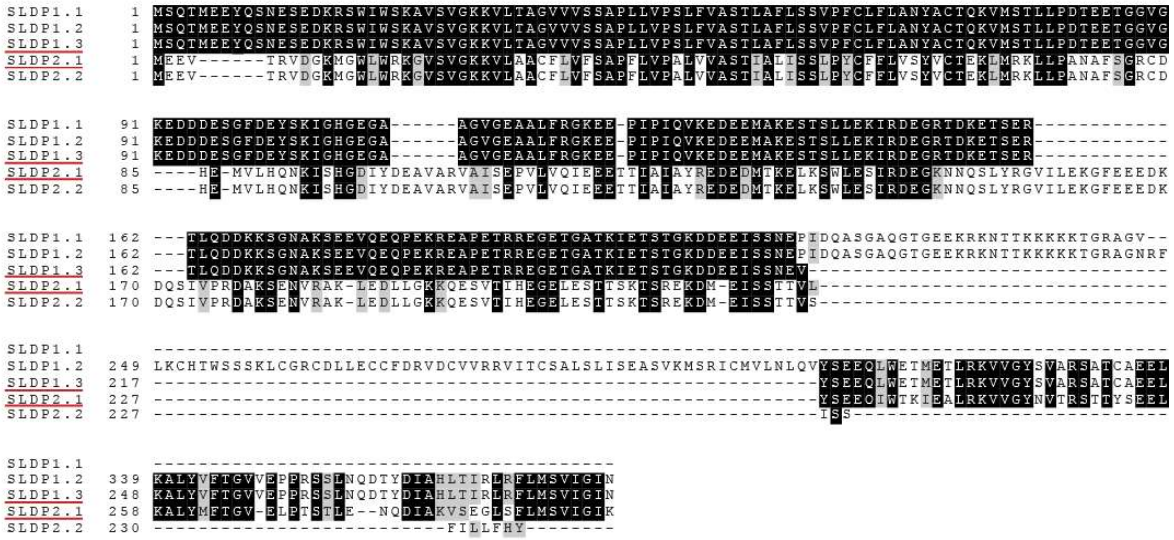

Supplementary Figure 1: Alignment of all SLDP1 and SLDP2 protein variants
Alignment was generated using T-Coffee (http://tcoffee.crg.cat/apps/tcoffee/do:regular), shading was performed using BoxShade (https://embnet.vital-it.ch/software/BOX_form.html). The splice variants analysed in the present study are underlined.

Supplementary Figure 2

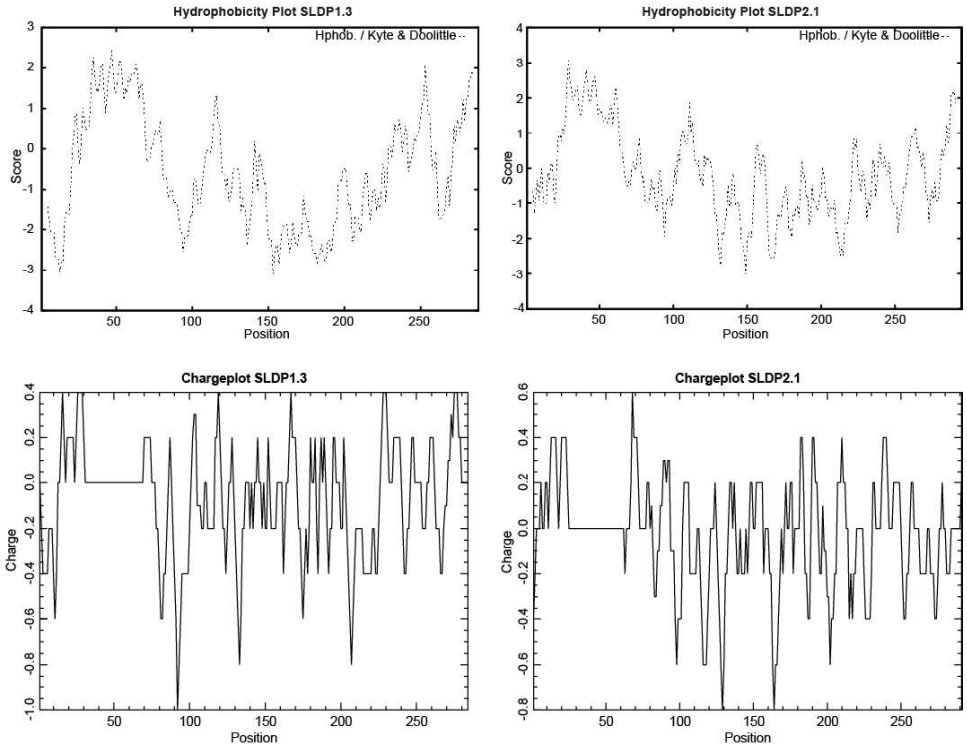

Supplementary Figure 2: *In silico* analysis of SLDP
Protein sequences of SLDP1.3 and SLDP2.1 were analysed for hydrophobicity and charges. Protein hydrophobicity plots were generated using ProtScale. Kyte & Doolittle scale was used with a window size of 9. Protein charge plots were generated using EMBOSS explorer charge with a window length of 5.

Supplementary Figure 3

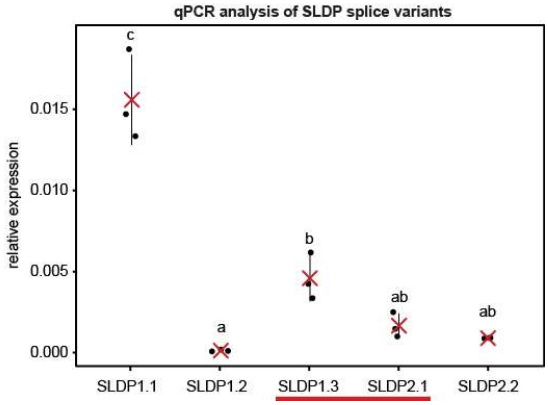

Supplementary Figure 3: qPCR analysis of *SLDP* splice variants
Total RNA was extracted from 24 h imbibed wild-type seeds and analysed by real-time quantitative PCR. Primers were designed to detect single splice variants. *UBQ10* was used as reference gene and relative expression is presented as normalised expression differences between reference and target gene of all replicates (red cross = mean, lines = SD). One-way ANOVA was performed, followed by Tukey post-hoc analysis (F (4.10) = 58.62, p = 6.63e-07, n = 3). Results are presented as compact letter display of all pair-wise comparisons in increasing order. The splice variants analysed in the present study are underlined.

Supplementary Figure 4

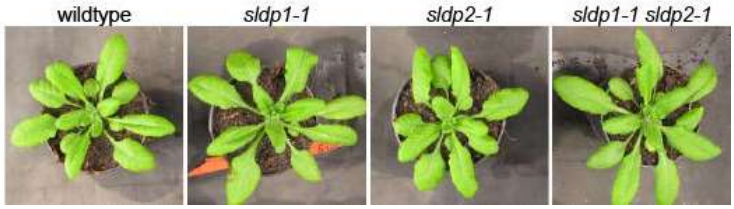

Supplementary Figure 4: Images of *sldp* mutants
Seeds of wild type and *sldp* single and double mutants were stratified for 72 h at 4 °C in the dark and grown in 16-h/8-h day/night cycle. Pictures are representative of average sized plants after 3 weeks of growth. No obvious macroscopic phenotype was observed.

Supplementary Figure 5

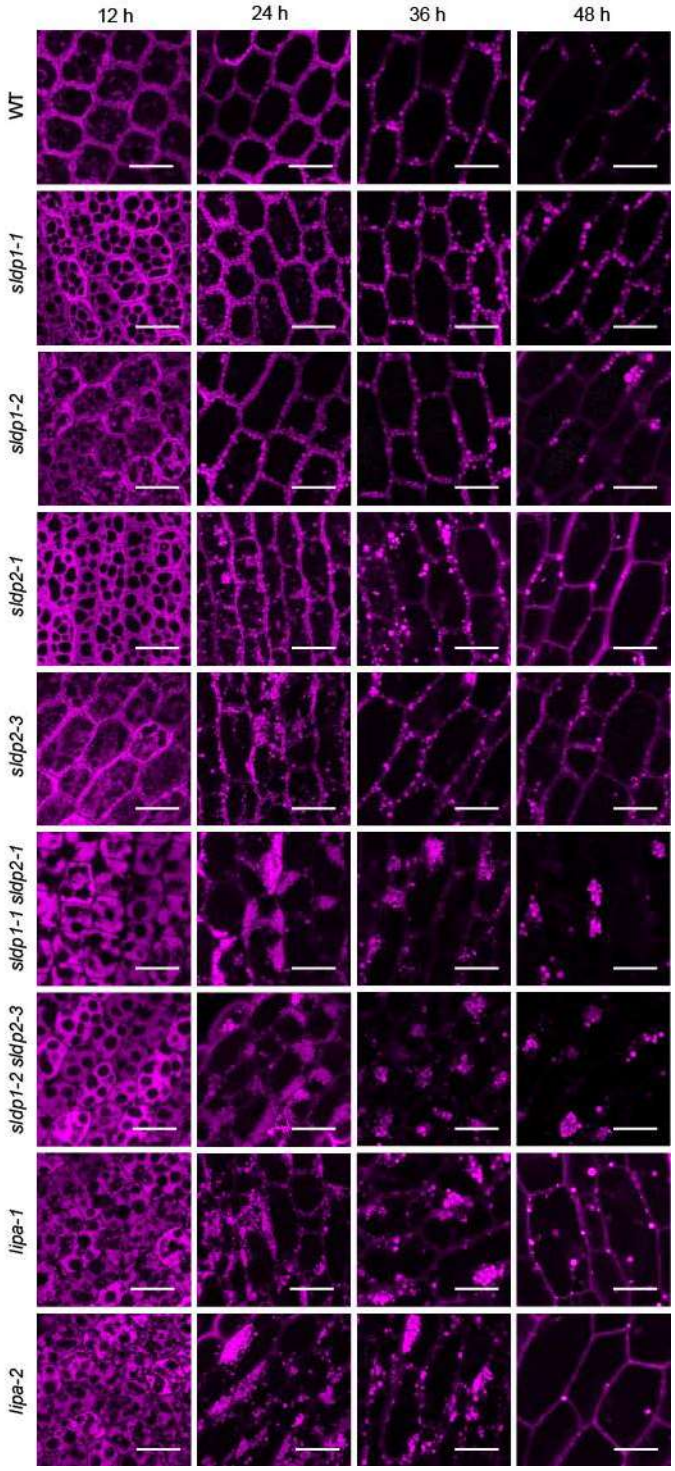

Supplementary Figure 5: Time-course analysis of *SLDP* and *LIPA* mutant line LDs in hypocotyls
Confocal laser scanning microscopy images of germinating wild-type, *sldp1-1*, *sldp1-3*, *sldp2-1*, *sldp2-2*, *sldp1-1 sldp2-1*, *sldp1-3 sldp2-2*, *lipa-1* and *lipa-2* seedlings (hypocotyls). Surface-sterilised seeds were placed on solid half-strength MS medium supplemented with 1 % sucrose, stratified for 4 days at 4 °C in the dark and LDs were microscopically analysed 12, 24, 36 and 48 h (± 2 h) after stratification. For analysis, LDs were stained with Nile red. Images are single plane images from the middle of the cell (similar planes were chosen for all images). Representative images for each stage and genotype were chosen, at least 5 images were taken. Bars: 10 µm.

Supplementary Figure 6

a

	WT	*sldp1-1*	*sldp2-1*	*sldp1-1 sldp2-1*	all
TE fraction	1031	1058	1066	1068	1078
LD fraction	636	663	646	660	666
all	1167	1203	1194	1205	1218

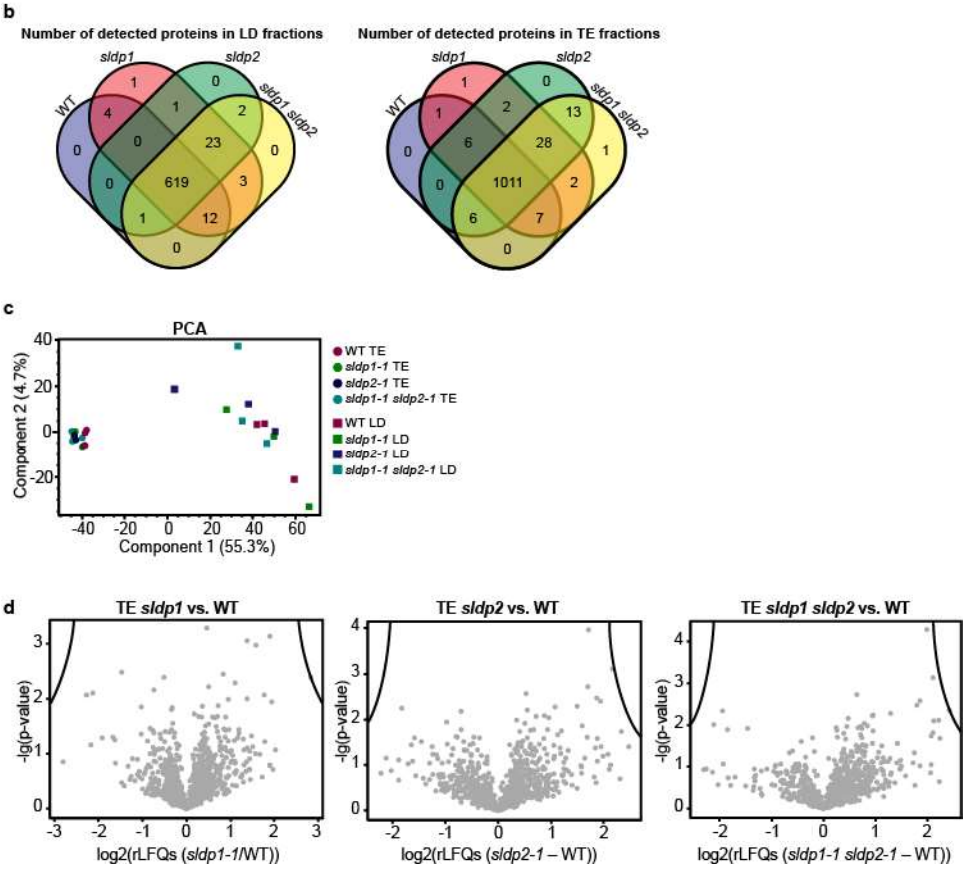

Supplementary Figure 6: Proteomic Analyses of *sldp* mutants.
Proteins were isolated from germinating seedlings 36 h after stratification (n=3). Proteins from LD enriched fractions and total extract (TE) fractions. Proteins were filtered for those detected at least three times in at least one group and identified by at least two peptides.
a Tabular overview of the number of detected proteins in the respective fractions of the respective lines.
b Venn diagrams of detected proteins in LD and total extract (TE) fractions in the respective lines.
c PCA-plots of filtered rawLFQs.
d LFQs were normalised as ‰ of total sum of all LFQs per replicate and log_2-transformed (rLFQ). Imputations were performed, missing values were replaced from normal distribution (width 0.3 and down shift 1.8 for TE, width 0.5 and down shift 1.8 for LD fractions). Imputed rLFQ values were used to create different volcano plots (significance threshold: FDR < 0.01 and log_2(FC) > 2): Wild-type versus *sldp1-1, sldp2-1* and *sldp1-1 sldp2-1* total extract (TE) fractions, respectively to detect proteins differentially accumulating in the respective genotype. No proteins were statistically significantly differentially accumulated.

Supplementary Figure 7

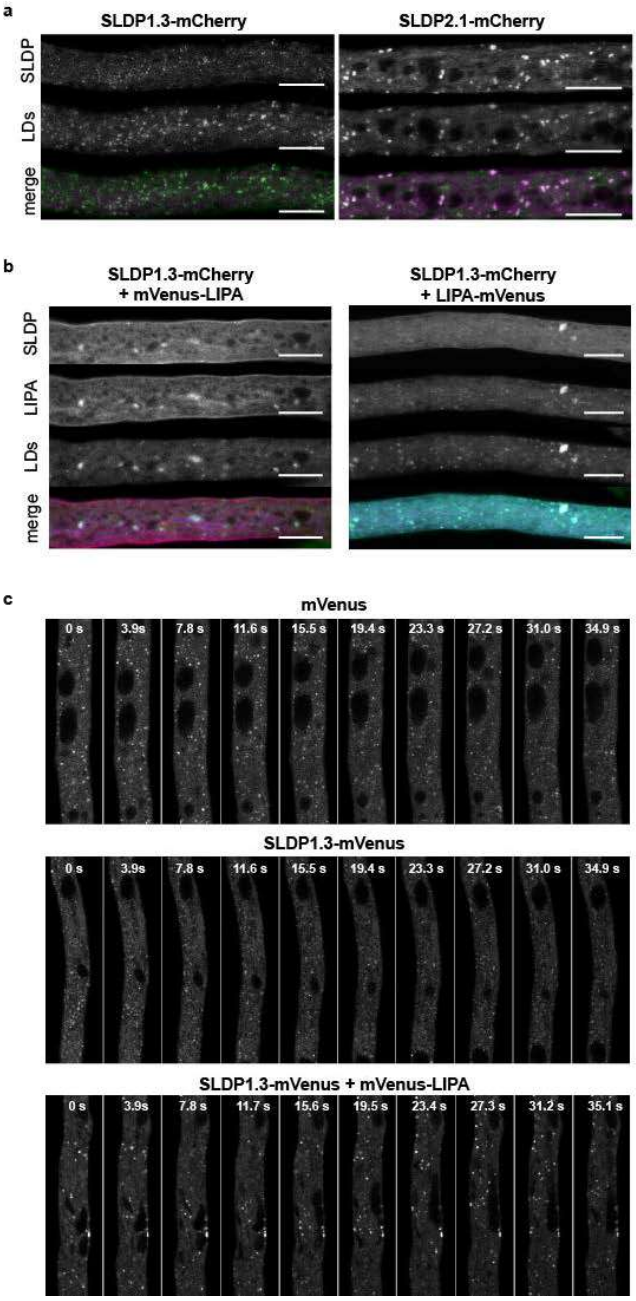

Supplementary Figure 7: Co-localisation analysis of SLDP and LIPA.

a SLDP-localisation in Tobacco pollen tubes. Transient expression of LAT52::SLDP1.3-mCherry and LAT52::SLDP2.1-mCherry in *Nicotiana tabacum* pollen tubes grown for ~ 5 h. Pollen tubes were fixed in formaldehyde and LDs were stained with Lipi-Blue. Images are representative of at least 10 observed pollen tubes. In merged channel: Magenta: mCherry-tagged proteins; green: Lipi-Blue-stained LDs; white: co-localisation. Bars: 10 µm.

b Transient expression of LAT52::mVenus-LIPA and LAT52::LIPA-mVenus alone and co-expressed with LAT52::SLDP1.3-mCherry in *Nicotiana tabacum* pollen tubes grown for ~ 5 h. Pollen tubes were fixed in formaldehyde and LDs were stained with Lipi-Blue. At least 10 pollen tubes were analysed for each transformation, images of at least 5 pollen tubes were taken. For merged image with two channels: magenta: mVenus (LIPA); green: LDs. For merged images with three channels red: mVenus (LIPA), blue: mCherry (SLDP), green: LDs. Bars: 10 µm.

c Pollen tube time series. Transient expression of LAT52::mVenus, LAT52::mVenus-LIPA and LAT52::SLDP1.3-mVenus alone and co-expressed in *Nicotiana tabacum* pollen tubes grown for ~ 5 h. Pollen tubes were fixed in formaldehyde. LDs were stained with Nile red (Sigma Aldrich) and Nile red fluoresence was recorded every 0.97 seconds. Every fifth image is presented here. Bars: 10 µm.

Supplementary Figure 8

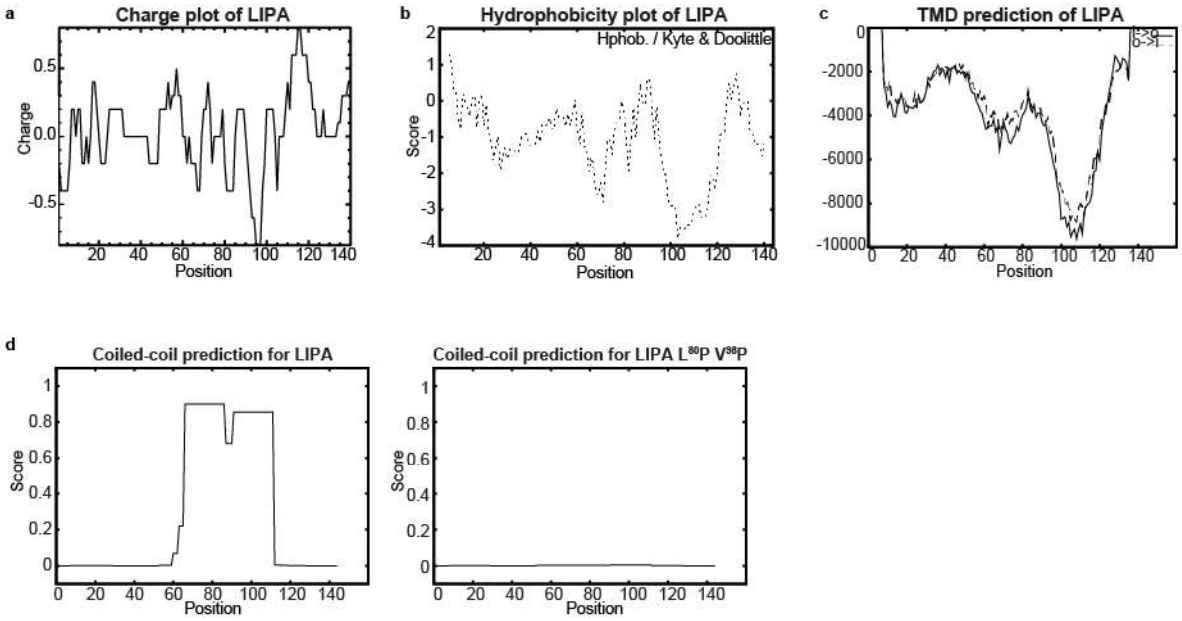

Supplementary Figure 8: *In silico* analysis of LIPA
Protein sequence of LIPA was analysed for hydrophobicity (**a**), charges (**b**), transmembrane domains (**c**) and coiled-coils (**d**). No hydrophobic stretches or TMDs were detected. A putative coiled-coil was predicted between residues 64 - 113 and is abolished by introduction of two proline residues at position 80 and 98.

Supplementary Figure 9

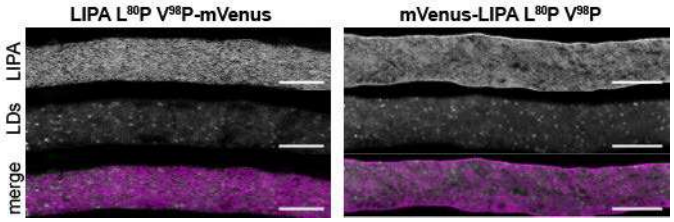

Supplementary Figure 9: Coiled-coil mutants of LIPA
Transient expression of LAT52::LIPA $L^{80}P$ $V^{98}P$-mVenus and LAT52::mVenus-LIPA $L^{80}P$ $V^{98}P$ in *Nicotiana tabacum* pollen tubes grown for ~ 5 h. Pollen tubes were fixed in formaldehyde and LDs were stained with Lipi-Blue. Images are representative of at least 10 observed pollen tubes. In merged channel: Magenta: mVenus-tagged proteins; green: Lipi-Blue-stained LDs; white: co-localisation. Bars: 10 µm.

5 Manuscript II: Lipidomic, metabolomic and transcriptomic adaptations to heat stress in *Nicotiana tabacum* pollen tubes

The manuscript is being prepared for submission. Supplementary figures are attached at the end. Supplementary datasets containing raw and processed data are available on the data drive included in this thesis and will be available online after publication.

Supplementary Material

Supplementary Figure 1: Boxplot and Biological Coefficient of Variation plots of transcript raw counts.
Supplementary Datasets 1-4: Lipidomics
Supplementary Datasets 5-6: Sterols
Supplementary Datasets 7-8: Metabolites
Supplementary Datasets 9-11: Transcriptomics
Supplementary Datasets 12-15: GO-term analysis
Supplementary Datasets 16-17: Transcriptomics – transcription factors
Supplementary Datasets 18-19: Transcriptomics – lipid genes

Author contribution:

H. E. Krawczyk contributed to designing experiments. She performed the growth analyses; lipid extractions, GC-FID measurements and data processing/analysis for TAG analysis; aided in the lipid and metabolite extraction and sample preparation for LC-MS and GC-MS and processed all pre-analysed data; she conducted all analyses on mapped transcript raw counts, including DE and GO analyses. She prepared the figures and wrote the manuscript.

List of author contributions

HEK, AHR and TI designed experiments and performed data analysis; HEK and TI wrote the manuscript; HEK prepared figures; HEK performed growth analyses; AHR, HEK, CH and IF performed lipidomic analyses; AHR executed RNA isolation; OS and GSR carried out library preparation, RNAseq analysis and mapping; HEK conducted transcript DE analysis; HEK and TI performed metabolome and sterole analysis.

Short title: Multi-omic analyses of Tobacco pollen tubes

Author for correspondence: Till Ischebeck

Lipidomic, metabolomic and transcriptomic adaptations to heat stress in *Nicotiana tabacum* pollen tubes

Hannah Elisa Krawczyk[1], Alexander Helmut Rotsch[1], Cornelia Herrfurth[1,2], Ivo Feussner[1,2], Orr Shomroni[3], Gabriela Salinas-Riester[3], Till Ischebeck[1,2]

[1]University of Göttingen, Albrecht-von-Haller-Institute for Plant Sciences and Göttingen Center for Molecular Biosciences (GZMB), Department of Plant Biochemistry, 37077 Göttingen, Germany

[2]University of Goettingen, Albrecht-von-Haller-Institute for Plant Sciences, Göttingen Metabolomics/Lipidomics Platform, 37077 Göttingen, Germany

[3]University Medical Center Göttingen (UMG), Institute of Human Genetics, NGS Integrative Genomics Core Unit (NIG), 37077 Göttingen

One sentence summary: *Nicotiana tabacum* pollen tubes react to heat stress with metabolomic adaptations, transcriptional adjustments, and a rapid and reversible lipid remodelling.

Abstract

After reaching the stigma, pollen grains germinate and form a pollen tube that transports the sperm cells to the ovule. Due to selection pressure between pollen tubes, they must have evolved mechanisms to quickly adapt to temperature changes to sustain an elongation at the highest possible rate. We investigated these adaptions in *Nicotiana tabacum* pollen tubes grown *in vitro* under 22°C and 37°C by a multi-omic approach including lipidomic, metabolomic and transcriptomic analysis. Both phospholipids and galactolipids increased in saturated acyl chains under heat stress while triacylglycerols changed less in respect to desaturation but showed higher levels. Most amino acids increased during heat stress (HS), including the non-codogenic amino acids γ-amino butyrate and pipecolate. Furthermore the sugars sedoheptulose and sucrose showed higher levels. Also the transcriptome underwent massive changes with 1570 of 23,053 detected genes being differentially up- and 813 being downregulated. Transcripts coding for heat shock proteins and many transcriptional regulators were most strongly upregulated, but also transcripts that have so far not been linked to heat stress. Transcripts involved in TAG synthesis was upregulated, while the modulation of acyl chain desaturation seemed not to be transcriptionally controlled.

Introduction

Around 80 % of the more than 350,000 known plant species are flowering plants (angiosperms) that mainly rely on sexual reproduction to pass on their genes to the next generation (Christenhusz and Byng, 2016). Sexual reproduction is also the prerequisite for seed and fruit set in crop plants. In most angiosperms, the male gametophyte – the pollen containing the sperm cells or the generative cell that later divides into the two sperm cells – double-fertilises the female gametophyte. To this end, the pollen has to land on the stigma of a pistil and adhere, rehydrate and germinate there. Since seed plant sperm cells are immotile, they have to be delivered through the female reproductive tissues to the ovule by tip-growing pollen tubes that are formed by the vegetative cells of the pollen (Sprunck, 2020). In some species, pollen tubes have to grow several centimetres to reach the egg-cell containing ovule. Maize pollen tubes, for example, can grow up to 50 cm in length with a speed of more than 1 cm per hour (Mascarenshas, 1993). Especially for these very long pollen tubes it is unlikely that enough lipids for the elongation are stored in the pollen grain, but the tubes rather depend on rapid de novo synthesis for their growth (Ischebeck, 2016). This assumption is supported by the fact that proteins involved in fatty acid synthesis are five to ten times more abundant in maturing pollen and growing pollen tubes of Tobacco than in leaves or roots (Ischebeck *et al.*, 2014; Ischebeck, 2016).

The process of sexual reproduction in plants is very sensitive to abiotic stresses like heat or cold stress. Male gametophytes are especially sensitive to heat stress during all stages of their

life and are generally more susceptible than female tissues (Hedhly, 2011; Santiago and Sharkey, 2019). One effect of heat stress on developing pollen is early tapetum degradation likely due to accumulation of reactive oxygen species (ROS) and the consequent disruption of concerted ROS signals (Zhao *et al.*, 2018). Furthermore, anthers can fail to release pollen grains, possibly due to heat-induced changes in cell wall composition, sucrose transport and water movement (Santiago and Sharkey, 2019). Also, the developing male gametophyte itself can encounter problems at different stages of development (Müller and Rieu, 2016; Raja *et al.*, 2019; Santiago and Sharkey, 2019).

The effects of heat stress on pollen germination and pollen tube growth are less well studied than those on pollen development but have also been addressed in several studies. It was shown that tomato pollen germination is negatively affected by heat stress in *in vitro* experiments (germination and pollen tube growth in medium outside of female tissues); an effect also attributed to elevated ROS levels (Luria *et al.*, 2019). Various sorghum genotypes show *in vitro* pollen germination reductions of 2 – 95 % under different heat stresses (Sunoj *et al.*, 2017). *In vivo* experiments with pollen from rice or the pine Pinus edulis gave similar results (Flores-Rentería *et al.*, 2018; Shi *et al.*, 2018).

Inhibited pollen tube growth has been observed as well. Experiments on *in vivo* grown cotton pollen tubes attribute reduced pollen tube growth to heat-stress-induced reduction of soluble carbohydrate content in the pistil (Snider, Oosterhuis and Kawakami, 2011; Snider, Oosterhuis, Loka, *et al.*, 2011). Heat-induced pollen tube growth inhibition in rice was described to be likely due to altered auxin homeostasis within the pistil (Zhang *et al.*, 2018). These experiments highlight the importance of biochemical interactions between pollen tubes and the surrounding pistil tissue during stress. However, pollen tube growth inhibition is also observed *in vitro*. Experiments with tomato pollen showed maximal germination rates at 15 °C and maximal pollen tube lengths at 25 °C, higher (or lower) temperatures were inhibitory (Karapanos *et al.*, 2010). Another *in vitro* study in tomato showed that high-temperature-induced ROS inhibit pollen tube growth and that elevated flavonol levels can counteract the heat-induced ROS-imbalance (Muhlemann *et al.*, 2018). Also, *in vitro* pollen tube growth of cotton, rice and Arabidopsis is inhibited by high temperatures (Boavida and McCormick, 2007; Song *et al.*, 2015; Coast *et al.*, 2016), indicating that growth inhibitions are not solely due to altered crosstalk with the female tissue, but also due to effects in the pollen tube itself.

A challenge all organs of plants have to meet during elevated temperatures, is maintaining membrane fluidity and integrity; this holds true for the plasma membrane (PM) as well as for intracellular membranes (Niu and Xiang, 2018). Among the challenges plant membranes have to meet under elevated temperatures are the prevention of bilayer disintegration (because of membrane hyperfluidity under high temperatures) and peroxidation of unsaturated fatty acids by ROS (Higashi and Saito, 2019).

The effects of long- and short-term heat stress on the leaf lipidome of different species has been reviewed recently (Higashi and Saito, 2019): Levels of phospholipids containing saturated or mono-unsaturated acyl chains increase; while most phospholipid species with polyunsaturated acyl-chains decrease. For glycolipids, 18:2 containing species (including 36:4-monogalactosyl diacylglycerol (MGDG), 36:5-MGDG, 34:2-digalactosyl diacylglycerol (DGDG), 36:4-DGDG, 36:5-DGDG, 34:2-sulfoquinovosyl diacylglycerol (SQDG), 36:4-SQDG, and 36:5-SQDG) increase and lipids harbouring two 16:3 or 18:3 acyl chains decrease. At the same time, triacyl glycerol (TAG) levels increase.

Nicotiana tabacum used in this study is a versatile model organism that is also very suited to study pollen tube growth. Here we show that Tobacco pollen tubes can grow well at a relatively high temperature of 37°C and monitor the adaptions of the pollen tubes on its lipidome, transcriptome and metabolome.

Results

Tobacco in vitro pollen tube growth is not inhibited by elevated temperatures

The *Nicotiana tabacum* genome has been sequenced, Tobacco flowers are large and rich in pollen that germinates and grows tubes effectively *in vitro* (Read *et al.*, 1993; Edwards *et al.*, 2017). First, we tested if Tobacco pollen tubes also grow at higher temperatures, and thereby pose a possible model organism to study successful heat adaptation. For this, we analysed pollen tube elongation under five different conditions (Figure 1a) with or without heat stress (HS): 3 h of growth at room temperature (22°C, RT 3 h), 6 h of growth at RT (RT 6 h), 3 h growth at RT and then 3 h growth under HS (HS 3+3 h), 3 h growth at RT and then 6 h growth under HS (HS 3+6 h) and 3 h growth at RT followed by 3 h growth under HS and finally 3 h at RT for heat stress relief (HSR 3+3+3 h). As shown in Figure 1b and 1c, pollen tubes grown at RT for 3 h reach an average length of 0.45 mm, after 6 h they on average elongate by another 0.6 mm. If shifted to HS after 3 h, they only elongate by 0.38 mm, meaning an average reduction of around 38 % in comparison to RT 6 h. If subjected to prolonged heat stress of 6 h, the picture slightly changes: Heat stressed tubes reach an average length of 1.27 mm, while heat stress relieved pollen tubes only reach 1.19 mm.

Figure 1

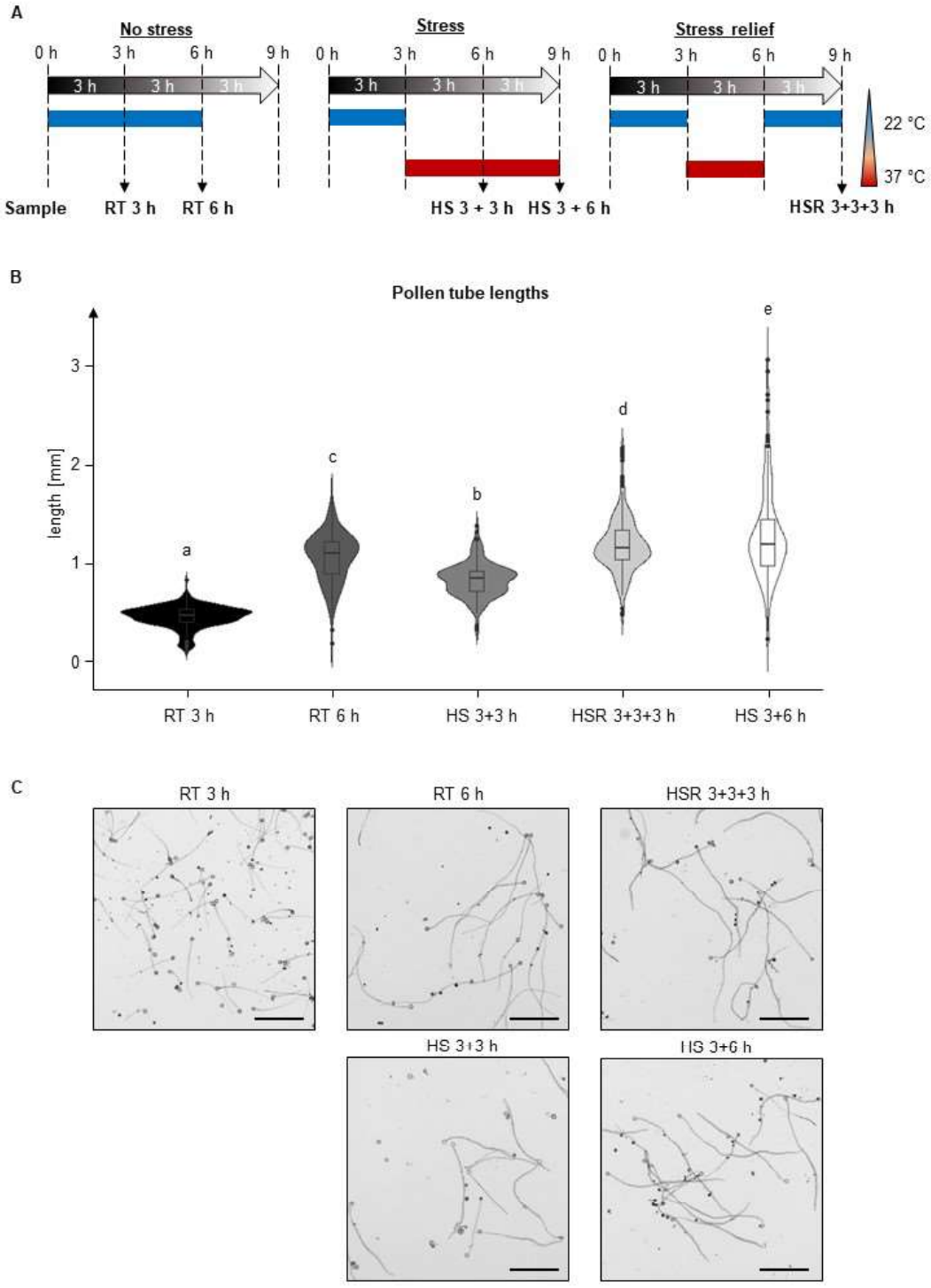

Figure 1: A Schematic depiction of the experimental setup. Pollen tubes were grown under five different conditions: either unstressed for 3 or 6 h at room temperature (22 °C; RT 3h, RT 6h); at RT for 3 h followed by either 3 or 6 h of heat stress (37 °C; HS 3+3 h, HS 3+6 h); or with heat stress relief for 3 h at RT, followed by 3 h HS at 37 °C and then another 3 h at RT (HSR 3+3+3 h).
B Violin plot of measured pollen tube lengths under the different conditions. Boxplots are shown within the diagram. ANOVA was performed, followed by Post-hoc Tukey analysis. Results are presented as compact letter display of all pair-wise comparisons in increasing order. n = 183 – 201.
C Images of pollen tubes grown under the indicated conditions. Bars = 0.5 mm

Relative phospholipid and galactolipid composition changes upon heat stress

Heat stress usually induces membrane remodelling in order to maintain membrane integrity. Sustaining pollen tube growth under elevated temperatures thus likely requires lipidomic adaptations, too. To assay such a remodelling, pollen tubes were grown at different temperature regimes (Figure 1a) and the lipid classes PC, PG, PE, PS, MGDG, DGDG, DAG and TAG were analysed by UPLC-nanoESI-MS/MS (Figure 2, 3, 4a). SQDG species could not be detected in any of the samples.

In total, 164 species were detected and quantified (Supplementary Dataset 1-4). On a total lipid level, heat stress had only mild effects on relative abundances (normalised to the values after 3 h of RT growth) of most lipid classes (Figure 2a). For PC and PE, only subtle to no changes in abundance were observed when the tubes were grown for an additional 3 h at RT or 3 h under heat stress (total growth of 6 h). After a total growth of 9 h, the amounts of PC and PE increased, but accumulation was slightly reduced in heat stressed tubes when compared to stress relieved tubes. Stronger relative increases were observed for the other membrane lipids, especially so after prolonged pollen tube growth. Particularly DGDG and PS showed strong relative increases upon heat treatment in comparison to control or stress-relieved samples. Furthermore, the neutral storage lipid TAG showed a strong increase over time and under heat stress. Its synthesis and breakdown intermediate DAG showed a less pronounced increase under heat stress.

Looking at overall saturation levels, the proportion of saturated acyl chains increased in all membrane lipid classes except for PS and DAG, while the relative abundance of polyunsaturated acyl chains decreased (Figure 2b). The changes were more pronounced in DGDG and PG in comparison to PC, PE and MGDG and were further increased after prolonged heat exposure. Shifting the tubes back to RT partly led to a reversion of the effects in PC, PE, and PG while levels in MGDG and DGDG remained approximately constant.

Regarding fatty acid composition of major lipid species (> 1 % of the total lipid class in at least one condition, shown in Figures 3, 4a), a relative increase in most 16:0-containing phospholipid species was observed after 3 h of HS. Exceptions are 34:2-PG and 34:3-species of PC, PE and PG. Similar results were obtained for species containing 18:0, while species without saturated acyl chains generally decreased in relative abundance. After prolonged HS for 6 h, the picture slightly changed. Some palmitate-containing species further increased (34:2-PC and -PS, 32:0-PG), others were mostly unchanged in comparison to 3 h of HS and two species even decrease again (34:1-PC, 34:3-PS). Were the pollen tubes shifted back to RT, most species containing 16:0 and 18:0 decreased again; while lipids containing no saturated acyl chains increased. PS containing 18:2 and 24:0 decreases under HS and recovered after stress relief.

The general trend observed in MGDG and DGDG is the same as for phospholipids: 16:0-species increase, while 18:3 containing species decrease. Stress relief partially reverses the observed effects again for some species but not for all.

Fewer changes were observed in the acyl-chain composition of the storage lipids DAG and TAG. DAG profile remained more or less constant under all tested conditions. For TAG, some changes over time but almost no changes in response to heat stress were observed. Strongest changes were observed for short-chain containing species (50:1 – 50:3), that strongly increase over time and accumulate after 3 h of HS (but not after prolonged stress); and for 54:6 – 54:8-TAG, that showed a decrease over time (but no changes upon HS).

To further validate the increase of TAG levels under HS, and to get information on absolute TAG levels, TAGs were also quantified by GC-FID (Figure 4b). Heat stressed pollen tubes (3 h RT + 3 h HS) produce more than twice the amount of TAG as control pollen tubes (6 h RT) did. Looking at the fatty acid profile, 16:0 shows a strong relative increase, while 18:1 and 18:3 show relative decreases. Intriguingly, proportion of 18:0 also decreased significantly.

Figure 2

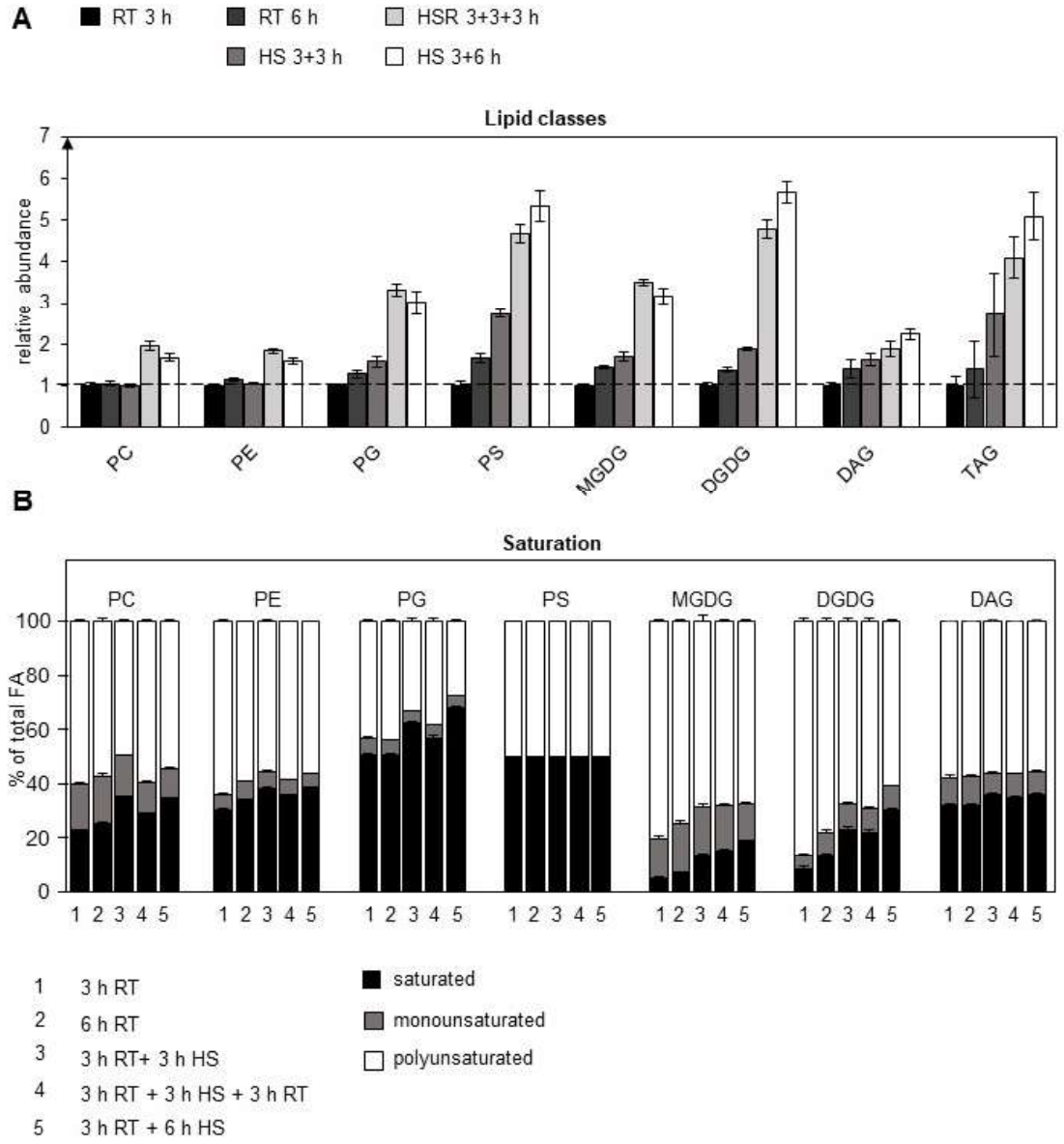

Figure 2*:* A Relative amounts of the lipid classes PC, PE, PG, PS, MGDG, DGDG, DAG and TAG in pollen tubes. Amounts after 6 h RT, 3 h RT + 3 h HS, 3 h RT + 6 h HS and 3 h RT + 3 h HS + 3 h RT were normalised to the respective amounts after 3 h RT, each lipid class was calculated separately. Total lipid class amounts were determined as sums of all detected lipid species per class, measured by UPLC-nanoESI-MS/MS. Statistic analyses are presented separately in Table 1.
B Relative saturation of the respective lipid class after 3 h RT, 6 h RT, 3 h RT + 3 h HS, 3 h RT + 6 h HS and 3 h RT + 3 h HS + 3 h RT. Relative amounts of all saturated (black), monounsaturated (grey) and polyunsaturated (white) fatty acid per class were summed up and divided by the number of fatty acids per respective lipid molecule.

Figure 3

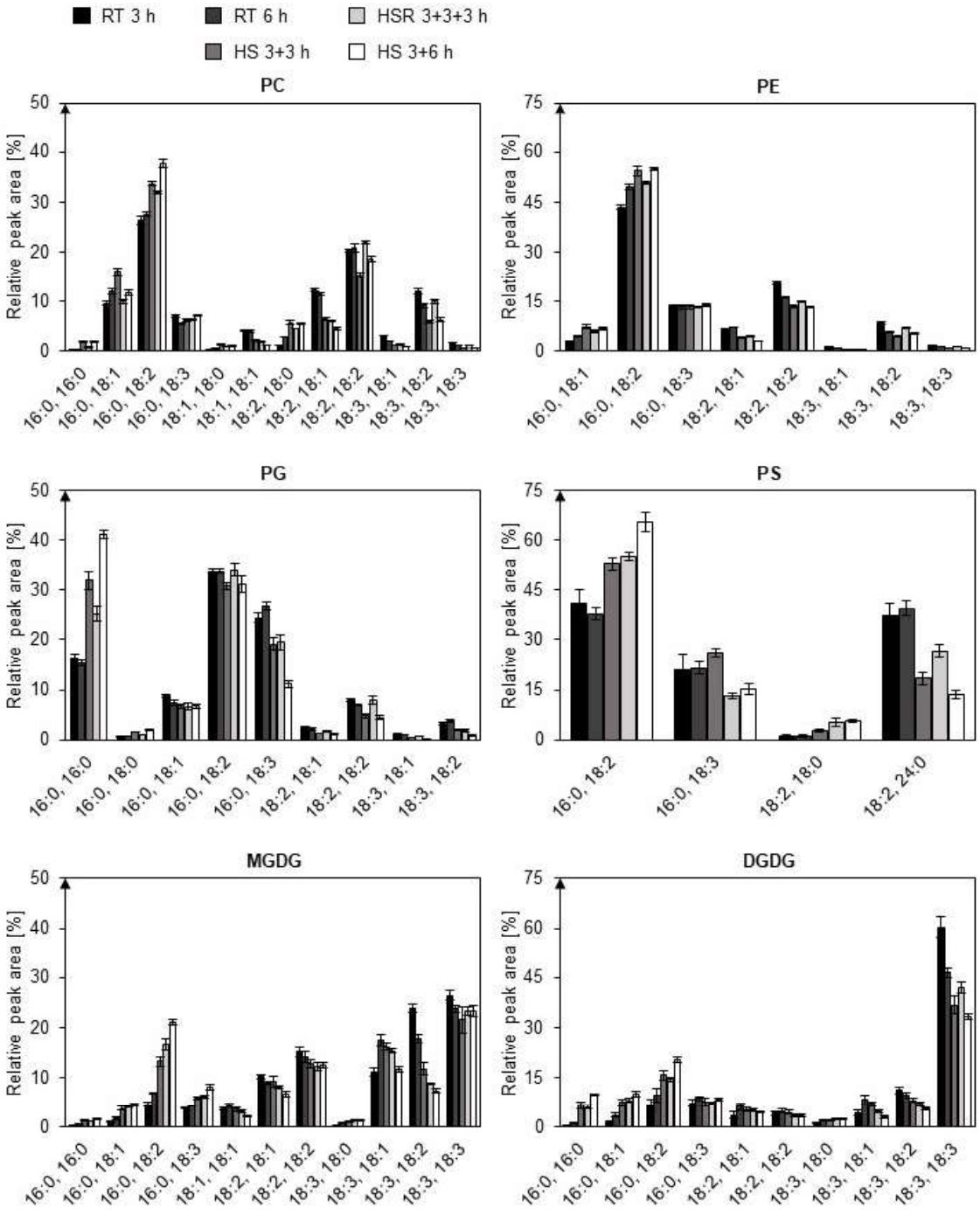

Figure 3: Relative fatty acid composition of the membrane lipids PC, PG, PE, PS, MGDG and DGDG from pollen tubes grown at 3 h RT, 6 h RT, 3 h RT + 3 h HS, 3 h RT + 6 h HS and 3 h RT + 3 h HS + 3 h RT. Lipid species were quantified as peak areas measured by UPLC-nanoESI-MS/MS, normalised to the peak sum of all lipid species per class, only major lipid species (< 1 % of total) are depicted. Statistic analyses are presented separately in Table 2.

Figure 4

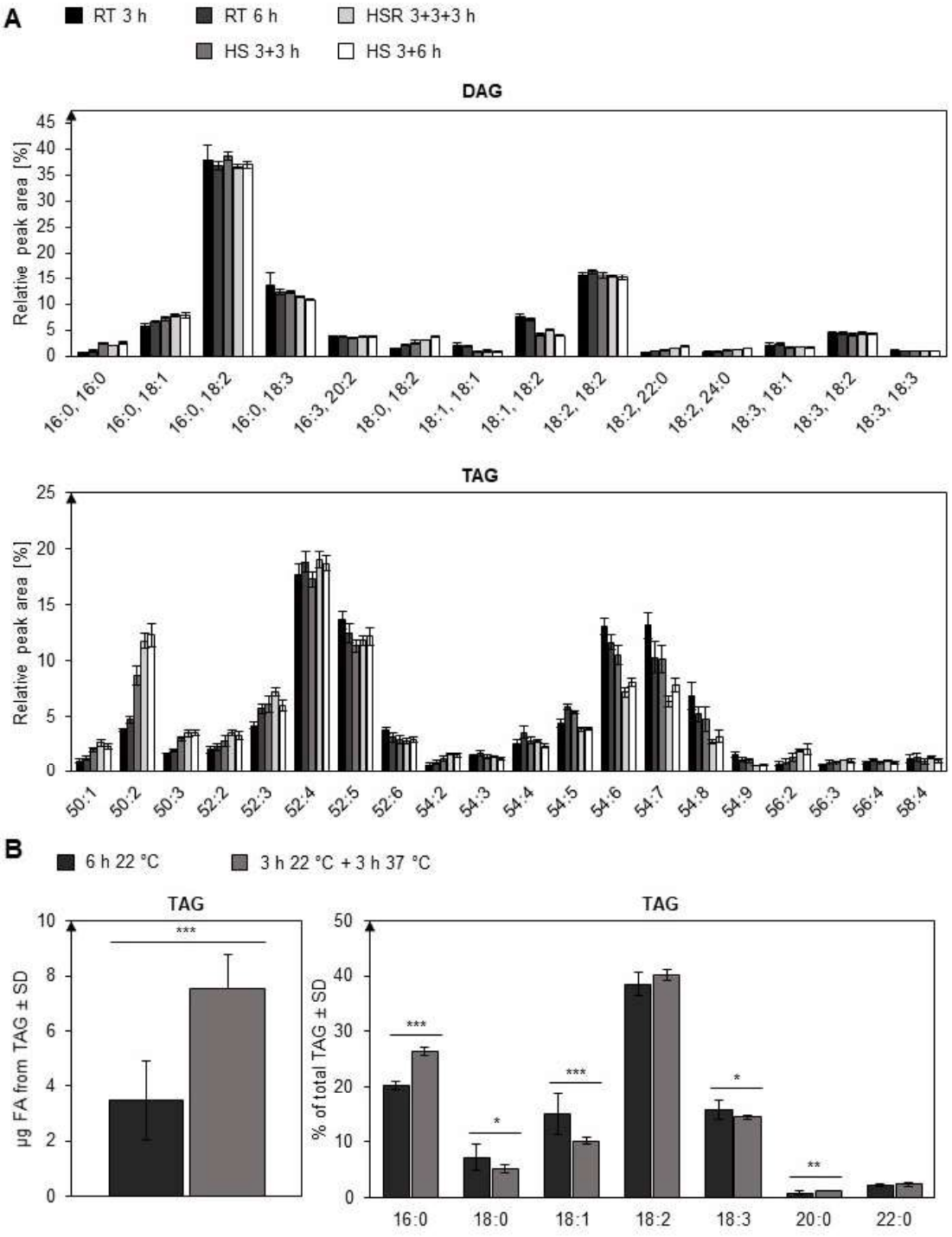

Figure 4: **A** Relative fatty acid composition of the neutral lipids DAG and TAG, extracted from pollen tubes grown at 3 h RT, 6 h RT, 3 h RT + 3 h HS, 3 h RT + 6 h HS and 3 h RT + 3 h HS + 3 h RT. Lipid species were quantified as peak areas measured by UPLC-nanoESI-MS/MS, normalised to the peak sum of all measured lipid species per class. Only major lipid species (< 1 % of total) are depicted. Statistic analyses are presented separately in Table 3. **B** Absolute quantification of TAG from heat stressed (3 h RT+ 3 h HS) and non-stressed (6h RT) pollen tubes per 1 mg of dry pollen. Also shown is the relative contribution of the respective fatty acids to the total TAG amount. Measurements were performed with GC-FID and quantified as peak areas. *** $p < 0.005$; ** $p < 0.001$; * $p < 0.05$; determined by two-sided Student's *t*-test.

Table 1: Statistics on lipid class analyses

	PC	PE	PG	PS	MGDG	DGDG	DAG	TAG
RT 3 h	a	a	a	a	a	a	a	a
RT 6 h	a	b	ab	b	b	b	b	ab
HS 3+3 h	a	ab	b	c	c	c	bc	b
HSR 3+3+3 h	b	c	c	d	d	d	c	c
HS 3+6 h	c	d	c	e	e	e	d	c

Statistics on membrane lipid analyses (Figure 2a). Analysis of variance (ANOVA) was performed, followed by Post-hoc Tukey analysis. Analyses were performed between all conditions, but separately for all lipid classes. Results are presented as compact letter display of all pair-wise comparisons in increasing order.

Table 2: Statistics on membrane lipid analyses

	16:0, 16:0	16:0, 18:0	16:0, 18:1	16:0, 18:2	16:0, 18:3	18:1, 18:0	18:1, 18:1	18:2, 18:0	18:2, 18:1	18:2, 18:2	18:2, 24:0	18:3, 18:0	18:3, 18:1	18:3, 18:2	18:3, 18:3
PC															
RT 3 h	a	-	a	a	c	a	c	a	d	c	-	-	e	c	c
RT 6 h	a	-	b	a	a	b	c	b	c	cd	-	-	d	b	b
HS 3+3 h	c	-	c	c	b	d	b	d	b	a	-	-	b	a	a
HSR 3+3+3 h	b	-	a	b	b	c	b	c	b	d	-	-	c	b	b
HS 3+6 h	c	-	b	d	c	c	a	d	a	b	-	-	a	a	a
PE															
RT 3 h	-	-	a	a	a	-	-	-	c	d	-	-	d	d	d
RT 6 h	-	-	b	b	a	-	-	-	d	c	-	-	c	b	b
HS 3+3 h	-	-	d	c	a	-	-	-	b	a	-	-	b	a	a
HSR 3+3+3 h	-	-	c	b	a	-	-	-	b	b	-	-	b	c	c
HS 3+6 h	-	-	c	c	a	-	-	-	a	a	-	-	a	b	a
PG															
RT 3 h	a	a	b	b	c	-	-	-	d	c	-	-	c	c	-
RT 6 h	a	a	a	b	d	-	-	-	c	b	-	-	c	d	-
HS 3+3 h	c	c	a	a	b	-	-	-	a	a	-	-	a	b	-
HSR 3+3+3 h	b	b	a	b	b	-	-	-	b	c	-	-	b	b	-
HS 3+6 h	d	d	a	a	a	-	-	-	a	a	-	-	a	a	-
PS															
RT 3 h	-	-	-	a	b	-	-	a	-	-	c	-	-	-	-
RT 6 h	-	-	-	a	b	-	-	a	-	-	c	-	-	-	-
HS 3+3 h	-	-	-	b	b	-	-	b	-	-	a	-	-	-	-
HSR 3+3+3 h	-	-	-	b	a	-	-	c	-	-	b	-	-	-	-
HS 3+6 h	-	-	-	c	a	-	-	c	-	-	a	-	-	-	-

MGDG															
RT 3 h	a	-	a	a	a	-	bc	-	c	c	-	a	a	d	b
RT 6 h	b	-	b	b	a	-	c	-	bc	bc	-	b	c	c	ab
HS 3+3 h	c	-	c	c	b	-	bc	-	bc	ab	-	c	bc	b	a
HSR 3+3+3 h	c	-	cd	d	b	-	b	-	ab	a	-	d	b	a	a
HS 3+6 h	d	-	d	e	c	-	a	-	a	ab	-	d	a	a	a
DGDG															
RT 3 h	a	-	a	a	a	-	-	-	a	ab	-	a	a	d	c
RT 6 h	a	-	b	a	a	-	-	-	c	b	-	b	b	c	b
HS 3+3 h	b	-	c	b	a	-	-	-	bc	ab	-	b	b	bc	a
HSR 3+3+3 h	b	-	c	b	a	-	-	-	bc	a	-	b	a	b	b
HS 3+6 h	c	-	d	c	a	-	-	-	ab	a	-	b	a	a	a

Statistics on membrane lipid analyses (Figure 3). Analysis of variance (ANOVA) was performed, followed by Post-hoc Tukey analysis. Analyses were performed between all conditions, but separately for all lipid species. Results are presented as compact letter display of all pair-wise comparisons in increasing order.

Table 3: Statistics on glycerolipid analyses

	DAG													
	16:0, 16:0	**16:0, 18:1**	**16:0, 18:2**	**16:0, 18:3**	**16:3, 20:2**	**18:1, 18:1**	**18:2, 18:0**	**18:2, 18:1**	**18:2, 18:2**	**18:2, 22:0**	**18:2, 24:0**	**18:3, 18:1**	**18:3, 18:2**	**18:3, 18:3**
RT 3 h	a	a	a	b	a	b	a	c	ab	a	a	b	a	a
RT 6 h	a	ab	a	ab	a	b	b	c	b	b	a	b	a	a
HS 3+3 h	c	bc	a	ab	a	a	c	a	ab	c	b	a	a	a
HSR 3+3+3 h	b	c	a	ab	a	a	d	b	a	d	b	ab	a	a
HS 3+6 h	c	c	a	a	a	a	e	a	a	c	c	a	a	a

	TAG																			
	50:1	**50:2**	**50:3**	**52:2**	**52:3**	**52:4**	**52:5**	**52:6**	**54:2**	**54:3**	**54:4**	**54:5**	**54:6**	**54:7**	**54:8**	**54:9**	**56:2**	**56:3**	**56:4**	**58:4**
RT 3 h	a	a	a	a	a	ab	b	b	a	ab	a	b	c	c	d	c	a	a	ab	a
RT 6 h	a	a	a	ab	b	ab	ab	ab	a	b	b	d	b	b	cd	b	a	ab	b	a
HS 3+3 h	b	b	b	bc	bc	a	a	a	b	ab	a	c	b	b	bc	b	ab	ab	a	a
HSR 3+3+3 h	c	c	c	c	c	b	a	a	b	ab	a	a	a	a	a	s	bc	b	ab	a
HS 3+6 h	bc	c	c	c	b	ab	ab	a	b	a	a	a	a	a	ab	s	x	ab	ab	a

Statistics on membrane lipid analyses (Figure 4 a-b). Analysis of variance (ANOVA) was performed, followed by Post-hoc Tukey analysis. Analyses were performed between all conditions, but separately for all lipid species. Results are presented as compact letter display of all pair-wise comparisons in increasing order.

Sterol synthesis in pollen tubes is upregulated under heat stress conditions

Sterols are important structural lipid constituents of membranes, especially the plasma membrane, and are important for membrane microdomain (lipid raft) formation and through this involved in diverse cellular processes, including polar cell growth (Simons and Ikonen, 1997; Beck *et al.*, 2007; Simon-Plas *et al.*, 2011).

The sterol profile in pollen from various species differs greatly from that in leaves or other sporophytic tissues and it was shown that the sterol synthesis pathway in growing Tobacco pollen tubes is truncated with only two species being de novo synthesised: presumably methylenepollinastanol and its precursor cycloeucalenol (Villette *et al.*, 2015; Rotsch *et al.*, 2017). Relative abundance of these sterol species increases during pollen tube growth (Rotsch *et al.*, 2017), as can be seen in the presented data (Figure 5, Supplementary Dataset S5-6). Especially cycloeucalenol accumulated strongly under HS and less at RT. After heat stress relief, increased accumulation ceased and levels remained constant.

Figure 5

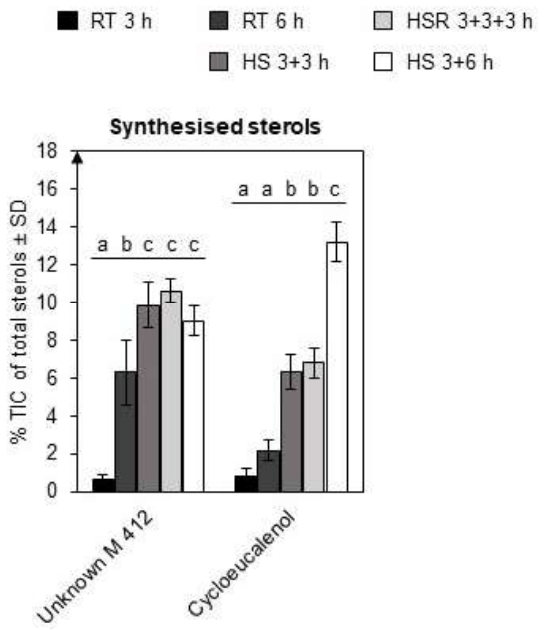

Figure 5: Relative amounts of newly synthesised sterol species. Only two sterol species are newly synthesised in growing Tobacco pollen tubes: Unknown M412 and Cycloeucalenol. Presented are relative abundances of the respective sterol based on the total ion current as measured by GC-MS, pollen tubes were grown 23°C for 3 h or 6 h, or shifted to 37 °C after 3 h for 3 h or 6 h (3+3h HS, 3+6h HS). Another batch of tubes was grown for 23°C for 3 h shifted to 37 °C for 3 h and then shifted back (3+3+3h HSR). ANOVA was performed, followed by Post-hoc Tukey analysis. Results are presented as compact letter display of all pair-wise comparisons in increasing order.

Metabolomic adaptations

In our study, we identified 51 metabolites by GC-MS that are mostly part of central metabolism including organic acids, amino acids and sugars (Supplementary Dataset S7-8). In addition, 17 markers were identified. Values of all timepoints were normalised to the values after 3 h of RT. While most metabolites accumulated during prolonged pollen tube growth, not all of these were affected by HS. Most amino acids increased during HS, including the non-codogenic amino acids β-lactate, γ-amino butyrate (GABA) and pipecolate (Figure 6d, Supplementary Dataset S5-6). Proline and glutamate levels, however, were not strongly affected by temperature. Also, sugar levels were only mildly affected by HS with the exception of the 7-carbon sugar sedoheptulose that increased ~ 3-fold, and sucrose that increased 2-fold after HS in comparison to the control (Figure 6b). Among the organic acids an increase in 2-isopropylmalate, an intermediate in leucine biosynthesis, and 2-oxoglutarate (2-OG) was observed (Figure 6c). Interestingly, fumarate and malate were not affected by HS but strongly increased after stress relief. Further metabolites that show an increase under HS include Glycerol-3-phosphate (G3P, Figure 6e and 6f, Supplementary Dataset S5-6) and the so far unidentified marker A171005 deposited in the Golm metabolome database (Kopka *et al.*, 2005).

Figure 6

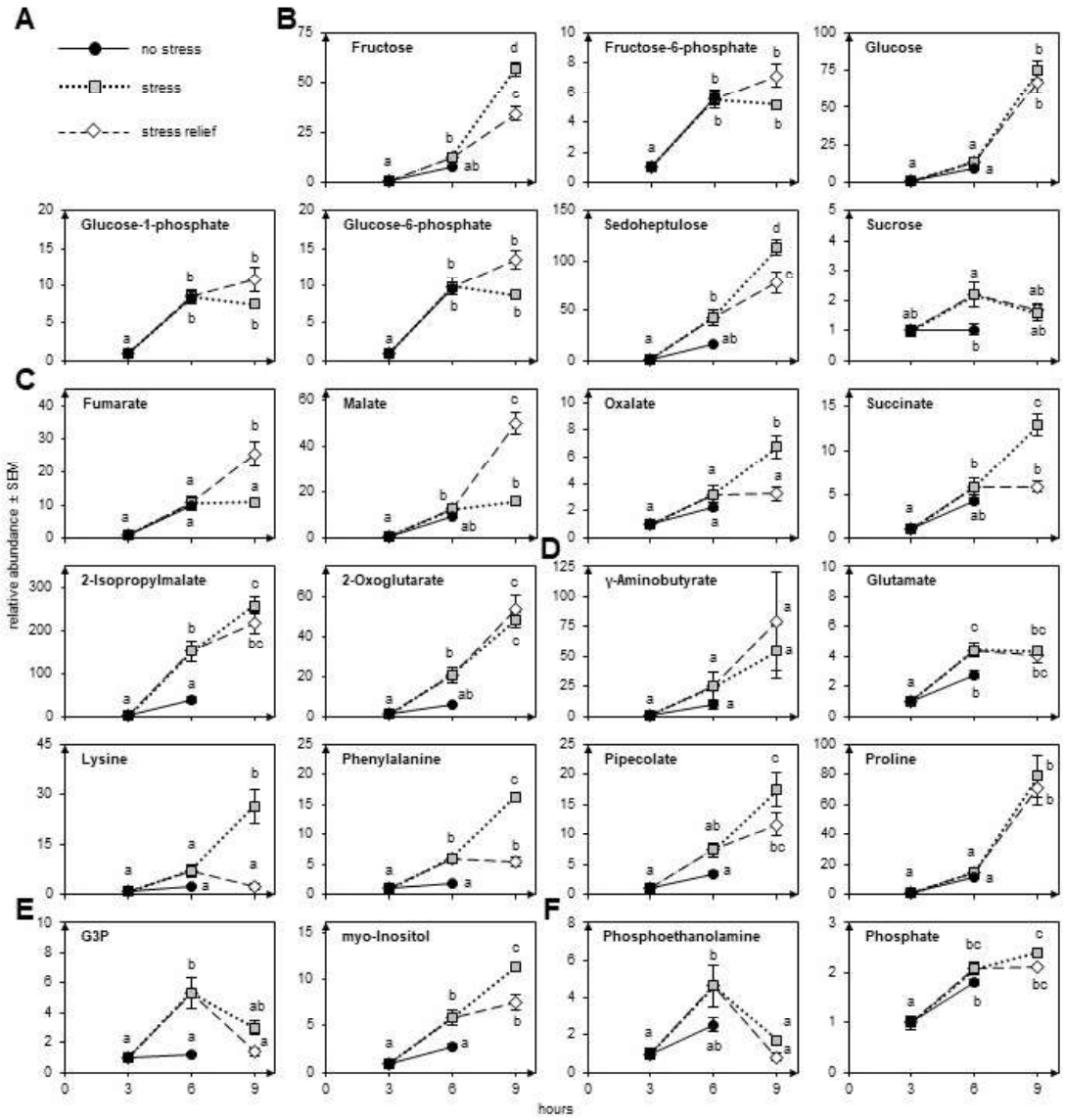

Figure 6*:* Relative amount of a selection of detected metabolites, normalised to RT 3h. **A** legend: black line and filled black circles: no stress (RT 3h and RT 6); dotted line and grey squares: stress (HS 3+3h and HS 3+6h); dashed lines and white rhombus: stress relief (HSR 3+3+3h). Shown are a selection of detected sugars (**B**), a selection of detected organic acids (**C**), a selection of detected amino acids (**D**), a selection of detected polyols (**E**) and others (**F**). ANOVA was performed, followed by Post-hoc Tukey analysis. Results are presented as compact letter display of all pair-wise comparisons in increasing order.

Heat stress leads to strong alteration on the transcriptome level

To assess whether the different adaptations are reflected on a transcriptional level, transcriptome analyses of pollen tubes grown for 3 or 6 h at RT or 3 h at RT followed by 3 h at HS were performed by RNA sequencing (Figure 7).

Overall, 26743 genes were detected, 24013 of which with more than 0.5 counts per million (CPM) in at least 2 libraries and 21241 of these could be assigned a UniProt protein ID (Table 4). The respective protein sequences were then blasted vs the TAIR 10 Arabidopsis protein

library and to 19,798 Tobacco proteins, Arabidopsis homologues with an Expect value (E-value) < 10^{-5} were found. The respective Arabidopsis protein identifiers were later used for functional annotation.

In the analysis of pollen tubes grown for three versus six hours at room temperature, 561 genes were differentially expressed (abs. log2FC > 1; FDR ≤ 0.005), 306 of which were up-regulated and 255 of which were down-regulated (Figure 7b).

In the comparison of heat-stress versus non heat-stressed pollen tubes, 2383 genes were differentially expressed, 1570 of which were up-regulated and 813 of which were down-regulated (Figure 7c). For analyses of gene functions, we further explored the second comparison making use of the functional annotation of the Arabidopsis genome and proteome.

Figure 7

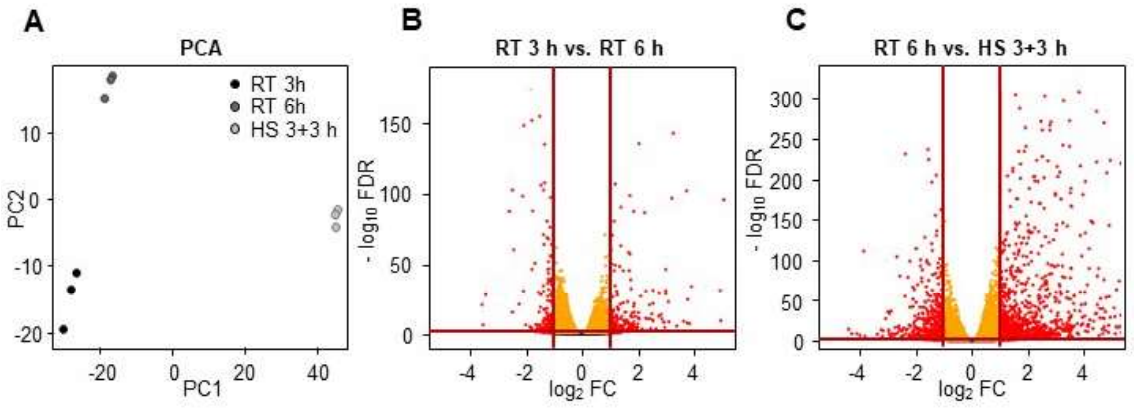

Figure 7: Analysis of transcriptome data. A Principle component analysis (PCA) of RT 3 h, RT 6 h and HS 3+3 h. B and C Volcano plots of RT 3h vs. RT 6h and RT 6h vs. HS 3+3 h, respectively. Red lines indicate threshold for differential expression (abs. log2FC > 1, red dots and FDR < 0.005, orange dots).

Table 4: Number of detected and annotated genes in the respective analysis.

Analysis	Detected genes	UniProt ID	Arabidopsis homolog
RT 3 h vs. RT 6 h	23,043	20,459	19,162
RT 6 h vs. HS 3+3 h	23,053	20,445	19,779
total	24,013	21,241	19,798
total unfiltered	26,743	-	-

Number of detected genes in total and in the two comparisons and number of total detected genes (unfiltered). For DE analyses, genes were filtered for a CPM < 0.5 in at least two of the respective analysed libraries. Genes were annotated a UniProt identifier (UniProt ID), some genes could not be annotated, number of annotated genes is given. Annotated Tobacco proteins were blasted against Arabidopsis to find closest homologs, only hits with E-value < 10^{-5} were considered. Number of genes with an Arabidopsis protein homolog hit is given.

GO-term analysis gives first insights

For gene ontology (GO) analysis, the GO terms assigned to the annotated Arabidopsis homologues were analysed. For the analysis of RT 6 h versus HS 3+3 h, 20,370 genes were assigned with 5994 different GO terms, giving a total of 152,469 GO term-gene combinations. RPKM values of all genes belonging to the same GO term were summed up and averaged for the respective condition to calculate log2FCs. The summed up RPKM values were also analysed by a Student's T-test for significances. The number of total detected genes belonging to the respective GO-term was determined as well as the number of genes within the term that, according to statistical testing (Supplementary Dataset S10), showed differential expression (Table 5 and Supplementary Dataset S12-15).

A selection of the most changed GO terms between RT 6 h and HS 3+3 h are presented in Table 5, grouped by sub-ontology (for complete lists see Supplementary Dataset S12-15). Among them are several heat shock-related GO terms containing many up-regulated genes and only few down-regulated genes. The terms include "functions in Hsp90 protein binding", "has unfolded protein binding", and "involved in response to heat". Another strongly changed GO term is "involved in response to reactive oxygen species" with 76 detected genes, 46 of which showed statistically significant up-regulation. Other changed GO terms like "has pre-mRNA 3'-splice site binding" and "involved in positive regulation of mRNA splicing, via spliceosome" might hint at a role of alternative splicing under heat stress, which has been shown before, e.g. in tomato pollen (Keller *et al.*, 2017). Interestingly, several changed GO terms suggest that auxin metabolism and/or signalling might be affected ("has auxin receptor activity", "involved in auxin catabolic process", and "involved in regulation of auxin biosynthetic process"). Up-regulation of the GO term "auxin catabolic process" as well as "auxin biosynthetic process" are due to up-regulation of putative Tobacco DIOXYGENASE FOR AUXIN OXIDATION 1 (DAO1) and REVEILLE1 (RVE1) homologues; while "auxin receptor activity" contains two down-regulated homologues of the Arabidopsis auxin receptor TRANSPORT INHIBITOR RESPONSE 1 (TIR1).

Table 5: List of selected GO-terms, their IDs, log_2-fold changes (6 h 22 °C vs. 3 h 22 °C + 3 h 37 °C), p-values, the number of detected genes within the GO-term and the number of differentially expressed genes (up- and down-regulated) within the term.

GO ID	GO term	log_2FC	*p-value*	genes	DEG up	DEG down
	Molecular Function					
GO:0043621	functions in protein self-association	4.09	1.4E-07	126	47	5
GO:0051879	functions in Hsp90 protein binding	3.38	9.8E-08	21	12	0
GO:0051082	has unfolded protein binding	2.20	5.7E-07	225	102	1
GO:0009916	has alternative oxidase activity	1.44	7.1E-07	8	4	0
GO:0004765	has shikimate kinase activity	1.06	0.0006	3	2	0
GO:0030628	has pre-mRNA 3'-splice site binding	1.06	2.2E-05	20	7	0
GO:0000064	has L-ornithine transmembrane transporter activity	-1.07	8.3E-05	5	0	2
GO:0005476	has carnitine:acyl carnitine antiporter activity	-1.08	9.4E-05	3	0	2
GO:0008792	has arginine decarboxylase activity	-1.35	9.2E-06	4	0	3
GO:0005244	has voltage-gated ion channel activity	-1.46	0.0029	3	0	2
GO:0038198	has auxin receptor activity	-2.01	0.0005	2	0	2
	Cellular Component					
GO:0089701	located in U2AF	1.29	1.4E-05	18	7	0
	Biological Process					
GO:0009061	involved in anaerobic respiration	9.36	2.6E-05	2	2	0
GO:0061077	involved in chaperone-mediated protein folding	3.27	8.4E-07	33	11	2
GO:0010187	involved in negative regulation of seed germination	2.73	5.1E-06	28	11	1
GO:0006457	involved in protein folding	2.26	5.4E-07	202	97	1
GO:0048026	involved in positive regulation of mRNA splicing, via spliceosome	1.80	1.0E-06	11	2	0
GO:0009852	involved in auxin catabolic process	1.72	4.6E-05	2	1	0
GO:0000302	involved in response to reactive oxygen species	1.68	6.5E-08	76	46	0
GO:0034605	involved in cellular response to heat	1.65	1.7E-06	47	20	0
GO:0009408	involved in response to heat	1.29	6.6E-08	266	116	10
GO:0010600	involved in regulation of auxin biosynthetic process	1.17	0.0032	4	3	0

GO:0010508	involved in positive regulation of autophagy	1.11	7.8E-06	14	3	0
GO:0043618	involved in regulation of transcription from RNA polymerase II promoter in response to stress	1.06	1.3E-05	22	9	0
GO:0033388	involved in putrescine biosynthetic process from arginine	-1.33	9.6E-06	6	0	3
GO:0071456	involved in cellular response to hypoxia	0.743	7.12E-07	211	67	11
GO:0009446	involved in putrescine biosynthetic process	-1.33	9.6E-06	6	0	3
GO:0006527	involved in arginine catabolic process	-1.33	9.8E-06	7	0	3

A selection of GO terms grouped by sub-ontologies (molecular function, cellular component, biological process) that show a strong log_2-fold change (log_2FC) between pollen tubes grown for 6 h at 22 °C and tubes grown for 3 h at 22 °C followed by 3 h at 37 °C. GO terms were quantified summing RPKM-values of all detected genes within one GO term (number of genes is given) for the respective condition (6 h 22 °C or 3 h 22 °C + 3 h 37 °C) and log_2FC of the summed RPKMs was calculated. P-values were calculated using Student's T-test on summed RPKM-values of the two conditions. Number of differentially expressed genes (DEG; $log_2FC > |1|$, FDR < 0.005 according to DE analysis with EdgeR, Suppl. Dataset S12-15) within the GO term are given.

Transcripts of transcriptional regulators are strongly affected

The GO term analysis revealed that the term “has transcription coactivator activity” was 3.2-fold upregulated, with 9 of 46 genes being differentially upregulated. The terms “functions in transcription regulatory region DNA binding” and “has DNA-binding transcription factor activity” showed 34 of 395 and 72 of 654 differentially upregulated but also 31 and 15 downregulated genes, respectively. The total transcript abundance within these terms was, however, only little changed (Supplementary Dataset S14). To get a closer look at putative transcriptional regulators important during heat stress, the transcript data was mined for genes homologous to Arabidopsis transcriptional regulators according to the Arabidopsis Plant Transcription Factor Database with 2192 gene entries (Pérez-Rodríguez *et al.*, 2009). Overall, 1319 Tobacco genes could be assigned to transcriptional regulators (117 up- and 42 differentially downregulated, Supplementary Dataset S16-17). The highest proportion of upregulated genes was found among the heat shock transcription factors (HSF, 9 of 19) and DNA-binding protein phosphatases (DBP, 6 of 10). Three of the HSFs were among the top 100 upregulated genes but also two members of the multiprotein bridging factor (MBF1) family with fold changes ranging from 155 to 421. The MBF1 family is part of a heat stress regulon in Arabidopsis (Suzuki *et al.*, 2011). Furthermore, the transcription factor families MYB-related and AP2-EREBP showed a comparably high number of upregulated genes (14 and 9 respectively).

Transcripts related to lipid metabolism are barely affected by heat stress

To find out whether lipid adaptations are mirrored on a transcriptional level, a list of 746 Arabidopsis genes with a role or putative role in glycerolipid, sphingolipid and sterol metabolism was compiled from several sources (see method section and Supplementary Dataset S18). Comparing our transcript data to this list, 713 Tobacco transcripts were assigned a putative function in lipid metabolism (Supplementary Dataset S19). Of these, only 43 genes were differentially expressed, 20 of which were up- and 23 down-regulated (Table 6).

This result already indicates that lipid adaptations are not strongly reflected on a transcriptional level. To take a closer look at the differentially expressed genes, lipid genes were grouped according to their pathways.

Table 6: List of all detected transcription factor families with differentially expressed genes.

Transcription factor family	Type	Arabidopsis genes	Detected genes	DEG up	DEG down
ABI3VP1	TF	57	27	1	1
Alfin-like	TF	7	10	0	1
AP2-EREBP	TF	146	34	9	1
ARF	TF	23	15	2	1
ARID	Other	10	17	1	1
AUX/IAA	Other	28	1	1	0
BES1	TF	8	10	0	1
bHLH	TF	136	44	5	3
bZIP	TF	70	49	1	5
C2C2-CO-like	TF	17	4	0	1
C2C2-GATA	TF	29	13	2	0
C2H2	TF	99	43	3	3
C3H	TF	68	90	7	1
CCAAT	TF	43	39	3	0
Coactivator p15	Other	3	2	2	0
CSD	TF	4	3	2	0
DBP	TF	4	10	6	0
EIL	TF	6	8	2	0
FAR1	TF	17	26	2	1
FHA	TF	17	20	3	0
G2-like	TF	40	20	2	0
GNAT	Other	32	34	1	0
GRAS	TF	33	17	3	3
HB	TF	91	19	1	0
HSF	TF	23	19	9	0
LOB	TF	43	14	1	0
LUG	Other	2	6	1	0
MADS	TF	105	30	2	2
MBF1	Other	3	7	2	0
mTERF	TF	34	11	1	1
MYB	TF	147	55	2	2
MYB-related	TF	65	71	14	1
NAC	TF	104	26	3	0
Orphans	TF	83	35	4	1
PHD	Other	45	92	3	1
Pseudo ARR-B	Other	5	5	1	1
RWP-RK	TF	14	10	2	1
SET	Other	33	46	3	0
Sigma70-like	TF	6	6	3	0

SNF2	Other	38	57	0	3
SWI/SNF-BAF60b	Other	16	10	1	0
TCP	TF	24	5	0	1
Tify	TF	15	9	0	1
TRAF	Other	25	16	0	2
TUB	TF	10	15	2	0
ULT	TF	2	4	0	1
VOZ	TF	2	4	1	0
WRKY	TF	72	22	3	1

List of all detected transcription factor families that contain differentially expressed genes. As reference, the Arabidopsis Plant Transcription Factor Database PlnTFDB with 2192 gene entries was used (Pérez-Rodríguez *et al*. 2009; accessed on 4th June 2020). Given are the transcription factor family names, their type (TF = transcription factor, Other = other transcriptional regulator), the number of Arabidopsis genes belonging to the respective family, the number of detected Tobacco genes putatively belonging to the respective family and the number of differentially expressed genes (DEG; $\log_2$FC > |1|, FDR < 0.005) within the family.

Fatty acid synthesis is not transcriptionally upregulated

Pollen tube growth requires fatty acid synthesis in the plastids to cope with the increasing need for membrane lipids in growing pollen tubes (Ischebeck, 2016). Under HS, pollen tubes seem to need slightly more membrane lipids, as several minor lipid classes as well as TAG levels accumulated stronger at high temperature (Figure 2a). However, neither of the pathways leading to acetyl-CoA synthesis via the pyruvate dehydrogenase or pyruvate decarboxylase seem to be strongly affected (Supplementary Dataset S19). The same is true for fatty acid synthesis itself, as only one relevant gene, one of six putative Ketoacyl-ACP Reductases (KAR) was up-regulated; on the other hand, a hydroxyacyl-ACP dehydrase (HAD) homologue was down-regulated. It was previously shown that downregulation of the ketoacylsynthase KASII/FAB1, which is responsible for the elongation from C16 to C18 acyl chains, leads to strongly increased levels of C16 acyl chains in Arabiodopsis (Pidkowich *et al.*, 2007). Interestingly, none of the four isoforms was considerably downregulated in Tobacco pollen tubes under heat stress, despite the increase of 16:0 acyl chains across lipid classes (Figure 3). Furthermore, an upregulation of thioesterase expression that could result in an increased release of C16 fatty acids, was not observed. On the contrary, three of the six thioesterases detected were even significantly downregulated.

What is more, no differentially expressed fatty acid desaturases (FADs) were detected in our screen. FAD2 and FAD3, the desaturases that catalyse the desaturation from 18:1- to 18:2- and 18:2- to 18:3-PC, respectively, are not downregulated but several isoforms were slightly upregulated. No homologues of FAD4, the enzyme catalysing the desaturation of 16:0 to 16:1 PG, were detected; neither were FAD5 homologues, desaturating 16:0 MGDG to 16:1. Two homologues of FAD6, the enzyme responsible for the desaturation of 16:1 and 18:1 MGDG and PG to 16:2 and 18:2 and of 18:1 SQDG and DGDG to 18:2, were detected, none of which

showed differential expression; neither did the FAD7 homologue or the two FAD8 homologues that desaturate 18:2 and 16:2 MGDG, DGDG, SQDG and PG to 18:3 and 16:3, respectively. Genes involved in fatty acid degradation were mostly unchanged, too. Only the transcript of one (of two detected) acyl-coenzyme A oxidases (ACX, involved in fatty acid degradation via fatty acid beta-oxidation) was down-regulated.

Transcript does not reflect adaptations in glycerolipid profiles

The expression levels of enzymes involved in glycerolipid metabolism gave a rather indifferent picture. While some individual isoforms were differentially expressed (Table 7), only few clear trends could be observed. Among the upregulated, but not differentially expressed genes, two putative PA phosphatases homologous to Arabidopsis LPP1/PAP1 which had a very high abundance level that increased by 25 and 55 %, respectively. Also two of three CGI58-type lysophosphatidic acid acyltransferases that are involved in membrane and neutral lipid homeostasis (Ghosh *et al.*, 2009; James *et al.*, 2010) were slightly upregulated by 32 and 35 %, respectively (Supplementary dataset S19). Regarding galactolipids, the adaptations were equally indifferent: Some transcripts involved in galactolipid synthesis showed a trend towards slight upregulation, while others showed a tendency towards downregulation. However, none of the changes met the threshold for differential expression.

Transcripts important for sulfolipid metabolism were not detected, indicating again that these lipids do not occur in Tobacco pollen tubes.

Table 7: List of differentially expressed genes with putative involvement in lipid metabolism.

Tobacco Gene	Tobacco Protein	Arabidopsis Gene	Arabidopsis Protein	Putative Function	log_2FC	FDR
Acetyl CoA and Fatty Acid Synthesis						
LOC107779989	A0A1S3YUM8	AT1G23800	ALDH2B7	Aldehyde dehydrogenase	1.59	1.8E-23
LOC107811394	A0A1S4BSN2	AT1G24360	KAR	Ketoacyl-ACP Reductase	1.24	8.1E-08
LOC107789406	A0A1S3ZQ73	AT2G38040	α-CT/CAC3	Carboxyltransferase alpha Subunit of Heteromeric ACCase	-1.02	9.0E-22
LOC107829909	A0A1S4DHM5	AT5G10160	HAD	Hydroxyacyl-ACP Dehydrase	-1.06	5.2E-08
LOC107789890	A0A1S3ZSC9	AT5G54960	PDC2	Pyruvate decarboxylase	-1.215	5.8E-04
LOC107769281	A0A1S3XVK6	AT1G65290	MTACP1	Acyl carrier protein, mitochondrial	-1.47	5.2E-06
LOC107790423	A0A1S3ZU33	AT4G13050	FATA2	Acyl-ACP Thioesterase A	-1.17	0.0166
LOC107818291	A0A1S4CF02	AT2G34590	PDH (E1 beta)	Pyruvate Dehydrogenase beta subunit	-1.57	1.1E-22
Fatty Acid Elongation, Desaturation and Export						
LOC107791219	A0A1S3ZWG6	AT5G10480	PAS2/HCD	Hydroxyacyl-CoA Dehydratase	1.14	3.6E-11
LOC107789797	A0A1S3ZRX0	AT2G28630	KCS12	3-ketoacyl-CoA synthase	-1.28	0.0040
Fatty Acid Degradation						
LOC107829745	A0A1S4DH57	AT5G42250		Zinc-binding alcohol dehydrogenase family protein	-1.04	1.7E-28
LOC107785996	A0A1S3ZEK9	AT1G06290	ACX3	Acyl-CoA Oxidase	-1.17	2.8E-31
Glycerolipid metabolism						
LOC107761528	A0A1S3X5P8	AT4G26770	CDP-DAGS	CDP-DAG Synthase	-1.05	2.8E-23
LOC107759316	A0A1S3WYH5	AT5G10170	MIPS3	myo-inositol-3-phosphate synthase	-1.17	1.5E-20
LOC107800182	A0A1S4AQG0	AT3G17770		Dihydroxyacetone kinase	1.96	5.7E-08
LOC107827585	A0A1S4DAJ3	AT3G05510		Phospholipid/glycerol acyltransferase family protein	1.10	2.2E-11
LOC107773804	A0A1S3Y9M0	AT4G30340	DGK7	diacylglycerol kinase 7	-2.13	8.5E-05
Triacylglycerol Synthesis						
LOC107830919	A0A1S4DLP1	AT2G19450	DGAT1/TAG1	Acyl-CoA : Diacylglycerol Acyltransferase	2.86	4.5E-25
LOC107789692	A0A1S3ZR81	AT2G19450	DGAT1/TAG1	Acyl-CoA : Diacylglycerol Acyltransferase	2.50	1.8E-07
LOC107775049	A0A1S3YDY1	AT2G19450	DGAT1/TAG1	Acyl-CoA : Diacylglycerol Acyltransferase	2.10	1.7E-08

LOC107779882	U5JD04	AT3G51520	DGAT2	Acyl-CoA : Diacylglycerol Acyltransferase	1.39	0.0002
LOC107811379	A0A1S4BSB8	AT1G48300	DGAT3	Acyl-CoA : Diacylglycerol Acyltransferase	1.12	4.3E-12
Lipid droplet-associated proteins						
LOC107774779	A0A1S3YCP8	AT4G10020	HSD5	Steroleosin	6.97	3.2E-51
LOC107821969	A0A1S4CS64	AT3G01570	OLE5	Oleosin family protein	5.87	4.3E-21
LOC107804268	A0A1S4B436	AT1G67360	LDAP1	Lipid droplet associated protein	1.14	3.8E-127
LOC107776898	A0A1S3YJQ0	AT1G10740	LDAH1	Lipid droplet associated hydrolase	1.10	6.4E-45
LOC107780677	A0A1S3YX57	AT3G18570	OLE8	Oleosin family protein	-1.22	3.3E-26
Acylglycerol Degradation						
LOC107786500	A0A1S3ZGS3	AT5G04040	SDP1	Patatin-like phospholipase family protein	1.09	3.6E-72
LOC107779568	A0A1S3YTI2	AT2G39420	MAGL8	Monoacylglycerol Lipase (MAGL)	-1.11	0.0001
LOC107815121	A0A1S4C4N0	AT3G62860	MAGL12	Monoacylglycerol Lipase (MAGL)	-1.15	2.4E-59
LOC107774655	A0A1S3YC93	AT4G18550	DSEL	cytosolic DAD1-like acylhydrolase, sn-1-specific lipase	-1.50	0.0007
Further Lipases						
LOC107789128	A0A1S3ZPC3	AT2G03140		alpha/beta-Hydrolases superfamily protein	1.92	1.4E-123
LOC107827574	A0A1S4D9U6	AT1G31480	SGR2	phosphatidic acid-preferring phospholipase A1 (PA-PLA1) ?	1.19	8.5E-10
LOC107811391	A0A1S4BSF2	AT3G48090	EDS1	alpha/beta-Hydrolases superfamily protein	1.16	3.7E-10
LOC107786539	A0A1S3ZGY2	AT1G71250	GDSL-like	GDSL-like Lipase/Acylhydrolase superfamily protein	-1.09	6.8E-86
LOC107797353	A0A1S4AGE5	AT2G26560	PLP2	Phospholipase A 2A	-1.26	7.3E-14
LOC107779233	A0A1S3YSB9	AT1G29120		Hydrolase-like protein family	-1.27	1.6E-53
LOC107799608	A0A1S4ANI7	AT1G29120		Hydrolase-like protein family	-1.29	2.2E-32
Steroid Biosynthesis						
LOC107795609	A0A1S4AAX4	AT2G29390	SMO2-2	sterol 4-alpha-methyl-oxidase 2-2	3.03	9.1E-11
LOC107795958	A0A1S4AC88	AT3G19820	DWF1	cell elongation protein / DWARF1 / DIMINUTO (DIM)	-1.06	0.0003
Sphingolipid Biosynthesis						
LOC107767458	A0A1S3XPT1	AT1G14290	SBH2	Sphingobase C4-Hydroxylase	1.01	1.1E-65
LOC107826684	A0A1S4D6W9	AT4G36830	ELO4	ELO family protein	-1.03	5.2E-07

LOC107808708	A0A1S4BIQ7	AT2G46210	SLD2	Sphingobase-D8 Desaturase	-1.05	1.1E-85

List of all differentially expressed Tobacco genes with a putative involvement in lipid metabolism. Given are the Tobacco gene name, the annotated UniProt ID Tobacco protein name, the closest Arabidopsis homolog (gene name and protein name) and the assigned putative Tobacco protein function according to the Arabidopsis homology. Differential expression analysis was performed with EdgeR, log_2 fold changes (log_2FC) and false discovery rates (FDR) are given.

Transcripts hint at a dynamic turnover of TAG upon heat stress

Taking a closer look at TAG metabolism, we found that diacylglycerol acyltransferase 1 (DGAT1), DGAT2 and DGAT3 homologues are strongly transcriptionally up-regulated after 3h of HS. However, a homologue of the major TAG lipase SUGAR DEPENDENT 1 (SDP1) is also up-regulated, so is another putative TAG lipase. A putative cytosolic DAD1-like seedling establishment-related lipase (DSEL) homologue is down-regulated, a lipase that in Arabidopsis showed preference for DAG and MAG *in vitro* and is supposed to be a negative regulator of seedling establishment by inhibiting break-down of storage oils (Kim *et al.*, 2011). Thus, down-regulation of this lipase might promote TAG break-down. The concomitant up- and down-regulation of different TAG synthesis and break-down genes hints at increased TAG turn-over rather than just an increase in TAG synthesis (as could be expected from lipidomic results; Figure 2a and 4b).

Up-regulated genes also include some known LD-localised proteins, a 11-beta-hydroxysteroid dehydrogenase-like 5 isoform is very strongly upregulated (125 fold), which is interesting as previously no HSDs were found on LDs of Tobacco pollen tubes on the protein level (Kretzschmar *et al.*, 2018). Also, an oleosin, a lipid droplet-associated protein (LDAP) and a putative lipid droplet associated hydrolase (LDAH) (Kretzschmar *et al.*, 2020) show upregulation; while another putative oleosin family protein is down regulated. Some low but significant changes can be observed in the scaffold protein plant UBX-domain containing protein (PUX10), that plays a role in the degradation of LD proteins (Deruyffelaere *et al.*, 2018; Kretzschmar *et al.*, 2018). All four detected putative homologues show slight upregulation (Supplementary Dataset S19).

Several genes involved in sterol and sphingolipid metabolism show differential expression

A transcript encoding for a methylsterol monooxygenase 2 (SMO2)-like isoform showed 8-fold upregulation. SMO proteins are involved in sterol synthesis, to be more precise SMO2-1 and SMO2-2 are involved in the reaction from 24-methylenelophenol to episterol (precursor of campesterol, brassinosteroids and brassicasterol) and from 24-ehtylenelophenol to δ7-avenasterol (that can be converted to isofucosterol, sitosterol and stigmasterol later). Furthermore, a putative delta(24)-sterol reductase shows two-fold upregulation. Its closest Arabidopsis homologue is DWARF1 (DWF1), which among others catalyses the reactions from isofucosterol to sitosterol and from 24-methylenecholesterol to 24-epi-campesterol and campesterol. However, neither of the mentioned sterols showed differential accumulation upon heat stress (Supplementary Dataset S5-6) and also are not believed to be newly synthesised in pollen tubes (Villette *et al.*, 2015; Rotsch *et al.*, 2017).

Regarding sphingolipid metabolism, a delta(8)-fatty-acid desaturase-like protein that shares 62 % sequence identity with the Arabidopsis SPHINGOID LONG CHAIN BASE DESATURASE 2 (SLD2) is two-fold downregulated on transcript level, while other homologues of this enzyme show upregulation (Table 7, Supplementary Dataset S19). The transcript of a putative sphingoid base hydroxylase 2 (SBH2) showed two-fold upregulation. Both, SBH2 and SLD2 have previously been reported to be highly expressed in Arabidopsis pollen, leading to a distict sphingolipid profile in Arabidopsis pollen that is high in glucosylceramides (GlcCers) and N-acetyl-glycosylated glycosylinositolphosphoceramides (GIPCs) (Luttgeharm *et al.*, 2015).

Differentially expressed genes among others suggest involvement of hormones and polyamines in heat stress adaptation

Some other interesting differentially expressed genes that have not been covered so far are highlighted in Table 8. The gene displaying the strongest up-regulation is annotated as “uncharacterised protein” in Tobacco and its closest Arabidopsis homologue, AT3G10020, is annotated as “plant/protein”. Publications suggest that it is a stress-responsive gene. Strongest downregulation was observed for a homologue of BON association protein 2 (BAP2), a reported inhibitor of programmed cell death (Yang *et al.*, 2007).

While auxins were already mentioned in the GO-terms, some other hormones might also play a role in heat stress adaptation of Tobacco pollen tubes. Strong upregulation was observed for a homologue of Arabidopsis JASMONATE-INDUCED OXYGENASE2 (JAO2), annotated as a protein with similarity to flavonol synthases and involved in the detoxification of polycyclic aromatic hydrocarbons (Hernández-Vega *et al.*, 2017). JASMONATE-ZIM-DOMAIN PROTEIN 8 (JAZ8) on the other hand was transcriptionally downregulated. Transcript of a putative homologue of BRI1-associated receptor kinase 1 (BAK1), a receptor-like kinase in brassinosteroid sensing, was downregulated under HS.

Also, an involvement of polyamines including spermine and spermidine in HS response, as has been reported (Fu *et al.*, 2019; Toumi *et al.*, 2019; Jing *et al.*, 2020; Zhou, R. *et al.*, 2020;), is reflected in the transcriptome. A putative SPERMINE SYNTHASE 3 (SPDS3) was more than 8-fold and a putative POLYAMINE OXIDASE 2 (PAO2) was 2-fold upregulated. PAO2 was recently shown to be involved in regulating excess spermidine contents in Arabidopsis seeds and seedlings (Takahashi *et al.*, 2019). Several other putative PAO1-4 homologues were detected and showed up- and down-regulation, however none had FC > 2. Also involved in polyamine metabolism is ARGININE DECARBOXYLASE 2 (ADC2), of which 4 putative Tobacco homologues were detected, 3 were differentially downregulated (and one log2FC of -0.977). ADCs catalyse the first and rate-limiting step in polyamine synthesis.

Table 8: Selection of other differentially expressed genes of interest

Tobacco Gene	Tobacco Protein	Arabidopsis Gene	Arabidopsis Protein	Putative Function	log_2FC	log_2CPM	FDR
LOC107766703	A0A1S3XM78	AT3G10020	unknown protein	plant/protein	12.07	3.38	0
LOC107778746	A0A1S3YRE7	AT5G05600	JAO2	2-oxoglutarate (2OG) and Fe(II)-dependent oxygenase superfamily protein	10.23	3.19	0
LOC107817403	A0A1S4CCK8	AT3G22370	AOX1a	alternative oxidase	9.05	0.41	9.24E-59
LOC107759427	A0A1S3WZ93	AT3G10020	unknown protein	plant/protein	7.89	2.57	2.52E-241
LOC107804414	A0A1S4B4D1	AT5G03370		acylphosphatase family	6.96	-1.40	2.73E-15
LOC107774730	A0A1S3YCX4	AT3G09640	APX2	ascorbate peroxidase	5.29	-1.31	3.20E-14
LOC107788327	A0A1S3ZM96	AT3G47520	MDH	malate dehydrogenase	4.07	-0.51	5.52E-20
LOC107795525	A0A1S4AAK3	AT1G14130	DAO1	2-oxoglutarate (2OG) and Fe(II)-dependent oxygenase superfamily protein	3.88	2.70	4.11E-184
LOC107801843	A0A1S4AVW8	AT5G47530		Auxin-responsive family protein	3.44	-0.79	2.59E-14
LOC107769851	A0A1S3XY09	AT3G21865	PEX22	peroxin	3.40	0.28	4.42E-27
LOC107764611	A0A1S3XFN6	AT5G53120	SPDS3	spermidine synthase	3.15	2.26	6.03E-95
LOC107808988	A0A1S4BJJ5	AT5G24240	ATPI4KGAMMA3	phosphatidylinositol 4-kinase gamma-like protein	2.97	3.59	1.35E-219
LOC107817192	A0A1S4CB63	AT4G27510		2-isopropylmalate synthase	2.36	-0.94	1.05E-07
LOC107762352	A0A1S3X8G8	AT1G49340	ATPI4KALPHA	Phosphatidylinositol 3- and 4-kinase family protein	2.36	1.92	7.99E-50
LOC107770164	A0A075EYT2	AT1G17710	PEPC1	phosphoethanolamine/phosphocholine phosphatase	2.34	3.66	1.55E-173
LOC107808981	A0A1S4BJF1	AT1G17710	PEPC1	phosphoethanolamine/phosphocholine phosphatase	2.00	5.00	9.42E-139
LOC107817132	A0A1S4CB76	AT1G17710	PEPC1	phosphoethanolamine/phosphocholine phosphatase	1.50	2.74	3.69E-38
LOC107799822	A0A1S4APJ5	AT2G43020	PAO2	polyamine oxidase	1.17	4.50	2.81E-72
LOC107768947	A0A1S3XUI8	AT1G65930	cICDH	cytosolic NADP+-dependent isocitrate dehydrogenase	-1.01	3.04	6.39E-13
LOC107828000	A0A1S4DBY9	AT2G28350	ARF10	auxin response factor	-1.46	0.28	1.39E-07
LOC107767522	A0A1S3XQ16	AT4G33430	BAK1	BRI1-associated receptor kinase	-1.47	-0.85	0.00091587
LOC107798522	T1WMC3	AT1G30135	JAZ8	jasmonate-zim-domain protein	-1.49	-0.40	0.00010296
LOC107759371	A0A1S3WYR7	AT4G34710	ADC2	arginine decarboxylase	-1.54	6.27	4.78E-241
LOC107819571	A0A1S4CJ33	AT1G02170	MC1	metacaspase	-2.00	-1.31	0.00123282
LOC107832546	A0A1S4DR37	AT5G25260	FLOT2	Flotillin	-2.07	-0.44	1.32E-06

LOC107820452	A0A1S4CLU4	AT1G02170	MC1	metacaspase	-2.57	1.00	7.54E-20
LOC107820447	A0A1S4CLX5	AT1G02170	MC1	metacaspase	-2.72	-0.41	1.84E-09
LOC107805149	A0A1S4B6Y7	AT5G04200	MC9	metacaspase	-2.86	-1.31	1.93E-06
LOC107824234	A0A1S4CZ94	AT2G19800	MIOX2	myo-inositol oxygenase	-2.89	-0.54	2.29E-09
LOC107773293	A0A1S3Y7Q9	AT2G19800	MIOX2	myo-inositol oxygenase	-3.17	0.20	1.86E-15
LOC107799833	A0A1S4APP9	AT2G45760	BAP2	BON association protein	-4.32	-0.46	7.69E-16

Selection of differentially expressed Tobacco genes (including the gene with the strongest up- and down-regulation, respectively), the annotated UniProt ID Tobacco protein name, the closest Arabidopsis homolog (gene name and protein name) and the assigned putative Tobacco protein function according to the Arabidopsis homology. Differential expression analysis was performed with EdgeR, log2 fold changes (log2FC), log2 counts per million (log_2CPM) and false discovery rates (FDR) are given.

Discussion

Tobacco pollen tube transcriptome shows expected but also unique adaptations to heat stress

As shown in several previous studies on plants, heat stress leads to a rapid and strong remodelling of the transcriptome (Kotak *et al.*, 2007; Mittal *et al.*, 2012; Rahmati Ishka *et al.*, 2018). One reaction conserved across pro- and eukaryotes is the upregulation of heat shock proteins (HSPs) (Jacob *et al.*, 2017). Accordingly, most transcripts strongly upregulated in response to heat stress encode HSPs in this study as well (Supplementary dataset S10). This upregulation has also been found to be a key response under heat stress in developing pollen, prior to pollen tube growth (Fragkostefanakis *et al.*, 2016; Keller *et al.*, 2018).

Other genes previously reported to be upregulated under heat stress show an increase in pollen tubes as well. These include genes encoding a homologue of ATFKBP62 (AT3G25230), which is known to mediate thermo-tolerance through interaction with a complex of HSP90.1 and the transcription factor HsfA2. Thereby ATFKBP62 sustains high levels of small HSPs (Meiri and Breiman, 2009). Another example is a homologue to the Bax inhibitor-1 family protein (AT1G03070) that is also upregulated under heat stress in vegetative tissues of Arabidopsis (Kilian *et al.*, 2007), where it might act as a ER-localized cell death repressor (Ishikawa *et al.*, 2011).

However, we also found differences between heat stress responses in Tobacco pollen tubes and vegetative tissues of Arabidopsis, as several heat-induced genes in Arabidopsis are expressed, but not upregulated upon heat stress in Tobacco pollen tubes. These include genes encoding for LATE EMBRYOGENESIS ABUNDANT (LEA) proteins, which protect other proteins and membranes especially during desiccation but are also upregulated by heat stress (Priya, Dhanker, *et al.*, 2019). Similarly, the HSF binding protein 1 (HSBP1), which is heat-induced, but a negative regulator of heat stress responses in Arabidopsis leaves (Hsu *et al.*, 2010), was present albeit not upregulated in Tobacco pollen tubes. Further examples are homologues of genes coding for the Arabidopsis serine protease PARK13/DEG14 (AT5G27660) (Basak *et al.*, 2014), the phytocystatin CYS5 (AT5G47550) (Song *et al.*, 2017), a putative inhibitor of cysteine proteases, or a temperature induced lipocalin (AT5G58070) (Chi *et al.*, 2009). All these proteins mediate thermotolerance and are upregulated during heat stress in Arabidopsis but not in the present study.

On the contrary, we found genes upregulated that have so far not been associated with heat stress. These include for example a Flotillin-like gene with homology to Arabidopsis FLOT2. Flotillins are involved in formation of membrane microdomains (Haney and Long, 2010; Li *et al.*, 2012). Moreover, Arabidopsis FLOT1 was shown to be involved in callose deposition upon bacterial infection, and it was suggested to play a role in different endocytotic processes, e.g. the regulation of respiratory burst oxidase homolog D (RbohD) activity through clathrin- and

microdomain-dependent endocytosis (Hao *et al.*, 2014; Daněk *et al.*, 2020). Medicago truncatula FLOT4 was shown to exclusively localise to tips of elongating root hairs upon inoculation with bacteria (Haney and Long, 2010). These data suggest, that Flotillins might also play an important role during pollen tube growth, maybe especially so under stress. The presence of sterol-rich membrane microdomains containing flotillin-like protein in rice pollen has recently been shown (Han *et al.*, 2018).

Another example is a Tobacco homologue of PEROXIN22 (PEX22), which to our knowledge has not been connected to heat stress so far. It was reported, however, that mutations in yeast PEX22 led to increased malate production and mislocalisation of a peroxisomal malate dehydrogenase to the cytosol (Negoro *et al.*, 2018). Interestingly, in pollen tubes, an increased transcript expression of a putative chloroplastic malate dehydrogenase (MDH) was observed and malate concentrations were significantly reduced by prolonged HS as compared to heat stress relieved pollen tubes, hinting at an involvement of malate in heat stress adaptation of pollen tubes.

Heat induced lipid remodelling is not controlled transcriptionally

The expression data shows no conclusive picture as to how the membrane lipid composition is altered. Nevertheless, several conclusions can be drawn from membrane lipid remodelling: Especially striking is the increase of the saturated acyl chains 16:0 and 18:0, while the ratio of monounsaturated and polyunsaturated acyl chains is not altered severely. This result suggests a regulation of fatty acid synthesis in the plastids, where it is determined if the acyl carrier protein (ACP)-connected acyl chains are initially elongated and desaturated. Only after elongation and desaturation from 16:0 to 18:1 the acyl chains can be precursors for further extraplastidial desaturation.

Arabidopsis and likely also other plant species harbour three types of ketoacylsynthases (KAS) with only one, KASII/FAB1, being responsible for the elongation of 16:0-ACP to 18:-ACP (Wu *et al.*, 1994; Pidkowich *et al.*, 2007). KASII/FAB1 would thus pose a good target for regulation. Regulation of the Δ9 desaturase OLE1 could be a further factor, as it introduces the first double bond to form 18:1. Thioesterases might also play a role, as knockout of FATB leads to a strong reduction of saturated acyl-chains (Bonaventure *et al.*, 2003), and knockdown of the two FATA genes also influences acyl-composition (Moreno-Pérez *et al.*, 2012).

One can speculate that the de novo synthesised fatty acids are even stronger saturated than reflected by the membrane lipid composition, as some acyl chains were probably already synthesised prior to heat stress. This would imply a rapid and strong adaptation of the above mentioned enzymes, likely through protein degradation, post-translational modification or a direct influence of temperature on the enzymatic activities. A transcriptional regulation is unlikely, as respective transcripts were little or not changed.

Role of PS and galactolipids in heat stress adaptation

Some lipid classes increase comparably stronger under heat stress. This is especially true for PS and DGDG. PS is found in the cytosolic leaflets of the plasma membrane and in endosomes and is negatively charged. It can form nanodomains in the plasma membrane that are important for Rho signalling (Platre *et al.*, 2019). These small G proteins have also been shown to be very important for the regulation of pollen tube growth (Scholz *et al.*, 2020), but it remains to be studied if they also depend on PS, how PS is distributed in the pollen tube, and if this distribution changes under heat stress.

PS is synthesized by just one enzyme in Arabidopsis, PHOSPHATIDYLSERINE SYNTHASE1 (PSS1). In Tobacco we found three homologues of PSS1, none of them is transcriptionally affected by heat stress. Due to its mode of synthesis, PS has to flip leaflet sides; AMINOPHOSPHOLIPID ATPASEs (ALAs) are flippases that have been shown to be able to flip PS in yeast (Noack and Jaillais, 2020). Although it does not explain increased PS levels, it is interesting to note that 6 putative homologues of ALA1 were detected, five of which were upregulated, two of them meeting the threshold for differential expression. Knockdown of ALA1 in Arabidopsis has been reported to render plants more sensitive to cold stress (Gomes *et al.*, 2000). On the other hand, 4 detected putative homologues of ALA3 were tendentially downregulated (not meeting the threshold for differential expression). Knockout of ALA3 in Arabidopsis did not only result in impaired pollen tube growth, but pollen fitness was further reduced under heat or cold stress (McDowell *et al.*, 2013). Moreover, ALA3 has recently been shown to be important for polar localisation of apical PS distribution in pollen tubes (Zhou, Y. *et al.*, 2020).

Galactolipids are the most abundant lipids of thylakoids and the effect of chloroplast galactolipids remodeling under temperature stress in Arabidopsis (Chen *et al.*, 2006; Higashi *et al.*, 2015) and tomato (Spicher *et al.*, 2016). In agreement with studies concerning other class of membranes lipids, the level of unsaturation in galactolipids is inversely correlated with growth temperature. Furthermore, heat acclimation at 38°C in wild-type Arabidopsis increases DGDG, DGDG to MGDG ratio and saturation level of DGDG lipid (Higashi *et al.*, 2015). Also, a role for galactolipids in acquired thermotolerance was already described in a study in 2006, when the authors did a mutant screen for plants defective in the acquisition of thermotolerance and found a mutant of DGD1 (Chen *et al.*, 2006). While pollen tubes contain plastids, these harbour no thylakoids (Staff *et al.*, 1989) and galactolipids in pollen tubes were discussed to be especially important in extraplastidial membranes, where they are also formed in phosphate-starved vegetative tissues (Härtel, *et al.* 2000). Evidence for the abundance of galactolipids in the male gametophyte comes from glycerolipid profiling of lily pollen tubes before and after elongation revealing a 5.7-fold increase in DGDG and a 2.8-fold increase in the MGDG levels (Nakamura *et al.*, 2009). The use of the MGDG synthase inhibitor

galvestine-1 developed by the team in Grenoble further highlighted an important role of galactolipids in pollen tube growth and the use of a specific antibody indicated a DGDG localization at the periphery of Arabidopsis pollen tubes most probably at the plasma membrane (Botté *et al.*, 2011). Also, the fact that galactolipids account for 11 % of all membrane forming glycerolipids in Tobacco pollen tubes (Müller and Ischebeck, 2017) speaks for their presence in extraplastidial membranes.

Transcript and lipidome suggest dynamic adaptations in LD-turnover and TAG metabolism

While transcripts involved in lipid metabolism were mostly unaffected by heat stress, transcripts coding for genes involved in TAG turnover and LD biology showed more dynamic adaptations to heat stress. Homologs of all 3 DGAT isoforms were found to be upregulated, so were different TAG lipases. Also, two oleosin-homologues were found to be differentially up- and down-regulated, respectively. A HSD5 homologue was even 125-fold up-regulated. These results indicate that LDs and the stored TAG reserves play an important role during heat stress adaptation.

An increase of TAG levels under heat stress has already been observed, e.g. in the algal species *Nannochloropsis oculata* (Converti *et al.*, 2009), *Ettlia oleoabundans* (Yang *et al.*, 2013), *Coccomyxa subellipsoidea* C169 (Allen *et al.*, 2018), or *Chlamydomonas reinhardtii* (Légeret *et al.*, 2016), but also in *Arabidopsis thaliana* leaves (Higashi *et al.*, 2015; Shiva *et al.*, 2020) and seedlings (Mueller *et al.*, 2015) or tomato fruits (Almeida *et al.*, 2020). In Arabidopsis seedlings, PHOSPHOLIPID:DIACYLGLYCEROL ACYLTRANSFERASE1 (PDAT1), an enzyme transferring a fatty acid from the acyl-CoA pool or from PC to DAG to yield TAG, is necessary for heat-induced TAG accumulation. Also, pdat1 mutant seedlings were more sensitive to heat-stress, indicating that PDAT1-mediated TAG accumulation mediates thermotolerance (Mueller *et al.*, 2017). In our screen, five putative PDAT1 homologues were identified and showed comparably high expressions, however their transcript abundance did not react strongly to heat stress. PDATs might already be so highly expressed in Tobacco pollen tubes that a further increase in transcript upon heat stress is not necessary to mediate thermotolerance. Also, in Tobacco pollen tubes no reduction of membrane lipids could be observed, including PC and PE which are the most abundant glycerolipids (Müller and Ischebeck, 2017). A study on *Chlamydomonas reinhardtii* observed that heat-stressed cells did not accumulate significantly higher amounts of total fatty acids, nor did total fatty acid profile change. However, more differentiated analyses of single lipid classes revealed increases in TAG levels at the expense of mainly MGDG, diacylglyceryl-O-4′-(N,N,N,-trimethyl)- homoserine (DGTS), PE and PG, suggesting a flux from different lipid classes into TAG. Moreover, a concomitant decrease in 18:3/16:4-MGDG and an increase in 18:3/16:4-DAG and 18:3/16:4/18:3-TAG was observed (Légeret *et al.*, 2016). Such an effect could not

be observed in the present study. In contrast, the average number of double bonds in TAG decreased from 1.68 to 1.38 after 6 h growth under heat stress. As of this, we speculate that the synthesis of saturated fatty acids is increased and FAs are then incorporated into membrane lipids. In parallel, there might be an increased, unspecific push of FAs released from membrane lipids into TAG that does not discriminate between acyl moieties.

Another interesting fact hinting at an involvement of not just TAG but LDs as organelles in heat stress adaptations is the 125-fold upregulation of a putative HSD5 homologue suggests involvements of LDs in heat stress adaptation beyond TAG accumulation. HSDs, also called steroleosins, are important for plant development and are involved in stress responses as well as wax metabolism (Li *et al.*, 2007; Zhang *et al.*, 2016; Shao *et al.*, 2019). Steroleosins are presumably involved in brassinosteroid metabolism (Li *et al.*, 2007) but were previously not found on LDs of Tobacco pollen tubes (Kretzschmar *et al.*, 2018). In this study only two transcripts with very low expression levels were detected at non-stressed conditions.

Metabolomic adaptations might facilitate thermotolerance

In previous studies on heat stressed shoot tissues of Arabidopsis (Kaplan *et al.*, 2004; Harsh *et al.*, 2016; Zinta *et al.*, 2018; Lawas *et al.*, 2019), it was found that different sugars accumulated, including glucose, fructose and in some cases sucrose. In Tobacco pollen tubes, the heat-induced accumulation of sugars was rather modest in comparison and the somewhat higher increase in sucrose has to be considered with care, as sucrose was also contained in the growth medium. Interestingly though, we found a strong increase in sedoheptulose, a seven carbon sugar normally occurring in its phosphorylated form in the Calvin-Benson cycle and the pentose phosphate pathway. It is unclear if this sugar has any protective function, but it was also found to highly accumulate in the alga Phaeodactylum tricornutum under nitrogen deprivation (Popko *et al.*, 2016).

In addition, an increase in free amino acids was observed in the above mentioned studies. Exceptions were methionine, β-alanine, aspartate and serine as well as glutamate and proline. Especially proline levels stay relatively stable upon heat stress and although it accumulates very strongly after 9 hours of pollen tube growth, it does so under normal as well as stress conditions. This is interesting, as proline was found to be clearly heat-inducible in studies on shoot tissues (Harsh *et al.*, 2016; Zinta *et al.*, 2018; Lawas *et al.*, 2019). However, a study on potato leaves showed that heat stress alone does not have significant influence on proline levels, neither in stress susceptible nor in resistant potato cultivars. In the study, proline only accumulated after drought or combined heat and drought stress (Demirel *et al.*, 2020). The same study observed an increase in lysine in one of the stress susceptible cultivars following heat stress It is possible that pipecolate, similar in structure to proline, plays a role in adaptation to heat in pollen tubes, as pipecolate was more heat-responsive than proline in the present

study. Pipecolate was also shown to strongly accumulate during Tobacco pollen development (Rotsch *et al.*, 2017) and it increases in shoot tissues upon pathogen infection (Ding *et al.*, 2016).

Glutamate amounts do not increase strongly and stay relatively stable from 6 to 9 hours of growth, without regard of heat stress. This indicates important roles for these two amino acids as likely their homeostasis is tightly controlled to keep up constant levels under heat stress. The glutamate derivative GABA has been reported to play an important role in sexual reproduction of angiosperms (Bouché *et al.*, 2003; Biancucci *et al.*, 2015; Domingos *et al.*, 2019; Lora *et al.*, 2019). It has long been known that GABA levels increase upon exposure to different abiotic stresses and reports on a role in biotic stress response accumulate, too (Tarkowski *et al.*, 2020).

Also, GABA and especially the GABA shunt pathway that bypasses two steps of the tricarboxylic acid (TCA)-cycle have been linked to heat tolerance (Ludewig *et al.*, 2008; Cao *et al.*, 2013; Li *et al.*, 2016; Yu *et al.*, 2017; Priya *et al.*, 2019). Although GABA showed a tendency of increased accumulation upon heat stress, this increase was not significant. 2-Oxoglutarate (2-OG, also α-ketoglutarate) a glutamate and thereby GABA precursor showed strong accumulation after 3 hours of heat stress.

Other factors influencing heat adaptation

Another part of the heat stress response could be alternative splicing, as 12 of 159 genes in the GO-term “involved in RNA splicing” were differentially upregulated as well as 7 of 20 in “has pre-mRNA 3'-splice site binding”. Alternative splicing has been observed in tomato pollen under heat stress (Keller *et al.*, 2017) and the alternative splicing of the transcription factor HsfA2 from tomato has been previously shown to be an important factor for thermotolerance (Hu *et al.*, 2020).

Important for the abundance of proteins is not only their transcription and translation rates but also the rate of their degradation via autophagy or the ubiquitin-proteasome pathway. Alterations here are indicated by strong changes in the GO terms “involved in positive regulation of autophagy”, “involved in endoplasmic reticulum unfolded protein response” (49 genes, 10 up), “involved in protein ubiquitination” (582, 50 up, 20 down), and “involved in ubiquitin-dependent protein catabolic process” (425, 26, 14). Apart from degrading proteins to adapt the proteome to the elevated temperatures, these proteins could also be involved in the degradation of an increased number of misfolded proteins.

Conclusion

Since adaptation to heat stress is a complex and multi-layered trait that requires intricate interplay of different cellular processes, no conclusive picture as to how thermotolerance of Tobacco pollen tubes is mediated can be drawn. A rapid lipid remodelling that is not controlled transcriptionally is equally as important as metabolomic adaptations and transcriptional changes. However, the present study with its different large datasets poses a useful mean for datamining.

Materials and Methods

Plant material and growth conditions

Tobacco (*Nicotiana tabacum* L. cv. Samsun-NN) plants were grown in the greenhouse as previously described (Rotsch *et al.*, 2017): plants were kept under 14 h of light from mercury-vapor lamps in addition to sunlight with light intensities of 150 – 300 µmol m^{-2} sec^{-1} at flowers and 50 – 100 µmol m^{-2} sec^{-1} at mid-height leaves. Temperature was set to 16 °C at night and 21 °C during the day with a relative humidity of 57–68 %.

Anthers were harvested from flower buds right before anthesis and dried at room temperature for up to four days before pollen from the anthers was collected by sieving. Pollen were weighed and rehydrated for 10 minutes in liquid pollen tube medium (5 % w/v sucrose, 12.5 % w/v PEG-4000, 15 mM MES-KOH pH 5.9, 1 mM CaCl2,1 mM KCl, 0.8 mM MgSO4, 0.01 % H3BO3 v/v, 30 µM CuSO4, modified from (Read *et al.*, 1993). The indicated amounts were spread onto cellophane foil (Max Bringmann KG) and placed on 50 ml of solid pollen tube medium (2 % Agarose w/v, 5 % sucrose w/v, 6 % PEG-4000 w/v, 15 mM MES-KOH pH 5.9, 1 mM CaCl2,1 mM KCl, 0.8 mM MgSO4, 0.01 % H3BO3 v/v, 30 µM CuSO4) inside square petri dishes (120 mm x 120 mm x 17 mm with vents, Greiner Bio-One), sealed with MicroporeTM (3M). All pollen tubes were grown for 3 hours at room temperature (RT). Control pollen tubes were kept at RT for another 3 hours, while heat stressed (HS) pollen tubes were transferred to 37 °C for 3 hours. For stress relief, pollen tubes were then transferred to RT again for the next 3 hours, while non-relieved pollen tubes remained at 37 °C.

RNA extraction, library preparation, and sequencing

Total RNA was extracted from 200 mg of pollen tubes using Spectrum™ Plant Total RNA Kit (Sigma-Aldrich, St. Louis, Missouri, USA). RNA-seq libraries were performed using the non-stranded mRNA Kit from Illumina (Cat. N°RS-122-2001). Quality and integrity of RNA was assessed with the Fragment Analyzer from Advanced Analytical by using the standard sensitivity RNA Analysis Kit (DNF-471). All samples selected for sequencing exhibited an RNA

integrity number over 8. After library generation, for accurate quantitation of cDNA libraries, the fluorometric based system QuantiFluor™dsDNA (Promega) was used. The size of final cDNA libraries was determined using the dsDNA 905 Reagent Kit (Fragment Analyzer, Advanced Bioanalytical) exhibiting a sizing of 300 bp in average. Libraries were pooled and sequenced on an Illumina HiSeq 4000 (Illumina), generating 50 bp single-end reads (30-40 Mio reads/sample).

Raw read and quality check

Sequence images were transformed with Illumina software BaseCaller to BCL files, which was demultiplexed to fastq files using bcl2fastq 2.17.1.14. The sequencing quality was asserted using FastQC (version 0.11.5) (Andrews, 2010: FastQC: A quality control tool for high throughput sequence data. babraham Bioinforma: http://www.bioinformatics.babraham.ac.uk/projects/).

Mapping and normalisation

Samples were aligned to the reference genome *Nicotiana tabacum* (Ntab version TN90, https://www.ncbi.nlm.nih.gov/assembly/GCF_000715135.1/) using the STAR aligner (version 2.5.2a) (Dobin *et al.*, 2013) allowing for 2 mismatches within 50 bases. Subsequently, reads were quantified for all Ntab version TN90 genes in each sample using featureCounts (version 1.5.0-p1) (Liao *et al.*, 2014).

Differential gene expression analysis

Read counts were analysed in the R/Bioconductor environment (Release 3.10, www.bioconductor.org) using edgeR package (version 3.28.1) (Robinson *et al.*, 2009; McCarthy *et al.*, 2012) gene names were translated to UniProt protein identifiers. For more detailed functional analyses, these Tobacco proteins were blasted against the TAIR 10 Arabidopsis protein library (TAIR10, https://www.arabidopsis.org/download_files/Proteins/TAIR10_protein_lists/TAIR10_pep_20101214) using Protein-Protein BLAST 2.5.0+ with a maximum target sequence of 1. Only those hits with an Expect value (E-value, describes amount of hits to be expected by chance for the respective database size) < 10^{-5} were considered. The obtained Arabidopsis AGI-codes were then assigned GO-terms for GO-term analysis The GO term annotations were obtained from the The Arabidopsis Information Resource (www.arabidopsis.org) in a version updated on 1.1.2020.

To analyse genes with a putative involvement in lipid metabolism, a compiled list of lipid genes was generated using the The Arabidopsis Acyl-Lipid Metabolism Website (Li-Beisson *et al.*, 2013), KEGG pathway (https://www.genome.jp/kegg/pathway.html, latest update 10th March

2020), and genes from Kretzschmar *et al.*, 2020, Kelly and Feussner, 2016 and Luttgeharm *et al.*, 2016.

Lipid extraction and fatty acid methyl esterification

For analyses by gas chromatography flame ionisation detection (GC-FID), total lipids from pollen tubes grown from 20 mg of dry pollen were extracted by methyl-tert-butyl ether (MTBE) extraction (modified from Matyash *et al.*, 2008). Pollen tubes were harvested into 2 mL of pre-heated isopropanol (75 °C) and kept at 75 °C for 5 – 10 minutes. 0.05 mg Tri-17:0-Triacylglycerol (Sigma-Aldrich, St. Louis, Missouri, USA) in 50 µL chloroform as internal standard for absolute quantification was directly added to the isopropanol. Isopropanol was transferred to a new vial and evaporated under N2-stream, the pollen tubes were covered with 2 mL of MTBE/methanol (3:1, v/v). Pollen tube tissue was disrupted with a spatula, vortexed and then shaken at 4 °C for one hour. After 5 minutes of centrifugation at 1000 x g, the supernatant was transferred to the vial with the evaporated isopropanol and 1 mL of 0.9 % (w/v) NaOH was added. Samples were vortexed and centrifuged again before the upper phase was transferred to a new vial. Solvent was evaporated under N_2-stream and samples dissolved in 250 µL chloroform/methanol/water 65:56:8 (v/v/v).

The total lipids were then separated by thin layer chromatography (TLC). 80 µL of the dissolved samples were spotted with a TLC spotter to TLC plates (TLC Silica gel 60, Merck KGaA). For extraction of TAGs, plates were run in hexane/diethylether/acetic acid 80:20:1 (v/v/v). The bands comigrating with the TAG-standard were scratched out. To obtain fatty acid methyl esters (FAMEs), samples were then subjected to 1 mL FAME reagent (2.5 % v/v H2SO4, 2 % v/v Dimethoxypropane in Methanol/Toluol 2:1, v/v) (Miquel and Browse, 1992) and under constant shaking incubated at 80 °C in a water bath for one hour. The reaction was stopped by adding 1 mL of saturated NaCl-solution and vortexing. FAMEs were then extracted adding 1 mL of hexane, centrifuging 10 minutes at 2,000 x g and transferring the upper phase to a new vial. Hexane was evaporated and samples resuspended in 25 µL of acetonitrile for subsequent GC-FID analysis.

For lipidomic analyses by liquid chromatography mass spectrometry (LC-MS), samples were extracted according to Grillitsch et al., 2014 with minor modifications. Briefly, pollen tubes grown from 20 mg of dry pollen were extracted. They were first lyophilised and ground with a bead mill and resuspended in isopropanol/hexane/water (60:26:14 v/v/v) and incubated at 60 °C for 30 min. After centrifugation at 635 x g for 20 min, the supernatant was dried under nitrogen stream and dissolved in tetrahydrofuran/methanol/water (4:4:1, v/v/v).

Central metabolite and sterol extraction and derivatisation

Primary metabolite and sterol extraction were performed as previously described (Rotsch *et al.*, 2017). Per time point, pollen tubes grown from 5 mg of pollen were harvested and freeze-dried overnight. After tissue disruption, 500 µL extraction solution ($MeOH/ChCl_3/H_2O$ 32.25:12.5:6.25, v/v/v) were added per sample, vortexed and incubated for 30 minutes at 4 °C under constant shaking. Supernatant was transferred to a new tube and pollen tubes were extracted again with another 500 µL of extraction solution. Incubation was repeated and supernatants combined. 0.0125 mg allo-inositol in 0.5 ml H_2O were added, incubated again at 4 °C for 30 minutes, centrifuged 5 minutes at full speed and the aqueous phase containing the metabolites was transferred. 20 µL were evaporated under N_2 and used for derivatisation with 15 µL of methoxyamine hydrochloride in pyridine (30 mg/mL) overnight at room temperature. Derivatisation with 30 µL N-methyl-N-(trimethylsilyl) trifluoroacetamide (MSTFA) followed for at least 1 h to obtain methoxyimino (MEOX)- and trimethylsilyl (TMS)-derivatives of the metabolites (Bellaire *et al.*, 2014).

For the analysis of sterols, 2 ml of MTBE/MeOH 3:1 (v/v) and 1 ml of 0.9% NaCl were added to 200 µl of the organic phase (200 µL) and evaporated under N_2-stream. Samples were dissolved in 20 µL pyridine, 10 µl of which were used for MSTFA-derivatisation with 10 µL of MSTFA 1-6 h prior to analysis.

GC-FID and GC-MS

GC-FID analysis of fatty acid methyl esters was performed as described in (Hornung *et al.*, 2002): an Agilent GC 6890 system (Agilent, Waldbronn, Germany) coupled with an FID detector equipped with a capillary HP INNOWAX column (30 m × 0.32 mm, 0.5 µm coating thickness, Agilent, Waldbronn, Germany) was used. Helium served as carrier gas (30 cm s^{-1}), with an injector temperature of 220 °C. The temperature gradient was 150 °C for 1 min, 150 – 200 °C at 15 °C min^{-1}, 200–250 °C at 2 °C min^{-1}, and 250 °C for 10 min.

For quantification, peak integrals were determined using Agilent ChemStation for LC 3D systems (Rev. B.04.03) and used to calculate absolute amounts of TAG as well as relative fatty acid contributions.

For the measurement of central metabolites and sterols, GC-MS measurements were performed as previously described in Touraine *et al.* 2019 for metabolites and Rotsch *et al.* 2017 for sterols. If the metabolites were not identified by an external standard, the spectra were identified with the Golm metabolome database (GMD) and the National Institute of Standards and Technology (NIST) spectral library 2.0f. The chemical information on metabolites identified with the GMD can be obtained at http://gmd.mpimp-golm.mpg.de/search.aspx (Kopka *et al.*, 2005). Due to the high levels, sucrose was measured in separate runs using only one-tenth of the sample as used for the regular runs.

Data was analysed using MSD ChemStation (F.01.03.2357). Masses used for quantification are depicted in Supplementary Dataset S7.

LC-MS

Lipids were analyzed using an UPLC-nano ESI-MS/MS system equipped with a 6500 QTRAP® tandem mass spectrometer (AB Sciex, Framingham, MA, USA) and data were processed as previously described (Tarazona et al., 2015). Data of the molecular lipid species are shown as relative peak area (in %), where the peak areas of all lipid species from each lipid class per sample were summarized to 100 %.

Statistical analyses

Statistical analyses were performed as indicated for the respective experiments.

For multiple comparisons, ANOVA was performed, followed by Post-hoc Tukey analysis. Results are presented as compact letter display of all pair-wise comparisons in increasing order, either in the diagram or as a separate table.

Unpaired two-sample t-tests were performed if just two means were compared. Results are presented as * ($p < 0.05$), ** ($p < 0.01$) and *** ($p < 0.005$).

References

Allen, J.W., Tevatia, R., Demirel, Y., DiRusso, C.C. and Black, P.N. (2018) Induction of oil accumulation by heat stress is metabolically distinct from N stress in the green microalgae *Coccomyxa subellipsoidea* C169. *PLoS One*, **13**, 1–20.

Almeida, J., Perez-Fons, L. and Fraser, P.D. (2020) A transcriptomic, metabolomic and cellular approach to the physiological adaptation of tomato fruit to high temperature. *Plant. Cell Environ.*, pce.13854.

Basak, I., Pal, R., Patil, K.S., et al. (2014) Arabidopsis AtPARK13, which confers thermotolerance, targets misfolded proteins. *J. Biol. Chem.*, **289**, 14458–14469.

Beck, J.G., Mathieu, D., Loudet, C., Buchoux, S. and Dufourc, E.J. (2007) Plant sterols in "rafts": a better way to regulate membrane thermal shocks. *FASEB J.*, **21**, 1714–1723.

Bellaire, A., Ischebeck, T., Staedler, Y., Weinhaeuser, I., Mair, A., Parameswaran, S., Ito, T., Schönenberger, J. and Weckwerth, W. (2014) Metabolism and development - integration of micro computed tomography data and metabolite profiling reveals metabolic reprogramming from floral initiation to silique development. *New Phytol.*, **202**, 322–335.

Biancucci, M., Mattioli, R., Forlani, G., Funck, D., Costantino, P. and Trovato, M. (2015) Role of proline and GABA in sexual reproduction of angiosperms. *Front. Plant Sci.*, **6**, 1–11.

Boavida, L.C. and McCormick, S. (2007) Temperature as a determinant factor for increased and reproducible *in vitro* pollen germination in *Arabidopsis thaliana*. *Plant J.*, **52**, 570–582.

Bonaventure, G., Salas, J.J., Pollard, M.R. and Ohlrogge, J.B. (2003) Disruption of the FATB gene in Arabidopsis demonstrates an essential role of saturated fatty acids in plant growth. *Plant Cell*, **15**, 1020–1033.

Botté, C.Y., Deligny, M., Roccia, A., et al. (2011) Chemical inhibitors of monogalactosyldiacylglycerol synthases in *Arabidopsis thaliana*. *Nat. Chem. Biol.*, **7**, 834–842.

Bouché, N., Fait, A., Bouchez, D., Møller, S.G. and Fromm, H. (2003) Mitochondrial succinic-semialdehyde dehydrogenase of the γ-aminobutyrate shunt is required to restrict levels of reactive oxygen intermediates in plants. *Proc. Natl. Acad. Sci. U. S. A.*, **100**, 6843–6848.

Cao, J., Barbosa, J.M., Singh, N.K. and Locy, R.D. (2013) GABA shunt mediates thermotolerance in *Saccharomyces cerevisiae* by reducing reactive oxygen production. *Yeast*, **30**, 129–144.

Chen, J., Burke, J.J., Xin, Z., Xu, C. and Velten, J. (2006) Characterization of the Arabidopsis thermosensitive mutant atts02 reveals an important role for galactolipids in thermotolerance. *Plant, Cell Environ.*, **29**, 1437–1448.

Chi, W.T., Fung, R.W.M., Liu, H.C., Hsu, C.C. and Charng, Y.Y. (2009) Temperature-induced lipocalin is required for basal and acquired thermotolerance in Arabidopsis. *Plant, Cell Environ.*, **32**, 917–927.

Christenhusz, M.J.M. and Byng, J.W. (2016) The number of known plants species in the world and its annual increase. *Phytotaxa*, **261**, 201–217.

Coast, O., Murdoch, A.J., Ellis, R.H., Hay, F.R. and Jagadish, K.S.V. (2016) Resilience of rice (*Oryza spp*.) pollen germination and tube growth to temperature stress. *Plant Cell Environ.*, **39**, 26–37.

Converti, A., Casazza, A.A., Ortiz, E.Y., Perego, P. and Borghi, M. Del (2009) Effect of temperature and nitrogen concentration on the growth and lipid content of *Nannochloropsis oculata* and *Chlorella vulgaris* for biodiesel production. *Chem. Eng. Process. Process Intensif.*, **48**, 1146–1151.

Daněk, M., Angelini, J., Malínská, K., et al. (2020) Cell wall contributes to the stability of plasma membrane nanodomain organization of *Arabidopsis thaliana* FLOTILLIN2 and HYPERSENSITIVE INDUCED REACTION1 proteins. *Plant J.*, **101**, 619–636.

Demirel, U., Morris, W.L., Ducreux, L.J.M., et al. (2020) Physiological, biochemical, and transcriptional responses to single and combined abiotic stress in stress-tolerant and stress-sensitive potato genotypes. *Front. Plant Sci.*, **11**, 1–21.

Deruyffelaere, C., Purkrtova, Z., Bouchez, I., Collet, B., Cacas, J.L., Chardot, T., Gallois, J.L. and D'Andrea, S. (2018) PUX10 IS A CDC48A adaptor protein that regulates the extraction of ubiquitinated oleosins from seed lipid droplets in Arabidopsis. *Plant Cell*, **30**, 2116–2136.

Ding, P., Rekhter, D., Ding, Y., et al. (2016) Characterization of a pipecolic acid biosynthesis pathway required for systemic acquired resistance. *Plant Cell*, **28**, 2603–2615.

Dobin, A., Davis, C.A., Schlesinger, F., Drenkow, J., Zaleski, C., Jha, S., Batut, P., Chaisson, M. and Gingeras, T.R. (2013) STAR: Ultrafast universal RNA-seq aligner. *Bioinformatics*, **29**, 15–21.

Domingos, P., Dias, P.N., Tavares, B., Portes, M.T., Wudick, M.M., Konrad, K.R., Gilliham, M., Bicho, A. and Feijó, J.A. (2019) Molecular and electrophysiological characterization of anion transport in *Arabidopsis thaliana* pollen reveals regulatory roles for pH, Ca^{2+} and GABA. *New Phytol.*, **223**, 1353–1371.

Edwards, K.D., Fernandez-Pozo, N., Drake-Stowe, K., et al. (2017) A reference genome for *Nicotiana tabacum* enables map-based cloning of homeologous loci implicated in nitrogen utilization efficiency. *BMC Genomics*, **18**, 1–14.

Flores-Rentería, L., Whipple, A. V., Benally, G.J., Patterson, A., Canyon, B. and Gehring, C.A. (2018) Higher temperature at lower elevation sites fails to promote acclimation or adaptation to heat stress during pollen germination. *Front. Plant Sci.*, **9**, 1–14.

Fragkostefanakis, S., Mesihovic, A., Hu, Y. and Schleiff, E. (2016) Unfolded protein response in pollen development and heat stress tolerance. *Plant Reprod.*, **29**, 81–91.

Fu, Y., Gu, Q., Dong, Q., Zhang, Z., Lin, C., Hu, W., Pan, R., Guan, Y. and Hu, J. (2019) Spermidine enhances heat tolerance of rice seeds by modulating endogenous starch and polyamine metabolism. *Molecules*, **24**.

Ghosh, A.K., Chauhan, N., Rajakumari, S., Daum, G. and Rajasekharan, R. (2009) At4g24160, a soluble acyl-Coenzyme A-dependent lysophosphatidic acid acyltransferase. *Plant Physiol.*, **151**, 869–881.

Gomes, E., Jakobsen, M.K., Axelsen, K.B., Geisler, M. and Palmgren, M.G. (2000) Chilling tolerance in Arabidopsis involves ALA1, a member of a new family of putative aminophospholipid translocases. *Plant Cell*, **12**, 2441.

Grillitsch, K., Tarazona, P., Klug, L., Wriessnegger, T., Zellnig, G., Leitner, E., Feussner, I. and Daum, G. (2014) Isolation and characterization of the plasma membrane from the yeast *Pichia pastoris*. *Biochim. Biophys. Acta - Biomembr.*, **1838**, 1889–1897.

Han, B., Yang, N., Pu, H. and Wang, T. (2018) Quantitative proteomics and cytology of rice pollen sterol-rich membrane domains reveals pre-established cell polarity cues in mature pollen. *J. Proteome Res.*, **17**, 1532–1546.

Haney, C.H. and Long, S.R. (2010) Plant flotillins are required for infection by nitrogen-fixing bacteria. *Proc. Natl. Acad. Sci. U. S. A.*, **107**, 478–483.

Hao, H., Fan, L., Chen, T., Li, R., Li, X., He, Q., Botella, M.A. and Lin, J. (2014) Clathrin and membrane microdomains cooperatively regulate RbohD dynamics and activity in Arabidopsis. *Plant Cell*, **26**, 1729–1745.

Harsh, A., Sharma, Y.K., Joshi, U., Rampuria, S., Singh, G., Kumar, S. and Sharma, R. (2016) Effect of short-term heat stress on total sugars, proline and some antioxidant enzymes in moth bean (*Vigna aconitifolia*). *Ann. Agric. Sci.*, **61**, 57–64.

Härtel, H., Dörmann, P. and Benning, C. (2000) DGD1-independent biosynthesis of extraplastidic galactolipids after phosphate deprivation in Arabidopsis. *Proc. Natl. Acad. Sci. U. S. A.*, **97**, 10649–10654.

Hedhly, A. (2011) Sensitivity of flowering plant gametophytes to temperature fluctuations. *Environ. Exp. Bot.*, **74**, 9–16.

Hernández-Vega, J.C., Cady, B., Kayanja, G., et al. (2017) Detoxification of polycyclic aromatic hydrocarbons (PAHs) in *Arabidopsis thaliana* involves a putative flavonol synthase. *J Hazard Mater*, **176**, 139–148.

Higashi, Y., Okazaki, Y., Myouga, F., Shinozaki, K. and Saito, K. (2015) Landscape of the lipidome and transcriptome under heat stress in *Arabidopsis thaliana*. *Sci. Rep.*, **5**, 1–7.

Higashi, Y. and Saito, K. (2019) Lipidomic studies of membrane glycerolipids in plant leaves under heat stress. *Prog. Lipid Res.*, **75**, 100990.

Hornung, E., Pernstich, C. and Feussner, I. (2002) Formation of conjugated Δ11 Δ13-double bonds by Δ12-linoleic acid (1,4)-acyl-lipid-desaturase in pomegranate seeds. *Eur. J. Biochem.*, **269**, 4852–4859.

Hsu, S.F., Lai, H.C. and Jinn, T.L. (2010) Cytosol-localized heat shock factor-binding protein, AtHSBP, functions as a negative regulator of heat shock response by translocation to the nucleus and is required for seed development in Arabidopsis. *Plant Physiol.*, **153**, 773–784.

Hu, Y., Mesihovic, A., Jiménez-Gómez, J.M., et al. (2020) Natural variation in HsfA2 pre-mRNA splicing is associated with changes in thermotolerance during tomato domestication. *New Phytol.*, **225**, 1297–1310.

Ischebeck, T. (2016) Lipids in pollen - They are different. *Biochim. Biophys. Acta - Mol. Cell Biol. Lipids*, **1861**, 1315–1328.

Ischebeck, T., Valledor, L., Lyon, D., Gingl, S., Nagler, M., Meijón, M., Egelhofer, V. and Weckwerth, W. (2014) Comprehensive cell-specific protein analysis in early and late pollen development from diploid microsporocytes to pollen tube growth. *Mol. Cell. Proteomics*, **13**, 295–310.

Ishikawa, T., Watanabe, N., Nagano, M., Kawai-Yamada, M. and Lam, E. (2011) Bax inhibitor-1: A highly conserved endoplasmic reticulum-resident cell death suppressor. *Cell Death Differ.*, **18**, 1271–1278.

Jacob, P., Hirt, H. and Bendahmane, A. (2017) The heat-shock protein/chaperone network and multiple stress resistance. *Plant Biotechnol. J.*, **15**, 405–414.

James, C.N., Horn, P.J., Case, C.R., Gidda, S.K., Zhang, D., Mullen, R.T., Dyer, J.M., Anderson, R.G.W. and Chapman, K.D. (2010) Disruption of the Arabidopsis CGI-58 homologue produces Chanarin-Dorfman-like lipid droplet accumulation in plants. *Proc. Natl. Acad. Sci. U. S. A.*, **107**, 17833–17838.

Jing, J., Guo, S., Li, Y. and Li, W. (2020) The alleviating effect of exogenous polyamines on heat stress susceptibility of different heat resistant wheat (*Triticum aestivum* L.) varieties. *Sci. Rep.*, **10**, 1–12.

K, S. and E., I. (1997) Functional rafts in cell membranes. *Nature*, **387**, 569–572.

Kaplan, F., Kopka, J., Haskell, D.W., et al. (2004) Exploring the temperature-stress metabolome. *Plant Physiol.*, **136**, 4159–4168.

Karapanos, I.C., Akoumianakis, K.A., Olympios, C.M. and Passam, H.C. (2010) Tomato pollen respiration in relation to *in vitro* germination and pollen tube growth under favourable and stress-inducing temperatures. *Sex. Plant Reprod.*, **23**, 219–224.

Keller, M., Hu, Y., Mesihovic, A., Fragkostefanakis, S., Schleiff, E. and Simm, S. (2017) Alternative splicing in tomato pollen in response to heat stress. *DNA Res.*, **24**, 205–217.

Keller, M., Simm, S., Bokszczanin, K.L., et al. (2018) The coupling of transcriptome and proteome adaptation during development and heat stress response of tomato pollen. *BMC Genomics*, **19**, 1–20.

Kelly, A. a. and Feussner, I. (2016) Oil is on the agenda: Lipid turnover in higher plants. *Biochim. Biophys. Acta - Mol. Cell Biol. Lipids*, **1861**, 1253–1268.

Kilian, J., Whitehead, D., Horak, J., et al. (2007) The AtGenExpress global stress expression data set: Protocols, evaluation and model data analysis of UV-B light, drought and cold stress responses. *Plant J.*, **50**, 347–363.

Kim, E.Y., Seo, Y.S. and Kim, W.T. (2011) AtDSEL, an Arabidopsis cytosolic DAD1-like acylhydrolase, is involved in negative regulation of storage oil mobilization during seedling establishment. *J. Plant Physiol.*, 3–7.

Kopka, J., Schauer, N., Krueger, S., et al. (2005) GMD@CSB.DB: The Golm metabolome database. *Bioinformatics*, **21**, 1635–1638.

Kotak, S., Larkindale, J., Lee, U., Koskull-Döring, P. von, Vierling, E. and Scharf, K.-D. (2007) Complexity of the heat stress response in plants. *Curr. Opin. Plant Biol.*, **10**, 310–316.

Kretzschmar, F.K., Doner, N.M., Krawczyk, H.E., Scholz, P., Schmitt, K., Valerius, O., Braus, G.H., Mullen, R.T. and Ischebeck, T. (2020) Identification of low-abundance lipid droplet proteins in seeds and seedlings. *Plant Physiol.*, **182**, 1326–1345.

Kretzschmar, F.K., Mengel, L.A., Müller, A.O., Schmitt, K., Blersch, K.F., Valerius, O., Braus, G.H. and Ischebeck, T. (2018) PUX10 Is a lipid droplet-localized scaffold protein that interacts with CELL DIVISION CYCLE48 and is involved in the degradation of lipid droplet proteins. *Plant Cell*, **30**, 2137–2160.

Lawas, L.M.F., Li, X., Erban, A., Kopka, J., Jagadish, S.V.K., Zuther, E. and Hincha, D.K. (2019) Metabolic responses of rice cultivars with different tolerance to combined drought and heat stress under field conditions. *Gigascience*, **8**, 1–21.

Légeret, B., Schulz-Raffelt, M., Nguyen, H.M., Auroy, P., Beisson, F., Peltier, G., Blanc, G. and Li-Beisson, Y. (2016) Lipidomic and transcriptomic analyses of *Chlamydomonas reinhardtii* under heat stress unveil a direct route for the conversion of membrane lipids into storage lipids. *Plant Cell Environ.,* **39**, 834–847.

Li-Beisson, Y., Shorrosh, B., Beisson, F., et al. (2013) Acyl-Lipid Metabolism. *Arab. B.*, **11**.

Li, F., Asami, T., Wu, X., Tsang, E.W.T. and Cutler, A.J. (2007) A putative hydroxysteroid dehydrogenase involved in regulating plant growth and development. *Plant Physiol.*, **145**, 87–97.

Li, R., Liu, P., Wan, Y., et al. (2012) A membrane microdomain-associated protein, Arabidopsis Flot1, is involved in a clathrin-independent endocytic pathway and is required for seedling development. *Plant Cell*, **24**, 2105–2122.

Li, Z., Yu, J., Peng, Y. and Huang, B. (2016) Metabolic pathways regulated by γ-aminobutyric acid (GABA) contributing to heat tolerance in creeping bentgrass (*Agrostis stolonifera*). *Sci. Rep.*, **6**, 1–16.

Liao, Y., Smyth, G.K. and Shi, W. (2014) FeatureCounts: An efficient general purpose program for assigning sequence reads to genomic features. *Bioinformatics*, **30**, 923–930.

Lora, J., Laux, T. and Hormaza, J.I. (2019) The role of the integuments in pollen tube guidance in flowering plants. *New Phytol.*, **221**, 1074–1089.

Ludewig, F., Hüser, A., Fromm, H., Beauclair, L. and Bouché, N. (2008) Mutants of GABA transaminase (POP2) suppress the severe phenotype of succinic semialdehyde dehydrogenase (ssadh) mutants in arabidopsis. *PLoS One*, **3**.

Luria, G., Rutley, N., Lazar, I., Harper, J.F. and Miller, G. (2019) Direct analysis of pollen fitness by flow cytometry: implications for pollen response to stress. *Plant J.*, **98**, 942–952.

Luttgeharm, Kyle D Kimberlin, A.N. and Cahoon, E.B. (2016) Plant sphingolipid metabolism and function. In Y. Nakamura and Y. Li-Beisson, eds. *Lipids in Plant and Algae Development*. Springer International Publishing, pp. 249–286.

Luttgeharm, K.D., Kimberlin, A.N., Cahoon, R.E., Cerny, R.L., Napier, J. a., Markham, J.E. and Cahoon, E.B. (2015) Sphingolipid metabolism is strikingly different between pollen and leaf in Arabidopsis as revealed by compositional and gene expression profiling. *Phytochemistry*, **115**, 121–129.

Mascarenshas, J.P. (1993) Molecular Mechanisms of Pollen Tube Growth and Differentiation. *Plant Cell*, **5**, 1303–1314.

Matyash, V., Liebisch, G., Kurzchalia, T. V., Shevchenko, A. and Schwudke, D. (2008) Lipid extraction by methyl-terf-butyl ether for high-throughput lipidomics. *J. Lipid Res.*, **49**, 1137–1146.

McCarthy, D.J., Chen, Y. and Smyth, G.K. (2012) Differential expression analysis of multifactor RNA-Seq experiments with respect to biological variation. *Nucleic Acids Res.*, **40**, 4288–4297.

McDowell, S.C., López-Marqués, R.L., Poulsen, L.R., Palmgren, M.G. and Harper, J.F. (2013) Loss of the *Arabidopsis thaliana* P4-ATPase ALA3 reduces adaptability to temperature stresses and impairs vegetative, pollen, and ovule development. *PLoS One*, **8**, 1–11.

Meiri, D. and Breiman, A. (2009) Arabidopsis ROF1 (FKBP62) modulates thermotolerance by interacting with HSP90.1 and affecting the accumulation of HsfA2-regulated sHSPs. *Plant J.*, **59**, 387–399.

Miquel, M. and Browse, J. (1992) Arabidopsis mutants deficient in polyunsaturated fatty acid synthesis: Biochemical and genetic characterization of a plant oleoyl-phosphatidylcholine desaturase. *J. Biol. Chem*., **267**, 1502–1509**.**

Mittal, D., Madhyastha, D.A. and Grover, A. (2012) Genome-wide transcriptional profiles during temperature and oxidative stress reveal coordinated expression patterns and overlapping regulons in rice. *PLoS One*, **7**.

Moreno-Pérez, A.J., Venegas-Calerón, M., Vaistij, F.E., Salas, J.J., Larson, T.R., Garcés, R., Graham, I.A. and Martínez-Force, E. (2012) Reduced expression of FatA thioesterases in Arabidopsis affects the oil content and fatty acid composition of the seeds. *Planta*, **235**, 629–639.

Mueller, S.P., Krause, D.M., Mueller, M.J. and Fekete, A. (2015) Accumulation of extra-chloroplastic triacylglycerols in Arabidopsis seedlings during heat acclimation. *J. Exp. Bot.*, **66**, 4517–4526.

Mueller, S.P., Unger, M., Guender, L., Fekete, A. and Mueller, M.J. (2017) Phospholipid: Diacylglycerol acyltransferase-mediated triacylglyerol synthesis augments basal thermotolerance. *Plant Physiol.*, **175**, 486–497.

Muhlemann, J.K., Younts, T.L.B. and Muday, G.K. (2018) Flavonols control pollen tube growth and integrity by regulating ROS homeostasis during high-temperature stress. *Proc. Natl. Acad. Sci. U. S. A.*, **115**, E11188–E11197.

Müller, A.O. and Ischebeck, T. (2017) Characterization of the enzymatic activity and physiological function of the lipid droplet-associated triacylglycerol lipase AtOBL1. *New Phytol.,* **1,** 1062–1076.

Müller, F. and Rieu, I. (2016) Acclimation to high temperature during pollen development. *Plant Reprod.*, **29**, 107–118.

Nakamura, Y., Kobayashi, K. and Ohta, H. (2009) Activation of galactolipid biosynthesis in development of pistils and pollen tubes. *Plant Physiol. Biochem.*, **47**, 535–539.

Negoro, H., Sakamoto, M., Kotaka, A., Matsumura, K. and Hata, Y. (2018) Mutation in the peroxin-coding gene PEX22 contributing to high malate production in *Saccharomyces cerevisiae*. *J. Biosci. Bioeng.*, **125**, 211–217.

Niu, Y. and Xiang, Y. (2018) An overview of biomembrane functions in plant responses to high-temperature stress. *Front. Plant Sci.*, **9**, 1–18.

Noack, L.C. and Jaillais, Y. (2020) Functions of anionic lipids in plants. *Annu. Rev. Plant Biol.*, **71**, 71–102.

Pérez-Rodríguez, P., Riaño-Pachón, D.M., Corrêa, L.G.G., Rensing, S.A., Kersten, B. and Mueller-Roeber, B. (2009) PlnTFDB: Updated content and new features of the plant transcription factor database. *Nucleic Acids Res.*, **38**, 822–827.

Pidkowich, M.S., Nguyen, H.T., Heilmann, I., Ischebeck, T. and Shanklin, J. (2007) Modulating seed β-ketoacyl-acyl carrier protein synthase II level converts the composition of a temperate seed oil to that of a palm-like tropical oil. *Proc. Natl. Acad. Sci. U. S. A.*, **104**, 4742–4747.

Platre, M.P., Bayle, V., Armengot, L., et al. (2019) Developmental control of plant Rho GTPase nano-organization by the lipid phosphatidylserine. *Science*, **364**, 57–62.

Popko, J., Herrfurth, C., Feussner, K., et al. (2016) Metabolome analysis reveals betaine lipids as major source for triglyceride formation, and the accumulation of sedoheptulose during nitrogen-starvation of *Phaeodactylum tricornutum*. *PLoS One*, **11**, 1–23.

Priya, M., Dhanker, O.P., Siddique, K.H.M., et al. (2019) Drought and heat stress-related proteins: an update about their functional relevance in imparting stress tolerance in agricultural crops. *Theor Appl Genet.,* **132**, 1607-1638.

Priya, M., Sharma, L., Kaur, R., Bindumadhava, H., Nair, R.M., Siddique, K.H.M. and Nayyar, H. (2019) GABA (γ-aminobutyric acid), as a thermo-protectant, to improve the reproductive function of heat-stressed mungbean plants. *Sci. Rep.*, **9**, 1–14.

Rahmati Ishka, M., Brown, E., Weigand, C., Tillett, R.L., Schlauch, K.A., Miller, G. and Harper, J.F. (2018) A comparison of heat-stress transcriptome changes between wild-type Arabidopsis pollen and a heat-sensitive mutant harboring a knockout of cyclic nucleotide-gated cation channel 16 (cngc16). *BMC Genomics*, **19**, 1–19.

Raja, M.M., Vijayalakshmi, G., Naik, M.L., Basha, P.O., Sergeant, K., Hausman, J.F. and Khan, P.S.S.V. (2019) Pollen development and function under heat stress: from effects to responses. *Acta Physiol. Plant.*, **41**, 1–20.

Read, S.M., Clarke, A.E. and Bacic, A. (1993) Stimulation of growth of cultured *Nicotiana tabacum* W 38 pollen tubes by poly(ethylene glycol) and Cu(II) salts. *Protoplasma*, **177**, 1–14.

Robinson, M.D., McCarthy, D.J. and Smyth, G.K. (2009) edgeR: A Bioconductor package for differential expression analysis of digital gene expression data. *Bioinformatics*, **26**, 139–140.

Rotsch, A.H., Kopka, J., Feussner, I. and Ischebeck, T. (2017) Central metabolite and sterol profiling divides Tobacco male gametophyte development and pollen tube growth into eight metabolic phases. *Plant J.*, **92**, 129–146.

Santiago, J.P. and Sharkey, T.D. (2019) Pollen development at high temperature and role of carbon and nitrogen metabolites. *Plant Cell Environ.*, **42**, 2759–2775.

Scholz, P., Anstatt, J., Krawczyk, H.E. and Ischebeck, T. (2020) Signalling pinpointed to the tip: The complex regulatory network that allows pollen tube growth. *Plants*, **9**, 1098.

Shao, Q., Liu, X., Su, T., Ma, C. and Wang, P. (2019) New insights into the role of seed oil body proteins in metabolism and plant development. *Front. Plant Sci.*, **10**, 1–14.

Shi, W., Li, X., Schmidt, R.C., Struik, P.C., Yin, X. and Jagadish, S.V.K. (2018) Pollen germination and *in vivo* fertilization in response to high-temperature during flowering in hybrid and inbred rice. *Plant Cell Environ.*, **41**, 1287–1297.

Shiva, S., Samarakoon, T., Lowe, K.A., et al. (2020) Leaf lipid alterations in response to heat stress of *Arabidopsis thaliana*. *Plants*, **9**, 845.

Simon-Plas, F., Perraki, A., Bayer, E., Gerbeau-Pissot, P. and Mongrand, S. (2011) An update on plant membrane rafts. *Curr. Opin. Plant Biol.*, **14**, 642–649.

Snider, J.L., Oosterhuis, D.M. and Kawakami, E.M. (2011) Diurnal pollen tube growth rate is slowed by high temperature in field-grown *Gossypium hirsutum* pistils. *J. Plant Physiol.*, **168**, 441–448.

Snider, J.L., Oosterhuis, D.M., Loka, D.A. and Kawakami, E.M. (2011) High temperature limits *in vivo* pollen tube growth rates by altering diurnal carbohydrate balance in field-grown Gossypium hirsutum pistils. *J. Plant Physiol.*, **168**, 1168–1175.

Song, C., Kim, T., Chung, W.S. and Lim, C.O. (2017) The Arabidopsis phytocystatin AtCYS5 enhances seed germination and seedling growth under heat stress conditions. *Mol. Cells*, **40**, 577–586.

Song, G., Wang, M., Zeng, B., Zhang, J., Jiang, C., Hu, Q., Geng, G. and Tang, C. (2015) Anther response to high-temperature stress during development and pollen thermotolerance heterosis as revealed by pollen tube growth and *in vitro* pollen vigor analysis in upland cotton. *Planta*, **241**, 1271–1285.

Spicher, L., Glauser, G. and Kessler, F. (2016) Lipid antioxidant and galactolipid remodeling under temperature stress in tomato plants. *Front. Plant Sci.*, **7**, 1–12.

Sprunck, S. (2020) Twice the fun, double the trouble: gamete interactions in flowering plants. *Curr. Opin. Plant Biol.*, **53**, 106–116.

Staff, I.A., Taylor, P., Kenrick, J. and Knox, R.B. (1989) Ultrastructural analysis of plastids in angiosperm pollen tubes. *Sex. Plant Reprod.*, **2**, 70–76.

Sunoj, V.S.J., Somayanda, I.M., Chiluwal, A., Perumal, R., Prasad, P.V.V. and Jagadish, S.V.K. (2017) Resilience of pollen and post-flowering response in diverse sorghum genotypes exposed to heat stress under field conditions. *Crop Sci.*, **57**, 1658–1669.

Suzuki, N., Sejima, H., Tam, R., Schlauch, K. and Mittler, R. (2011) Identification of the MBF1 heat-response regulon of *Arabidopsis thaliana*. *Plant J.*, **66**, 844–851.

Takahashi, Y., Uemura, T. and Teshima, Y. (2019) Polyamine oxidase 2 is involved in regulating excess spermidine contents during seed germination and early seedling development in *Arabidopsis thaliana*. *Biochem. Biophys. Res. Commun.*, **516**, 1248–1251.

Tarazona, P., Feussner, K. and Feussner, I. (2015) An enhanced plant lipidomics method based on multiplexed liquid chromatography-mass spectrometry reveals additional insights into cold- and drought-induced membrane remodeling. *Plant J.*, **84**, 621–633.

Tarkowski, Ł.P., Signorelli, S. and Höfte, M. (2020) γ-Aminobutyric acid and related amino acids in plant immune responses: Emerging mechanisms of action. *Plant Cell Environ.*, 1–14.

Toumi, I., Pagoulatou, M.G., Margaritopoulou, T., Milioni, D. and Roubelakis-Angelakis, K.A. (2019) Genetically modified heat shock protein90s and polyamine oxidases in Arabidopsis reveal their interaction under heat stress affecting polyamine acetylation, oxidation and homeostasis of reactive oxygen species. *Plants*, **8**.

Touraine, B., Vignols, F., Przybyla-Toscano, J., et al. (2019) Iron-sulfur protein NFU2 is required for branched-chain amino acid synthesis in Arabidopsis roots. *J. Exp. Bot.*, **70**, 1875–1889.

Villette, C., Berna, A., Compagnon, V. and Schaller, H. (2015) Plant sterol diversity in pollen from angiosperms. *Lipids*, **50**, 749–760.

Wu Jingrui, James Jnr, D.W., Dooner, H.K. and Browse, J. (1994) A mutant of Arabidopsis deficient in the elongation of palmitic acid. *Plant Physiol.*, **106**, 143–150.

Yang, H., Yang, S., Li, Y. and Hua, J. (2007) The arabidopsis BAP1 and BAP2 genes are general inhibitors of programmed cell death. *Plant Physiol.*, **145**, 135–146.

Yang, Y., Mininberg, B., Tarbet, A. and Weathers, P. (2013) At high temperature lipid production in *Ettlia oleoabundans* occurs before nitrate depletion. *Appl. Microbiol. Biotechnol.*, **97**, 2263–2273.

Yu, J., Li, R., Fan, N., Yang, Z. and Huang, B. (2017) Metabolic pathways involved in carbon dioxide enhanced heat tolerance in bermudagrass. *Front. Plant Sci.*, **8**, 1–22.

Zhang, C., Li, G., Chen, T., et al. (2018) Heat stress induces spikelet sterility in rice at anthesis through inhibition of pollen tube elongation interfering with auxin homeostasis in pollinated pistils. *Rice*, **11**.

Zhang, Z., Cheng, Z., Gan, L., et al. (2016) OsHSD1, a hydroxysteroid dehydrogenase, is involved in cuticle formation and lipid homeostasis in rice. *Plant Sci.*, **249**, 35–45.

Zhao, Q., Zhou, L., Liu, J., Du, X., Asad, M.-A.-U., Huang, F., Pan, G. and Cheng, F. (2018) Relationship of ROS accumulation and superoxide dismutase isozymes in developing anther with floret fertility of rice under heat stress. *Plant Physiol. Biochem.*, **122**, 90–101.

Zhou, R., Hu, Q., Pu, Q., et al. (2020) Spermidine enhanced free polyamine levels and expression of polyamine biosynthesis enzyme gene in rice spikelets under heat tolerance before heading. *Sci. Rep.*, **10**, 1–9.

Zhou, Y., Yang, Y., Niu, Y., et al. (2020) The tip-localized phosphatidylserine established by Arabidopsis ALA3 is crucial for Rab GTPase-mediated vesicle trafficking and pollen tube growth. *Plant Cell*, **32**, 3170–3187.

Zinta, G., Abdelgawad, H., Peshev, D., Weedon, J.T., Ende, W. Van Den, Nijs, I., Janssens, I.A., Beemster, G.T.S. and Asard, H. (2018) Dynamics of metabolic responses to periods of combined heat and drought in *Arabidopsis thaliana* under ambient and elevated atmospheric CO_2. *J. Exp. Bot.*, **69**, 2159–2170.

Supplementary Figure 1

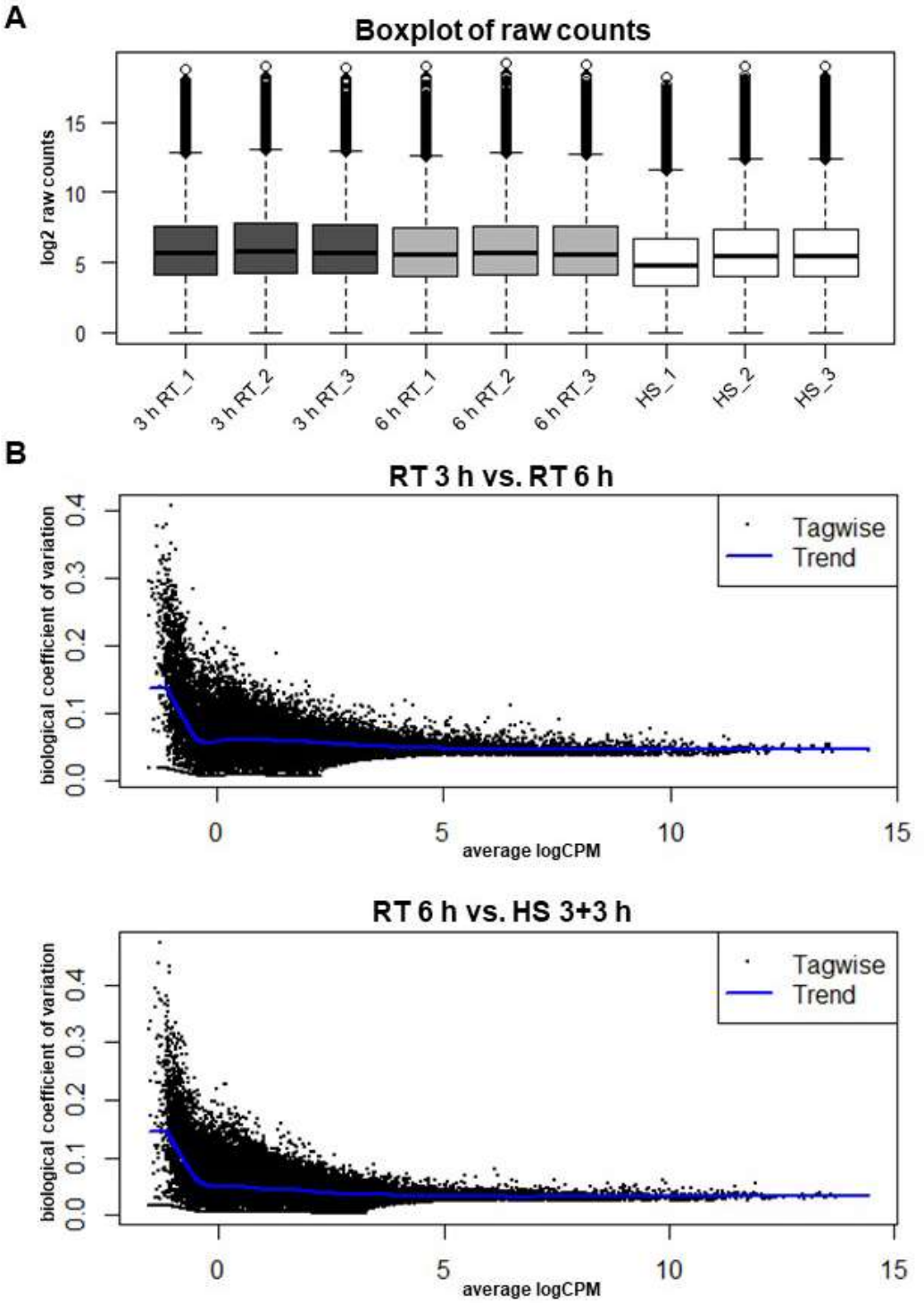

Supplementary Figure 1: A Boxplot of raw counts from transcriptome analysis. **B** Biological coefficient of variation (BCV) plots of RT 3h vs RT 6h and RT 6h vs. HS 3+3 h. Displayed are trended (blue line) and genewise (tagwise, black dots) BCV estimates (empirical robust bayes tagwise dispersions for negative binomial GLMs using observation weights).

6 Additional results: Further characterisation of *sldp* mutants

Obtained results as well as methods not included in the manuscript “Identification of a putative lipid droplet-plasma membrane tethering complex” are presented in this chapter. For the manuscript, we concentrated on cell biological phenotypes of *sldp* and *lipa* mutants and less on physiological functions. However, these are also of great importance and some experiments focusing on the physiological impact of SLDP have been conducted. So far, results are only available for T-DNA mutants of *SLDP* and not for CRISPR mutant lines and also not for *LIPA* lines. Still, obtained data give valuable insight into putative physiological functions of SLDP.

Contributions:

All additional data were acquired and processed by H. Elisa Krawczyk, except for the SLDP1.3 Y2H screen.

Acknowledgements:

Thanks to John M. Dyer (US Arid-Land Agricultural Research Center) for performing Y2H analysis and providing the Y2H results table.

Results

The clustered LD phenotype is already detectable during embryogenesis

The LD-clustering phenotype described in manuscript II was analysed in detail during post-germinative growth and thereby during TAG breakdown. We were interested if the phenotype is already visible during TAG accumulation throughout embryogenesis. Figure 7a shows an overview of LDs in wild-type embryos in the course of embryo development. Aligning of LDs along the PM, similar to the LD distribution in post-germinative growth, is also observable during TAG accumulation, most prominently during walking stick and upturned U stages, when cells are not yet completely filled with LDs. To analyse if *sldp* mutant embryos are impaired in this LD distribution, embryos from late walking stick/early upturned U stage were analysed. Figure 7b shows hypocotyls and cotyledons of wild-type and *sldp1-1 sldp2-1* mutant embryos. Nile red staining of LDs displayed that already during embryo development the phenotype of clustered LDs becomes visible, albeit to a lesser extent and not as clear as during post-germinative growth. However, the phenotype is visible, especially in cotyledons.

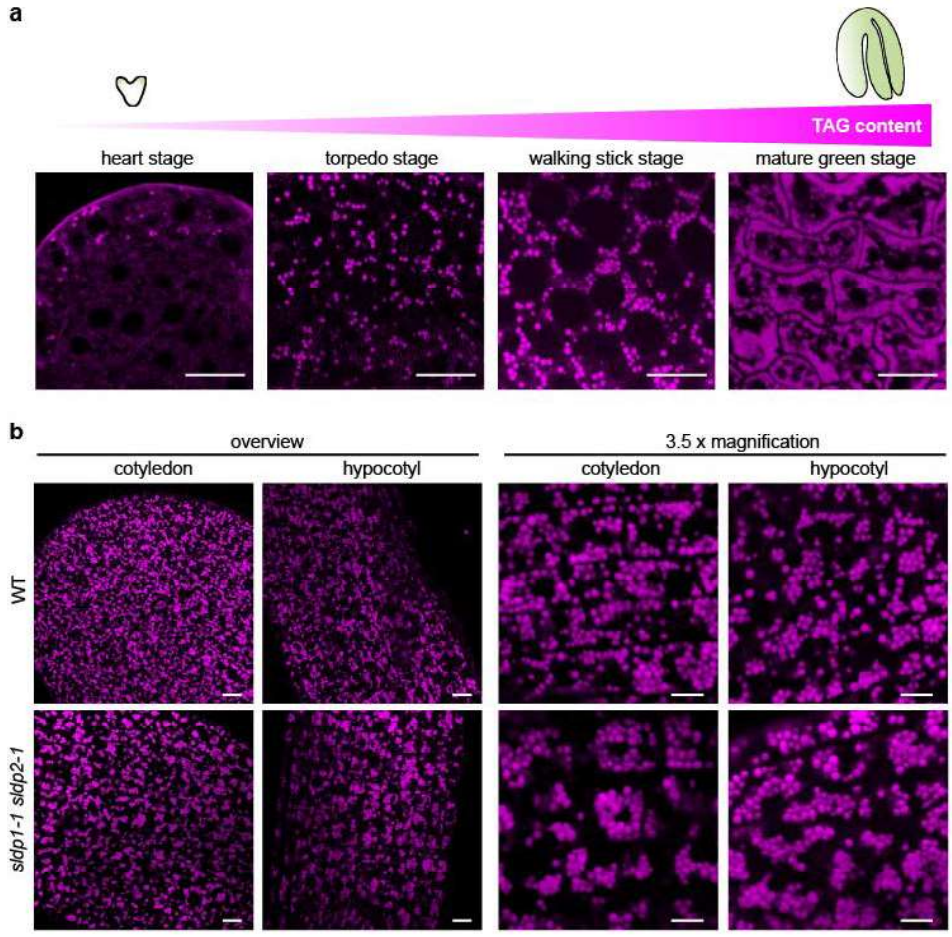

Figure 7: LDs in embryos. a LD accumulation in developing wild type embryos from heart stage to mature green stage. LDs are visualised by Nile red staining of stored neutral lipids. **b** Late walking stick/early upturned U stage wild-type and *sldp1-1 sldp2-1* embryos. An overview as well as 3.5x magnification of a cotyledon and a hypocotyl are presented. A representative image for each stage and genotype were chosen, at least 10 embryos each were analysed and at least 5 images taken. Bars: 10 µm.

Seed weight of sldp1 sldp2 is increased

To get an idea about physiological impacts, different seed traits of wild-type, *sldp1-1, sldp2-1* and *sldp1-1 sldp2-1* seeds were analysed. Analyses of seed size did not result in significant differences between the genotypes. 200 to 258 dry seeds of each genotype (all grown and harvested together) were measured to obtain lengths and width and ratios of length/width. Moreover, ImageJ was used for automated seed area detection. Figure 8 shows the results presented as violin plots with mean points. Data show that seed sizes are not severely altered. Wild-type seeds have a slightly increased seed area as compared to mutant seeds, however, there were no differences in seed width and only *sldp2-1* seeds are (significantly) slightly longer. The ratio of length to width, as a mean to measure roundness of the seeds, was not different between the mutants and the wild type. Overall, no major differences in seed size were measurable.

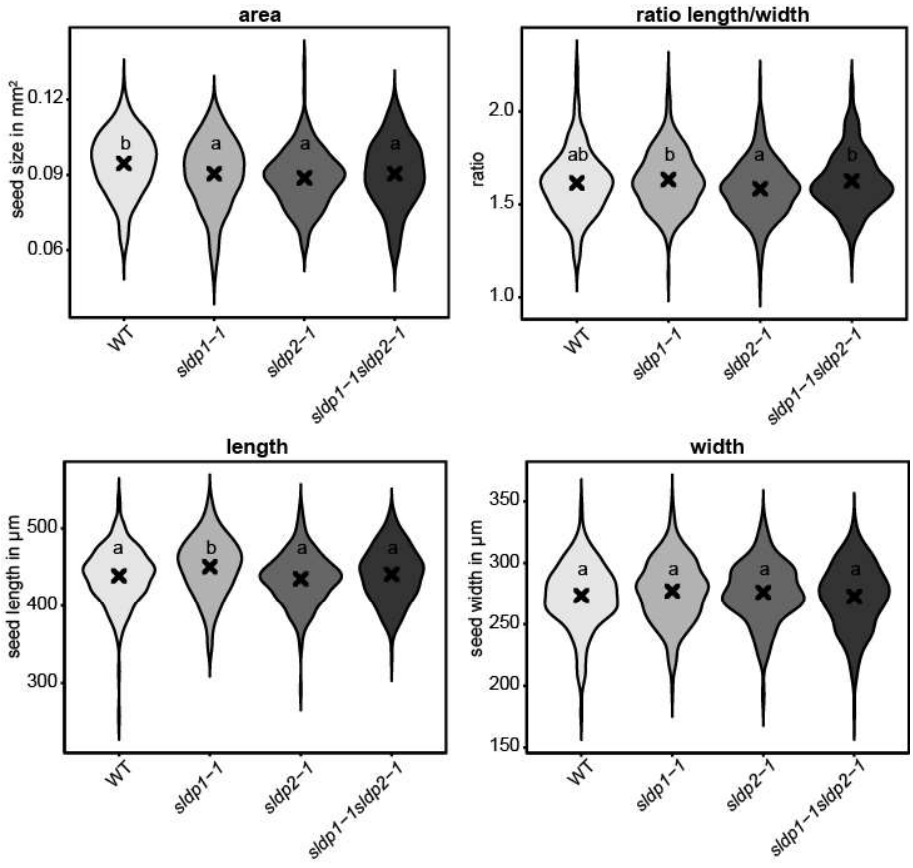

Figure 8: Analysis of seed morphology. Dry seeds from the wild type, sldp1-1, sldp2-1 and sldp1-1 sldp2-1 were manually measured for length and width, the ration length/width was calculated and ImageJ was used for automated area calculation. One-way ANOVAs were performed, followed by Tukey post-hoc analysis. Results are presented as compact letter display of all pair-wise comparisons in increasing order.

Another analysed trait was seed weight. For this, 5 times 500 seeds from the wild-type and *sldp1-1 sldp2-1* were counted and weighed. The obtained weights were used to calculate the per seed weight. Data revealed that *sldp1-1 sldp2-1* seeds are statistically significantly heavier than wild-type seeds: While one wild-type seed from the analysed batch weighed on average

19.4 µg, one *sldp1-1 sldp2-1* seed from the same batch weighed 20.8 µg and is thereby around 1.4 µg heavier (Figure 9a). The presented results are consistent with another independent experiment with another seed batch. To further analyse the increased seed weight, a water loss experiment was conducted. Defined amounts of seeds (8-14 mg) from the wild type and *sldp1-1 sldp2-1* mutants in three replicates were placed at 100 °C over night (15 h) and weighed again the next day to analyse water loss and thereby find out if increased seed weight is due to higher amounts of water in the dry seed. However, analysis revealed that both the wild type and *sldp1-1 sldp2-1* lost around 5.2 % of their initial seed weight (Figure 9b), indicating that the dry weight of the mutant seeds is also increased.

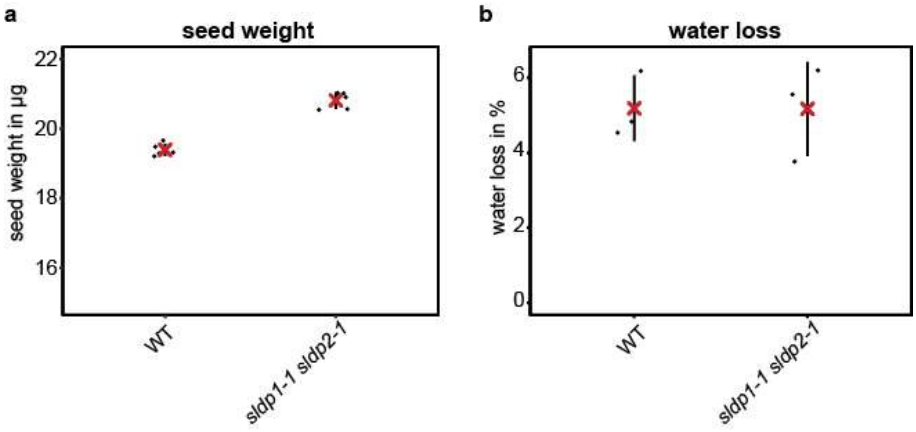

Figure 9: Seed weight analysis. For seed weight analyses **(a)**, 5 times 500 seeds of the wild type and sldp1-1 sldp2-1 were weighed and the per seed weight was calculated. Dry seed water content was analysed **(b)** by putting a defined amount of dry seeds at 100 °C over night and % water loss (relative to per seed dry weight) was calculated.

Mutant seeds accumulate more FAs but are not impaired in TAG degradation

The aberrant clustering of LDs in *sldp* and *lipa* knockout mutants suggested that accessibility of lipases to the LD-stored TAGs might be impaired. Therefore, TAG degradation rates of wild-type, *sldp1-1*, *sldp2-1* and *sldp1-1 sldp2-1* seedlings were analysed in dry seeds, during germination and post-germinative growth. In Arabidopsis seeds, 20:1 FA is a marker for TAG, as it is only incorporated to TAG. By following the amount of 20:1 FA, the fate of TAG can thus be monitored, assuming that the proportion of 20:1 acyl-chains in TAG is constant. As shown in Figure 10a, the relative TAG FA composition is not altered. Surprisingly, Figure 10b shows that no major differences in TAG degradation rates were observed. Despite the striking aberrant LD clustering, breakdown of TAG, as monitored by 20:1 FA breakdown, is not impaired. However, when looking at total lipid contents of the analysed seeds and seedlings, a significant increase especially in dry seeds of *sldp1-1* and *sldp1-1 sldp2-1* is observable Figure 10c. For dry seeds, one *sldp1-1 sldp2-1* seed contains around 5.74 ± 0.19 µg FAs and a wild-type seed contains around 4.87 ± 0.48 µg.

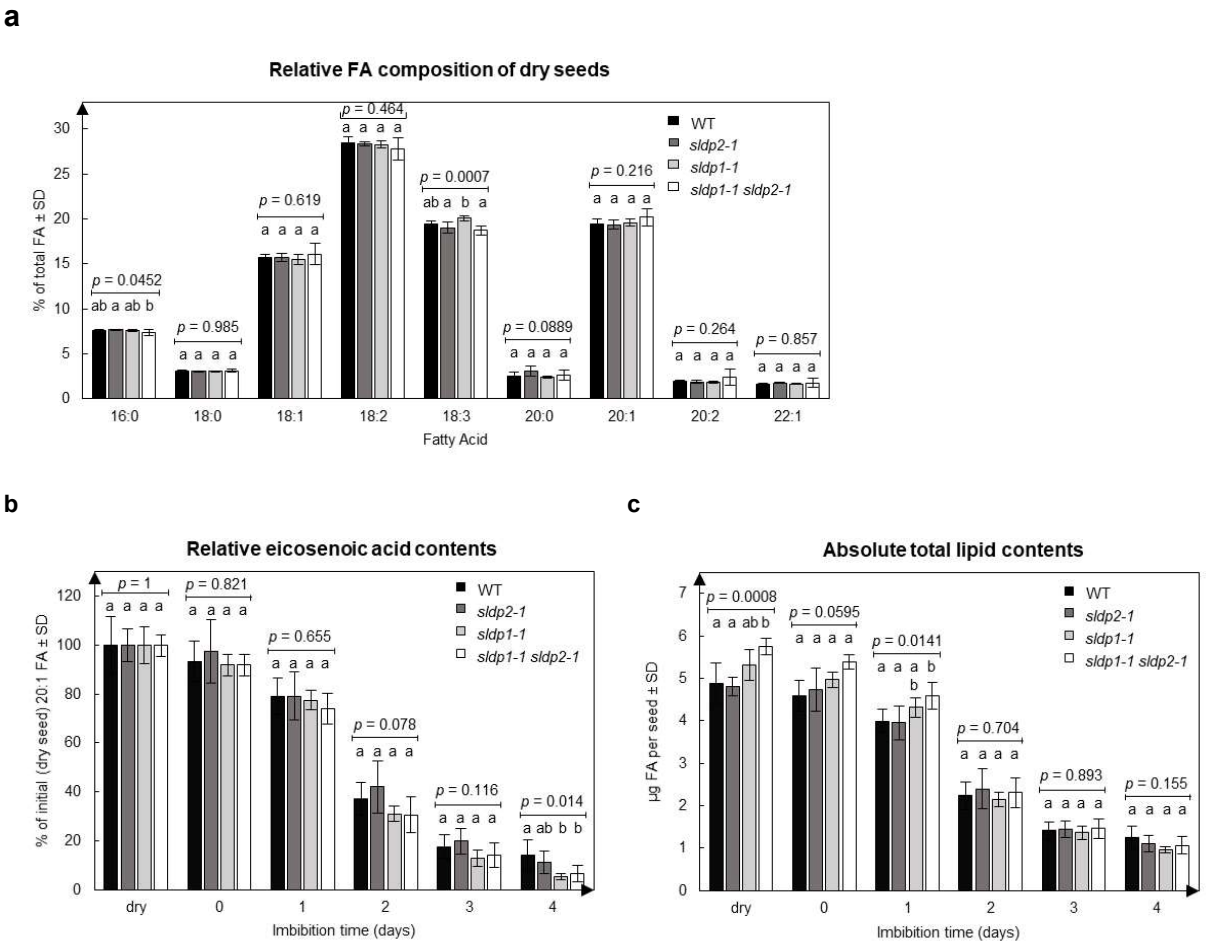

Figure 10: Lipid analyses of dry and germinating seeds. Total lipid contents from dry seeds, stratified seeds (0) and 1-4 day imbibed seeds of the wild type*, sldp1-1, sldp2-1* and *sldp1-1 sldp2-1* were extracted and analysed by GC-FID. For TAG breakdown analysis. **a** Total FA composition of dry seeds was analysed, relative to the total FA amount. **b** Relative 20:1 FA amounts, as measurement for TAG content, in the course of germination (normalised to the amount in dry seeds) were monitored. **c** Absolute lipid contents of the described seeds and seedlings over the time course were analysed. One-way ANOVAs were performed, followed by Tukey post-hoc analyses. Results are presented as compact letter display of all pair-wise comparisons in increasing order. n=5, the presented results are representative of another, independent experiment with another seed batch.

Seedling growth under normal conditions is not altered

Apart from dry seeds, also seedlings were analysed for their capacity to germinate in the light or in the dark in the absence of exogenous sucrose supply. In the dark, wild-type hypocotyls reached around 0.92 mm length and *sldp1-1 sldp2-1* hypocotyls reached 0.9 mm. In the light, wild-type as well as *sldp1-1 sldp2-1* hypocotyls were on average 0.14 mm long. No statistically significant differences were obtained for light- or dark-grown hypocotyls (Figure 11). Data stem from one experiment only, with 97 – 215 seedlings analysed per condition and genetic background.

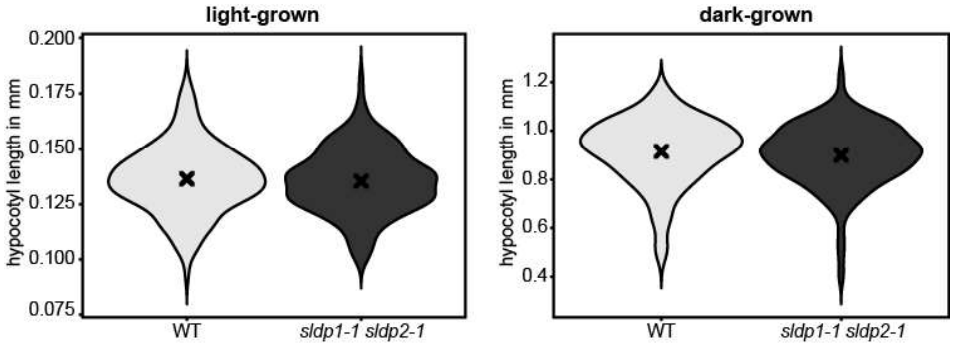

Figure 11: Hypocotyl lengths in the light and the dark without exogenous sucrose supply. Seeds (sieved to a size of 250-300 µm) were analysed for their capacity to establish a seedling in the absence of exogenous sucrose in the light and in the dark. Seeds were placed on solid half-strength MS-medium without sucrose, stratified for four days in the dark and grown for 5 days prior to measurements. n = 97 – 215

Yeast-2-hybrid analysis reveals putative interaction partners

As SLDP1 and 2 are small proteins without a predicted enzymatic function or known domain, their function could be to interact with other proteins. One likely interaction partner, LIPA, was identified by the proteomic analysis of LDs from *sldp1 sldp2* mutant lines in comparison to wild-type LDs. This interaction was further supported by cell biological and genetic experiments. However, it is possible that SLDP1 and 2 have additional interaction partners.

To find further potential interaction partners of SLDP1, a yeast-2-hybdrid (Y2H) screen was performed. A truncated version SLDP1 (∆1-81, lacking the first 81 amino acids containing a hydrophobic stretch) was used as bait (with the full length version no protein expression in yeast was observed, which might be due to instability and degradation of the full-length protein in yeast). A leaf cDNA bank was used as prey. Y2H association was classified as strong, moderate or weak based on the relative growth of yeast on selective media. Results are presented in Table 2. Several putative interaction partners were identified by strong Y2H association, among them voltage dependent anion channel 3 (VDAC3), SYT1, clathrin light chain protein, pyrophosphorylase 5 (PPa5), DNAJ heat shock family protein 6 (DJA6) and molecular chaperone Hsp40/DNAJ family protein (DJA5). No formation of homodimers of SLDP1.3 were observed.

Table 2: Results from Y2H-screen. A truncated version of SLDP1 (SLDP1 ∆1-81) was used as bait, a leaf cDNA bank was used as prey. Identified potential interaction partners are named and described, Y2H association as assessed by yeast growth on selective media is given

Gene	Y2H association	Description
AT5G15090	Strong	**Voltage dependent anion channel 3 (VDAC3).** Prominently localized in outer mitochondrial membrane, involved in metabolite exchange b/w organelle and cytosol, involved in defence response to bacterium.
AT2G20990	Strong	**Arabidopsis synaptotagmin A (SYTA/SYT1).** Encodes a protein specifically localized to the ER-PM boundary with similarity to synaptotagmins, a class of membrane trafficking proteins. SYT1 is expressed in all tissues. Loss of

		function mutations show hypersensitivity to NaCl and electrolyte leakage from the plasma membrane. SYT1 also affects calcium dependent freezing tolerance and mechanical stress response. Regulates endocytosis endosome recycling at the plasma membrane, but not membrane traffic along the secretory pathway. SYT1 may have a role in membrane repair such as membrane resealing after freezing induced damage. SYT1 binds to phosphatidylinositol phosphates *in vitro*. It is distributed to immobile tubules and likely plays an important role in the formation of the tubular ER network as well as in cellular ER-PM tethering.
AT2G40060	Strong	**Clathrin light chain protein**. Encodes a clathrin that is localized to the cortical division zone and the cell plate, co-localises with TPLATE during cell plate anchoring.
AT4G01480	Strong	**Pyrophosphorylase 5 (PPa5)**. Encodes a protein that might have inorganic pyrophosphatase activity.
AT2G22360	Strong	**DNAJ heat shock family protein 6 (DJA6)**. Functions in unfolded protein binding, heat shock protein binding, protein folding, and heat response.
AT4G39960	Strong	**Molecular chaperone Hsp40/DNAJ family protein (DJA5)**. Functions in unfolded protein binding, heat shock protein binding, protein folding, and heat response.
AT3G52200	Moderate	**Dihydrolipoamide acetyltransferase, long form protein (LTA3)**. Involved in acetyl-CoA biosynthetic process from pyruvate and metabolic processes.
AT2G32910	Moderate	**Development and cell death (DCD) domain protein**. Unknown function.
AT1G22930	Moderate	**T-complex protein 11**. Unknown function.
AT2G37940	Weak	**Inositol phosphorylceramide synthase 2 (AtIPCS2)**. Encodes plant inositolphosphorylceramid (IPC) synthase and plays an important role in modulating plant programmed cell death.
AT2G28590	Weak	**Protein kinase superfamily protein**. Involved in protein serine/threonine kinase activity and aa phosphorylation.
AT3G02690	Weak	**Nodulin MtN21/EamA-like transporter family protein**. Unknown function, located in chloroplasts and membranes.
AT5G62850	Weak	**Vegetative cell expressed 1 (AtVEX1)**. Nodulin MtN3 family protein. Encodes a protein that is expressed in vegetative cells of pollen. Member of the SWEET sucrose efflux transporter family proteins.
AT3G51230	Weak	**Chalcone-flavanone isomerase family protein**. Plant enzyme responsible for isomerization of chalcone to naringenin, a key step in the biosynthesis of flavonoids.
AT1G15200	Weak	**Protein-protein interaction regulator family protein.**
AT3G16220	Weak	**Putative eukaryotic LigT**. Molecular function unknown, located in the cytoplasm.
AT3G53670	Weak	Unknown/hypothetical protein.
AT5G67110	Weak	**Basic helix-loop-helix (bHLH) DNA-binding superfamily protein**. Encodes a myc/bHLH transcription factor-like protein, gene product involved in fruit dehiscence.
AT1G52580	Weak	**Rhomboid-like protein 5 (RBL5).** Functions in serine-type endopeptidase activity.
AT1G79230	Weak	**Mercaptopyruvate sulfurtransferase 1 (MST1)**. Involved in sulfate transport and aging. Encodes sulfurtransferase/rhodaneses, which belongs to a group of enzymes widely distributed in all three phyla that catalyze transfer of sulfur from a donor to a thiophilic acceptor substrate. Evidence suggests sulfutransferases are involved in cyanide detoxification.
AT3G22200	Weak	**Pollen-pistil incompatibility 2 (POP2)**. Pyridoxal phosphate (PLP)-dependent transferases superfamily protein. Genetically redundant with POP3; mediates pollen tube guidance.
AT1G43800	Weak	**Plant stearoyl-acyl-carrier-protein desaturase family protein (AKA Floral transition at the meristem 1)**. Involved in oxidation reduction, fatty acid metabolic processes, fatty acid biosynthetic processes.

AT1G49340	Weak	**1-phosphatidylinositol 4-kinase alpha (ATPI4K Alpha)**. Involved in aa phosphorylation and has found to be expressed in inflorescences and shoots.
AT2G47470	Weak	**Unfertilized embryo sac 5 (UNE5)**. Thioredoxin family protein. Encodes a protein disulfide isomerase-like protein. Transcript levels are upregulated in response to three different chemical inducers of ER stress – dithiothreitol, betamercaptoethanol, and tunicamycin).
AT2G20130	Weak	**Like COV1 protein (LCV2)**. Protein of unknown function in A.thaliana.
AT1G74010	Weak	**Calcium-dependent phosphotriesterase superfamily protein**. Functions in strictosidine synthase activity and is involved in a number of biological processes.
AT1G62480	Weak	**Vacuolar calcium-binding protein-like protein**. Involved in cadmium ion and salt stress response.
AT5G20740	Weak	**Plant invertase/pectin methylesterase inhibitor superfamily protein**. Located in the endomembrane system. Displays enzyme inhibitor and pectinesterase inhibitor activity.
AT3G47520	Weak	**Malate dehydrogenase (MDH)**. Encodes a protein with NAD-dependent malate dehydrogenase activity, located in chloroplasts.
AT5G59880	Weak	**Actin depolymerizing factor 3 (ADF3)**. Involved in response to oxidative stress and cadmium ions. Located in mitochondrion, intracellularly, chloroplasts, and plasma membrane.
AT3G16920	Weak	**Chitinase-like protein 2 (CTL2)**. Encodes a chitinase-like protein expressed predominantly in stems. Mutants accumulate ligning in etiolated hypocotyls.
AT1G18197	Weak	**GCK domain protein**. Unknown function.
AT2G29550	Weak	**Tubulin beta-7 chain (TUB7)**. Encodes a beta-tubulin that is expressed in leaves, roots, and flowers. Involved in response to salt stress and cadmium ions.
AT5G17920	Weak	**Cobalamin-independent methionine synthase (ATMS1)**. Involved in methionine regeneration via the activated methyl cycle (SAM cycle). Protein undergoes thiolation following treatment with the oxidant tert-butylhydroperoxide.
AT4G29450	Weak	**Leucine-rich repeat protein kinase family protein**. Involved in protein aa phosphorylation and located in the endomembrane system.
AT1G53970	Weak	**GDSl esterase/lipase-like protein**. Unknown function.
AT3G16500	Weak	**Phytochrome-associated protein 1 (PAP1)**. Functions in sequence-specific DNA binding transcription factor activity and response to auxin stimuli.
AT1G67440	Weak	**Embryo defective 1688 (EMB1688)**. Functions in GTP binding and embryo development ending in seed dormancy.
AT3G60210	Weak	**GroES-like family protein**. Functions in ATP binding and protein folding.

Experimental procedures

Seed measurements (size, weight)

To analyse seed size, dry seeds were placed on white paper (Whatman® filter paper grade 6, Whatman plc, Little Chalfont, United Kingdom) and images were recorded with the Ocular scientific image acquisition software (version 1.0, Digital Optics Ltd, Auckland, New Zealand) on a binocular (Olympus SZX12 binocular, Olympus Corporation, Tokyo, Japan) attached to a camera (R6 Retiga camera, QImaging, Surrey, Canada). Seed length as well as width was measured with ImageJ software (1.52p) (Rueden *et al.*, 2017) and ratio of width/length as a

measurement for seed roundness was determined. Automated seed area measurements were performed with the 'analyse particles' functions implemented in ImageJ. To assess seed weight, 5 times 500 seeds were counted manually and weighed three times on a micro scale (KERN & SOHN GmbH, Balingen-Frommern, Germany). Means of the three technical replicates were calculated and used for further analyses. Means and SDs of the 5 replicates were calculated and divided by 500 to obtain the average per seed weight and per seed SD.

Seed lipid analysis

All seeds used for seed lipid analyses were sieved to a size of 250 – 300 µm prior to analyses to ensure observed effects are really comparable and not due to differences in seed size that influence lipid content. Six biological replicates were performed (seeds from six different mother plants were harvested and 25 seeds each were analysed per time point and genotype). Seeds were germinated on wet filter papers (Whatman® filter paper grade 6, Whatman plc, Little Chalfont, United Kingdom) soaked in 1.6 ml H_2O and put in a petri dish in humid environment. Apart from seeds for dry seed analysis, seeds were stratified for 4 days at 4 °C in the dark prior to imbibition. After 4 days of stratification, 0 day samples were harvested; the other samples were placed into 16-h/8-h day/night cycle (light period: 08:00 – 24:00) in a Percival (CU-36L/D, Percival Scientific Inc., Perry, USA) and harvested after the indicated time points. Total lipid contents of dry seeds and seedlings after 0, 24, 48, 72 and 96 h of imbibition were analysed by gas chromatography flame ionisation detection (GC-FID). For this, seeds and seedlings were harvested into 1 ml fatty acid methyl ester (FAME) reagent (2.5 % v/v H_2SO_4, 2 % v/v dimethoxypropane in methanol/toluol 2:1, v/v) (Miquel and Browse, 1992) with 30 µl of 0.33 mg/ml tri-15:0 TAG (1,2,3-tripentadecanoylglycerol ≥99%, Sigma-Aldrich, St. Louis, Missouri, USA) in toluol (ROTIPURAN® ≥ 99.5 %, Carl Roth, Karlsruhe, Deutschland) as internal standard and ground with a glass stick. Samples were then incubated at 80 °C in a water bath under constant shaking for one hour to esterify all FAs to methanol. The reaction was stopped with 1 ml of saturated NaCl-solution and vortexing. FAMEs were then extracted twice adding 1 ml of hexane, centrifuging 10 min at 2,000 x g and transferring the upper phase to a new glass tube. Hexane was evaporated and samples resuspended in 30 µl of acetonitrile (HPLC Gradient grade, Fisher Chemical, Thermo Fisher Scientific, Waltham, Massachusetts, USA). Subsequent GC-FID analysis was performed as described in (Hornung *et al.*, 2002): an Agilent GC 6890 system (Agilent, Waldbronn, Germany) coupled to an FID detector equipped with a capillary HP INNOWAX column (30 m × 0.32 mm, 0.5 µm coating thickness, Agilent, Waldbronn, Germany) was used. Helium served as carrier gas (30 cm × s−1), with an injector temperature of 220 °C. The temperature gradient was 150 °C for 1 min, 150–200 °C at 15 °C min^{-1}, 200–250 °C at 2 °C min^{-1}, and 250 °C for 10 min. Quantification was performed as described in manuscript II.

Embryo preparation and microscopy

For microscopic analyses of embryos, green siliques from wild-type or *sldp1-1 sldp2-1* plants were harvested and embryos were dissected from developing seeds. Using a binocular (Olympus SZX12 binocular, Olympus Corporation, Tokyo, Japan), embryo stage was determined according to Goldberg *et al*. (1994). Embryos were then harvested and stained with 0.5 µg/ml Nile red (Sigma Aldrich, St. Louis, Missouri, USA) in water. Microscopic analysis was performed as described in manuscript I for seedling time course microscopy.

Hypocotyl measurements

All seeds used for hypocotyl analyses were sieved to a size of 250 – 300 µm prior to analyses and stratified for 4 days at 4 °C in the dark. They were surface-sterilised in 6 % sodium hypochlorite solution for 15 – 20 minutes and placed on half-strength MS medium (Murashige and Skoog, 1962) supplemented with 0.8 % (w/v) without sucrose. Seedlings were grown vertically in the light for 7 days under 16-h/8-h day/night regime (light period: 08:00 – 24:00) or 4 h in the light and then 7 days in the dark in a Percival (CU-36L/D, Percival Scientific Inc., Perry, USA) and hypocotyls were recorded with the Ocular scientific image acquisition software (version 1.0, Digital Optics Ltd, Auckland, New Zealand) on a binocular (Olympus SZX12 binocular, Olympus Corporation, Tokyo, Japan) attached to a camera (R6 Retiga camera, QImaging, Surrey, Canada). Hypocotyl length was measured with ImageJ software (1.52p) (Rueden *et al.*, 2017) and violin plots with mean points were generated using ggplot2 package (version 3.3.2) in the R environment (version 4.0.1).

Y2H analysis

A Y2H library, consisting of Arabidopsis cDNA from leaf tissues cloned into the appropriate prey vector, was screened with the Matchmaker Gold Y2H System (Clontech Laboratories, Inc., http://www.clontech.com/) as described by the manufacturer, using a truncated version of Arabidopsis SLDP1.3 (pGBKT7/SLDP1.3Δ1-81) as bait. Screening was performed as described previously (Pyc *et al.*, 2017).

7 Discussion

In the present thesis, LDs in two different reproductive tissues, seeds and pollen tubes, were analysed. One study resulted in the identification of a putative MCS between LDs and the PM in seeds and seedlings, functional consequence of which still has to be elucidated. The other study illuminated a putative function of LDs as a FA sink in heat stress-induced lipid remodelling.

7.1 On the putative LD-PM contact site

In manuscript I, we have shown that SLDP and LIPA most likely form a protein complex that tethers LDs to the PM during post-germinative growth and probably embryogenesis in Arabidopsis. So far, the physiological consequences of the presence or absence of this contact site are still unclear.

7.1.1 True MCS have to be distinguished from non-functional contacts of organelles

An important aspect in the analysis of MCS is the distinction of true MCS and mere stochastic, non-functional contacts of organelles (reviewed in Prinz *et al.*, 2020). Especially in the presented case of LDs at the PM, the possibility of passive pushing of LDs against the PM by the expanding vacuole has to be excluded. The existence of a true MCS between LDs and the PM could be verified by various approaches. Methods for detection, analysis and visualisation of true MCS, as well as their pros and cons, have been discussed in Scorrano *et al.* (2019) and Baillie *et al.* (2020). The imaging methods by confocal microscopy used here could be supplemented by using e.g. split fluorescent reporters. Among the fluorescence tag-based methods, FRET/FLIM (Förster resonance energy transfer/ fluorescence lifetime imaging) (Osterrieder *et al.*, 2009; Csordás *et al.*, 2010; Venditti *et al.*, 2019) and BiFC (Bimolecular fluorescence complementation) (Yang *et al.*, 2018; Cieri *et al.*, 2018) are commonly used methods for MCS analysis. Other microscopy-based approaches include electron microscopy (EM), e.g. in combination with immuno-gold labelling (Pérez-Sancho *et al.*, 2015; Cui *et al.*, 2016; Wang *et al.*, 2016), as well as the super-resolution microscopy techniques SIM (Structured illumination microscopy) and dSTORM (direct Stochastic Optical Reconstruction Microscopy) (Modi *et al.*, 2019). Furthermore, three dimensional electron tomography has been used to visualise MCS (De Brito and Scorrano, 2008; Fernández-Busnadiego *et al.*, 2015) and could help in the present example to exclude that LDs are just passively pushed to the PM by other organelles. There are also more sophisticated methods available than mere imaging, e.g. electrical tweezers (Andersson *et al.*, 2007; Sparkes *et al.*, 2009; Gao *et al.*, 2016; Osterrieder *et al.*, 2017; White *et al.*, 2020) or femtosecond laser shock waves (Oikawa *et al.*, 2015) for quantitative measurements of physical interactions between MCS components. These methods could potentially also provide further proof for the putative LD-PM MCS discussed here.

For confirmation or also identification of further MCS-components putatively interacting with SLDP or LIPA, proximity labelling-based techniques like BioID (van Vliet *et al.*, 2017) or APEX2 (Jing *et al.*, 2015) could be used, both of which are biotinylation probes. In addition, simple co-immunoprecipitation assays of SLDP or LIPA or co-purification of associated membranes (and pretended contaminants) in cell fractionation and organelle-specific proteome analyses could reveal further LD-PM MCS components (Kriechbaumer *et al.*, 2015).

7.1.2 Putative role of LD-PM contacts in resource allocation

The observed clustering effect of LDs is already conceivable during embryogenesis (Figure 7). Also, the presented additional data in Chapter 6 showed that the distribution of LDs along the PM is dispensable for TAG breakdown – lipases obviously still can access the LD core to degrade the contents and deliver them to peroxisomes, as TAG contents of analysed mutant seeds decreased similarly to wild-type seeds (Figure 10b). Moreover, under all so far analysed conditions, no growth phenotype of the *sldp1 sldp2* knockout lines was observed. The need for a putative LD-PM tether during post-germinative growth is thus not directly tangible. However, we showed that total lipid contents in dry seeds of *sldp1 sldp2* mutants were increased (Figure 10c). This increased lipid content of *sldp1 sldp2* seeds might be due to increased rates of fatty acid synthesis during early embryo maturation. However, as an overall increase in seed weight, rather than just increased lipid contents, is observed (Figure 9), SLDP and LIPA might be important even earlier, during seed filling, and clustering during germination might just be a remnant of a function that comes into effect earlier.

Seeds are heterotrophic organs and as such fully depend on nutrients supplied by parental tissues for development (Zhang *et al.*, 2007). Although highly speculative, it is an intriguing thought that the putative LD-PM anchoring might be needed for proper organelle inheritance during seed development, similar to what has been reported for organelle-inheritance in budding yeast. In yeast, as described in section 1.2.1, LDs can be retained in mother cells during cell division through MCS anchoring them to the perinuclear ER, while other LDs are inherited to daughter cells (Knoblach and Rachubinski, 2015). During development of the embryo sac (the female gametophyte), a certain subset of LDs might be transmitted to filial tissues, while another subset could be retained in maternal tissues. The lack of an LD-PM anchor might cause an oversupply of LDs, TAG or sucrose to filial tissues, already during transition from somatic to germline identity, during gametophyte development or later during division of the embryo sac (female gametophyte) into the zygote and the endosperm precursor cell. The embryo-sac will be double-fertilised by the two sperm nuclei inside a pollen grain, resulting in a diploid zygote (2n) and the triploid primary endosperm cell (3n). While the zygote will develop into the embryo and its suspensor (the small structure carrying the embryo), the primary endosperm cell develops into the endosperm by several rounds of mitosis without

subsequent cell division. It is known and shown in Figurer 7 that the embryo, will start to accumulate LDs and TAG during maturation (reviewed in Baud *et al.*, 2008). For this, it depends in the endosperm. During nutrient loading, released nutrients from maternal tissues first accumulate in the endosperm, which will then nourish the embryo, mainly in the form of starch (Hill *et al.*, 2003; Baud *et al.*, 2008). An oversupply of LDs or TAG to the endosperm could allow increased nutrient availability for the embryo and hence increased seed weight and oil content of the mature seed.

However, seed weight is influenced by a wide array of other maternal factors (Bennett *et al.*, 2012) and resource allocation is just one of the possibilities. All in all, influence of a putative LD-PM MCS in organelle inheritance and resource allocation remains highly speculative. More detailed analyses on the amount of produced seeds and siliques and also the duration of seed production have to be conducted to get a more complete picture and see if resource allocation in *sldp1 sldp2* mutants might be altered.

7.1.3 Synaptotagmin is a putative interaction partner of SLDP

As shown in Table 2, SYT1 was identified as a putative strong interaction partner of SLDP1.3 in a Y2H screen. For the screen, a leaf database was used and SLDP1.3 is not expressed in leaves. Interaction of SLDP1.3 and SYT1 might thus also be due to the non-native expression of SLDP and might not occur in seeds. However, according to the Arabidopsis eFP browser, SYT1 is ubiquitously expressed, also in seeds (Schmid *et al.*, 2005; Nakabayashi *et al.*, 2005; Winter *et al.*, 2007; Waese *et al.*, 2017). It is therefore still possible that SLDP1.3 and SYT1 interact in seeds and/or seedlings.

Arabidopsis SYT1 (also called SYTA) has been reported to maintain PM integrity (Schapire *et al.*, 2008; Eckardt, 2008), plays a role in virus movement (Lewis and Lazarowitz, 2010; Levy *et al.*, 2015), is involved in endocytosis (Lewis and Lazarowitz, 2010) and in Ca^{2+}-dependent freezing tolerance (through membrane resealing) (Yamazaki *et al.*, 2008). Subcellular localisation analyses revealed that it is enriched at ER-PM contact sites, where it confers resistance to mechanical stresses and is likely involved in plasmodesmata formation (Pérez-Sancho *et al.*, 2015; Ishikawa *et al.*, 2018; Levy and Tilsner, 2020). These SYT1-enriched ER-PM contact sites often co-localise with VAP27-1-enriched ER-PM contact sites, which SYT1 seems to stabilise (Siao *et al.*, 2016). VAP27-1 was recently found to also interact with ER-LD contact site-localised Seipin (Greer *et al.*, 2020). Localisation of Arabidopsis SYT1 to ER-PM contact sites is resembling the localisation of mammalian extended synaptotagmins (E-SYTs), which have been reported to be involved in e.g. lipid transfer through a synaptotagmin-like mitochondrial and lipid binding protein (SMP) domain (Schauder *et al.*, 2014; Yu *et al.*, 2016; Nath *et al.*, 2020). Arabidopsis SYT1 also contains an SMP domain (Levy and Tilsner, 2020). The SYT1-mediated ER-PM contact is enhanced under ionic stress (E., Lee *et al.*, 2019).

Regarding the described functions and homology to mammalian E-SYTs, SYT1 likely plays an important role in membrane repair and/or stabilisation under salt, cold and mechanical stresses.

A putative interaction of SLDP and SYT1 or even an involvement of SYT1 in the LD-PM tether is therefore conceivable. SLDP, LIPA and SYT1 might act together to form a tri-organellar, rather than a bi-organellar, tether between the ER, LD and PM. The functions of SYT1 in membrane repair and/or stabilisation and in lipid transfer might require LDs in proximity as buffering system. This is supported by the fact that SYT1 also interacts with VAP27-1, which interacts with LD-ER junction-localised Seipins, hinting at another putative LD-ER-PM tether. Redundancies in tethers are often observed and complicate functional analysis of MCS. In yeast for example, where up to 40 % of the PM is connected to the ER, at least seven different tethers are involved in ER-PM tethering. Three of these tethers are tricalbins, orthologs of the mammalian extended synaptotagmins (Manford *et al.*, 2012; Quon *et al.*, 2018; Jorgensen *et al.*, 2020). One putative yeast ER-PM tether, Ice2, is also a known LD-ER tether (together with Ldb16) coupling LD lipolysis to phospholipid formation in the ER (Shpilka *et al.*, 2015), again supporting the existence of a putative three-way contact of LDs, the PM and the ER.

Taken together, these data might hint at a tri-organellar MCS rather than a bi-organellar contact, where SLDP, LIPA and SYT1 might act together to tether the ER, LDs and the PM to mediate and buffer lipid transfer for membrane repair upon mechanical, salt or freezing stress.

7.1.4 PM-anchored LDs – Not LD-PM but rather LD-PM-ER contact site?

All these data undermine the importance of not just LD-PM contacts, but rather of tri-organellar contacts involving the ER and LDs in contact with another organelle. MCS involving LDs have been shown to be tri-organellar rather than just connecting two organelles. This is the case for MIGA2, a human protein connecting LDs, the ER and mitochondria (Freyre *et al.*, 2019); Snz, a drosophila protein connecting LDs, the ER and the PM (Ugrankar *et al.*, 2019); and Mdm1, a yeast protein connecting the LDs, the ER and the vacuole (Hariri *et al.*, 2018; Hariri *et al.*, 2019). Looking at the functions of MCS in lipid transfer on the one hand and the roles of LDs in balancing lipid fluxes and buffering lipids, it seems likely that for these functions, LDs and the ER have to be in contact. LDs, as well as MCS, have been shown to be involved in stress responses. Various cellular stresses were shown to shift lipid fluxes and often TAG serves as a lipid hub with lipids being channelled through TAG prior to degradation or other uses. One example was already described: to protect the mitochondrion from accumulating acylcarnitines, lipids are channelled into LDs in a DGAT1-dependent manner first (Nguyen *et al.*, 2017). Taking into account that mitochondria are not connected to vesicular trafficking pathways (reviewed in Prinz, 2010) and that enzymes catalysing the last step in TAG synthesis reside in the ER (reviewed in Bates, 2016), it is not surprising that a tri-organellar contact between the ER, LDs and mitochondria has to exist for LDs to be able to buffer toxic or excess

lipids as TAG. A similar mechanism might also occur during heat stress – heat-induced PM remodelling causes reduction of unsaturated FA levels in membranes. For unsaturated FAs cannot be turned saturated again, they either have to be stored or degraded. As shown in TAG analysis of manuscript II, not just TAGs containing unsaturated FAs increase upon heat stress, but rather there is an overall, unspecific increase of TAGs. It might therefore be that heat stress causes a bulk membrane lipid degradation and phospholipids are unspecifically degraded, regardless of their saturation level, and replaced by saturated FAs. This bulk degradation of phospholipids could, similarly to what has been observed during autophagy, lead to lipotoxicity, therefore prior to their degradation via β-oxidation, these lipids might be channelled through TAG. As described previously, apart from vesicular transport, these channelling mechanisms might also rely on close contacts with the ER (where the final step of TAG synthesis takes place), LDs (where TAGs are then stored), and the site from where the bulk lipid release stems – e.g. the PM or other cellular membranes that are being degraded.

For putative buffering/detoxification functions of LDs at different organelles, it is thus possible that tri-organellar contacts between the ER, LDs and the respective organelle have to exist, so that FAs can be channelled into LDs via action of DGAT (or other TAG synthesising enzymes in the ER).

7.2 Evolution of LD proteins

LDs are highly conserved from archaea to eukaryotes – many, if not all, eukaryotes and bacterial cells contains LDs and also several archaea contain LDs (Murphy, 2012; Zhang and Liu, 2017). It was suggested that LDs evolved as transient depots for dietary lipids that were exceeding cellular needs and only later evolved their functions as long-term carbon storages and obtained their diverse and specialised functions (reviewed in Murphy, 2012). These specialised functions could likely evolve with the concomitantly evolving diversifying LD proteome. Prokaryotic LDs likely indeed merely serve as energy/carbon stores, as opposed to the various functions of eukaryotic LDs. Differences between eu- and prokaryotic LDs are also found in their stored lipids. While eukaryotes mostly store TAG in their LDs, prokaryotes often store polymeric lipids, most commonly polyhydroxyalkanoates such as polyhydroxybutyrate or polyhydroxyvalerate (reviewed in Murphy, 2012). Focus here will be put on eukaryotic LDs.

7.2.1 SLDP and LIPA likely evolved in flowering plants

Regarding LDs' primary function in lipid storage, proteins uniform to all LDs are lipid metabolic enzymes, such as lipases or acyltransferases, but also enzymes involved in sterol metabolism (Lundquist *et al.*, 2020). Enzymes involved in TAG synthesis, e.g. DGAT, show strong eukaryotic conservation (reviewed in de Vries and Ischebeck, 2020).

While the lipid metabolism machinery is highly conserved among species, there seems to be more variability in other LD proteins, such as structural proteins or proteins involved in biogenesis. LD biogenesis protein Seipin for example is conserved among eukaryotes, although Seipins diversified during e.g. plant evolution (de Vries and Ischebeck, 2020). Other LD biogenesis proteins, however, are species-specific, such as PEX30 that is only involved in fungal LD biogenesis, or LDAP that is specific to plants (reviewed in Lundquist *et al.*, 2020). Major structural proteins are diverse, as well. Perilipins for example are found in all eukaryotes except for the plant lineage. In flowering plants, lycopods, mosses and algae, oleosins are major structural proteins and overtake similar scaffolding functions (reviewed in Lundquist *et al.*, 2020). In some algae, e.g. *Chlamydomonas reinhardtii*, MAJOR LD PROTEIN (MLDP) is found instead of oleosins (Moellering and Benning, 2010). Oleosins, MLDP and perilipins do not show sequence homology and although these proteins differ in some specialised functions, they all serve the same function in stabilising LDs and preventing uncontrolled fusion. They might be examples of a convergent evolution, where proteins evolved in independent events to fulfil the same function.

In the present study, three proteins, SLDP1 and 2 and LIPA, were analysed. As discussed in manuscript I, SLDP1, SLDP2 and LIPA transcripts are reported to be highly seed-specific in different transcript databases (Nakabayashi *et al.*, 2005; Schmid *et al.*, 2005; Winter *et al.*, 2007; Klepikova *et al.*, 2016; Waese *et al.*, 2017). Amino acid sequence analysis reveals that all three proteins are specific for vascular plants, where homologues of SLDP and LIPA are found in diverse species. However, no homologues are found in liverworts, mosses or hornworts and also within the vascular plants, homologues are restricted to magnoliopsida. Interestingly, protein blast analysis of SLDP2.1 reveals a distinct homologue in the lycophyte *Selaginella moellendorffii*. This spike moss from an ancient lineage shares similarities with vascular plants but also with non-seed plants and harbours one of the smallest plant genome sizes reported (Banks, 2009; Banks *et al.*, 2011; de Vries and Ischebeck, 2020). The 65 C-terminal amino acid residues of SLDP2.1 share 34 % sequence identity with the C-terminus of four *S. moellendorffii* proteins annotated as midasin isoforms. Midasins are nuclear chaperones aiding in exporting pre-60S ribosome subunits from the nucleus and in Arabidopsis are reported to be involved in seed proteome establishment and de-repression of ABI5 for proper seed germination (Li *et al.*, 2019). Interestingly, it was suggested that spermatophytes co-opted the already existing LD protein framework, evolved to tolerate drought and desiccation, for the development of seeds and seed-specific programs (de Vries and Ischebeck, 2020). Not only SLDP2.1 has a distinct homologue in a non-seed species, but also e.g. LIPID DROPLET PROTEIN OF SEEDS (LDPS), another LD-protein in seeds, has homologues in streptophyte algae. Regarding the homologues of LD proteins from Arabidopsis seeds in non-seed species, authors speculate that seed-specific LD proteins might already

have evolved before seeds did, which is certainly true for some LD proteins (de Vries and Ischebeck, 2020). In the case of SLDP2.1 a homology outside of seed plants was only observed for the C-terminus of the *S. moellendorffii* midasin isoform (the last 65 of around 405 amino acids) and the C-terminus of SLDP2.1 (last 65 amino acids of 295). This part of the annotated *S. moellendorffii* midasin does not harbour any particular domains. However, the C-terminus of SLDP2 is highly conserved in angiosperm SLDP2 homologues. LIPA homologues, as well as SLDP1.1, SLDP1.2, SLDP1.3 and SLDP2.2 homologues, are only found in flowering plants.

In conclusion, the protein homology analyses implicate a role of SLDP and LIPA specific to seeds of flowering plants, although a distinct relative of SLDP2.1 might already have existed in a non-seed plant and might have been lost in other species. Either, SLDP and LIPA indeed fulfil a function that is specific to seeds, or the proteins represent an example of convergent evolution in LD proteins and do have functional analogues but lack sequence homologues, similar to what is observed e.g. for oleosins and perilipins. Similar to oleosins, SLDP and LIPA might be restricted to non-vegetative tissues with other proteins taking over their functions in vegetative tissues (and putatively non-seed species). However, in contrast to oleosins, SLDP and LIPA transcripts, at least in Arabidopsis, are not found in other reproductive tissues, such as pollen. A more detailed functional analysis of SLDP and LIPA in seeds and seedlings as well as their physiological implication will shed more light on the evolution of this two protein families.

7.2.2 SLDP targeting to LDs via its N-terminus might be a conserved mechanism

Interestingly, transgenic expression of various LD proteins across species was shown to result in proper LD-localisation, suggesting a conserved targeting mechanism, however no specific targeting signal for LDs has been identified so far (reviewed in Zhang and Liu, 2017; Olzmann and Carvalho, 2019).

Generally, LD-localised proteins have been classified in two groups: Class I proteins that associate to the LD monolayer through hydrophobic domains and Class II proteins that associate via amphipathic helices or FA modifications (Kory *et al.*, 2016; Bersuker and Olzmann, 2017). The classification of proteins into these two groups is a generalisation, as actiual protein topologies often remain unknow, but was described to provide a ‘conceptual framework for discussing how proteins associate with the LD membrane’ (Bersuker and Olzmann, 2017) and is therefore used here. Class I proteins enter the LD membrane by lateral diffusion from the ER, where they are inserted into the membrane, through lipidic ER-LD bridges. Most of them adopt a hairpin conformation, so that often the C- as well as the N-terminus are located towards the cytosol. Typically, these proteins can be accommodated in ER bilayers as well as LD monolayers. In the absence of LDs, these proteins localise

throughout the ER (reviewed in Olzmann and Carvalho, 2019). Regulation of the partitioning of class I LD proteins from the ER to LDs and their asymmetric distribution between the organelles still poses an open question in LD biology.

Class II proteins insert directly from the cytosol and several modes of association have been reported. Examples are binding via lipid modifications or via interactions with another LD-localised protein. Often, however, class II proteins contain an amphipathic helix, adopting a topology where all hydrophobic residues face one side of the helix and all polar residues face the other side (Kory *et al.*, 2016; Olzmann and Carvalho, 2019). Proteins only fold into this helical structure upon contact with polar-apolar interfaces, such as lipid surfaces, and thereby can adsorb to membranes and anchor proteins there (Giménez-Andrés *et al.*, 2018). Such amphipathic helices can have various properties, depending on their length, the density and size of hydrophobic residues per turn as well as the charge and distribution of polar residues. Interestingly, amphipathic helices do not only serve localisation purposes. They were also shown to be able to sense membrane curvatures and packing defects or levels of lipid desaturation, and they can act as a protective shield for membranes. Perilipin4 for example adopts a giant amphipathic helix structure of 968 amino acids that coats LDs and was suggested to replace the LD monolayer upon LD growth (Čopič *et al.*, 2018). The same study showed that amphipathic helix length, hydrophobicity, and charge influence LD targeting. Some proteins, as e.g. plant LDAP3, completely lack concise targeting sequences and the whole sequence was shown to be needed for proper LD localisation (Gidda *et al.*, 2016).

SLDP, analysed in the present study, likely enters LDs from the ER and is thus a class I protein. Expression analyses in pollen tubes often not only revealed LD-localisation but upon strong expression also ER-like patterning of SLDP. A motif at the N-terminus of SLDP was shown to be necessary (and sufficient) for LD-localisation and is also highly conserved. This part contains an amphipathic helix and a hydrophobic stretch. This hydrophobic stretch is around 40 amino acids long, similar to other class I LD proteins, such as PUX10 or GPAT4 (Wilfling *et al.*, 2013; Kretzschmar *et al.*, 2018). GPAT4, a protein that targets only a subpopulation of LDs in *Drosophila melanogaster*, contains a 44 amino acid hairpin, consisting of two hydrophobic helices linked by three amino acids. This hairpin alone was shown to be sufficient to mediate ER localisation and subsequent LD re-localisation. Similar proteins, as e.g. AGPAT1 or DGAT1 that remain in the ER membrane and are not relocated to LDs, have similar topologies but with longer and hydrophilic linker regions within the hairpin. If the hairpin linker region of GPAT4 is replaced by such a longer hydrophilic linker sequence, GPAT4 localises to the ER but fails to relocate to LDs. On the other hand, if the hairpin itself is replaced by a hydrophilic linker sequence, GPAT4 fails to insert into the ER but is directly recruited to LDs from the cytosol (Wilfling *et al.*, 2013). Thus, the hairpin is likely needed for ER localisation and

the linker allows for re-localisation to LDs, however yet another C- or N-terminal region contributes to LD localisation. An interplay of a positively charged region followed by a central hydrophobic domain was also shown to be necessary for proper LD localisation of mammalian class I LD proteins and it was hypothesised that the hydrophobic domain mediates ER membrane localisation, while the positively charged stretch then mediates sorting and loading onto LDs (Ingelmo-Torres *et al.*, 2009).

Similarly, in the present study, the hydrophobic stretch of SLDP might mediate ER localisation of SLDP1 and SLPD2 and the amphipathic helix might facilitate loading of the protein onto LDs. More detailed analyses on the amphipathic helix and the hydrophobic stretch alone have to be conducted to clarify the exact mode of localisation. Interestingly, by their chemical diversity, amphipathic helixes can mediate specificities of proteins to just certain lipids – thereby allowing for specific targeting to organellar subdomains or formation of subpopulations of organelles, if there is a compositional bias in the membranes. This way, subpopulations of LDs with a certain protein coat might be created by varying the phospholipid composition (and/or curvature/desaturation) of LDs. This mechanism could explain, why only a portion of LDs in seedlings are in contact to the PM but not all. The putative amphipathic helix of SLDP might only adsorb to certain, 'matching' LDs and only these LDs will be anchored to the PM by the subsequent interaction of SLDP and LIPA. However, *in silico* analysis does not provide sufficient proof for true amphipathic helix formation of SLDP. The putative adoption of this conformation for LD targeting could e.g. be verified by systematic cysteine mutagenesis and subsequent solvent accessibility analysis via PEGylation assays as described in (Pataki *et al.*, 2018).

PM-localised LIPA would be a class II LD protein that most likely binds LDs from the cytosol through interaction with another LD-localised protein. Masking the C-terminus leads to re-localisation of LIPA to the cytosol and not e.g. retention in the ER. LIPA is thus likely not a subject of the secretory pathway, but probably recruited to the PM from the cytosol. Concomitantly, SLDP probably recruits LIPA to LDs directly from the cytosol or when LIPA is already bound to the PM.

The exact mechanism by which SLDP and LIPA are targeted to LDs and the putative creation of LD subpopulations by differential protein recruiting poses a promising topic for future studies and might contribute to a general understanding of LD targeting, not just in plants but in all eukaryotes.

7.3 Functional diversity of LDs in vegetative and reproductive tissues

There are differences of LDs in vegetative and reproductive tissues. LDs in reproductive tissues have mostly been implicated in FA storage and supply, while LDs in vegetative tissues are often associated to stress responses. Generally, less is known about stress responses of LDs in reproductive tissues. In manuscript II, we show a clear correlation of LD-stored TAGs and stress response in a reproductive tissue, the pollen tube.

7.3.1 Specific functions of LDs in vegetative tissues

Usually, vegetative tissues do not accumulate LDs in higher amounts. Various abiotic and biotic stresses as well as senescence have however been reported to induce LD accumulation in vegetative tissues (reviewed in Yang and Benning, 2018; Lu *et al.*, 2020).

Major functional differences between LDs in vegetative and reproductive tissues are determined by the coating proteins. Oleosins represent by far the most abundant proteins on seed LDs, followed by caleosins (Katavic *et al.*, 2006; Thakur and Bhatla, 2016; Zhi *et al.*, 2017; Hamada *et al.*, 2020; Kretzschmar *et al.*, 2020). LD proteomes in non-seed tissues are less well studied, but as described in section 1.1.2, some proteome data are available. In mesocarp tissues, neither oleosins nor caleosins were detected, but LDAP is one of the most abundant proteins in Chinese tallow and avocado mesocarp (Horn *et al.*, 2013; Zhi *et al.*, 2017). In leaves, oleosins are not detected in ageing or in *Pseudomonas*-infected leaves. A study on senescing Arabidopsis leaves instead reported CLO3 and LDAP1 to be the most abundant LD-proteins (Brocard *et al.*, 2017) and in a study on infected leaves in comparison to senescing leaves, similar results were obtained: Two of the four most abundant proteins in infected, as well as senescing leaves, were again CLO3 and LDAP1. Some other proteins like LDAP3 or α-DOX were only detected in LD proteomes of infected leaves (Fernández-Santos *et al.*, 2020), suggesting a dynamic adaptation of the LD protein coat, according to cellular needs. Interestingly, in *Nicotiana tabacum* pollen tubes, caleosin and oleosin isoforms (NtOLE6, NtCLO1) were found most abundant on LDs, but also a Tobacco LDAP1 isoform is amongst the most abundant proteins on LDs (Kretzschmar *et al.*, 2018).

Generally, the proteins found on vegetative LDs are often involved in stress responses, reflecting the observed increase of LDs in vegetative tissues upon various stresses (Singer *et al.*, 2016; Yang and Benning, 2018). Arabidopsis LDAPs were shown to be involved in abiotic stress responses and are needed for LD proliferation in leaves following heat or cold stress (Gidda *et al.*, 2016). LDAPs are also involved in drought stress response and double knockout of *LDAP1* and *LDAP3* renders plants more susceptible to drought stress, while overexpression increases drought tolerance in Arabidopsis (E., Y., Kim *et al.*, 2016). Also, LDs in leaves are diurnally controlled in a process requiring LDAP1-3 and increase in abundance towards the end of the night (Gidda *et al.*, 2016). CLO3 and α-DOX1 have been reported to act together in

response to senescence or fungal infections in leaves to produce antimicrobial phytoalexins (Shimada *et al.*, 2014) but are also found in seedlings grown under sterile conditions (Kretzschmar *et al.*, 2020). CLO3, also called RESPONSIVE TO DEHYDRATION20 (RD20) moreover plays a role in oxidative stress (Blée *et al.*, 2014) as well in drought tolerance, as knockout leads to increased stomatal apertures and transpiration rates (Aubert *et al.*, 2010). Involvement in stomatal opening and closure is therefore another supposed function of LDs in vegetative tissues (reviewed in Yang and Benning, 2018). Indeed, guard cells accumulate LDs in larger amounts than other leaf cells. ATP generated from β-oxidation of TAGs was hypothesised to drive light-induced stomatal opening, as opening is delayed after genetic or chemical inhibition of TAG catabolism (McLachlan *et al.*, 2016). Supporting a putative role of TAG-derived FAs in stomatal closure and opening, knockout of the β-oxidation enzyme 3-ketoacyl-CoA thiolase-2 (KAT2), that influences abscisic acid (ABA)-induced stomatal closure, was shown to reduce stomatal closure (Jiang *et al.*, 2011).

Cross talk of LDs and ABA is also observed in seedlings (a vegetative tissue). The transcription factor ABA insensitive (ABI) 4, a key regulator in ABA signalling, was shown to bind the promoter of *DGAT1* under nitrogen-deficiency, increasing *DGAT1* expression and consequently TAG accumulation (Yang *et al.*, 2011). Both, ABI4 and ABI5 transcription factors were later shown to synergistically regulate *DGAT1* in 7-day-old seedlings under different stresses, including e.g. salt or osmotic stress (Kong *et al.*, 2013). In drought-stressed seedlings, ABA-dependent TAG accumulation was shown to be regulated by the transcription factor MYB96, in drought-stressed seedlings (H., G., Lee *et al.*, 2019). Based on these data, a tight correlation of stress-induced ABA accumulation and stress-induced TAG accumulation in vegetative tissues was suggested (Lu *et al.*, 2020).

Concluding, all these data show that LDs in vegetative tissues are involved in a wealth of abiotic and biotic stress responses.

7.3.2 Specific functions of LDs in reproductive tissues

Generally, less is known about LDs in stress response in seeds. There, stress-inducible LDs might be masked by the sheer mass of storage LDs. It is thinkable, that in seeds, different subpopulations of LDs exist: the huge subpopulation dedicated to storage purposes and a small, ‘basal’ subpopulation that is needed for stress response. The few LDs detected in leaves might reflect this basal amount of LDs. Especially MCS have been reported to be involved in the creation of organellar subpopulations within one cell. The putative LD-PM MCS analysed in the present thesis did not seem to have an impact on TAG degradation rates, nor was any phenotype observable after knocking the tether out. It is therefore possible, that the LD-PM anchor is only important for a subset of LDs in seeds and a physiological role only comes into effect under stress conditions. The MCS might therefore pose an example for creating different

subpopulations of LDs, which could be important for stress-related functions of LDs in reproductive tissues (the seed) and/or vegetative tissues (the seedling).

A specific role of LDs in reproductive tissues is during fertilisation. LDs have been shown to accumulate in flower petals, tapetum cells of anthers, pollen grains, and wet stigmata and have several functions there, e.g. forming the pollen coat or providing energy and carbons for pollen germination and tube growth (reviewed in Yang and Benning, 2018; Ischebeck *et al.*, 2020). Indeed, TAGs are crucial for pollen, as *pdat1 dgat1* double knockout pollen grains, that are incapable of accumulating TAGs and LDs, are male sterile (Zhang *et al.*, 2009). Also, mutants defective in Seipin, that produce enlarged LDs that cannot enter the growing pollen tube from the pollen grain, are also strongly impaired in male fertility (Taurino *et al.*, 2018). However, the amount of TAGs accumulated in pollen was calculated to be insufficient to generate enough energy and/or membrane lipids to fuel pollen tube growth and fertilisation alone (Ischebeck, 2016) and at least in tobacco pollen tubes, peroxisomes do not seem to get in contact with peroxisomes (Müller *et al.*, 2017). Instead, pollen tubes depend on nourishment from female tissues (Selinski and Scheibe, 2014). Therefore, LDs in pollen likely have further functions. Pollen tube penetration and directional pollen tube growth are two such processes shown to require TAGs (reviewed in Yang and Benning, 2018). Polyunsaturated TAGs in the exudate of wet stigmata for example (e.g. in *Nicotiana tabacum*) are sufficient and necessary for directional pollen tube penetration (Wolters-Arts *et al.*, 1998; Yang and Benning, 2018). Also, LDs are e.g. involved in pollen coat formation, a layer covering the pollen grain involved in pollen protection and stigma-interaction (Lévesque-Lemay et al., 2016).

What is more, OIL BODY ASSOCIATED LIPASE 1 (OBL1), a lipase shown to be important for Tobacco pollen tube growth (Müller and Ischebeck, 2017), is also reported to be involved in the production of oxylipin-derived volatiles in tomato leaves (Garbowicz *et al.*, 2018) and was suggested to play a similar role in Tobacco pollen tubes (Ischebeck *et al.*, 2020).

Another function of LDs especially in pollen and seeds might be involvement in brassinosteroid (BR) metabolism. BRs are a class of polyhydroxysteroid phytohormones first discovered in the 1970s (Mitchell *et al.*, 1970; Mitchell and Gregory, 1972). They are involved in a plethora of cellular processes and play crucial roles in plant growth, development and stress tolerance. Several lines of evidence might hint at an involvement of LDs in BR metabolism. Firstly, BRs by far accumulate strongest in immature seeds and pollen with 1–100 µg/kg fresh weight – both of which are organs rich in LDs – while e.g. leaves (containing few LDs) usually only accumulate amounts of 0.01–0.1 µg/kg fresh weight (Bajguz, 2011). Also, BRs are for example involved in in seed dormancy and post-germinative growth (Hu and Yu, 2014), they play a role in leaf senescence (Chory *et al.*, 1991), stress responses (Anwar *et al.*, 2018), plant immunity (Lozano-Durán and Zipfel, 2015; Shigenaga and Argueso, 2016), pollen viability and tube

growth and pollen exine patterning (reviewed in Ye *et al.*, 2010). As already reviewed in this thesis, LDs were shown to play a role in all of these processes, too. What is more, overexpression of the LD-protein HYDROXYSTEROID DEHYDROGENASE 1 (HSD1) in Arabidopsis was shown to result in similar phenotypes as overproduction of BRs. Plants exhibited hypersensitivity towards exogenous BR, while germination was hyposensitive to the BR antagonist abscisic acid (ABA) (Li *et al.*, 2007). Although the exact function of plant HSDs remain elusive, they have been suggested to play a role in BR synthesis (L.,-J., Lin *et al.*, 2002; Ischebeck *et al.*, 2020). Lastly, BRs are synthesised in cycloartenol- or cycloartanol-dependent pathways (Bajguz *et al.*, 2020). In plants, two key sterol synthesis genes have been shown to localise to LDs: CAS1, catalysing the reaction from squalene to cycloartenol and SMT1, catalysing the conversion of cycloartenol to 24-methylencycloartenol (Kretzschmar *et al.*, 2018). Taken together, all these data strongly suggest a role of LDs in BR metabolism.

Interestingly, in the present study on heat stressed pollen tubes, a 125-fold increase of a Tobacco *HSD5* isoform was observed. Indeed, exogenously applied BRs have been reported to convey tolerance against heat stress in e.g. Arabidopsis seedlings or turf grass (reviewed in Divi *et al.*, 2010; Alam *et al.*, 2018). What is more, BRASSINAZOLE RESISTANT 1 (BZR1), one of the main transcription factors regulating BR-responses, was shown to be involved in heat stress tolerance in tomato (Yin *et al.*, 2018). Taken together, the increase of LDs, as measured by increased TAG-levels, in heat-stressed pollen tubes might also mediate thermotolerance by playing a role in BR accumulation through increased *HSD5* levels. Analysis of BR levels in heat stressed pollen tubes might give further insights into a putative correlation of LDs, BRs and thermotolerance.

Another putative role for LDs in heat-stressed pollen tubes was demonstrated in the present thesis. Heat stress induces lipid remodelling of phospholipids, causing a decrease of unsaturated FAs in phospholipids and an unspecific increase in TAG species. Putatively, TAGs in pollen tubes can serve as a sink for released membrane lipids that are likely channelled into TAGs in a DGAT-dependent manner. Interestingly, although an increase in several *DGAT* isoforms was observed in the present study, none of the transcription factors involved in stress-induced *DGAT*-expression in vegetative tissues, such as MYB96 (H., G., Lee *et al.*, 2019) or ABI4/ABI5 (Kong *et al.*, 2013), were induced by heat stress. This suggests that in pollen tubes, other transcription factors might be involved in stress-induced expression of *DGATs*, potentially MYB-related transcription factors, which showed transcriptional up-regulation. Also, in contrast to what has been described for e.g. heat-stressed *Chlamydomonas reinhardtii* (Légeret *et al.*, 2016), very few significant expression differences of transcripts encoding enzymes involved in lipid metabolism were observed here.

Further analyses of heat stressed pollen tubes, impaired in TAG accumulation (e.g. *dgat1* or *pdat1* mutants) could give further insights on putative heat stress adaptation mechanisms in pollen tubes.

7.4 Concluding remarks

The aim of this thesis was to shed light on functions of LDs in two different plant organs – seeds and pollen tubes. For this, two approaches were used: In a bottom-up approach, unknown proteins localising to LDs were analysed to find out about their functions and thereby potentially unravel previously unknown processes involving LDs. In a top-down approach, a process already known to involve LDs but through uncertain molecular mechanisms and proteins was analysed. Concludingly, both approaches used in this thesis gave new insights into the intricate and versatile biology of LDs: one identified a previously unknown putative tethering complex, anchoring LDs to the PM during post-germinative growth. The other shed light on the involvement of LDs as putative lipid hubs for heat-induced lipid remodelling in pollen tubes.

Regarding the identification of an LD-PM tethering complex, two previously unknown LD-proteins, SLDP1 and SLDP2, were identified from a proteomic screen of LD-enriched *Arabidopsis thaliana* seedling fractions. Their localisation to LDs was confirmed and knockout phenotypes, such as increased oil accumulation in seeds and aberrant cellular LD distribution, were discovered. Moreover, an interaction partner, LIPA, another previously unknown protein, was identified by a proteomic analyses of *sldp* knockouts. Knockout of LIPA causes the same aberrant LD localisation as SLDP knockout. It was found that the interaction partner alone does not localise to LDs but to the PM. It can however be recruited to LDs in a non-native tissue by co-expressing SLDP and LIPA. What is more, it can relocate SLDP-decorated LDs to the PM and immobilise them there in pollen tubes. So far, no physiological consequences of losing this tethering mechanism in its native tissue could be observed. We speculate that SLDP and LIPA interact to form an MCS between the PM and LDs, importance of which might only come into effect upon stress conditions, such as salt, mechanic or cold stress. The ER, and putatively also LDs, are then be needed in proximity to the PM to facilitate membrane repair and LDs might act as a buffering system to protect the cell from free FAs.

Concerning the role of LDs in heat-induced lipid remodelling, we found that relative and absolute TAG levels unspecifically increase upon heat stress. Transcriptome analysis revealed increases of several *DGAT* homologues. To adapt membrane properties to the increased temperatures, unsaturated FAs have to be removed. As an increase of several TAG-derived FAs, not just unsaturated ones, is observed. We suggest that upon heat stress, there is an unspecific bulk degradation of membrane lipids. To prevent lipotoxicity of free FAs, acyl chains are putatively channelled into the TAG-pool, where they might be stored for later reuse or from where they might be channelled to degradation. As no relative decrease in most phospholipid species is observed, concomitant to bulk degradation, probably *de novo* synthesis might occur. This is however not reflected on a transcriptional level. Apart from this presumed TAG-

mediated thermotolerance, lipidome, transcriptome and metabolome data analyses revealed several other adaptations of pollen tubes to heat stress. The increase of pollen specific sterol species upon heat stress and the concomitant increased transcript expression of SMO2, an enzyme involved in sterol metabolism, are one example. Other examples are e.g. the observed differential accumulation of several TCA-intermediates and several other primary metabolites or the increased expression of several transcription factors of the MYB-related or the AP2-EREBP family. Taken together, the study provides multifaceted insights into the many layers of heat stress adaptation in Tobacco pollen tubes and contributes many incentives for future research.

References

Alam, M.N., Zhang, L., Yang, L., Islam, M.R., Liu, Y., Luo, H., Yang, P., Wang, Q. and Chan, Z. (2018) Transcriptomic profiling of tall fescue in response to heat stress and improved thermotolerance by melatonin and 24-epibrassinolide. *BMC Genomics*, **19**, 1–14.

Allen, J.W., Tevatia, R., Demirel, Y., DiRusso, C.C. and Black, P.N. (2018) Induction of oil accumulation by heat stress is metabolically distinct from N stress in the green microalgae *Coccomyxa subellipsoidea* C169. *PLoS One*, **13**, 1–20.

Almeida, J., Perez-Fons, L. and Fraser, P.D. (2020) A transcriptomic, metabolomic and cellular approach to the physiological adaptation of tomato fruit to high temperature. *Plant. Cell Environ.*, pce.13854.

Andersson, M.X., Goksör, M. and Sandelius, A.S. (2007) Optical manipulation reveals strong attracting forces at membrane contact sites between endoplasmic reticulum and chloroplasts. *J. Biol. Chem.*, **282**, 1170–1174.

Anwar, A., Liu, Y., Dong, R., Bai, L., Yu, X. and Li, Y. (2018) The physiological and molecular mechanism of brassinosteroid in response to stress: A review. *Biol. Res.*, **51**, 1–15.

Aubert, Y., Vile, D., Pervent, M., Aldon, D., Ranty, B., Simonneau, T., Vavasseur, A. and Galaud, J.P. (2010) RD20, a stress-inducible caleosin, participates in stomatal control, transpiration and drought tolerance in *Arabidopsis thaliana*. *Plant Cell Physiol.*, **51**, 1975–1987.

Baillie, A.L., Falz, A.L., Müller-Schüssele, S.J. and Sparkes, I. (2020) It started with a kiss: Monitoring organelle interactions and identifying membrane contact site components in plants. *Front. Plant Sci.*, **11**.

Bajguz, A. (2011) Brassinosteroids – occurence and chemical structures in plants. In *Brassinosteroids: A Class of Plant Hormone*. Dordrecht: Springer Netherlands, pp. 1–27.

Bajguz, A., Chmur, M. and Gruszka, D. (2020) Comprehensive overview of the brassinosteroid biosynthesis pathways: substrates, products, inhibitors, and connections. *Front. Plant Sci.*, **11**, 1–9.

Banks, J.A. (2009) Selaginella and 400 million years of separation. *Annu. Rev. Plant Biol.*, **60**, 223–238.

Banks, J.A., Nishiyama, T., Hasebe, M., et al. (2011) The selaginella genome identifies genetic changes associated with the evolution of vascular plants. *Science*, **332**, 960–963.

Barbosa, A.D., Savage, D.B. and Siniossoglou, S. (2015) Lipid droplet–organelle interactions: emerging roles in lipid metabolism. *Curr. Opin. Cell Biol.*, **35**, 91–97.

Barbosa, A.D., Sembongi, H., Su, W.M., Abreu, S., Reggiori, F., Carman, G.M. and Siniossoglou, S. (2015) Lipid partitioning at the nuclear envelope controls membrane biogenesis. *Mol. Biol. Cell*, **26**, 3641–3657.

Barbosa, A.D. and Siniossoglou, S. (2017) Function of lipid droplet-organelle interactions in lipid homeostasis. *Biochim. Biophys. Acta - Mol. Cell Res.*, **1864**, 1459–1468.

Bates, P.D. (2016) Understanding the control of acyl flux through the lipid metabolic network of plant oil biosynthesis. *Biochim. Biophys. Acta - Mol. Cell Biol. Lipids*, **1861**, 1214–1225.

Bates, P.D. and Browse, J. (2012) The significance of different diacylgycerol synthesis pathways on plant oil composition and bioengineering. *Front. Plant Sci.*, **3**, 1–11.

Bates, P.D., Stymne, S. and Ohlrogge, J. (2013) Biochemical pathways in seed oil synthesis. *Curr. Opin. Plant Biol.*, **16**, 358–364.

Baud, S., Dubreucq, B., Miquel, M., Rochat, C. and Lepiniec, L. (2008) Storage reserve accumulation in Arabidopsis: metabolic and developmental control of seed filling. *Arab. B.*, **6**.

Baumann, N.A., Sullivan, D.P., Ohvo-Rekilä, H., Simonot, C., Pottekat, A., Klaassen, Z., Beh, C.T. and Menon, A.K. (2005) Transport of newly synthesized sterol to the sterol-enriched plasma membrane occurs via nonvesicular equilibration. *Biochemistry*, **44**, 5816–5826.

Beaudoin, F., Wilkinson, B.M., Stirling, C.J. and Napier, J.A. (2000) *In vivo* targeting of a sunflower oil body protein in yeast secretory (sec) mutants. *Plant J.*, **23**, 159–170.

Benador, I.Y., Veliova, M., Mahdaviani, K., et al. (2018) Mitochondria bound to lipid droplets have unique bioenergetics, composition, and dynamics that support lipid droplet expansion. *Cell Metab.*, **27**, 869–885.

Benning, C. (2008) A role for lipid trafficking in chloroplast biogenesis. *Prog. Lipid Res.*, **47**, 381–389.

Bersuker, K. and Olzmann, J.A. (2017) Establishing the lipid droplet proteome: Mechanisms of lipid droplet protein targeting and degradation. *Biochim. Biophys. Acta - Mol. Cell Biol. Lipids*, **1862**, 1166–1177.

Binns, D., Januszewski, T., Chen, Y., et al. (2006) An intimate collaboration between peroxisomes and lipid bodies. *J. Cell Biol.*, **173**, 719–731.

Blée, E., Boachon, B., Burcklen, M., et al. (2014) The reductase activity of the Arabidopsis caleosin RESPONSIVE TO DESSICATION20 mediates gibberellin-dependent flowering time, abscisic acid sensitivity, and tolerance to oxidative stress. *Plant Physiol.*, **166**, 109–124.

Bohnert, M. (2019) Organelle contact sites: Lipid droplets hooked by metabolically controlled tethers. *Curr. Biol.*, **29**, R375–R377.

Bohnert, M. (2020) Tethering fat: Tethers in lipid droplet contact sites. *Contact*, **3**.

Booth, D.M., Enyedi, B., Geiszt, M., Várnai, P. and Hajnóczky, G. (2016) Redox nanodomains are induced by and control calcium signaling at the ER-mitochondrial interface. *Mol. Cell*, **63**, 240–248.

Bosma, M., Dapito, D.H., Drosatos-Tampakaki, Z., Huiping-Son, N., Huang, L.S., Kersten, S., Drosatos, K. and Goldberg, I.J. (2014) Sequestration of fatty acids in triglycerides prevents endoplasmic reticulum stress in an *in vitro* model of cardiomyocyte lipotoxicity. *Biochim. Biophys. Acta - Mol. Cell Biol. Lipids*, **1841**, 1648–1655.

Brito, O.M. De and Scorrano, L. (2008) Mitofusin 2 tethers endoplasmic reticulum to mitochondria. *Nature*, **456**, 605–610.

Brocard, L., Immel, F., Coulon, D., et al. (2017) Proteomic analysis of lipid droplets from Arabidopsis aging leaves brings new insight into their biogenesis and functions. *Front. Plant Sci.*, **8**.

Buhman, K.K., Chen, H.C. and Farese, R. V. (2001) The enzymes of neutral lipid synthesis. *J. Biol. Chem.*, **276**, 40369–40372.

Cai, Y., Goodman, J.M., Pyc, M., Mullen, R.T., Dyer, J.M. and Chapman, K.D. (2015) Arabidopsis SEIPIN proteins modulate triacylglycerol accumulation and influence lipid droplet proliferation. *Plant Cell*, **27**, 2616–2636.

Cartwright, B.R., Binns, D.D., Hilton, C.L., Han, S., Gao, Q. and Goodman, J.M. (2015) Seipin performs dissectible functions in promoting lipid droplet biogenesis and regulating droplet morphology. *Mol. Biol. Cell*, **26**, 726–739.

Chang, W., Zhang, M., Zheng, S., et al. (2015) Trapping toxins within lipid droplets is a resistance mechanism in fungi. *Sci. Rep.*, **5**, 1–11.

Chapman, K.D., Aziz, M., Dyer, J.M. and Mullen, R.T. (2019) Mechanisms of lipid droplet biogenesis. *Biochem. J.*, **476**, 1929–1942.

Chen, J.C.F., Tsai, C.C.Y. and Tzen, J.T.C. (1999) Cloning and secondary structure analysis of caleosin, a unique calcium-binding protein in oil bodies of plant seeds. *Plant Cell Physiol.*, **40**, 1079–1086.

Chitraju, C., Mejhert, N., Haas, J.T., et al. (2017) Triglyceride synthesis by DGAT1 protects adipocytes from lipid-induced ER stress during lipolysis. *Cell Metab.*, **26**, 407–418.

Chory, J., Nagpal, P. and Peto, C. (1991) Phenotypic and genetic analysis of det2, a new mutant that affects light-regulated seedling development in Arabidopsis. *Plant Cell*, **3**, 445–459.

Choudhary, V., Atab, O. El, Mizzon, G., Prinz, W.A. and Schneiter, R. (2020) Seipin and Nem1 establish discrete ER subdomains to initiate yeast lipid droplet biogenesis. *J. Cell Biol.*, **219**.

Choudhary, V., Ojha, N., Golden, A. and Prinz, W.A. (2015) A conserved family of proteins facilitates nascent lipid droplet budding from the ER. *J. Cell Biol.*, **211**, 261–271.

Choudhary, V. and Schneiter, R. (2020) Lipid droplet biogenesis from specialized ER subdomains. *Microb. Cell*, **7**, 218–221.

Cieri, D., Vicario, M., Giacomello, M., et al. (2018) SPLICS: A split green fluorescent protein-based contact site sensor for narrow and wide heterotypic organelle juxtaposition. *Cell Death Differ.*, **25**, 1131–1145.

Coleman, R.A. (2020) The “discovery” of lipid droplets: A brief history of organelles hidden in plain sight. *Biochim. Biophys. Acta - Mol. Cell Biol. Lipids*, **1865**, 1–9.

Converti, A., Casazza, A.A., Ortiz, E.Y., Perego, P. and Borghi, M. Del (2009) Effect of temperature and nitrogen concentration on the growth and lipid content of Nannochloropsis oculata and Chlorella vulgaris for biodiesel production. *Chem. Eng. Process. Process Intensif.*, **48**, 1146–1151.

Čopič, A., Antoine-Bally, S., Giménez-Andrés, M., Torre Garay, C. La, Antonny, B., Manni, M.M., Pagnotta, S., Guihot, J. and Jackson, C.L. (2018) A giant amphipathic helix from a perilipin that is adapted for coating lipid droplets. *Nat. Commun.*, **9**, 1–16.

Csordás, G., Várnai, P., Golenár, T., Roy, S., Purkins, G., Schneider, T.G., Balla, T. and Hajnóczky, G. (2010) Imaging interorganelle contacts and local calcium dynamics at the ER-mitochondrial interface. *Mol. Cell*, **39**, 121–132.

Cui, S., Hayashi, Y., Otomo, M., Mano, S., Oikawa, K., Hayashi, M. and Nishimura, M. (2016) Sucrose production mediated by lipid metabolism suppresses the physical interaction of peroxisomes and oil bodies during germination of *Arabidopsis thaliana*. *J. Biol. Chem.*, **291**, 19734–19745.

Datta, S., Liu, Y., Hariri, H., Bowerman, J. and Henne, W.M. (2019) Cerebellar ataxia disease-associated Snx14 promotes lipid droplet growth at ER-droplet contacts. *J. Cell Biol.*, **218**, 1335–1351.

Dawaliby, R. and Mayer, A. (2010) Microautophagy of the nucleus coincides with a vacuolar diffusion barrier at nuclear–vacuolar junctions. *Mol. Biol. Cell*, **21**, 4173–4183.

Deruyffelaere, C., Purkrtova, Z., Bouchez, I., Collet, B., Cacas, J.L., Chardot, T., Gallois, J.L. and D'Andrea, S. (2018) PUX10 IS A CDC48A adaptor protein that regulates the extraction of ubiquitinated oleosins from seed lipid droplets in Arabidopsis. *Plant Cell*, **30**, 2116–2136.

Dickson, E.J. and Hille, B. (2019) Understanding phosphoinositides: rare, dynamic, and essential membrane phospholipids. *Biochem. J.*, **476**, 1–23.

Ding, B., Turgeon, R. and Parthasarathy, M. V. (1992) Substructure of freeze-substituted plasmodesmata. *Protoplasma*, **169**, 28–41.

Divi, U.K., Rahman, T. and Krishna, P. (2010) Brassinosteroid-mediated stress tolerance in Arabidopsis shows interactions with abscisic acid, ethylene and salicylic acid pathways. *BMC Plant Biol.*, **10**, 151.

Domenico, S. De, Tsesmetzis, N., Sansebastiano, G. Pietro Di, Hughes, R.K., Casey, R. and Santino, A. (2007) Subcellular localisation of *Medicago truncatula* 9/13-hydroperoxide lyase reveals a new localisation pattern and activation mechanism for CYP74C enzymes. *BMC Plant Biol.*, **7**, 1–13.

Eastmond, P.J. (2004) Cloning and characterization of the acid lipase from Castor beans. *J. Biol. Chem.*, **279**, 45540–45545.

Eastmond, P.J. (2006) SUGAR-DEPENDENT1 encodes a patatin domain triacylglycerol lipase that initiates storage oil breakdown in germinating Arabidopsis seeds. *Plant Cell*, **18**, 665–675.

Eckardt, N.A. (2008) Arabidopsis synaptotagmin1 maintains plasma membrane integrity. *Plant Cell*, **20**, 3182.

Edqvist, J., Blomqvist, K., Nieuwland, J. and Salminen, T.A. (2018) Plant lipid transfer proteins: Are we finally closing in on the roles of these enigmatic proteins? *J. Lipid Res.*, **59**, 1374–1382.

Eisenberg-Bord, M., Shai, N., Schuldiner, M. and Bohnert, M. (2016) A tether is a tether is a tether: Tethering at membrane contact sites. *Dev. Cell*, **39**, 395–409.

Esnay, N., Dyer, J.M., Mullen, R.T. and Chapman, K.D. (2020) Lipid Droplet–Peroxisome Connections in Plants. *Contact*, **3**, 251525642090876.

Fahy, E., Subramaniam, S., Brown, H.A., et al. (2005) A comprehensive classification system for lipids. *Eur. J. Lipid Sci. Technol.*, **107**, 337–364.

Fan, J., Yu, L. and Xu, C. (2017) A central role for triacylglycerol in membrane lipid breakdown, fatty acid *β*-Oxidation, and plant survival under extended darkness. *Plant Physiol.*, **174**, 1517–1530.

Fan, J., Yu, L. and Xu, C. (2019) Dual role for autophagy in lipid metabolismin Arabidopsis. *Plant Cell*, **31**, 1598–1613.

Farmer, J.B. (1901) The Cell in development and inheritance. *Nature*, **63**, 437–438.

Fei, W., Shui, G., Gaeta, B., et al. (2008) Fld1p, a functional homologue of human seipin, regulates the size of lipid droplets in yeast. *J. Cell Biol.*, **180**, 473–482.

Fernández-Busnadiego, R., Saheki, Y. and Camilli, P. De (2015) Three-dimensional architecture of extended synaptotagmin-mediated endoplasmic reticulum-plasma membrane contact sites. *Proc. Natl. Acad. Sci. U. S. A.*, **112**, E2004–E2013.

Fernández-Santos, R., Izquierdo, Y., López, A., Muñiz, L., Martínez, M., Cascón, T., Hamberg, M. and Castresana, C. (2020) Protein profiles of lipid droplets during the hypersensitive defense response of Arabidopsis against Pseudomonas infection. *Plant Cell Physiol.*, **61**, 1144–1157.

Ferrer, A., Altabella, T., Arró, M. and Boronat, A. (2017) Emerging roles for conjugated sterols in plants. *Prog. Lipid Res.*, **67**, 27–37.

Feußner, I. and Kindl, H. (1992) A lipoxygenase is the main lipid body protein in cucumber and soybean cotyledons during the stage of triglyceride mobilization. *FEBS Lett.*, **298**, 223–225.

Freyre, C.A.C., Rauher, P.C., Ejsing, C.S. and Klemm, R.W. (2019) MIGA2 links mitochondria, the ER, and lipid droplets and promotes *de novo* lipogenesis in adipocytes. *Mol. Cell*, **76**, 811–825.e14.

Fuchs, C.D., Claudel, T., Kumari, P., et al. (2012) Absence of adipose triglyceride lipase protects from hepatic endoplasmic reticulum stress in mice. *Hepatology*, **56**, 270–280.

Funato, K. and Riezman, H. (2001) Vesicular and nonvesicular transport of ceramide from ER to the Golgi apparatus in yeast. *J. Cell Biol.*, **155**, 949–959.

Gao, G., Chen, F.J., Zhou, L., Su, L., Xu, D., Xu, L. and Li, P. (2017) Control of lipid droplet fusion and growth by CIDE family proteins. *Biochim. Biophys. Acta - Mol. Cell Biol. Lipids*, **1862**, 1197–1204.

Gao, H., Metz, J., Teanby, N.A., Ward, A.D., Botchway, S.W., Coles, B., Pollard, M.R. and Sparkes, I. (2016) *In vivo* quantification of peroxisome tethering to chloroplasts in Tobacco epidermal cells using optical tweezers1[OPEN]. *Plant Physiol.*, **170**, 263–272.

Garbowicz, K., Liu, Z., Alseekh, S., et al. (2018) Quantitative trait loci analysis identifies a prominent gene involved in the production of fatty acid-derived flavor volatiles in tomato. *Mol. Plant*, **11**, 1147–1165.

Gidda, S.K., Park, S., Pyc, M., et al. (2016) Lipid Droplet-Associated Proteins (LDAPs) are required for the dynamic regulation of neutral lipid compartmentation in plant cells. *Plant Physiol.*, **170**, 2052–2071.

Giménez-Andrés, M., Čopič, A. and Antonny, B. (2018) The many faces of amphipathic helices. *Biomolecules*, **8**, 1–14.

Goldberg, R.B., Paiva, G. de and Yadegari, R. (1994) Plant embryogenesis: Zygote to seed. *Science*, 266, 605–614.

Gong, J., Sun, Z., Wu, L., et al. (2011) Fsp27 promotes lipid droplet growth by lipid exchange and transfer at lipid droplet contact sites. *J. Cell Biol.*, **195**, 953–963.

Graham, I.A. (2008) Seed storage oil mobilization. *Annu. Rev. Plant Biol.*, **59**, 115–142.

Greer, M.S., Cai, Y., Gidda, S.K., et al. (2020) SEIPIN isoforms interact with the membrane-tethering protein VAP27-1 for lipid droplet formation. *Plant Cell*, **32**, 2932–2950.

Grippa, A., Buxó, L., Mora, G., et al. (2015) The seipin complex Fld1/Ldb16 stabilizes ER-lipid droplet contact sites. *J. Cell Biol.*, **211**, 829–844.

Gross, D.A., Zhan, C. and Silver, D.L. (2011) Direct binding of triglyceride to fat storage-inducing transmembrane proteins 1 and 2 is important for lipid droplet formation. *Proc. Natl. Acad. Sci. U. S. A.*, **108**, 19581–19586.

Haj, F.G., Sabet, O., Kinkhabwala, A., et al. (2012) Regulation of signaling at regions of cell-cell contact by endoplasmic reticulum-bound Protein-Tyrosine Phosphatase 1B. *PLoS One*, **7**, e36633.

Hamada, S., Kishikawa, A. and Yoshida, M. (2020) Proteomic analysis of lipid droplets in *Sesamum indicum*. *Protein J.*, **39**.

Hanada, K., Kumagai, K., Yasuda, S., Miura, Y., Kawano, M., Fukasawa, M. and Nishijima, M. (2003) Molecular machinery for non-vesicular trafficking of ceramide. *Nature*, **426**, 803–809.

Hanano, A., Almousally, I., Shaban, M., Rahman, F., Blee, E. and Murphy, D.J. (2016) Biochemical, transcriptional, and bioinformatic analysis of lipid droplets from seeds of date palm (*Phoenix dactylifera* L.) and their use as potent sequestration agents against the toxic pollutant, 2,3,7,8-tetrachlorinated dibenzo-p-dioxin. *Front. Plant Sci.*, **7**, 1–17.

Hariri, H., Rogers, S., Ugrankar, R., Liu, Y.L., Feathers, J.R. and Henne, W.M. (2018) Lipid droplet biogenesis is spatially coordinated at ER–vacuole contacts under nutritional stress . *EMBO Rep.*, **19**, 57–72.

Hariri, H., Speer, N., Bowerman, J., et al. (2019) Mdm1 maintains endoplasmic reticulum homeostasis by spatially regulating lipid droplet biogenesis. *J. Cell Biol.*, **218**, 1319–1334.

Henne, W.M., Reese, M.L. and Goodman, J.M. (2018) The assembly of lipid droplets and their roles in challenged cells. *EMBO J.*, **37**.

Henne, W.M., Zhu, L., Balogi, Z., Stefan, C., Pleiss, J.A. and Emr, S.D. (2015) Mdm1/Snx13 is a novel ER-endolysosomal interorganelle tethering protein. *J. Cell Biol.*, **210**, 541–551.

Higashi, Y., Okazaki, Y., Myouga, F., Shinozaki, K. and Saito, K. (2015) Landscape of the lipidome and transcriptome under heat stress in *Arabidopsis thaliana*. *Sci. Rep.*, **5**, 1–7.

Higashi, Y. and Saito, K. (2019) Lipidomic studies of membrane glycerolipids in plant leaves under heat stress. *Prog. Lipid Res.*, **75**.

Hill, L.M., Morley-Smith, E.R. and Rawsthorne, S. (2003) Metabolism of sugars in the endosperm of developing seeds of oilseed rape. *Plant Physiol.*, **131**, 228–236.

Horn, P.J., James, C.N., Gidda, S.K., Kilaru, A., Dyer, J.M., Mullen, R.T., Ohlrogge, J.B. and Chapman, K.D. (2013) Identification of a new class of lipid droplet-associated proteins in plants. *Plant Physiol.*, **162**, 1926–1936.

Hornung, E., Pernstich, C. and Feussner, I. (2002) Formation of conjugated Δ11 Δ13-double bonds by Δ12-linoleic acid (1,4)-acyl-lipid-desaturase in pomegranate seeds. *Eur. J. Biochem.*, **269**, 4852–4859.

Hu, Y. and Yu, D. (2014) BRASSINOSTEROID INSENSITIVE2 interacts with ABSCISIC ACID INSENSITIVE5 to mediate the antagonism of brassinosteroids to abscisic acid during seed germination in Arabidopsis. *Plant Cell*, **1**, 1–16.

Huang, C.Y. and Huang, A.H.C. (2017) Unique motifs and length of hairpin in oleosin target the cytosolic side of endoplasmic reticulum and budding lipid droplet. *Plant Physiol.*, **174**, 2248–2260.

Huang, S., Jiang, L. and Zhuang, X. (2019) Possible roles of membrane trafficking components for lipid droplet dynamics in higher plants and green algae. *Front. Plant Sci.*, **10**, 1–8.

Hugenroth, M. and Bohnert, M. (2020) Come a little bit closer! Lipid droplet-ER contact sites are getting crowded. *Biochim. Biophys. Acta - Mol. Cell Res.*, **1867**, 118603.

Hurlock, A.K., Roston, R.L., Wang, K. and Benning, C. (2014) Lipid trafficking in plant cells. *Traffic*, **15**, 915–932.

Ingelmo-Torres, M., González-Moreno, E., Kassan, A., et al. (2009) Hydrophobic and basic domains target proteins to lipid droplets. *Traffic*, **10**, 1785–1801.

Ischebeck, T. (2016) Lipids in pollen - They are different. *Biochim. Biophys. Acta - Mol. Cell Biol. Lipids*, **1861**, 1315–1328.

Ischebeck, T., Krawczyk, H.E., Mullen, R.T., Dyer, J.M. and Chapman, K.D. (2020) Lipid droplets in plants and algae: Distribution, formation, turnover and function. *Semin. Cell Dev. Biol.*

Ishikawa, K., Tamura, K., Ueda, H., Ito, Y., Nakano, A., Hara-Nishimura, I. and Shimada, T. (2018) Synaptotagmin-associated endoplasmic reticulum-plasma membrane contact sites are localized to immobile ER tubules. *Plant Physiol.*, **178**, 641–653.

Jacquier, N., Choudhary, V., Mari, M., Toulmay, A., Reggiori, F. and Schneiter, R. (2011) Lipid droplets are functionally connected to the endoplasmic reticulum in *Saccharomyces cerevisiae*. *J. Cell Sci.*, **124**, 2424–2437.

Jacquier, N., Mishra, S., Choudhary, V. and Schneiter, R. (2013) Expression of oleosin and perilipins in yeast promotes formation of lipid droplets from the endoplasmic reticulum. *J. Cell Sci.*, **126**, 5198–5209.

Jambunathan, S., Yin, J., Khan, W., Tamori, Y. and Puri, V. (2011) FSP27 promotes lipid droplet clustering and then fusion to regulate triglyceride accumulation. *PLoS One*, **6**, 1–12.

Jiang, T., Zhang, X.F., Wang, X.F. and Zhang, D.P. (2011) Arabidopsis 3-Ketoacyl-CoA Thiolase-2 (KAT2), an enzyme of fatty acid β-Oxidation, is involved in ABA signal transduction. *Plant Cell Physiol.*, **52**, 528–538.

Jing, J., He, L., Sun, A., et al. (2015) Proteomic mapping of ER-PM junctions identifies STIMATE as a regulator of Ca^{2+} influx. *Nat. Cell Biol.*, **17**, 1339–1347.

Jolivet, P., Boulard, C., Bellamy, A., Larré, C., Barre, M., Rogniaux, H., D'Andréa, S., Chardot, T. and Nesi, N. (2009) Protein composition of oil bodies from mature *Brassica napus* seeds. *Proteomics*, **9**, 3268–3284.

Jolivet, P., Roux, E., D'Andrea, S., Davanture, M., Negroni, L., Zivy, M. and Chardot, T. (2004) Protein composition of oil bodies in *Arabidopsis thaliana* ecotype WS. *Plant Physiol. Biochem.*, **42**, 501–509.

Jongsma, M.L.L.M., Berlin, I., Wijdeven, R.H.H.M., et al. (2016) An ER-associated pathway defines endosomal architecture for controlled cargo transport. *Cell*, **166**, 152–166.

Jorgensen, J.R., Tei, R., Baskin, J.M., Michel, A.H., Kornmann, B. and Emr, S.D. (2020) ESCRT-III and ER–PM contacts maintain lipid homeostasis. *Mol. Biol. Cell*, **31**, 1302–1313.

Joshi, A.S., Nebenfuehr, B., Choudhary, V., Satpute-Krishnan, P., Levine, T.P., Golden, A. and Prinz, W.A. (2018) Lipid droplet and peroxisome biogenesis occur at the same ER subdomains. *Nat. Commun.*, **9**, 1–12.

Kannan, M., Lahiri, S., Liu, L.K., Choudhary, V. and Prinz, W.A. (2017) Phosphatidylserine synthesis at membrane contact sites promotes its transport out of the ER. *J. Lipid Res.*, **58**, 553–562.

Kassan, A., Herms, A., Fernández-Vidal, A., et al. (2013) Acyl-CoA synthetase 3 promotes lipid droplet biogenesis in ER microdomains. *J. Cell Biol.*, **203**, 985–1001.

Katavic, V., Agrawal, G.K., Hajduch, M., Harris, S.L. and Thelen, J.J. (2006) Protein and lipid composition analysis of oil bodies from two *Brassica napus* cultivars. *Proteomics*, **6**, 4586–4598.

Kim, E.Y., Park, K.Y., Seo, Y.S. and Kim, W.T. (2016) Arabidopsis Small Rubber Particle Protein homolog SRPs play dual roles as positive factors for tissue growth and development and in drought stress responses. *Plant Physiol.*, **170**, 2494–2510.

Kim, R.J., Kim, H.J., Shim, D. and Suh, M.C. (2016) Molecular and biochemical characterizations of the monoacylglycerol lipase gene family of *Arabidopsis thaliana*. *Plant J.*, **85**, 758–771.

Klepikova, A. V., Kasianov, A.S., Gerasimov, E.S., Logacheva, M.D. and Penin, A.A. (2016) A high resolution map of the *Arabidopsis thaliana* developmental transcriptome based on RNA-seq profiling. *Plant J.*, **88**, 1058–1070.

Knoblach, B. and Rachubinski, R.A. (2015) Transport and retention mechanisms govern lipid droplet inheritance in *Saccharomyces cerevisiae*. *Traffic*, **16**, 298–309.

Knoblach, B., Sun, X., Coquelle, N., Fagarasanu, A., Poirier, R.L. and Rachubinski, R.A. (2013) An ER-peroxisome tether exerts peroxisome population control in yeast. *EMBO J.*, **32**, 2439–2453.

Knothe, G. and Dunn, R.O. (2009) A comprehensive evaluation of the melting points of fatty acids and esters determined by differential scanning calorimetry. *JAOCS, J. Am. Oil Chem. Soc.*, **86**, 843–856.

Kong, Y., Chen, S., Yang, Y. and An, C. (2013) ABA-insensitive (ABI) 4 and ABI5 synergistically regulate *DGAT1* expression in Arabidopsis seedlings under stress. *FEBS Lett.*, **587**, 3076–3082.

Kory, N., Farese, R. V. and Walther, T.C. (2016) Targeting fat: Mechanisms of protein localization to lipid droplets. *Trends Cell Biol.*, **26**, 535–546.

Kraemer, F.B., Khor, V.K., Shen, W.-J. and Azhar, S. (2013) Cholesterol ester droplets and steroidogenesis. *Mol. Cell. Endocrinol.*, **371**, 15–19.

Kretzschmar, F.K., Doner, N.M., Krawczyk, H.E., Scholz, P., Schmitt, K., Valerius, O., Braus, G.H., Mullen, R.T. and Ischebeck, T. (2020) Identification of low-abundance lipid droplet proteins in seeds and seedlings. *Plant Physiol.*, **182**, 1326–1345.

Kretzschmar, F.K., Mengel, L.A., Müller, A.O., Schmitt, K., Blersch, K.F., Valerius, O., Braus, G.H. and Ischebeck, T. (2018) PUX10 Is a lipid droplet-localized scaffold protein that interacts with CELL DIVISION CYCLE48 and Is involved in the degradation of lipid droplet proteins. *Plant Cell*, **30**, 2137–2160.

Kriechbaumer, V., Botchway, S.W., Slade, S.E., Knox, K., Frigerio, L., Oparka, K. and Hawes, C. (2015) Reticulomics: Protein-protein interaction studies with two plasmodesmata-localized reticulon family proteins identify binding partners enriched at plasmodesmata, endoplasmic reticulum, and the plasma membrane. *Plant Physiol.*, **169**, 1933–1945.

Kumagai, K. and Hanada, K. (2019) Structure, functions and regulation of CERT, a lipid-transfer protein for the delivery of ceramide at the ER–Golgi membrane contact sites. *FEBS Lett.*, **593**, 2366–2377.

Kvam, E. and Goldfarb, D.S. (2006) Nucleus-vacuole junctions in yeast: Anatomy of a membrane contact site. *Biochem. Soc. Trans.*, **34**, 340–342.

Laibach, N., Post, J., Twyman, R.M., Gronover, C.S. and Pr??fer, D. (2014) The characteristics and potential applications of structural lipid droplet proteins in plants. *J. Biotechnol.*, **201**, 15–27.

Lamberti, C., Nebbia, S., Balestrini, R., et al. (2020) Identification of a caleosin associated with hazelnut (*Corylus avellana* L.) oil bodies. *Plant Biol.*, **22**, 404–409.

Lara, J.A., Burciaga-Monge, A., Chávez, A., Revés, M., Lavilla, R., Arró, M., Boronat, A., Altabella, T. and Ferrer, A. (2018) Identification and characterization of sterol acyltransferases responsible for steryl ester biosynthesis in tomato. *Front. Plant Sci.*, **9**, 1–18.

Lee, E., Vanneste, S., Pérez-Sancho, J., Benitez-Fuente, F., Strelau, M., Macho, A.P., Botella, M.A., Friml, J. and Rosado, A. (2019) Ionic stress enhances ER–PM connectivity via phosphoinositide-associated SYT1 contact site expansion in Arabidopsis. *Proc. Natl. Acad. Sci. U. S. A.*, **116**, 1420–1429.

Lee, H.G., Park, M.E., Park, B.Y., Kim, H.U. and Seo, P.J. (2019) The Arabidopsis MYB96 transcription factor mediates ABA-dependent triacylglycerol accumulation in vegetative tissues under drought stress conditions. *Plants*, **8**, 1–12.

Légeret, B., Schulz-Raffelt, M., Nguyen, H.M., Auroy, P., Beisson, F., Peltier, G., Blanc, G. and Li-Beisson, Y. (2016) Lipidomic and transcriptomic analyses of *Chlamydomonas reinhardtii* under heat stress unveil a direct route for the conversion of membrane lipids into storage lipids. *Plant Cell Environ.*, **39**, 834–847.

Lévesque-Lemay, M., Chabot, D., Hubbard, K., Chan, J.K., Miller, S. and Robert, L.S. (2016) Tapetal oleosins play an essential role in tapetosome formation and protein relocation to the pollen coat. *New Phytol.*, **209**, 691–704.

Levy, A. and Tilsner, J. (2020) Creating Contacts Between Replication and Movement at Plasmodesmata – A role for membrane contact sites in plant virus infections? *Front. Plant Sci.*, **11**, 1–8.

Levy, A., Zheng, J.Y. and Lazarowitz, S.G. (2015) Synaptotagmin SYTA forms ER-plasma membrane junctions that are recruited to plasmodesmata for plant virus movement. *Curr. Biol.*, **25**, 2018–2025.

Lewis, J.D. and Lazarowitz, S.G. (2010) Arabidopsis synaptotagmin SYTA regulates endocytosis and virus movement protein cell-to-cell transport. *Proc. Natl. Acad. Sci. U. S. A.*, **107**, 2491–2496.

Li, F., Asami, T., Wu, X., Tsang, E.W.T. and Cutler, a. J. (2007) A putative Hydroxysteroid Dehydrogenase involved in regulating plant growth and development. *Plant Physiol.*, **145**, 87–97.

Li, P.C., Ma, J.J., Zhou, X.M., Li, G.H., Zhao, C.Z., Xia, H., Fan, S.J. and Wang, X.J. (2019) Arabidopsis MDN1 is involved in the establishment of a normal seed proteome and seed germination. *Front. Plant Sci.*, **10**, 1–10.

Li, Z. and Srivastava, P. (2003) Heat-shock proteins. *Curr. Protoc. Immunol.*, **58**.

Lin, L.-J., Sorgan, S.K.T., Peng, C.-C. and Tzen, J.T.C. (2002) Correction. *Plant Physiol.*, **129**, 1930–1930.

Lin, L.-J., Sorgan, S.K.T., Peng, C.-C. and Tzen, J.T.C. (2002) Steroleosin, a sterol-binding dehydrogenase in seed oil bodies. *Plant Physiol.*, **128**, 1200–1211.

Liu, H., Wang, C., Chen, F. and Shen, S. (2015) Proteomic analysis of oil bodies in mature *Jatropha curcas* seeds with different lipid content. *J. Proteomics*, **113**, 403–414.

Liu, L.K., Choudhary, V., Toulmay, A. and Prinz, W.A. (2017) An inducible ER-Golgi tether facilitates ceramide transport to alleviate lipotoxicity. *J. Cell Biol.*, **216**, 131–147.

Lozano-Durán, R. and Zipfel, C. (2015) Trade-off between growth and immunity: Role of brassinosteroids. *Trends Plant Sci.*, **20**, 12–19.

Lu, J., Xu, Y., Wang, J., Singer, S.D. and Chen, G. (2020) The role of triacylglycerol in plant stress response. *Plants*, **9**.

Lundquist, P.K., Poliakov, A., Bhuiyan, N.H., Zybailov, B., Sun, Q. and Wijk, K.J. van (2012) The functional network of the Arabidopsis plastoglobule proteome based on quantitative proteomics and genome-wide coexpression analysis. *Plant Physiol.*, **158**, 1172–1192.

Lundquist, P.K., Shivaiah, K.K. and Espinoza-Corral, R. (2020) Lipid droplets throughout the evolutionary tree. *Prog. Lipid Res.*, **78**, 101029.

Manford, A.G., Stefan, C.J., Yuan, H.L., MacGurn, J.A. and Emr, S.D. (2012) ER-to-plasma membrane tethering proteins regulate cell signaling and ER morphology. *Dev. Cell*, **23**, 1129–1140.

Masclaux-Daubresse, C., D'andrea, S., Bouchez, I., Cacas, J.L. and Raines, C. (2020) Reserve lipids and plant autophagy. *J. Exp. Bot.*, **71**, 2854–2861.

McLachlan, D.H., Lan, J., Geilfus, C.M., et al. (2016) The breakdown of stored triacylglycerols is required during light-induced stomatal opening. *Curr. Biol.*, **26**, 707–712.

Michaud, M. and Jouhet, J. (2019) Lipid trafficking at membrane contact sites during plant development and stress response. *Front. Plant Sci.*, **10**, 1–10.

Michaud, M., Prinz, W.A. and Jouhet, J. (2017) Glycerolipid synthesis and lipid trafficking in plant mitochondria. *FEBS J.*, **284**, 376–390.

Mikitova, V. and Levine, T.P. (2012) Analysis of the key elements of FFAT-like motifs identifies new proteins that potentially bind VAP on the ER, including two AKAPs and FAPP2. *PLoS One*, **7**, e30455.

Miquel, M. and Browse, J. (1992) Arabidopsis mutants deficient in polyunsaturated fatty acid synthesis: Biochemical and genetic characterization of a plant oleoyl-phosphatidylcholine desaturase. *J. Biol. Chem*., **267**, 1502–1509**.**

Miquel, M., Trigui, G., D'Andréa, S., et al. (2014) Specialization of oleosins in oil body dynamics during seed development in Arabidopsis seeds. *Plant Physiol.*, **164**, 1866–1878.

Mitchell, J., Mandava, N., Worley, J.F., Plimmer, J. and Smith, M. (1970) Brassins - a new family of plant hormones from rape pollen. *Nature*, **225**, 1065–1066.

Mitchell, J.W. and Gregory, L.E. (1972) Enhancement of overall plant growth, a new response to brassins. *Nature*, **239**, 253–254.

Modi, S., López-Doménech, G., Halff, E.F., et al. (2019) Miro clusters regulate ER-mitochondria contact sites and link cristae organization to the mitochondrial transport machinery. *Nat. Commun.*, **10**, 17–19.

Moellering, E.R. and Benning, C. (2010) RNA interference silencing of a major lipid droplet protein affects lipid droplet size in *Chlamydomonas reinhardtii*. *Eukaryot. Cell*, **9**, 97–106.

Mueller, S.P., Krause, D.M., Mueller, M.J. and Fekete, A. (2015) Accumulation of extra-chloroplastic triacylglycerols in Arabidopsis seedlings during heat acclimation. *J. Exp. Bot.*, **66**, 4517–4526.

Mueller, S.P., Unger, M., Guender, L., Fekete, A. and Mueller, M.J. (2017) Phospholipid: Diacylglycerol acyltransferase-mediated triacylglyerol synthesis augments basal thermotolerance. *Plant Physiol.*, **175**, 486–497.

Müller, A.O. and Ischebeck, T. (2017) Characterization of the enzymatic activity and physiological function of the lipid droplet-associated triacylglycerol lipase AtOBL1. *New Phytol.,* **1,** 1062–1076.

Murashige, T. and Skoog, F. (1962) A revised medium for rapid growth and bio assays with Tobacco tissue cultures. *Physiol. Plant.*, **15**, 473–497.

Murphy, D.J. (2012) The dynamic roles of intracellular lipid droplets: From archaea to mammals. *Protoplasma*, **249**, 541–585.

Nakabayashi, K., Okamoto, M., Koshiba, T., Kamiya, Y. and Nambara, E. (2005) Genome-wide profiling of stored mRNA in *Arabidopsis thaliana* seed germination: Epigenetic and genetic regulation of transcription in seed. *Plant J.*, **41**, 697–709.

Nath, V.R., Mishra, S., Basak, B., Trivedi, D. and Raghu, P. (2020) Extended synaptotagmin regulates membrane contact site structure and lipid transfer function *in vivo* . *EMBO Rep.*, 1–16.

Nettebrock, N.T. and Bohnert, M. (2020) Born this way – Biogenesis of lipid droplets from specialized ER subdomains. *Biochim. Biophys. Acta - Mol. Cell Biol. Lipids*, **1865**, 158448.

Nguyen, T.B., Louie, S.M., Daniele, J.R., Tran, Q., Dillin, A., Zoncu, R., Nomura, D.K. and Olzmann, J.A. (2017) DGAT1-Dependent lipid droplet biogenesis protects mitochondrial function during starvation-induced autophagy. *Dev. Cell*, **42**, 9–21.

Nguyen, T.B. and Olzmann, J.A. (2017) Lipid droplets and lipotoxicity during autophagy. *Autophagy*, **13**, 2002–2003.

Niu, Y. and Xiang, Y. (2018) An overview of biomembrane functions in plant responses to high-temperature stress. *Front. Plant Sci.*, **9**, 1–18.

Oikawa, K., Matsunaga, S., Mano, S., et al. (2015) Physical interaction between peroxisomes and chloroplasts elucidated by *in situ* laser analysis. *Nat. Plants*, **1**, 15035.

Oku, M., Maeda, Y., Kagohashi, Y., Kondo, T., Yamada, M., Fujimoto, T. and Sakai, Y. (2017) Evidence for ESCRT- and clathrin-dependent microautophagy. *J. Cell Biol.*, **216**, 3263–3274.

Olzmann, J.A. and Carvalho, P. (2019) Dynamics and functions of lipid droplets. *Nat. Rev. Mol. Cell Biol.*, **20**, 137–155.

Olzmann, J.A. and Kopito, R.R. (2011) Lipid droplet formation is dispensable for endoplasmic reticulum-associated degradation. *J. Biol. Chem.*, **286**, 27872–27874.

Osterrieder, A., Carvalho, C.M., Latijnhouwers, M., Johansen, J.N., Stubbs, C., Botchway, S. and Hawes, C. (2009) Fluorescence lifetime imaging of interactions between Golgi tethering factors and Small GTPases in plants. *Traffic*, **10**, 1034–1046.

Osterrieder, A., Sparkes, I.A., Botchway, S.W., Ward, A., Ketelaar, T., Ruijter, N. de and Hawes, C. (2017) Stacks off tracks: a role for the golgin AtCASP in plant endoplasmic reticulum-Golgi apparatus tethering. *J. Exp. Bot.*, **68**, 3339–3350.

Pataki, C.I., Rodrigues, J., Zhang, L., Qian, J., Efron, B., Hastie, T., Elias, J.E., Levitt, M. and Kopito, R.R. (2018) Proteomic analysis of monolayer-integrated proteins on lipid droplets identifies amphipathic interfacial α-helical membrane anchors. *Proc. Natl. Acad. Sci. U. S. A.*, **115**, E8172–E8180.

Peramuna, A., Morton, R. and Summers, M.L. (2015) Enhancing alkane production in cyanobacterial lipid droplets: A model platform for industrially relevant compound production. *Life*, **5**, 1111–1126.

Peramuna, A. and Summers, M.L. (2014) Composition and occurrence of lipid droplets in the cyanobacterium *Nostoc punctiforme*. *Arch. Microbiol.*, **196**, 881–890.

Pérez-Sancho, J., Tilsner, J., Samuels, A.L., Botella, M.A., Bayer, E.M. and Rosado, A. (2016) Stitching organelles: Organization and function of specialized membrane contact sites in plants. *Trends Cell Biol.*, **26**, 705–717.

Pérez-Sancho, J., Vanneste, S., Lee, E., McFarlane, H.E., Valle, A.E. del, Valpuesta, V., Friml, J., Botella, M.A. and Rosado, A. (2015) The Arabidopsis synaptotagmin1 is enriched in endoplasmic reticulum-plasma membrane contact sites and confers cellular resistance to mechanical stresses. *Plant Physiol.*, **168**, 132–143.

Poirier, Y., Antonenkov, V.D., Glumoff, T. and Hiltunen, J.K. (2006) Peroxisomal β-oxidation – A metabolic pathway with multiple functions. *Biochim. Biophys. Acta - Mol. Cell Res.*, **1763**, 1413–1426.

Popluechai, S., Froissard, M., Jolivet, P., Breviario, D., Gatehouse, A.M.R., O'Donnell, A.G., Chardot, T. and Kohli, A. (2011) *Jatropha curcas* oil body proteome and oleosins: L-form JcOle3 as a potential phylogenetic marker. *Plant Physiol. Biochem.*, **49**, 352–356.

Poxleitner, M., Rogers, S.W., Lacey Samuels, A., Browse, J. and Rogers, J.C. (2006) A role for caleosin in degradation of oil-body storage lipid during seed germination. *Plant J.*, **47**, 917–933.

Price, A.M., Doner, N.M., Gidda, S.K., et al. (2020) Mouse Fat-Specific Protein 27 (FSP27) expressed in plant cells localizes to lipid droplets and promotes lipid droplet accumulation and fusion. *Biochimie*, **169**, 41–53.

Prinz, W.A. (2014) Bridging the gap: Membrane contact sites in signaling, metabolism, and organelle dynamics. *J. Cell Biol.*, **205**, 759–769.

Prinz, W.A. (2010) Lipid trafficking sans vesicles: Where, why, how? *Cell*, **143**, 870–874.

Prinz, W.A., Toulmay, A. and Balla, T. (2020) The functional universe of membrane contact sites. *Nat. Rev. Mol. Cell Biol.*, **21**, 7–24.

Pyc, M., Cai, Y., Gidda, S.K., Yurchenko, O., Park, S., Kretzschmar, F.K., et al. (2017) Arabidopsis lipid droplet-associated protein (LDAP) – interacting protein (LDIP) influences lipid droplet size and neutral lipid homeostasis in both leaves and seeds. *Plant J.*, **92**, 1182–1201.

Qu, R., Wang, S.M., Lin, Y.H., Vance, V.B. and Huang, A.H. (1986) Characteristics and biosynthesis of membrane proteins of lipid bodies in the scutella of maize (*Zea mays* L.). *Biochem. J.*, **235**, 57–65.

Quon, E., Sere, Y.Y., Chauhan, N., et al. (2018) Endoplasmic reticulum-plasma membrane contact sites integrate sterol and phospholipid regulation. *PLOS Biol.*, **16**.

Rahman, F., Hassan, M., Rosli, R., Almousally, I., Hanano, A. and Murphy, D.J. (2018) Evolutionary and genomic analysis of the caleosin/peroxygenase (CLO/PXG) gene/protein families in the Viridiplantae. *PLoS One*, **13**.

Rossini, M., Pizzo, P. and Filadi, R. (2020) Better to keep in touch: investigating inter-organelle cross-talk. *FEBS J.*, 1–16.

Rueden, C.T., Schindelin, J., Hiner, M.C., DeZonia, B.E., Walter, A.E., Arena, E.T. and Eliceiri, K.W. (2017) ImageJ2: ImageJ for the next generation of scientific image data. *BMC Bioinformatics*, **18**, 1–26.

Sadali, N.M., Sowden, R.G., Ling, Q. and Jarvis, R.P. (2019) Differentiation of chromoplasts and other plastids in plants. *Plant Cell Rep.*, **38**, 803–818.

Salogiannis, J., Egan, M.J. and Reck-Peterson, S.L. (2016) Peroxisomes move by hitchhiking on early endosomes using the novel linker protein PxdA. *J. Cell Biol.*, **212**, 289–296.

Schapire, A.L., Voigt, B., Jasik, J., et al. (2008) Arabidopsis synaptotagmin 1 is required for the maintenance of plasma membrane integrity and cell viability. *Plant Cell*, **20**, 3374–3388.

Schauder, C.M., Wu, X., Saheki, Y., Narayanaswamy, P., Torta, F., Wenk, M.R., Camilli, P. De and Reinisch, K.M. (2014) Structure of a lipid-bound extended synaptotagmin indicates a role in lipid transfer. *Nature*, **510**, 552–555.

Schmid, M., Davison, T.S., Henz, S.R., Pape, U.J., Demar, M., Vingron, M., Schölkopf, B., Weigel, D. and Lohmann, J.U. (2005) A gene expression map of *Arabidopsis thaliana* development. *Nat. Genet.*, **37**, 501–506.

Schmidt, M.A. and Herman, E.M. (2008) Suppression of soybean oleosin produces micro-oil bodies that aggregate into oil body/ER complexes. *Mol. Plant*, **1**, 910–924.

Schrader, M. (2001) Tubulo-reticular clusters of peroxisomes in living COS-7 cells: Dynamic behavior and association with lipid droplets. *J. Histochem. Cytochem.*, **49**, 1421–1429.

Schuldiner, M. and Bohnert, M. (2017) A different kind of love – lipid droplet contact sites. *Biochim. Biophys. Acta - Mol. Cell Biol. Lipids*, **1862**, 1188–1196.

Scorrano, L., Matteis, M.A. De, Emr, S., et al. (2019) Coming together to define membrane contact sites. *Nat. Commun.*, **10**, 1–11.

Seibert, J.T., Najt, C.P., Heden, T.D., Mashek, D.G. and Chow, L.S. (2020) Muscle lipid droplets: Cellular signaling to exercise physiology and beyond. *Trends Endocrinol. Metab.*, 1–11.

Selinski, J. and Scheibe, R. (2014) Pollen tube growth: Where does the energy come from? *Plant Signal. Behav.*, **9**, e977200-1-e977200-9.

Senoo, H., Kojima, N. and Sato, M. (2007) Vitamin A-storing cells (stellate cells). *Vitam. Horm.*, **75**, 131–159.

Shai, N., Yifrach, E., Roermund, C.W.T. Van, et al. (2018) Systematic mapping of contact sites reveals tethers and a function for the peroxisome-mitochondria contact. *Nat. Commun.*, **9**.

Shigenaga, A.M. and Argueso, C.T. (2016) No hormone to rule them all: Interactions of plant hormones during the responses of plants to pathogens. *Semin. Cell Dev. Biol.*, **56**, 174–189.

Shimada, T.L., Shimada, T., Okazaki, Y., et al. (2019) HIGH STEROL ESTER 1 is a key factor in plant sterol homeostasis. *Nat. Plants*, **5**, 1154–1166.

Shimada, T.L., Shimada, T., Takahashi, H., Fukao, Y. and Hara-Nishimura, I. (2008) A novel role for oleosins in freezing tolerance of oilseeds in *Arabidopsis thaliana*. *Plant J.*, **55**, 798–809.

Shimada, T.L.T., Takano, Y., Shimada, T.L.T., et al. (2014) Leaf oil body functions as a subcellular factory for the production of a phytoalexin in Arabidopsis. *Plant Physiol.*, **164**, 105–18.

Shiva, S., Samarakoon, T., Lowe, K.A., et al. (2020) Leaf lipid alterations in response to heat stress of *Arabidopsis thaliana*. *Plants*, **9**, 845.

Shpilka, T., Welter, E., Borovsky, N., Amar, N., Mari, M., Reggiori, F. and Elazar, Z. (2015) Lipid droplets and their component triglycerides and steryl esters regulate autophagosome biogenesis. *EMBO J.*, **34**, 2117–2131.

Siao, W., Wang, P., Voigt, B., Hussey, P.J. and Baluska, F. (2016) Arabidopsis SYT1 maintains stability of cortical endoplasmic reticulum networks and VAP27-1-enriched endoplasmic reticulum-plasma membrane contact sites. *J. Exp. Bot.*, **67**, 6161–6171.

Siloto, R.M.P., Findlay, K., Lopez-Villalobos, A., Yeung, E.C., Nykiforuk, C.L. and Moloney, M.M. (2006) The accumulation of oleosins determines the size of seed oilbodies in Arabidopsis. *Plant Cell*, **18**, 1961–74.

Singer, S.D., Zou, J. and Weselake, R.J. (2016) Abiotic factors influence plant storage lipid accumulation and composition. *Plant Sci.*, **243**, 1–9.

Sparkes, I.A., Ketelaar, T., Ruijter, N.C.A. De and Hawes, C. (2009) Grab a golgi: Laser trapping of golgi bodies reveals *in vivo* interactions with the endoplasmic reticulum. *Traffic*, **10**, 567–571.

Spicher, L. and Kessler, F. (2015) Unexpected roles of plastoglobules (plastid lipid droplets) in vitamin K1 and E metabolism. *Curr. Opin. Plant Biol.*, **25**, 123–129.

Stefano, G., Renna, L., Wormsbaecher, C., Gamble, J., Zienkiewicz, K. and Brandizzi, F. (2018) Plant endocytosis requires the ER membrane-anchored proteins VAP27-1 and VAP27-3. *Cell Rep.*, **23**, 2299–2307.

Szabadkai, G., Bianchi, K., Várnai, P., Stefani, D. De, Wieckowski, M.R., Cavagna, D., Nagy, A.I., Balla, T. and Rizzuto, R. (2006) Chaperone-mediated coupling of endoplasmic reticulum and mitochondrial Ca^{2+} channels. *J. Cell Biol.*, **175**, 901–911.

Taurino, M., Costantini, S., Domenico, S. De, et al. (2018) SEIPIN proteins mediate lipid droplet biogenesis to promote pollen transmission and reduce seed dormancy. *Plant Physiol.*, **176**, pp.01430.2017.

Thakur, A. and Bhatla, S.C. (2016) Proteomic analysis of oil body membrane proteins accompanying the onset of desiccation phase during sunflower seed development. *Plant Signal. Behav.*, **10**.

Thazar-Poulot, N., Miquel, M., Fobis-Loisy, I. and Gaude, T. (2015) Peroxisome extensions deliver the Arabidopsis SDP1 lipase to oil bodies. *Proc. Natl. Acad. Sci. U. S. A.*, **112**, 4158–63.

Thiam, A.R., Antonny, B., Wang, J., Delacotte, J., Wilfling, F., Walther, T.C., Beck, R., Rothman, J.E. and Pincet, F. (2013) COPI buds 60-nm lipid droplets from reconstituted water-phospholipid- triacylglyceride interfaces, suggesting a tension clamp function. *Proc. Natl. Acad. Sci. U. S. A.*, **110**, 13244–13249.

Thiam, A.R. and Beller, M. (2017) The why, when and how of lipid droplet diversity. *J. Cell Sci.*, **130**, 315–324.

Thiam, A.R. and Dugail, I. (2019) Lipid droplet-membrane contact sites - From protein binding to function. *J. Cell Sci.*, **132**, jcs230169.

Tnani, H., López, I., Jouenne, T. and Vicient, C.M. (2011) Protein composition analysis of oil bodies from maize embryos during germination. *J. Plant Physiol.*, **168**, 510–513.

To, M., Peterson, C.W.H., Roberts, M.A., Counihan, J.L., Wu, T.T., Forster, M.S., Nomura, D.K. and Olzmann, J.A. (2017) Lipid disequilibrium disrupts ER proteostasis by impairing ERAD substrate glycan trimming and dislocation. *Mol. Biol. Cell*, **28**, 270–284.

Traber, M.G. and Kayden, H.J. (1987) Tocopherol distribution and intracellular localization in human adipose tissue. *Am. J. Clin. Nutr.*, **46**, 488–495.

Ugrankar, R., Bowerman, J., Hariri, H., et al. (2019) Drosophila Snazarus regulates a lipid droplet population at plasma membrane-droplet contacts in adipocytes. *Dev. Cell*, **50**, 557–572.

Valachovic, M., Garaiova, M., Holic, R. and Hapala, I. (2015) Squalene is lipotoxic to yeast cells defective in lipid droplet biogenesis. *Biochem. Biophys. Res. Commun.*, 1–6.

Valitova, J.N., Sulkarnayeva, A.G. and Minibayeva, F. V (2016) Plant sterols: diversity, biosynthesis, and physiological functions. *Biochemistry. (Mosc).*, **81**, 819–834.

Valm, A.M., Cohen, S., Legant, W.R., et al. (2017) Applying systems-level spectral imaging and analysis to reveal the organelle interactome. *Nature*, **546**, 162–167.

Vance, J.E., Aasman, E.J. and Szarka, R. (1991) Brefeldin A does not inhibit the movement of phosphatidylethanolamine from its sites of synthesis to the cell surface. *J. Biol. Chem.*, **266**, 8241–8247.

Velázquez, A.P., Tatsuta, T., Ghillebert, R., Drescher, I. and Graef, M. (2016) Lipid droplet-mediated ER homeostasis regulates autophagy and cell survival during starvation. *J. Cell Biol.*, **212**, 621–631.

Venditti, R., Rega, L.R., Masone, M.C., et al. (2019) Molecular determinants of ER–Golgi contacts identified through a new FRET–FLIM system. *J. Cell Biol.*, **218**, 1055–1065.

Vevea, J.D., Garcia, E.J., Chan, R.B., Zhou, B., Schultz, M., Paolo, G. Di, McCaffery, J.M. and Pon, L.A. (2015) Role for lipid droplet biogenesis and microlipophagy in adaptation to lipid imbalance in yeast. *Dev. Cell*, **35**, 584–599.

Vliet, A.R. van, Giordano, F., Gerlo, S., et al. (2017) The ER stress sensor PERK coordinates ER-plasma membrane contact site formation through interaction with Filamin-A and F-Actin remodeling. *Mol. Cell*, **65**, 885–899.

Vries, J. de and Ischebeck, T. (2020) Ties between stress and lipid droplets pre-date seeds. *Trends Plant Sci.*, **25**, 1203–1214.

Waese, J., Fan, J., Pasha, A., et al. (2017) ePlant: Visualizing and exploring multiple levels of data for hypothesis generation in plant biology. *Plant Cell*, **29**, 1806–1821.

Walther, T.C., Chung, J. and Farese, R. V. (2017) Lipid droplet biogenesis. *Annu. Rev. Cell Dev. Biol.*, **33**, 491–510.

Wang, H., Sreenevasan, U., Hu, H., Saladino, A., Polster, B.M., Lund, L.M., Gong, D.W., Stanley, W.C. and Sztalryd, C. (2011) Perilipin 5, a lipid droplet-associated protein, provides physical and metabolic linkage to mitochondria. *J. Lipid Res.*, **52**, 2159–2168.

Wang, P., Richardson, C., Hawkins, T.J., Sparkes, I., Hawes, C. and Hussey, P.J. (2016) Plant VAP27 proteins: Domain characterization, intracellular localization and role in plant development. *New Phytol.*, **210**, 1311–1326.

Wang, S., Idrissi, F.Z., Hermansson, M., Grippa, A., Ejsing, C.S. and Carvalho, P. (2018) Seipin and the membrane-shaping protein Pex30 cooperate in organelle budding from the endoplasmic reticulum. *Nat. Commun.*, **9**, 1–12.

Wasternack, C. and Feussner, I. (2018) The oxylipin pathways: Biochemistry and function. *Annu. Rev. Plant Biol.*, **69**, 363–386.

Welte, M.A. and Gould, A.P. (2017) Lipid droplet functions beyond energy storage. *Biochim. Biophys. Acta - Mol. Cell Biol. Lipids*, **1862**, 1260–1272.

White, R.R., Lin, C., Leaves, I., et al. (2020) Miro2 tethers the ER to mitochondria to promote mitochondrial fusion in Tobacco leaf epidermal cells. *Commun. Biol.*, **3**, 1–8.

Wilfling, F., Thiam, A.R., Olarte, M.J., et al. (2014) Arf1/COPI machinery acts directly on lipid droplets and enables their connection to the ER for protein targeting. *Elife*, **2014**, 1–20.

Wilfling, F., Wang, H., Haas, J.T., et al. (2013) Triacylglycerol synthesis enzymes mediate lipid droplet growth by relocalizing from the ER to lipid droplets. *Dev. Cell*, **24**, 384–399.

Winter, D., Vinegar, B., Nahal, H., Ammar, R., Wilson, G. V. and Provart, N.J. (2007) An "electronic fluorescent pictograph" browser for exploring and analyzing large-scale biological data sets. *PLoS One*, **2**, 1–12.

Wolters-Arts, M., Lush, W.M. and Mariani, C. (1998) Lipids are required for directional pollen-tube growth. *Nature*, **392**, 818–821.

Wong, L.H., Gatta, A.T. and Levine, T.P. (2019) Lipid transfer proteins: the lipid commute via shuttles, bridges and tubes. *Nat. Rev. Mol. Cell Biol.*, **20**, 85–101.

Xu, D., Li, Y., Wu, L., et al. (2018) Rab18 promotes lipid droplet (LD) growth by tethering the ER to LDs through SNARE and NRZ interactions. *J. Cell Biol.*, jcb.201704184.

Yamaguchi, T., Fujikawa, N., Nimura, S., Tokuoka, Y., Tsuda, S., Aiuchi, T., Kato, R., Obama, T. and Itabe, H. (2015) Characterization of lipid droplets in steroidogenic MLTC-1 Leydig cells: Protein profiles and the morphological change induced by hormone stimulation. *Biochim. Biophys. Acta - Mol. Cell Biol. Lipids*, **1851**, 1285–1295.

Yamazaki, T., Kawamura, Y., Minami, A. and Uemura, M. (2008) Calcium-dependent freezing tolerance in arabidopsis involves membrane resealing via synaptotagmin SYT1. *Plant Cell*, **20**, 3389–3404.

Yang, Y. and Benning, C. (2018) Functions of triacylglycerols during plant development and stress. *Curr. Opin. Biotechnol.*, **49**, 191–198.

Yang, Y., Mininberg, B., Tarbet, A. and Weathers, P. (2013) At high temperature lipid production in *Ettlia oleoabundans* occurs before nitrate depletion. *Appl. Microbiol. Biotechnol.*, **97**, 2263–2273.

Yang, Y., Yu, X., Song, L. and An, C. (2011) ABI4 activates *DGAT1* expression in Arabidopsis seedlings during nitrogen deficiency. *Plant Physiol.*, **156**, 873–883.

Yang, Z., Zhao, X., Xu, J., Shang, W. and Tong, C. (2018) A novel fluorescent reporter detects plastic remodeling of mitochondria-ER contact sites. *J. Cell Sci.*, **131**.

Ye, Q., Zhu, W., Li, L., Zhang, S., Yin, Y., Ma, H. and Wang, X. (2010) Brassinosteroids control male fertility by regulating the expression of key genes involved in Arabidopsis anther and pollen development. *Proc. Natl. Acad. Sci. U. S. A.*, **107**, 6100–6105.

Yin, Y., Qin, K., Song, X., Zhang, Q., Zhou, Y., Xia, X. and Yu, J. (2018) BZR1 transcription factor regulates heat stress tolerance through FERONIA receptor-like kinase-mediated reactive oxygen species signaling in tomato. *Plant Cell Physiol.*, **59**, 2239–2254.

Yu, H., Liu, Y., Gulbranson, D.R., Paine, A., Rathore, S.S. and Shen, J. (2016) Extended synaptotagmins are Ca^{2+}-dependent lipid transfer proteins at membrane contact sites. *Proc. Natl. Acad. Sci. U. S. A.*, **113**, 4362–4367.

Zaaboul, F., Raza, H., Chen, C. and Liu, Y. (2018) Characterization of peanut oil bodies integral proteins, lipids, and their associated phytochemicals. *J. Food Sci.*, **83**, 93–100.

Zahradka, P., Neumann, S., Aukema, H.M. and Taylor, C.G. (2017) Adipocyte lipid storage and adipokine production are modulated by lipoxygenase-derived oxylipins generated from 18-carbon fatty acids. *Int. J. Biochem. Cell Biol.*, **88**, 23–30.

Zhang, C. and Liu, P. (2017) The lipid droplet: A conserved cellular organelle. *Protein Cell*, **8**, 796–800.

Zhang, M., Fan, J., Taylor, D.C. and Ohlrogge, J.B. (2009) DGAT1 and PDAT1 acyltransferases have overlapping functions in Arabidopsis triacylglycerol biosynthesis and are essential for normal pollen and seed development. *Plant Cell*, **21**, 3885–3901.

Zhang, W.H., Zhou, Y., Dibley, K.E., Tyerman, S.D., Furbank, R.T. and Patrick, J.W. (2007) Review: Nutrient loading of developing seeds. *Funct. Plant Biol.*, **34**, 314–331.

Zhang, X., Lin, K. and Li, Y. (2020) Highlights to phytosterols accumulation and equilibrium in plants: Biosynthetic pathway and feedback regulation. *Plant Physiol. Biochem.*, **155**, 637–649.

Zhi, Y., Taylor, M.C., Campbell, P.M., et al. (2017) Comparative lipidomics and proteomics of lipid droplets in the mesocarp and seed tissues of Chinese tallow (*Triadica sebifera*). *Front. Plant Sci.*, **8**, 1–20.

Zuidmeer-Jongejan, L., Fernández-Rivas, M., Winter, M.G.T., et al. (2014) Oil body-associated hazelnut allergens including oleosins are underrepresented in diagnostic extracts but associated with severe symptoms. *Clin. Transl. Allergy*, **4**, 1–10.

Acknowledgements

Mein erster und größter Dank gebührt PD Dr. Till Ischebeck. Lieber Till, danke, dass du mich und meine Doktorarbeit die letzten Jahre betreut hast. Du hast mich in die spannende Welt der Lipid Droplets eingeführt und mir ein tolles Projekt mit vielen Freiheiten gegeben. Du hast mir die Bioanalytik nahegebracht und es (quasi) geschafft, mich auch für Pollenschläuche zu begeistern! Auch wenn wir hin und wieder mal unsere kleinen Meinungsverschiedenheiten hatten, auch das gehört dazu und bringt die Wissenschaft voran! Ich möchte dir für all deine Unterstützung, wissenschaftlich und moralisch, danken. Ich weiß es sehr zu schätzen, in dir einen so engagierten und bemühten Chef gehabt zu haben, mit dem man immer über alles reden kann und der immer das beste für seine Studenten im Sinn hat! Danke!

Auch meinen Thesis Advisory Committee Mitgliedern möchte ich Dank aussprechen. Prof. Dr. Jörg Stülke und PD Dr. Marcel Wiermer, vielen Dank, dass Sie Teil meines TAC waren, dass Sie sich meine Vorträge angehört und mir Feedback zu meinen Projekten gegeben haben.

Ebenfalls bedanken möchte ich mich bei Prof. Dr. Feußner. Sie geben der AG Ischebeck in Ihren Laboren ein Zuhause. Ein großer Dank auch für Ihre finanzielle Unterstützung und für allen wissenschaftlichen Input.

Many thanks go to all our collaboration partners and/or (going-to-be) co-authors, especially Prof. Dr. Robert Mullen, Prof. Dr. Kent Chapman, and Dr. John Dyer, for brainstorming together, critical discussions and also for socialising. Special thanks to Nathan Doner for reading and revising our manuscript so thoroughly and giving helpful advice!

I would also like to thank the whole current and former AG Ischebeck. Especially the PhD students that joined me part or whole of the way, Anna, Athanas, Franzi, Patricia, Philipp and Siqi; but also our master students, Magdiel, Max and Maurice and all our lab rotation students. Not only for creating a nice working environment, for scientific discussions, collaborations and great conference stays, but also for all the Ischegang meetings with BBQ, Pizza, Burger and one or two Amarula, for classical or Disney music days in the lab and especially also for coping with my rhinozeros-tantrums! Thank you all for making the AG Ischebeck so lively and loveable. Special thank also goes to the students whom I had the pleasure to supervise: Siqi Sun, Katharina Kohm and Alexander Rotsch.

Of course, I would also like to thank all current and former members of the AG Feussner. All of you contributed to me enjoying the work this thesis is based on and coming to the lab with joy. Although I did not specifically love the hiking parts, all our lab excursions, BBQs, Christmas parties and movie nights were always a great pleasure and lots of fun! As was working with you all in the department, having lunch together or meeting for a short coffee break. I am grateful for having had such great and amicable colleagues!

In this regard, I also want to thank Dr. Ellen Hornung, for always answering any questions at any time and never losing her good spirits; Dr. Agnieszka Zienkiewicz and Dr. Krzysztof Zienkiewicz for always sharing their knowledge and being supportive; Dr. Tegan Haslam for being so cooperative and always offering a helping hand (/reading eye) and Dr. Cornelia Herrfurth for measuring and analysing our samples!

A special thank also goes to all the PhD-students accompanying me on my way. A problem shared is a problem halved – thank you, Benji, Nodumo, Hanno, Anna, Sven, Milena, Dimi, Franzi, Athanas, Yi-Tse, Jasmin, Kathi, Patricia, Philipp, Alisa, Lennart, Siqi and Benedikt!

Ein großer Dank gebührt auch Susanne Mester, ohne die diverse meiner Pflanzen ein sehr viel kürzeres Leben gehabt hätten; Malte Bürsing, der sich jederzeit jedem noch so großen oder kleinen technischen Problem annimmt und die wunderbarsten bewegten und leuchtenden Doktorhüte zaubert; Tarek Morsi, der auch beim hundertsten Computer-Problem seine gute Laune nie verloren hat; Heike Lott und Anja Vogelpohl, die mich nicht nur kontinuierlich mit Tesa-Film, Eddings und neuen Hüllen für meine Laborkarte versorgt haben (und immer eine Gästekarte für mich parat hatten…), sondern die mir auch immer geholfen haben, Dienstreiseanträge zu finden und zu verstehen, meine verlorengegangenen Verträge wieder aufzutreiben, Urlaubsanträge zu managen und so viel mehr! Danke! Ein großer Dank auch ans GGNB-Office, das im Hintergrund das Management aller administrativen Angelegenheiten übernimmt und auf jede Frage eine schnelle und liebe Antwort hat!

Ein weiterer sehr großer Dank gebührt Sabine Freitag. Liebste Sabein, auch du hast sehr viel dazu beigetragen, dass ich diese Arbeit fertig stellen konte. Nicht nur hast du mir geholfen, mich in der Welt der Biochemie zurecht zu finden, hast mir unter die Arme gegriffen, wo du konntest und mir unzählige Fragen beantwortet. Du hast auch immer ein offenes Ohr für meine privaten Sorgen und Freuden gehabt und bist immer eine große moralische Unterstützung gewesen! Danke für alles!

Auch Dr. Amélie Kelly verdient ein großes Dankeschön. Liebe Amélie, erst einmal danke für deine Korrekturen und Anregungen zu meiner Arbeit! Du warst aber auch sonst nie müde, dich mit meinen Fragen, Problemen, Ideen und Wehwehchen auseinander zu setzen und hattest immer Anregungen für mich parat. Dein Rat und deine Hilfe haben mir immer sehr geholfen und waren und sind mir sehr viel wert! Danke auch dir!

Besonders dankbar bin ich auch Jasmin und Kathi. Wir haben uns gegenseitig den gesamten Weg des Doktors begleitet und alle Hochs und Tiefs miterlebt. Wie gesagt: geteiltes Leid ist halbes Leid. Aber: geteilte Freude ist doppelte Freude – ich bin euch unendlich dankbar in euch Freundinnen gefunden zu haben, mit denen ich auch alle Freuden des Lebens teilen kann. Vielen Dank!

Auch bei meinen Freunden außerhalb des Labors möchte ich mich bedanken. All eure kleinen und großen Gesten der Unterstützung waren mir in den letzten Monaten unendlich viel Wert und ich bin unglaublich dankbar, so tolle Menschen meine Freunde nennen zu können! Maike, vielen Dank, dass du trotz der Distanz, trotz der Zeitverschiebung und trotz meiner Igelei immer für mich da bist! Julia, vielen Dank für deine Unterstützung und dass du immer ein Instagram-Meme parat hast! Kathrin (und Dieter), danke für deinen moralischen Support! Nora und Anka, danke für euren Vor-Ort-Support und dass ich immer auf euch zählen kann! Sarah, Tanita, Malena – danke für eure Begeisterung, dass ich uns den Doktor nach Hause hole! Ricci und Jule, vielen Dank für euer Verständnis in den letzten Monaten und dass ihr mich schon so lange begleitet!

Natürlich möchte ich mich auch bei meiner Familie bedanken. Mama, Papa, Paul, Josi, ohne euch hätte ich es nicht so weit geschafft. Danke, dass ihr mich immer in allem unterstützt habt und vor allem danke, dass ich weiß, dass ich mich immer auf euch verlassen kann und ihr immer für mich da seid und mir Rückhalt gebt!

Moni, auch dir bin ich unbeschreiblich dankbar, dass du mich in den letzten Monaten des Doktors begleitet hast. Danke für all deine Geduld die letzten Wochen, deine Krisenbewältigungsstrategien (je nach Ausmaß der Krise in Form von Pringles oder Schnapspralinen), deine Unterstützung und einfach dafür, dass du da bist!

"I would maintain that thanks are the highest form of thought, and that gratitude is happiness doubled by wonder."

Gilbert K. Chesterton (1874 – 1936)